Mobilization and detoxification of carcinogenic oxyanions from a contaminated soil mediated by micro and nano-sized metallic particles

by

Mario Rivero-Huguet

Department of Food Science and Agricultural Chemistry
Faculty of Agricultural and Environmental Sciences
McGill University, Montréal
July 2009

A thesis submitted to McGill University in partial fulfilment of the requirements of the degree of Doctor of Philosophy *à Olivier*

Abstract

Soil washing is a treatment process that has been used extensively for toxicant extraction, yet the process does not detoxify the mobilized pollutants *per se*. The more common detoxification processes include redox reactions that are mediated by zero-valent metals (ZVMs). Reduction of Cr(VI) to Cr(III) is desirable, as the latter specie is toxicologically innocuous to most living organisms and also has a low mobility and bioavailability. The main goals of this project included the development of an efficient treatment for the extraction and inactivation of toxic inorganic anions using ZVMs from contaminated soils. A variety of micron-sized ZVMs (Al, Cu, Fe, Mg, Ni, Si, and Zn); metallic mixtures (Pd/Fe, Ag/Fe, Cu/Fe, Zn/Fe, Co/Fe, Mg/Fe, Ni/Fe, Al/Fe, Si/Fe, Pd/Cu, Pd/Zn, Pd/Cu/Fe, Pd/Zn/Fe, and Zn/Cu/Fe); Cu and Fe nano-sized particles (NPs), and selected nano-sized bimetallic analogs (Pd/Fe, Cu/Fe and Pd/Cu) were evaluated for reactivity towards the reduction of Cr(VI) in a surfactant preparation (Tween® 20) under a selection of reaction conditions. At circum neutral pHs, a rapid inactivation of the surface was observed for almost all the tested metals whereas complete reduction of Cr(VI) was achieved at acidic pH only by using Cu, Fe, Mg, or Zn. Relative to the reactivity of the zero-valent iron, the tested bimetallic mixtures (Pd/Fe > Pd/Zn> Ag/Fe > Ni/Fe> Zn/Fe > Pd/Cu > Cu/Fe) appreciably increased the pseudo-first order rate constant. The Zn/Cu/Fe, represented a cost-effective preparation providing comparable or improved kinetic parameters relative to the more expensive palladized bimetallic mixtures. The results suggest that the cementation of a noble metal serves not only as a reaction accelerator but also provides protection of the ZVM surface impeding its rapid inactivation. A considerable increase in reactivity (up to 100-fold) was observed with NPs. The formation of clusters of polymeric structures provided an extra protection of the NPs surface with a striking increase of their reactivity mainly at more alkaline conditions. The influence of the presence of various naturally-occurring inorganic and organic molecules were evaluated for the detoxification of Cr(VI). An appreciable enhancement (up to 50-fold) of the constant rate was achieved for certain organic compounds capable of reducing Cr(VI) (α-hydroxyl carboxylate, ascorbic acid, cysteine) and for certain chelating agents (EDTA derivates, siderophores). Moderate improvements in the Cr(VI) reduction were observed for certain inorganic oxyanions (ClO_4^-, NO_3^-, SeO_4^{2-}), likely caused by their redox reaction with zero-valent iron.

Résumé

Le lavage de sols est un processus de traitement qui a été employé intensivement pour l'extraction des produits toxiques, néanmoins le processus ne détoxique pas les polluants mobilisés. Les procédés plus communs de désintoxication incluent les réactions rédox qui sont négociées par les métaux nullivalents (MNVs). La réduction de Cr(VI) au Cr(III) est souhaitable, car la dernière espèce est moins toxique pour la plupart des êtres vivants, et a également une basse mobilité et disponibilité biologique. Les objectifs principaux de ce projet ont inclus le développement d'une méthode efficace pour l'extraction et la détoxication des anions inorganiques toxiques utilisant MNVs dès sols contaminés.

Une série de micro-MNVs (Al, Cu, Fe, Mg, Ni, Si, et Zn); de combinaison métalliques (Pd/Fe, Ag/Fe, Cu/Fe, Zn/Fe, Co/Fe, Mg/Fe, Ni/Fe, Al/Fe, Si/Fe, Pd/Cu, Pd/Zn, Pd/Cu/Fe, Pd/Zn/Fe, et Zn/Cu/Fe); de nano-particules (NPs) de Cu et Fe ; ainsi que des NPs bimétalliques (Pd/Fe, Cu/Fe et Pd/Cu) ont été évalués sur la réactivité vers la réduction de Cr(VI) dans une préparation d'agent tensioactif (Tween® 20) sous différentes conditions de réaction. Aux pHs près de la neutralité, on a observé une inactivation rapide de la surface pour presque tous les métaux examinés tandis que la réduction totale de Cr(VI) a été réalisée au pH acide seulement en employant le Cu, le Fe, le magnésium, ou le Zn. Au regard à la réactivité du fer nullivalente, les préparations bimétalliques testées (Pd/Fe > Pd/Zn> Ag/Fe > Ni/Fe> Zn/Fe > Pd/Cu > Cu/Fe) ont sensiblement augmentés la constante de vélocité de pseudo-première taux. La préparation métallique Zn/Cu/Fe, représente un mélange métallique rentable fournissant des paramètres cinétiques comparables ou améliorés par comparaison aux mélanges bimétalliques plus chers qui possèdent du palladium. Les résultats suggèrent, que la cémentation d'un métal noble serve non seulement d'accélérateur de réaction, mais en même temps, offre protection de la surface du MNV empêchant son inactivation très rapide. On a observé une augmentation considérable de la réactivité (jusqu'à 100 fois) en utilisant de NPs. La formation de clusters des structures polymériques a fourni une protection supplémentaire de la surface de NPs qui a provoqué une augmentation saisissante de leur réactivité, notamment à des conditions plus alcalines. L'influence de la présence de diverses molécules inorganiques et organiques, qui sont naturellement dans l'environnement, a été évaluée sur la désintoxication du Cr (VI). Une appréciable augmentation (jusqu'à 50

fois) de la vitesse de la réaction a été aperçue pour certaines molécules organiques capables de réduire le Cr(VI) (α-hydroxyle carboxylique, acide ascorbique, cystéine) et pour certains agents chélateurs (dérivé d'EDTA, siderophores). On a observé des améliorations modérées de la réduction de Cr (VI) pour certains oxyanions inorganiques ($ClO_4^-, NO_3^-, SeO_4^{2-}$) probablement causé par leur réaction rédox avec du fer nullivalent.

Contribution of co-authors

This research has been entirely supervised by Dr. William Marshall. Dr. Marshall was responsible for defining the problem and provided direct advisory input as the work progresses. The author of this thesis was responsible for the design of experiments, experimental work, and manuscripts preparation. The present work has been supported financially by the Natural Science and Engineering Research Council of Canada (NSERC).

Dr. Marshall is the co-author for the manuscripts that have been published, and co-author for the manuscript that have been submitted for publication or the manuscript under preparation.

Parts of these works have been published or submitted

M. Rivero-Huguet, W.D. Marshall. Uncertainties when using dual-wavelength or single-wavelength spectrophotometry to monitor the course of hexavalent chromium reduction mediated by zero-valent iron. **Accred. Qual. Assur. 13 (2008) 711-716**.

M. Rivero-Huguet, W.D. Marshall. Reduction of hexavalent chromium mediated by micro- and nano-scale zero valent metallic particles. ***J. Environ. Monit*. 11 (2009) 1072-1079.**

M. Rivero-Huguet, W.D. Marshall. Reduction of hexavalent chromium mediated by micro- and nano-sized mixed metallic particles. **J. Hazard. Mater. 169 (2009) 1081-1087.**

M. Rivero-Huguet, W.D. Marshall. Influence of various organic molecules on the reduction of hexavalent chromium mediated by zero-valent iron. **Chemosphere 76 (2009) 1240-1248.**

M. Rivero-Huguet, W.D. Marshall. Impact of various inorganic oxyanions on the removal rate of hexavalent chromium mediated by zero-valent iron. **Environ. Chem. 2009. *Submitted***.

Acknowledgements

First and foremost, I need to acknowledge the love, support and understanding of my love, Olivier. Without his constant and consistent support, patience, endless encouragement, finishing this degree would not have been possible. You and Chloé have changed my life, your love and encouragement mean the world to me. Merci mon cœur, sans ton amour et ton appui soutenu, finir ce diplôme n'aurait pas été envisageable.

I owe a special thank you to my mother and brothers for their generous love, moral support, encouragement, and inspiration throughout my studies.

I would like to thank my supervisor, Dr. William D. Marshall, for affording me the opportunity to work in his research group. His invaluable scientific guidance, logistic support, all-time availability, financial aid, support, as well as emotional encouragement and friendly conversations throughout my graduate studies have allowed me to take the most of my experience here.

I would like to express my sincere thanks Dr. Shiv Prasher, Dr. A. Ismail, and Dr. F.R. van de Voort for providing me lab facilities and technical help. The technical guidance and training of Dr. Kebba Sabally, Dr. Diego Gonzalez, and Dr. Pedro Alvarez are gratefully appreciated.

Appreciations are extended to Dr. V.A. Yaylayan for sharing his time and insight, scientific guidance, suggestions, valuable advice, and friendly conversations.

A very special thanks to my friends: Raquel, Carlos, Elena, Julio, Paty Co, Andrea, Gabriel, Paty Baklaya, Piero, Marcelo Z., Raul, Sergio, Heber, Francisco, Nadia, Sylvie&Nicolas, Françoise&Armande, Bernard&Frédéric, Marie-Hélène for your encouragement, unconditional friendship and patience; I could not have done it without you.

I would like to acknowledge my fellow graduate students at McGill University (both past and present) for all their help, advice, and above all lots of laughs.

The financial support of the Natural Science and Engineering Research Council (NSERC) of Canada and McGill University are gratefully acknowledged.

I would like to express my gratitude to my supervisors, colleagues, and friends at the International Development Research Centre (IDRC) for their support, scientific discussions, and encouragement during the last step of my studies.

Table of Contents

Abstract *i*
Résumé *ii*
Contribution of co-authors *iv*
Acknowledgements *v*
List of Tables *xi*
List of Figures *xiv*

One *Introduction* *1*

1.1 Rationale 1
1.2 Problem Assessment 3
1.3 Project Objectives 6
1.4 Scope of the Study 7
1.5 Organization of the Thesis 8

Two *Literature Review* *10*

2.1 General background of oxyanions compounds 10
2.2 Oxyanions of Chromium 14
  2.2.1 Physical and chemical properties 14
  2.2.2 Uses 15
  2.2.3 Sources for humans 16
  2.2.4 Toxicological effects 17
2.3 Oxyanions of Arsenic 19
  2.3.1 Physical and chemical properties 19
  2.3.2 Uses 22
  2.3.3 Sources for humans 24
  2.3.4 Toxicological effects 26
2.4 Oxyanions of Selenium 29
  2.4.1 Physical and chemical properties 29

2.4.2 Uses 31
2.4.3 Sources for humans 32
2.4.4 Toxicological effects 33
2.5 Remediation technologies for metal oxyanion-contaminated soils 36
2.5.1 Solidification/stabilisation technologies - Vitrification 37
2.5.2 Pyrometallurgical separation 39
2.5.3 Chemical treatment 39
2.5.4 Electrokinetics 40
2.5.5 Biological treatment 42
2.5.5.1 Bioleaching 42
2.5.5.2 Biochemical processes 42
2.5.6 Phytoremediation 44
2.5.7 Soil flushing/washing 45
2.5.7.1 Use of surfactants preparations in soil remediation 46
2.5.7.2 Decomposition of pollutants using Ionizing radiation 47
2.5.7.3 Removal of oxyanions using ultrafiltration 48
2.5.7.4 Tansformation of pollutants using micro-Zero-Valent Metals 48
2.5.7.5 Tansformation of pollutants using nano-sized metallic particles 51

Three *Preface* *53*
Reduction of hexavalent chromium mediated by micron- and nano-scale zero-valent metallic particles *54*

3.1 Introduction 54
3.2 Experimental 55
3.2.1 Reagents and materials 55
3.2.2 Acid pre-treatment of zero valent iron 56
3.2.3 Determination of hexavalent Chromium adapted to a microscale 56
3.2.4 Determination of Ferrous ion in the extract of surfactant solution 57
3.2.5 Metal determination by Atomic Spectroscopy 57
3.2.6 Preparation of nanometer sized metal particles (Cu and Fe) 57
3.2.7 Estimation of Uncertainties associated with concentration 58
3.3 Results and Discussion 58
3.3.1 Reduction of Cr(VI) using zero-valent metals (Al, Cu, Fe, Mg, Ni, Si or Zn) 58

3.3.2 Reaction Probes 64
3.3.3 Reduction of Cr(VI) using nano-sized metal particles 67
3.3.4 Comparisons of nano- *vs*. micron-scale ZV metals 71
3.4 Conclusions 73

Four *Preface* *74*
Reduction of hexavalent chromium mediated by micro- and nano-sized mixed metallic particles *75*

4.1 Introduction 75
4.2 Experimental 77
4.2.1 Reagents and materials 77
4.2.2 Acid pre-treatment of zero valent iron 77
4.2.3 Preparation of bi and trimetallic mixtures 78
4.2.4 Determination of hexavalent Chromium adapted to a microscale 78
4.2.5 Determination of Ferrous ion in surfactant extract 78
4.2.6 Metal determination by Atomic Spectroscopy 78
4.2.7 Preparation of nanometer sized bi-metallic particles (Cu and Fe) 79
4.2.8 Estimation of Uncertainties associated with concentration 80
4.3 Results and discussion 80
4.3.1 Reduction of Cr(VI) using micron-scale metallic mixtures 80
4.3.2 Reduction of Cr(VI) using nano-sized bimetallic particles 87
4.4 Conclusions 91

Five *Preface* *93*
Influence of various organic molecules on the reduction of hexavalent chromium mediated by zero-valent iron *94*

5.1 Introduction 94
5.2 Materials and methods 96
5.3 Results and discussion 98
5.3.1 Reduction of Cr(VI) in the presence of organic acids (with one to three carboxylic groups) 98
5.3.2 Reduction of Cr(VI) in the presence of polyamine carboxylates 104

5.3.3 Reduction of Cr(VI) in the presence of diverse organic structures 107
5.4 Conclusions 112

Six *Preface* *113*
Impact of various inorganic oxyanions on the removal rate of hexavalent chromium mediated by zero-valent iron *114*

6.1 Introduction 114
6.2 Material and methods 116
6.3 Results and discussion 117
6.4 Conclusions 126

Seven *Preface* *127*
Uncertainties when using dual-wavelength or single-wavelength spectrophotometry to monitor the course of hexavalent chromium reduction by zero-valent iron *128*

7.1 Introduction 128
7.2 The standard procedure 131
7.3 Identification of the uncertainties sources and their quantification 131
7.3.1 Uncertainty related to mass concentration, $u(\gamma_0)$ 134
7.3.2 Uncertainty related to mass, $u(M)$ 135
7.3.3 Uncertainty related to recovery, $u(R)$ 136
7.3.4 Uncertainty related to density, $u(d)$ 137
7.4 Calculation of combined and expanded uncertainty 138
7.5 Conclusions 141

Eight *Preface* *142*
Summary, conclusions, and recommendations for future research *143*

8.1 Summary 143
8.2 Conclusions 146
8.3 Recommendations for Future Research 147

Appendix 1 *149*
Appendix 2 *154*
Appendix 3 *156*
References *160*

List of Tables

Table 1.1 Inorganic contaminants and their sources **4**

Table 1.2 Canadian soil quality guidelines (total µg g^{-1}) **6**

Table 2.1 Most common oxyanions found in the environment **11**

Table 2.2 Selected properties of metal and non metal oxyanions analogues **13**

Table 2.3 Naturally occurring inorganic and organic arsenic species **20**

Table 2.4 Most important selenium species in environmental and biological systems **29**

Table 2.5 A summary of remediation technologies **37**

Table 3.1 Predicted surface area-normalized rate constant (k_{SA}), correlation coefficient and intersection time for the time dependant disappearance of Cr(VI) from unbuffered solution at various initial pHs (pH_i) in the presence of various micron-size ZVMs. **61**

Table 3.2 Variations in the observed pseudo-first order rate constant (*k*) following various pre-treatments of the micron sized Fe^0 surface prior to reactions at pH 2 or 5 for Cr(VI) and Fe concentration of 24.5 mg L^{-1} and 7.0 g L^{-1} respectively. **66**

Table 3.3 Pseudo-first order rate constant (*k*), surface-area normalized rate constant (k_{SA}), calculated half-life ($t_{1/2}$), surface area normalized half- life ($t_{SA\ 1/2}$), and correlation coefficient (r^2) for the pseudo-first order model of the time dependant disappearance of Cr(VI) from unbuffered solution at various initial pHs (pHi) in the presence of nano-size particles. **68**

Table 3.4 A comparison of calculated specific area normalized rate constants observed for micron-scale *vs*. nano-scale (either bound or unbound) zero-valent metal (Fe or Cu) at pH 2 or 6. **72**

Table 4.1 Predicted surface area-normalized rate constant (k_{SA}), and calculated surface-area normalized half-life ($t_{SA1/2}$) for the time dependant disappearance of Cr(VI) from unbuffered solution at various initial pHs (pH_i). **81**

Table 4.2 Predicted surface area-normalized rate constant (k_{SA}), and calculated surface-area normalized half-life ($t_{SA1/2}$) for the time dependant disappearance of Cr(VI) from unbuffered solution at various initial pHs (pH_i) for selected trimetallic mixtures. **88**

Table 4.3 Coefficient of correlation (r^2), pseudo-first order rate constant (k), surface area normalized rate constant (k_{SA}), half-life ($t_{1/2}$), surface area normalized half-life ($t_{1/2\ SA}$) and pH for Cr(VI) reduction with nano-size metallic particles in unbuffered solution. **89**

Table 5.1 Predicted surface area-normalized rate constant(s) (k_{SA}) in the presence of Fe(0) and test reagent for the time dependant disappearance of Cr(VI) from unbuffered solution at various initial pHs (pH_i). Only data of organic acids (up to three carboxylic acids groups) that increased the reduction rate of Cr(VI) more than 2-fold are included. **99**

Table 5.2 Predicted surface area-normalized rate constant (k_{SA}), and calculated surface-area normalized half-life ($t_{SA1/2}$) for the time dependant disappearance of Cr(VI) from unbuffered solution at various initial pHs (pH_i) when reacted in the presence of various ethlyendiamine tetracetic acid derivates. **105**

Table 5.3 Predicted surface area-normalized rate constant (k_{SA}), and calculated surface-area normalized half-life ($t_{SA1/2}$) for the time dependant disappearance of Cr(VI) from unbuffered solution at various initial pHs (pH_i) for selected organic molecules. **108**

Table 6.1 Predicted surface area-normalized rate constant(s) (k_{SA}) in the presence of Fe(0) and test reagent for the time dependant disappearance of Cr(VI) from unbuffered solution at various initial pHs (pH_i). **119**

Table A1.1 Kaolin-type soil properties **149**

Table A1.2 Mean concentration (± 1SD[a]) of the initial hexavlent chromium burden, mean recovery percent by the extracting surfactant (± 1SD[a]) and mean concentration of the final hexavalent chromium burden (± 1SD[a]). **151**

Table A1.3 Surface area normalized rate constant (k_{SA} ± 1SD[a]), coefficient of correlation (r^2) with the pseudo-first order model and parameters related to the one-way analysis of variance (ANOVA). **153**

Table A2.1 Cost comparison of soil washing with detoxification and precipitation using ZVI (Chapter Three), 2% Pd/Fe (Chapter Four), and ZVI with a 500 μM citric acid solution (Chapter Five). **155**

List of Figures

Figure 2.1 Redox potential (V) versus pH diagram for Chromium **15**

Figure 2.2 Schematic diagram of toxicity and mutagenicity of Cr(VI) **18**

Figure 2.3 The Eh-pH diagram for As at 25ºC and 1atm. Solid species are enclosed in parentheses **22**

Figure 2.4 Proposed metabolic pathway for inorganic arsenic. Arsenate (iAsV); arsenite (iAsIII); dimethylarsinous acid (DMAIII); dimethylarsinic acid (DMAV); dimethylthioarsinous acid (DMTAIII); dimethylthioarsinic acid (DMTAV); monomethylarsonous acid (MMAIII); monomethylarsonic acid (MMAV); arsenotriglutathione (iAsIII(GS)$_3$); (MMAIII(GS)$_2$) monomethylarsenodiglutathione and (DMAIII(GS) dimethylarsenodiglutathione) **27**

Figure 2.5 The Eh-pH diagram for Se at 25ºC and 1atm. **31**

Figure 2.6 Proposed metabolism pathways for important seleno-compounds. **35**

Figure 2.7 Microwave set-up for remediation purposes **38**

Figure 2.8 Electrokinetic process for soil remediation. **41**

Figure 2.9 A schematic diagram of the main features of the Cr(VI) reduction by ZVI. **50**

Figure 3.1 Plots of the variation with time of the ln of the mean Cr(VI) concentration (mg L^{-1}) when reacted at (A) pH 2.0± 0.1 or (B) 6.0± 0.1 with various micron-scale zero-valent metals. (■) Fe, (□) Cu, (●) Zn, (○) Mg, (▲) Ni, (△) Si and (⊞) Al. Uncertainty in the determination of selected Cr(VI) concentrations was omitted to facilitate the plot visualization. The vertical dotted line in pane B represents the *I*. time between the two exponential decay models. **62**

Figure 3.2 Variations, with time, in the soluble concentrations of total Cr, (■); Cr (VI), (□); total Fe, (●); or Fe^{+2}, (○).for reaction with initial conditions of pH 2.0±0.1 and [Cr(VI)] of 22.1 mg L^{-1} in the presence of Fe^0 granules (7.2 g L^{-1}). **65**

Figure 3.3 Plots of the variation with time of the mean Cr(VI) concentration (mg L^{-1}) when reacted at **(A)** pH 2.0± 0.1 or **(B)** 6.0± 0.1 with various nano-scale ZVM formulations. (■) Fe^0; (●) Fe^0/Al$_2$O$_3$; (o) Fe^0/soluble starch; (□) Fe0/CMC; (⊖) Cu^0; (∆) Cu^0/Al$_2$O$_3$; (▲) Cu^0/soluble starch; (▼) Cu^0/CMC. **69**

Figure 4.1 Plots of the variation, with time, of ln(C/C$_o$) or (C/C$_o$) where C is the concentration of Cr(VI) at time t and C$_o$ is the initial concentration (mg L^{-1}) when reacted (A) and (C) at pH 2.0± 0.1 or (B) and (D) at 6.0± 0.1 with various metallic mixtures at a ZVM to Cr(VI) ratio (~300)**:** Fe, (■)**;** 2% Pd/Fe, (□)**;** 2% Ag/Fe, (●); 2% Cu/Fe, (○);2% Zn/Fe, (▲);2% Co/Fe, (∆);2% Mg/Fe, (◊);5% Al/Fe, (▽);2% Ni/Fe, (♦);2% Si/Fe, (◁)**;** 2% Pd/Zn, (▼)**;** Pd/Cu/Fe, (◑)**;** Pd/Zn/Fe, (⊞); and Zn/Cu/Fe. , (⬖). In 1D, the *l*.time, 30 min for Fe, or 120 min for Pd/Cu/Fe and Pd/Zn/Fe has been identified with a dotted line or with a dashed line respectively. **83**

Figure 4.2 Variations, at pH 2.0± 0.1, in the mean surface area normalized pseudo-first order rate constant (k_{SA}, mL min^{-1} m^{-2}) for Fe^0 (■) or selected bimetallic mixtures (□) 0.2% Pd/Fe, (●) 1% Pd/Fe, (○) 2% Pd/Fe and (∆) 2% Ag/Fe as a function of the ratio of zero-valent iron to the concentration of Cr(VI). **86**

Figure 4.3 Plots of the variation with time of the mean Cr(VI) concentration (mg L^{-1}) when reacted at **(A)** pH 2.0± 0.1 or **(B)** 6.0± 0.1 with different nano-scale metallic formulations. (□) Fe; (●) Pd/Fe; (■) Cu/Fe; (○) Cu; (▲) Pd/Cu. **90**

Figure 5.1 Selected plots of the variation with time of the ln of the ratio of the mean Cr(VI) concentration at time t to the initial concentration (μM) when reacted (A) at pH 2.0± 0.1 or (B) at 6.0± 0.2 with ZVI at a Fe(0) to Cr(VI) ratio (~300): Fe, (■); citric acid, (□); glycolic acid, (●); L-cysteine, (○); picolinic acid, (▲); lactic acid, (∆); malic acid, (◑); pyruvic acid, (▽); and tartaric acid, (⊞), *l*.time (60 min) for glycolic, lactic, picolinic and pyruvic acids (dotted line). Uncertainties in the determinations of certain Cr(VI) concentrations were omitted to facilitate the plot visualization. **101**

Figure 5.2 Possible oxidation products for selected organic compounds. pK_a values are derived from Smith et al., 1993. **102**

Figure 5.3 Selected plots of the variation, with time, of the ln of the ratio of the mean Cr(VI) concentration at time t to the initial concentration (μM) when reacted (A) at pH 2.0± 0.1 or (B) at 6.0± 0.2 with ZVI at a Fe(0) to Cr(VI) ratio (~300): Fe, (■); EDTA, (□); EDDS, (●); DPTA, (▲); and HEDTA , (○), *l*.time (30 min) for Fe(0) alone (dotted line), *l*.time (60 min) for EDDS and HEDTA reaction systems (dashed line). Uncertainties in the determination of certain Cr(VI) concentrations were omitted to facilitate plot visualization. **106**

Figure 5.4 Selected plots of the variation with time of the ln of the ratio of the mean Cr(VI) concentration at time t to the initial concentration (μM) when reacted (A) at pH 2.0± 0.1 or (B) at 6.0± 0.2 with ZVI at a Fe(0) to Cr(VI) ratio (~300): Fe, (■); acac, (□); DFO, (●); tu, (Δ); ascorbic acid, (◑); and phen, (○),*l*.time (30 min) for Fe(0) alone (dotted line), *l*.time (60 min) for DFO and phen reaction systems (dashed line). Uncertainties in some the determinations of certain Cr(VI) concentrations were omitted to facilitate the plot visualization. **109**

Figure 6.1 Selected plots of the variation with time of the ln of the ratio of the mean Cr(VI) concentration at time t to the initial concentration (*μ*M) when reacted (A) at pH 2.0 ± 0.2 or (C) at pH 6.0 ± 0.2 with ZVI at a Fe(0) to Cr(VI) ratio (~300): Fe, (■); arsenate, (□); perchlorate, (●); molybdate, (○); nitrate, (▲); sulfate, (Δ); phosphate, (◑); and selenate, (⊞), *l*.time (30 min) for ZVI (dotted line C). Plot (B) is an expansion of the intersection of the 2 models when reacting Cr(VI) in the presence of phosphate and ZVI (some points of the Fe plot were removed to improve visualization). Some uncertainties in the determinations of certain Cr(VI) concentrations were omitted to facilitate the plot visualization. **120**

Figure 6.2 Variation with time of the C/Co the ratio of the mean Cr(VI), NO_3^-, and NH_4^+ concentration at time t to the initial concentration (μM) when reacted at pH 2.0 ± 0.1 with ZVI at a Fe(0) to Cr(VI) ratio (~300): Fe, (■); chromate and nitrite, (□); chromate and nitrate, (●); concentration of NH_4^+, (○); disappearance of nitrate, (▲). 122

Figure 6.3 Variation with time of the C/Co the ratio of the mean Cr(VI), MnO_4^-, and total Mn at time t to the initial concentration (μM) when reacted at pH 2.0 ± 0.2 with ZVI at a Fe(0) to Cr(VI) ratio (~300): Fe, (■);chromate and permanganate, (○); total Mn, (●); disappearance of MnO_4^-, (□); background variation of UV-VIS spectra of MnO_4^- at time t. 125

Figure 7.1 A summary of events to monitor the time dependant decline of γ(Cr) mediated by zero-valent iron. 132

Figure 7.2 An Ishikawa diagram (cause-and-effect) for the spectrophotometric determination of the mass concentration of hexavalent chromium, γ(Cr). 133

Figure 7.3 Plots of the variation with time of the mass concentration of hexavalent chromium, γ(Cr) in mg L^{-1}, together with their expanded uncertainty $U(\gamma(\text{Cr}))$, monitored by single-wavelength spectrophotometry (SWS) (■) or dual-wavelength spectrophotometry (DWS) (□). For clarity, the abscissa and ordinate for the (□) plot have been displaced by 2 min and 1 mg L^{-1} respectively. 139

Figure 7.4 Representation of the uncertainty contributions to the combined standard uncertainty, $u_c(\gamma(\text{Cr}))$, using single-wavelength (SWS) or dual-wavelength spectrophotometry (DWS) for the determination of Cr(VI) mass concentration (mg L^{-1}). γ_o; mass concentration extrapolated from the linear regression, d; density, M_o; sample mass and M_f is the final mass of the solution. 140

Chapter

One

Introduction

Let us not…flatter ourselves overmuch on account
of our human conquest over nature.
For each such conquest takes its revenge on us.

Frederick Engels, 1876

1.1 Rationale

Human activities have a large and important impact on the environment and pollution is frequently regarded as the bi-product of modern technological development. Older than civilization, pollution has been a problem since the appearance of our ancestors. The adulteration of water, soil, and air by physical and chemical waste products of human activity has accompanied our species since it first walked upon the earth. From prehistoric times, pollution has been linked inextricably to health and medicine. Actually, environmental pollution caused by heavy metals began with the domestication/exploitation of fire more than one-half million years ago. With the development of mining and metal-working techniques in ancient times, the close link between metals, metal pollution, and human history was created [1].

During the time of the Greek and Roman civilizations (2000-2500 years ago) mining and trade of mineral resources became a key feature of their economies. Metal recovery techniques have been considered to be indicators of technological improvement and economic power. During this era, large quantities of heavy metals, especially Pb (80,000 to 100,000 metric tons/year), Cu (15,000 metric tons/year), Zn (10,000 metric tons/year) and Hg (> 2 metric tons/year), as well as Sn and Zn contributed to the high standard of living. Although the mines were operated on a small scale, uncontrolled smelting of huge amounts of ores in open fires resulted in substantial emissions of trace metals into the atmosphere. The release of toxic metals to the environment was extremely serious even at that time and the interdiction of mining operations occurred in certain ancient cities in Italy [2]. Although some mines were re-opened in the beginning of the 11th century A.D., it was the improvement of large furnaces that significantly extended the industrial installations during the 16th century.

The arrival of the Industrial Revolution in the 18th century brought unprecedented demands for metals and an exponential increase in the problem of metal waste disposal. This, coupled with the focusing of populations within industrialised cities, resulted in an increased burden on the local environment.

During subsequent centuries, this disposal was amplified, making the cumulative industrial discharges of toxic metals massive indeed. The continued exploitation of mineral resources, on a massive scale, has generated enormous quantities of wastes that must be disposed in an economical but safe manner.

The realization that contaminated sites can pose serious hazards became widely recognised in the late 1970s when pollution disasters like the Love Canal in the United States and Lekkerkerk in the Netherlands received widespread coverage in the media [3]. The fact that toxic wastes were discovered in residential neighbourhoods focussed people’s attention on the grave risks to human health and to environmental integrity within a region that such sites posed.

It was only in the latter part of the 20th century that an increased awareness of human impacts on global environmental systems at the local, regional, and global scale became widely recognized. This has resulted in efforts to improve the degraded quality of natural systems (aquatic and soil environments), with an increase in the remediation-restoration of land in urban environments together with a more sensitive stewardship of these resources.

Once contaminants have been introduced into the environment, subsequent clean-up can be extremely difficult, time consuming, and costly. Due to the existence of many contaminated sites, appreciable research and development efforts have been directed to the improvement of efficient procedures for remediating these sites. These methods must be both economically viable and environmentally benign. The presence of inorganic pollutants (metals, metalloids, and inorganic radionuclides) in soil and groundwater at contaminated sites presents special challenges to environmental managers because options for remediation remain very limited.

Because these metal contaminants cannot be degraded (converted to other elements), detoxification alternatives are limited either to changing oxidation state or to fixing the toxic metal to some inert surface so that it becomes unavailable to contacting organisms.

Inorganic pollutants, which are present as anions (AsO_3^{3-}, AsO_4^{3-}, CrO_4^{2-}, MoO_4^{2-}, SeO_3^{2-}, SeO_4^{2-}, $^{99}TcO_4^-$, ClO_4^-, PO_4^{3-}, NO_3^-, VO_4^{3-}) at contaminated sites, are a particular problem as most soil particles have an excess of negative surface charge at near neutral pHs. The highly oxygenated nature impart appreciable water solubility to these ions and electrostatic repulsion limits sorption processes to soil particles. In turn, this results in an increased mobility for oxygenated anionic contaminants within a soil environment, which exacerbates the problems associated with their presence in both saturated and unsaturated subsurface environments [4].

The development of a decontamination regime that is efficient and economically viable remains the ultimate aim of remediation/restoration practitioners. A unique chemical that can be used for all applications and situations is sought. To achieve this aim certain criteria that must be kept in mind when developing such a reagent/procedure. It is necessary for processing to achieve complete destruction of the contaminant as quickly as possible. Logistical considerations further emphasise the need for a highly reactive decontaminant. A conflicting requirement is for the decontaminant to be non-destructive to non-target species (organisms or surfaces/substrates such as paints and rubbers). This leads to the difficult situation of developing a procedure that detoxifies to all contaminants selectively but reacts with nothing else. Also, the reagent should have not adversely affect the response of sensitive equipment, including monitors and detectors. The ease of application is also a desirable feature for logistical reasons.

The use of zero-valent metal particles for decontamination of common soil and water contaminants has been the subject of several studies. These zero-valent metal particles show promise in fulfilling the above requirements.

1.2 Problem Assessment

Elements present in natural materials (soils or sediments) at concentrations less than 1000 μg g^{-1} have been defined as trace elements [5]. Numerous trace metals have been identified as essential micronutrients (including chromium, cobalt, copper, iron, selenium and zinc) and as electron acceptors or donors in metabolic processes (iron). At elevated concentrations, however, all of these metals exhibit appreciable toxicities. As such, they can represent pollutants in sediment, soil, and groundwater and constitute one of the most pressing issues in modern environmental science. Arsenic contamination of drinking water, cadmium, chromium, lead, and zinc pollution in soils, the dispersal/transport of radionuclides over long time scales, and the cycling of mercury are a few examples. Contamination results from increased mobilisation from mine tailings, the disposal of concentrated metal wastes within incompletely isolated landfills, the fugitive escape of leaded gasoline and leaded paints, land application of fertilizer and pesticides, animal manures, biosolids, composts, coal combustion residues and atmospheric deposition.

Most of the inorganic contaminants listed in Table 1.1 bind strongly to the surfaces of soil and sediment particles depending on the solution conditions, with pH and ionic composition being the primary determining factors.

Because metal and radionuclide contaminations are generally non-degradable except by radioactive decay, conventional remediation technologies involve some form of immobilisation or containment.

Table 1.1 Inorganic contaminants and their sources [5]

Chemical classes	Contaminants	Sources or applications
Metals	Cr, Cu, Ni, Pb, Hg, Cd, Zn, As, Se	Mining, Pb-gasoline, batteries, paints, fungicides, pesticides
Organometallics	Trialkyltin, methylmercury	Paints, chemical manufacturing
Radionuclides	$^{238\text{-}240}$Pu, ^{235,238}U, ^{99}Tc, ^{60}Co, ^{90}Sr	Nuclear reactors, weaponry, medicine, food irradiation

The environmental impact of metallic contaminants in soils and sediments is dependent both on the chemical speciation of the metal and the response of the matrix to biological and physicochemical conditions. These factors are responsible for the mobilization of the metal from the solid into the aquatic phase and hence transport within the immediate vicinity, affecting the rate of dispersal, dilution, uptake, and transfer into living systems. As a result of their multifaceted biological functions, the significance of metals in the environment will depend on environmental factors that control their mobility and bioavailability [6].

Currently, environmental guidelines were established to help sustain the quality of the environment and to protect living organisms from the adverse effects of metallic contaminants. A mandatory ban on Pb-based paint was enacted in the late 1970s, and incentive programs to limit the use of lead in plumbing were implements in the 1980s and restrictive utilisation of leaded gasoline occurred in 1986 [7].

Nowadays, urban centres and agricultural areas are facing the serious problem of the accumulation of heavy metals in the soil where they have accumulated from the 19th century up until the late 1970s. Many of these contaminated sites now stand abandoned and are referred to as Brownfields. These sites pose a threat to humans who work or live near them (since As, Cr, Cd, Hg, Pb are considered to be cumulative poisons) and to plants because elevated amounts of micronutrients (such as Co, Cu, Mn, Zn) can be phytotoxic.

It is in this context that most industrialised nations have promulgated regulations that set maximum acceptable concentrations of toxic substances in the air, water, soil and sediments. In the 1990s the Canadian Council of Ministers of the Environment (CCME) published the “Protocol for the Derivation of Environmental and Human Health Soil Quality Guidelines” and the “Recommended Canadian Soil Quality Guidelines”, which contained soil quality guidelines for 20 substances (both inorganic, organic) within four types of land uses (agricultural, residential/parkland, commercial, and industrial) [8]. Table 1.2 provides an overview of the recommended Canadian soil quality guidelines regarding toxic metal contents.

An interesting storage concept, called Secure landfill, was set by the government of Québec in 2001 (and subsequently updated in 2006) and implemented to limit the disposal of highly contaminated soils imported from outside of the providence. Metal-contaminated soils with levels in excess of the D-level criteria (e.g. total levels of Cd<100, total Cr< 4000, Hg<50, Pb <5000 $\mu g\ g^{-1}$) cannot be excavated and sent to a secure landfill site, unless it has been treated chemically to remove 90% of the contaminants and stabilized against trace metal leaching (Règlement sur l’enfouissement de sol contaminés) [9].

The regulated values are intended to protect not only human receptors but also other organisms that may be exposed to contaminants through a range of exposure pathways associated with four broad land use categories.

Table 1.2 Recommended Canadian soil quality guidelines (total µg g^{-1}) [8]

Substance	Land Use			
	Agricultural	Residential/ Parkland	Commercial	Industrial
Arsenic (inorganic)	12	12	12	12
Cadmium	1.4	10	22	22
Chromium				
Total chromium	64	64	87	87
Hexavalent Chromium (VI)	0.4	0.4	1.4	1.4
Copper	63	63	91	91
Lead	70	140	260	600
Mercury (Inorganic)	6.6	6.6	24	50
Nickel	50	50	50	50
Selenium	1.0	1.0	3.0	3.9
Vanadium	130	130	130	130
Zinc	200	200	360	360

1.3 Project Objectives

In terms of remediation techniques and procedures, the appropriate methods accomplish three goals: the more efficient and rapid isolation of contaminants, their transformation into less hazardous products and last but not least decreased processing. The overall research objectives are to develop an efficient zero valent metal mediated treatment for the removal/inactivation of toxic inorganic anions from contaminated soil. In addition to the detoxification of the contaminants, the potential reuse of the pollutants was to be investigated. Specifically, the objectives of this research project were as follows:

I. To establish the mobilization efficiencies of several surfactants frequently used in remediation techniques regarding the extraction of inorganic anions,
II. To determine the transformation rates of hexavalent chromium with selected zero valent metals (ZVMs) and to identify conditions that optimize the reactions rates of the most promising candidate,

III. To prepare and evaluate metallic mixtures in order to improve the transformation rate of metallic contaminants,

IV. To synthesize nano-scale particles of ZVMs, bimetallic nano mixtures, and to evaluate their efficiency at mediating the conversion of toxic anions to less hazardous products,

V. To evaluate the influence of various organic materials (that can be normal constituents of virgin soils) on the detoxification of toxic anions from contaminates soils,

VI. To evaluate the influence of various inorganic anions that are normally present in contaminated soils on the detoxification toxic anions in this medium, and

VII. To measure and then estimate the uncertainties of the measurements in accordance with recommendations given by the Bureau International des Poids et Mesures.

1.4 Scope of the Study

This study project was to be carried out on a soil that was heavily-contaminated with hexavalent chromium. The soil was selected as the model soil as it represented a low permeability soil. The efficiency of mobilisation of metal oxyanion(s) was to be assessed in the presence of various commercial surfactants (three anionic, two cationic and six non-ionic formulations in the absence /presence of ion pairing reagent). Once the most efficient and least reactive mobilisation agent had been identified, kinetic studies were conducted with a variety of zero-valent metal (Al^0, Fe^0, Cu^0, Mg^0, Ni^0, $Pt^0/\gamma\text{-}Al_2O_3$, $Pd^0/\gamma\text{-}Al_2O_3$, Si^0 and Zn^0), or zero valent bimetallic mixtures (Ag^0/Fe^0, Al^0/Fe^0, Co^0/Fe^0, Cu^0/Fe^0, Mg^0/Fe^0, Ni^0/Fe^0, Pd^0/Fe^0, Pd^0/Cu^0, Pd^0/Zn^0, Si^0/Fe^0, and Zn^0/Fe^0) or trimetallic mixtures ($Pd^0/Cu^0/Fe^0$, $Pd^0/Zn^0/Fe^0$, and $Zn^0/Cu^0/Fe^0$).

The interactions of certain inorganic anions (arsenite, arsenate, borate, molybdate, nitrate, nitrite, phosphate, perchlorate, periodate, permanganate, selenate, selenite, silicates sulfate) with selected naturally-occurring organic compounds that included a variety of polyols (glycerol, polygalacturonic acid, soluble starch), aliphatic organic acids (ascorbic acid, citraconic acid, citric acid, oxalic acid, acetic acid, formic acid, succinic acid, lactic acid, tartaric acid, glycolic acid, malonic acid, phytic acid, pyruvic acid, malic acid), and aromatic acids (p-hydroxybenzoic acid, phtalic acid, picolinic acid, 2,6-pyridine dicarboxylic acid, salicylic acid) or compounds bearing carboxylic and/or amino groups (humic acid, glutamic acid, L-histidine, cysteine, urea, thiourea, glutathione). Additionally, a variety of chelating reagents (that include cyclodextrin, deferoxamine {DFO}, ethylenediamine tetraacetic acid {EDTA}, diethylenetriamine pentaacetic acid {DTPA}, ethylenediamine tetrapropionic acid {EDTPA}, [S,S]-ethylenediamine disuccinic acid {EDDS}, ethylenebis(oxyethylenenitrilo) tetraacetic acid {EOTA}, methylglicine diacetic acid {MGDA}, 1,6-diaminohexane N,N,N',N'-tetraacetic acid {DHTA}, 1,3-diamino-2-hydroxypropane-N,N,N',N'-tetraacetic acid {DPTA}, 1,2-diaminopropane- N,N,N',N'-tetraacetic acid {MEDTA}, N-(2-Hydroxyethyl)ethylenediamine-N,N′,N′-triacetic acid (HEDTA), 1,10-phenanthroline {phen} or acetylacetone {acac}) were to be evaluated.

The synthesis and purification of different zero valent nanoparticles and zero valent bimetallic nanoparticles was also to be investigated as well as the influence of various support materials as well as their performance during the detoxification of inorganic oxyanions.

1.5 Organization of Thesis

This thesis is organized into eight chapters and include the introduction and conclusions sections. The introductory chapter describes the problem and lists the overall objectives. Chapter 2 reviews the previous research conducted on inorganic oxyanions-contaminated sites and the available remediation technologies. This literature review supports the overall research objective. The subsequent chapters evaluate and discuss the efficiency and reactivity of various ZVMs, metallic mixtures, and nano-sized metallic particles towards the transformation of hexavalent chromium in a surfactant extract, as well as the influence of various inorganic and organic compounds that are often found in contaminated sites. Chapter 3 describes the evaluation of the reactivity of a variety of ZVMs and Cu and Fe nano-sized particles towards the reduction of hexavalent chromium in a surfactant extract. Mechanistic considerations were also investigated in the reaction between zero-valent iron and Cr(VI). Chapter 4 evaluates the reducting activity of selected micron-scale metallic particles and some nano-sized bimetallic analogs with Cr(VI) in a surfactant preparation under a variety of reaction conditions. Chapter 5 investigates the reducting activity of a variety of naturally-occurring organic molecules (containing α-hydroxyl carbonyl, α-hydroxyl carboxylate, α-carbonyl carboxylate, phenolate, carboxylates and/or thiol groups, siderophore, ascorbic acid); chelating agents (ethylenediaminetetraacetic acid derivates, acetyacetone) and others towards a surfactant preparation containing Cr(VI) and Fe(0) under a variety of reaction conditions. Chapter 6 examines the influence of several inorganic oxyanions, usually found in contaminated sites, on the reduction of Cr(VI) mediated by Fe(0) under a variety of reaction conditions. Chapter 7 identifies, measures, and estimates the major sources of uncertainty in the measurements of the dissapearence of Cr(VI) mediated by Fe(0) following the recommendations given by the Bureau International des Poids et Mesures and the EURACHEM/CITAC guide. Chapter 8 provides an overall conclusion to the project and suggests some future research. The final chapter of this thesis provides a list of the cited references to the technical literature provided in chronological order.

Chapter

Two

Literature Review

> *"All substances are poisons; there is none which is not a poison. The right dose differentiates a poison from a remedy..".*
>
> *Paracelsus, (1493-1541)*

This chapter provides a brief overview of transition metal and metal oxyanions in order to better understand the nature of contamination in the environment and particularly in water, soil, and sediments. Several remediation techniques concerning heavy metal and oxyanions and a more detailed discussion is focused on the decontamination of sites using mobilizing agents (chelating agents, surfactants) and/or zero valent metal. The potential of nano-sized particles for the detoxification and removal of inorganic oxyanions from soils is also examined in greater detail.

2.1 General background of oxyanions compounds

The earth's crust contains about 50% by weight of oxygen. Most inorganic chemistry is concerned with its compounds, if only in the sense that so much chemistry involves the most important oxygenated compound – water. The oxygen atom forms compounds with all the elements except helium, neon, and possibly argon, and it combines directly with all the other elements except the halogens, a few noble metals, and the noble gases, either at room or at elevated temperatures.

The chemistry of oxo compounds has been studied extensively over history. It is governed by the formation of at least one double bond (M=O) with another atom, either a non-metal or a metalloid or a transition metal (M). For most of the inorganic species, the opportunity for π interactions between M and the oxygen atom arises leading to increased stability [10].

In order to limit the length of this review, the coverage has been limited arbitrarily to compounds which contain discrete molecular units of the type $[MO_x]^{n-}$ with $n \neq 0$. This will exclude a large number of oxo-compounds, *i.e.* almost all uncharged metal oxocompounds, most isopoly- and hetero-poly-species and ternary oxides that contain polymeric units. A list of the common oxo anions that are known to be present in the environment is provided in Table 2.1.

Most of the oxo compounds share common properties, which facilitates their characterisation and identification. As an example, the bond distances corresponding to a double bond lies between the range of 1.59–1.66 Å, the spatial configuration corresponds to a tetrahedral structure while the M=O infrared stretching frequencies typically absorb in the 800 to 1000 cm^{-1} region for transition metal species [10, 11].

Table 2.1 Most common oxyanions found in the environment

Transition metal			Metalloid		Non-metal		
CrO_4^{2-}	$Cr_2O_7^{2-}$	MnO_4^-	AsO_3^{3-}	SeO_3^{2-}	CO_3^{2-}	PO_4^{3-}	ClO_4^-
MoO_4^{2-}	$Mo_2O_7^{2-}$	TcO_4^-	AsO_4^{3-}	SeO_4^{2-}	NO_3^-	SO_4^{2-}	IO_3^-
WO_4^{2-}		ReO_4^-	GeO_4^{4-}	TeO_4^{2-}	SiO_4^{4-}		IO_6^{5-}
VO_4^{3-}				TeO_6^{6-}			

A periodic tendency exists for the transition metal's tendency to form a metal-oxygen double bond. Increasing atomic number stabilises higher oxidation states {Cr(VI), Mn(VII), Os(VIII)} resulting in tetrahedral species like (CrO_4^{2-}, MnO_4^-, and OsO_4). All these metal ions share a d^0 electronic configuration and they behave as hard acids. The fact that they have no electrons to lose makes them poor reducing agents and an enhancement of the oxidizing properties is observed when the number of electrons is increased. Whereas the vanadate specie, VO_4^{3-}, is a mild oxidizing agent, CrO_4^{2-} and MnO_4^- are potent oxidizing agents especially in acidic solution.

In general, the coordination numbers of the elements of the second and third transition series tend to be greater than for the first series because of the ionic radii are larger (by about 0.15-0.20 Å) for corresponding species. Thus tetrahedral coordination is considerably less frequent although present in species such as MoO_4^-, TcO_4^-, ReO_4^-, and OsO_4. The filling up of the 4f orbitals results in chemistries of transition metals of the second and third row that are much more similar to each other than the corresponding transition metal from the first row. It can be explained because the filling of the fourteen 4f orbitals (comprising the fourteen lanthanide elements) occurs between filling the ten 4d orbitals (comprising the ten transition metals of the second row) and the 5d orbitals (comprising the ten transition metals of the third row). These fourteen 4f electrons do not effectively shield their associated positively charged species and thus the 5d electrons experience a relatively large effective nuclear charge and consequently are drawn closer to the nucleus. This effect is known as lanthanide contraction. Taking as an example the three elements of the Group VII of the periodic table (Mn, Tc, and Re), they form stable compounds in solution like, MnO_4^-, TcO_4^- and ReO_4^-, with rather different redox properties (the pertechnate and perrhenate ions are much weaker oxidants than the permanganate ion). On the basis of the above facts, it can be anticipated that the analogs, Tc and Re compounds, will have similar physical properties (such as size, shape, dipole moment and formal charge). As a result, under the same conditions (e.g. groundwater, soil, sediments) they are reasonably indistinguishable and can be handled in a similar manner [12,13].

On the other hand, there are certain transition metals in their higher oxidation states that have similarities with their non-metal homologs, for instance V(V), As(V) and P(V) in, VO_4^{3-}, AsO_4^{3-} and PO_4^{3-} respectively, Cr(VI) and S(VI) in CrO_4^{2-} and SO_4^{2-}, Mn(VII) and Cl(VII) in MnO_4^- and ClO_4^-. The correlation may be extended to polyanions, such as dichromate, $Cr_2O_7^{2-}$, however, the differences in behaviour between the metal anions and the non-metal anions are often more important than their similarities. Whereas polyphosphoric acids and polysulfuric acids form only under rather stringent dehydrating conditions, polymerization of certain metal anions occur spontaneously upon acidification. For example, the chromate ion is stable only at high pH, and as the pH is lowered, protonation and dimerization occur:

$$CrO_4^{2-} + H^+ \longrightarrow (OH)CrO_3^-$$
$$(OH)CrO_3^- + H^+ \longrightarrow (OH)_2CrO_2$$
$$2(OH)_2CrO_2 \longrightarrow Cr_2O_7^{2-} + 2H^+ + 2H_2O$$

Table 2.2 Selected properties of metal and non metal oxyanions analogues [14, 15]

	V(V)	P(V)	As(V)	Cr(VI)	S(VI)	Mn(VII)	Cl(VII)
Z^a	23	15	33	24	16	25	17
E.C.^{b}	$[Ar]3d^04s^0$	$[Ne]3s^03p^0$	$[Ar]3d^{10}4s^04p^4$	$[Ar]3d^04s^0$	$[Ne]3s^03p^0$	$[Ar]3d^04s^0$	$[Ne]3s^03p^0$
Oxyanion	VO_4^{3-}	PO_4^{3-}	AsO_4^{3-}	CrO_4^{2-}	SO_4^{2-}	MnO_4^-	ClO_4^-
V^c (Å^3)	55.9	56.5	63.9	57.9	51.0	57.9	57.9
r(X-O)^d ($Å$)	1.59	1.52	1.67	1.66	1.49	1.60	1.44
Geometry	tetrahedral	tetrahedral	tetrahedral	tetrahedral	tetrahedral	Tetrahedral	tetrahedral
	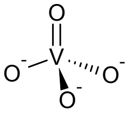	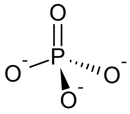	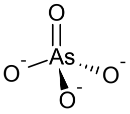	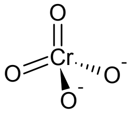	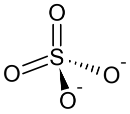	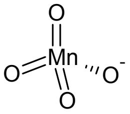	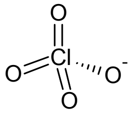
Crystal structure	orthorombic	orthorombic	orthorombic	orthorombic	orthorombic	Orthorhombic	Orthorhombic

[a] Z = Atomic Number, [b] E.C. = Electronic Configuration, [c] V = Ionic Volume, [d] r = bond length

The commercial importance of oxyanions is extensive; applications are found in nuclear medicine ($^{99m}TcO_4^-$, $^{186}ReO_4^-$ and $^{188}ReO_4^-$), pesticide and fungicide formulations (e.g. $PbAsO_4$, $CuSO_4$, etc.) and fertilizers (NH_4PO_4). Certain oxyanions are found naturally in soils as minerals (e.g., anglesite $PbSO_4$, crocoite $PbCrO_4$, ortophosphates) which makes almost impossible to establish further tendencies and subsequent discussion will be provided for each oxyanion separately. Because each oxyanion has a different impact on the environment, selected examples will be examined in more detail in the next sections.

2.2 Oxyanions of Chromium

2.2.1 Physical and Chemical Properties

In 1798, the French scientist Louis Nicholas Vaquelin discovered the element chromium in the mineral crocoite ($PbCrO_4$) [16]. Chromium is the sixth most abundant element in the earth's crust. Chromite ore is the major source of chromium, and even the highest grade of ore ($FeOCr_2O_3$) contains slightly more than 50% chromic oxide. Production of chromium involves the reduction of chromite ore with aluminium, carbon, or silicon followed by purification. The roasting of chromite ore with soda ash produces sodium chromate and dichromate. The latter two compounds are the starting mixtures for most other chromium compounds [16, 17].

In contrast to Cr(III), hexavalent chromium is not readily adsorbed to surfaces and, since most of its salts are soluble, much of the Cr(VI) released to aerobic environments is present as soluble ionic species including hydrochromate ($HCrO_4^-$), chromate (CrO_4^{2-}), and/or dichromate ($Cr_2O_7^{2-}$) which are mobile and biologically available in ecosystems.

Chromate is the second most stable chromium compound; it is a strong oxidizing agent and it reacts rapidly with numerous reducing agents found commonly in the environment (including ferrous ion, organic matter, sulphide compounds as well as through microbial processes). The effectiveness of these reducing agents varies with pH and redox conditions and an increase of the reduction of hexavalent chromium to trivalent species is observed while decreasing pH [18]. Though possible, the redox potential of the Cr(VI)/Cr(III) is so high, E^0= +1.33 V. There are few oxidants present in natural ecosystems capable of oxidizing Cr(III) to Cr(VI). The most likely of these oxidants include dissolved oxygen and manganese oxides. Recent studies have indicated that labile forms of Cr(III) can be oxidized photochemically to Cr(VI) in aerobic surface waters. A more detailed diagram of the variations in oxidising properties and stability with pH is provided in Figure 2.1.

Although hexavalent chromium compounds traverse cell membranes and are reduced to trivalent compounds intracellularly, there is no evidence that biological systems can convert trivalent compounds to Cr(VI) compounds [18].

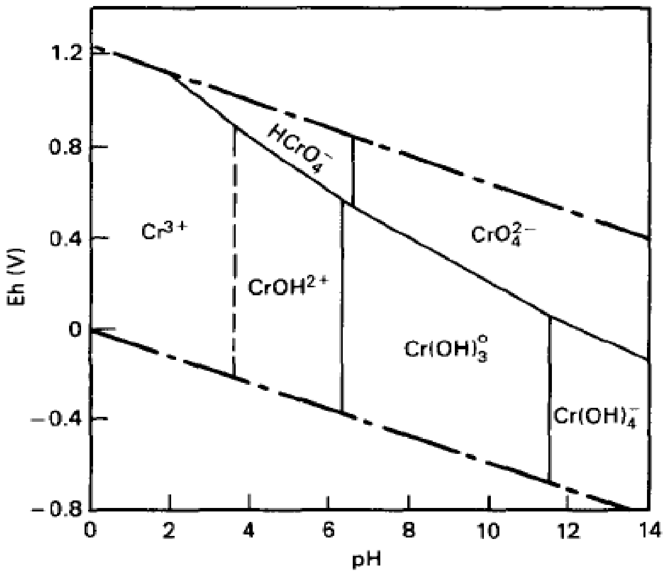

Figure 2.1 Redox potential (V) versus pH diagram for Chromium [18]

2.2.2 Uses

Chromate occurs only rarely in nature in the mineral crocoite ($PbCrO_4$); therefore, most environmental sources of chromate result from man-made production. The primary uses of chromium compounds are chemical (e.g. pigment production), metallurgical (resistant alloys as stainless steel) and refractory industries [19]. Chromate compounds have been used on a large scale as a rust inhibitor in cooling towers, in fertilizer and other heavy industries all over the planet owing to their excellent corrosion inhibiting and biocide properties. Consequently, effluents discharged from such industries can contain large quantities of hexavalent chromium [20, 21].

The waterborne wood preservative CCA (chromated copper arsenate) has been used extensively to treat wood since its development by Dr. Sonti Kamesan in 1933 [16-18]. The roles of Cu and As in the CCA formulation are to inhibit fungi and insects, respectively, while Cr plays a key role in the fixation process, which binds the formulation constituents to wood. Common uses of CCA-treated wood include decks, fences, boardwalks, playground equipment, picnic tables, raised garden beds, and retaining walls [16].

The major detriment of CCA-treated wood on the environment is considered to be the possible diffusion of arsenate and chromate into adjacent soil and leaching into ground water. However, the USEPA [22] recently announced a voluntary decision by industry to phase out consumer use of CCA-treated wood products by 31 December 2003. Thus in the year 2004 the USEPA no longer permitted the registration of CCA containing products for residential use. However, wood treated with CCA before this date can still be used in residential areas, and existing structures containing CCA-treated wood are not affected by this action.

2.2.3 Sources for humans

Most chromium released into the environment results from human activities at stationary point sources. Combustion and the processing of ore discharge primarily trivalent chromium into the environment as chromium oxide; however, small amounts of hexavalent chromium do appear in fly-ash of coal-fired power plants and from chromate manufacturing sites. The highest exposure to hexavalent chromium occurs during chromate production, ferrochrome and chrome pigment production, chrome plating, and stainless steel welding.

The USEPA has estimated that 64% of the total atmospheric chromium results from the emission of hexavalent chromium from fossil fuel combustion and steel production [16]. It was estimated that about 84 tonnes/year of chromium (including both tri- and hexa- valent forms) are released by industries into the Canadian atmosphere from anthropogenic sources each year. Of the 84 tonnes, approximately 51% is attributable to fossil fuel combustion and a further 29% to various industrial processes (iron and steel production, and refractory and chemical processing) [8].

Chromium levels vary widely in soil depending on the composition of the parent rock. Most of the hexavalent chromium contamination in the soils is the result of deposition of commercial products and therefore elevated concentrations are often found in landfills. Although somewhat controversial, CCA-treated wood is considered to diffuse high concentration of Cr to the adjacent soil and to the ground water by leaching and weathering of treated lumber exposed to acidic rainfall. In soil, trivalent chromium is not very mobile because most of it exists as the insoluble oxide ($Cr_2O_3 \cdot nH_2O$) but the very soluble hexavalent are rather mobile in the soil. Organic matter and other reducing agents, when present in soils, eventually promote the reduction of the hexavalent form to the insoluble chromic oxide.

From the Canadian context, it is considered that wastes containing more than 5,000 tonnes of chromium (in various forms) are dumped annually onto land throughout the country, mostly coming from Canadian metal-finishing sludges (1,600 tonnes), nonferrous base smelters and refineries (2,100 tonnes), solid wastes from Canadian households (up to 1,200 tonnes). Due to its toxicity and carcinogenicity, total chromium and in particular the hexavalent chromium content in soil are strictly regulated. The government of Canada has imposed a maximum amount of total Cr that ranges from 64 to 87 $\mu g\ g^{-1}$, depending the category of the soil, and 0.4 to 1.4 for hexavalent chromium depending the use of the soil [8].

The amount of chromium in aquatic systems is also regulated. The USEPA has established a maximum allowable level in drinking water of 50 $\mu g\ L^{-1}$ [23]. The major sources of contamination of Cr in water systems are domestic wastewater effluents, metal and chemical manufacturing, processing of nonferrous metals, and atmospheric fallout (a minor contributor).

2.2.4 Toxicological effects

At ultra- trace levels, chromium is an essential element for living organisms. Trivalent chromium is considered to play an essential role in the metabolism of glucose in mammals (it is a key component of the glucose tolerance factor) and in the metabolism of insulin [16, 19, 24-26].

In general, hexavalent chromium species penetrate biological membranes much more readily than trivalent species. Based on a review of available literature, estimates of the proportion of trivalent chromium that is absorbed from the gastrointestinal tract range up to about 3%, whereas up to about 10% of ingested hexavalent chromium is estimated to be absorbed; organic complexes are even more readily absorbed. Much of ingested hexavalent chromium is reduced to trivalent chromium before absorption. Absorption of inhaled chromium is believed to be greater, with estimated proportions of up to 12% and 30% for Cr(III) and Cr(VI) compounds respectively [16].

Absorption is also dependent on the physical/chemical properties of the specific compound. After absorption, chromium binds to glycoproteins in plasma and becomes widely distributed throughout the body, including the foetus, via the bloodstream. It is eliminated from the body largely in the urine, while most of the unabsorbed portion is excreted in the faeces [25, 26].

In contrast to trivalent chromium, the chromate structure resembles sulphate and phosphate oxyanions, which are used extensively in humans for many diverse biochemical processes. The individual cells of the body need to take up these oxyanions and have active systems that transport/incorporate these nutrients. Because chromate resembles phosphate and sulphate structurally, it can be taken up accidentally on the active phosphate pathway. After crossing cellular membranes and under normal physiological conditions, hexavalent chromium reacts spontaneously with intracellular reductants (e.g., ascorbate and glutathione) to generate short-lived intermediates Cr(V) and/or Cr(IV) oxygen free radicals and the end-product trivalent chromium. Cr(V) undergoes a one-electron redox cycle to regenerate Cr(VI) and transferring a reactive oxygen specie (ROS) that easily combines with DNA-protein complexes. The production of oxidative DNA damage may be the underlying basis for the genotoxicity of hexavalent chromium compounds. On the other hand, Cr(IV) can bind to cellular materials and interfere with their normal physiological functions [24-27]. These numerous processes are summarised in Figure 2.2.

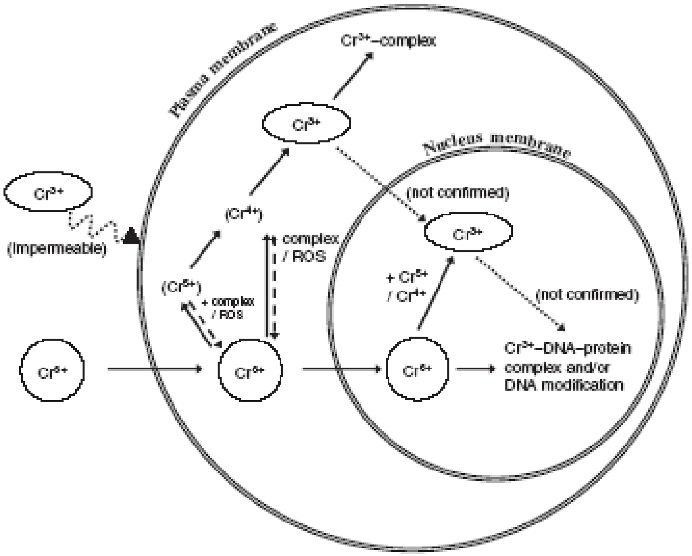

Figure 2.2 Schematic diagram of toxicity and mutagenicity of Cr(VI) [26]

In humans, several traumata are associated with Cr(VI) exposure. The carcinogenicity of hexavalent chromium compounds was first recognised in the late 19th century when nasal tumours were described in Scottish chrome pigment workers exposed to concentrations greater than 20 μg m^{-3}. The appearance of ulcerations and subsequent perforations of the nasal septum is considered to be one of the markers of toxic effects resulting from exposure to hexavalent chromium compounds. In fact, hexavalent chromium compounds are considered to be both skin and pulmonary sensitizers. Among other symptoms of the Cr(VI) contact are conjunctivitis, lacrimation, nose and throat irritation, skin irritation, eardrum perforation, rhinitis and epistaxis [24-26].

Case reports that date back to the 1930s focused attention on the incidence of lung cancer in chromate workers. Lung cancer in German chromate workers was accepted as a work-related disease in 1936. Since then, the carcinogenicity of hexavalent chromium has been investigated in a wide range of occupationally exposed populations [16]. In the chrome plating, chromate production, and chromate pigment industries, exposure to Cr(VI) compounds has been demonstrated consistently to be associated with increased mortality due to cancer of the respiratory system [19].

Currently, the International Agency for Research on Cancer (IARC) and the US Toxicology Program recognise hexavalent chromium as a known human carcinogen [27]. Based on positive responses in assays for genotoxicity, chromate is the most potent genotoxic chromium compound and today is ranked as one of the 17 chemicals posing the greatest threat to humans [17]. For this reason the Occupational Safety and Health Administration (OSHA) regulates exposure to Cr(VI) and forces employers and employees to extreme health precautions while handling and/or producing hexavalent chromium compounds [28].

2.3 Oxyanions of Arsenic

2.3.1 Physical and Chemical Properties

Arsenic is a metalloid and is the twentieth most abundant element in the earth's crust. It can exist in four valence states; –3, 0, +3, and +5. In strongly reducing environments, elemental arsenic As(0) and arsine (AsH_3) can exist. The most common oxidation states of As in soils are three and five and the oxidized forms of these elements exit in soils and solutions as the oxyanions arsenate, (AsO_4^{3-}) and arsenite, (AsO_3^{3-}). Under moderately reducing conditions, arsenite may be the dominant form whereas arsenate is generally the stable oxidation state in oxygenated environments [29-32]. Arsenic occurs as a major constituent in more than 200 minerals [30]. As the chemistry of arsenic follows closely that of sulphur, the greatest concentrations of the element tend to occur in sulphide minerals, of which the most abundant arsenic-containing minerals include arsenopyrite (FeAsS), realgar

(AsS), orpiment (As_2S_3), niccolite (NiAs), and cobaltite (CoAsS). The greatest concentrations of these minerals therefore occur in mineralize areas and are commonly found in close association with the transition metals as well as Cd, Pb, Ag, Au, Sb, P, W and Mo [31].

Arsenic and its compounds occur in crystalline, powder, amorphous or vitreous forms. They usually occur in trace quantities in all rock, soil, water and air. However, concentrations may be higher in certain areas as a result of weathering and anthropogenic activities including metal mining and smelting, fossil fuel combustion and pesticide use [29-30].

There are many arsenic compounds of environmental importance and a brief list is of the most common naturally occurring arsenic-containing compounds can be seen in Table 2.3.

Table 2.3 Naturally occurring inorganic and organic arsenic species (adapted from [29, 31])

Name	Abbreviation	Structure
Arsenite	As(III)	AsO_3^{3-}
Arsenate	As(V)	AsO_4^{3-}
Monomethylarsonous acid	MMA(III)	$CH_3As(OH)_2$
Monomethylarsonic acid	MMA(V)	$CH_3AsO(OH)_2$
Dimethylarsinous acid	DMA(III)	$(CH_3)_2AsOH$
Dimethylarsenic acid	DMA(V)	$(CH_3)_2AsO(OH)$
Dimethylarsenoylethanol	DMAE	$(CH_3)_2AsOCH_2CH_2OH$
Trimethylarsine oxide	TMAO	$(CH_3)_3AsO$
Tetramethylarsonium ion	Me_4As^+	$(CH3)_4As^+$
Arsenobetaine	AsB	$(CH_3)_3As^+CH_2COO^-$
Arsenobetaine	AsB-2	$(CH_3)_3As^+CH_2CH_2COO^-$
Arsenocholine	AsC	$(CH_3)_3As^+CH_2CH_2OH$
Trimethylarsine	TMA(III)	$(CH_3)_3As$
Arsines	AsH_3, $MeAsH_2$, Me_2AsH	$(CH_3)_xAsH_{3-x}$ (x = 0-3)
Ethylmethlarsines	Et_xAsMe_{3-x}	$(CH_3CH_2)_xAs(CH_3)_{3-x}$ (x = 0-3)

Phenylarsonic acid	PAA	$C_6H_5AsO(OH)_2$
p-arsanilic acid	*p*-ASA	$NH_2C_6H_4AsO(OH)_2$
4-nitrophenylarsonic acid	4-NPAA	$NO_2AsO(OH)_2$
p-ureidophenylarsonic acid	*p*-UPAA	$NH_2CONHC_6H_4AsO(OH)_2$
Arsinoylribosides	Arsenosugars X-XV	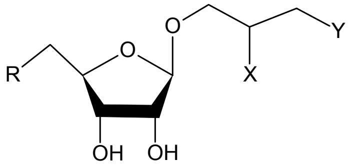

	R	X	Y
X	$(CH_3)_2As(O)$-	-OH	-OH
XI	$(CH_3)_2As(O)$-	-OH	$-PO_3HCH_2CH(OH)CH_2OH$
XII	$(CH_3)_2As(O)$-	-OH	$-SO_3H$
XIII	$(CH_3)_2As(O)$-	-OH	$-OSO_3H$
XIV	$(CH_3)_2As(O)$-	$-NH_2$	$-SO_3H$
XV	$(CH_3)_3As^+$	-OH	$-OSO_3H$

Speciation determines how arsenic compounds interact with their environment. For example, the behaviours of arsenate and arsenite in environmental matrices differ considerably. Movement in environmental matrices is a strong function of speciation and soil type. In a non-absorbing sandy loam, arsenite is 5–8 times more mobile than arsenate [33]. Soil pH also influences arsenic mobility. At a pH of 5.8 arsenate is slightly more mobile than arsenite, but when pH changes from acidic to neutral to basic, arsenite increasingly tends to become the more mobile species, though mobility of both arsenite and arsenate increases with increasing pH [33]. In strongly adsorbing soils, transport rate and speciation are influenced by organic carbon content and microbial population. Both arsenite and arsenate are transported at a slower rate in strongly adsorbing soils than in sandy soils.

Under oxidizing and aerated conditions, the predominant form of arsenic in water and soil is arsenate. Under reducing and waterlogged conditions (< 200 mV), arsenites are anticipated to be the predominant arsenic compounds. The rate of conversion is dependent on the redox potential (Eh) and pH of the soil as well as on other physical, chemical and biological factors. In brief, at moderate or high Eh, arsenic can be stabilized as a series of pentavalent oxyanions, H_3AsO_4, $H_2AsO_4^-$, $HAsO_4^{2-}$, and AsO_4^{3-}. However, under most reducing (acid and mildly alkaline) conditions, arsenite predominates. The Pourbaix diagram is presented in Figure 2.3.

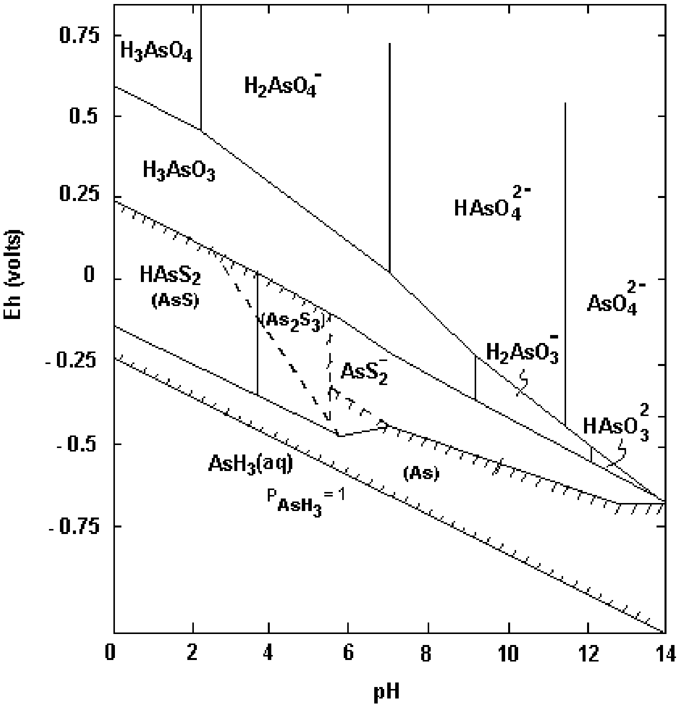

Figure 2.3 The Eh-pH diagram for As at 25ºC and 1atm. Solid species are enclosed in parentheses (adapted from [30]).

When As_2O_3 is deposited directly into aerobic surface waters, it hydrolyses to form As(III) species, mainly H_3AsO_3. Arsenite is thermodynamically unstable, and therefore tends to oxidize to dissolved As(V) species, principally arsenates species as $H_2AsO_4^-$ and $HAsO_4^{2-}$. This oxidation is relatively slow, but can be accelerated by chemical oxidizing agents such as manganese and iron oxyhydroxides or by the action of certain bacteria [29].

2.3.2 Uses

Arsenic is probably the most famous and notorious poison of all time. The poison of kings and the king of poisons [1]. It is well known that during the 15th and 16th centuries, the Italian family of Borgias used arsenic as their favorite poison for political assassinations [1]. Some historians support the suggestion that even Napoleon has been killed by arsenic-tainted wine served to him while in exile [1].

On the other hand, it was reported early in history that arsenic compounds were used to treat several health disorders. It fact, the father of medicine, Hippocrates, used arsenic to treat ulcers, in the early 1900s the scientist Paul Ehrlich designed some organic arsenicals (Salvarsan) as treatment for syphilis and in the late 1800s Sir William Osler stated that arsenic was the best treatment of acute promyelocytic leukemia [2].

Arsenical compounds have been used in agriculture as insecticides and herbicides for more than 100 years. Inorganic arsenic compounds historically were used as pesticides. Lead arsenate ($PbHAsO_4$) was widely used as a pesticide in orchards for the control of the codling moth from the beginning of the 20th century up to the early 1950s [34-36]. In United States, its use was discontinued following the introduction of DDT (Dichloro- Diphenyl- Trichloroethane) in 1948 and the organophosphorus insecticides in the early 1950s [34]. In Canada, the use of inorganic arsenical pesticides in fruit and vegetable production was stopped in 1975 [28]. Today, because the toxicity of most organoarsenicals is less than that of inorganic arsenic species, some organoarsenicals (mono- and disodium methylarsonate and dimethylarsinic acid) are used to control weeds in cotton fields and as defoliation agents prior to cotton harvesting [36].

Arsenic is an active component of antifungal wood preservatives (CCA, which contains 25% sodium arsenite). It is estimated that in the United States, 74% of arsenic is contained in products used for wood preservation [30]. Since 1975, it is estimated that more than 300,000 metric tons of inorganic arsenic has been used in CCA-treated wood in the United States [32]. As previously mentioned the major effect of CCA-treated wood on the environment is the potential leaching of arsenate and chromate into adjacent soil and since the year 2004 the USEPA will not allow CCA products for residential use [22].

Arsenic compounds are also used in the pharmaceutical and glass industries, and in the formulation of sheep-dips, leather preservatives and poisonous baits. Arsenicals are employed in the manufacture of pigments while metallic arsenic is utilised in the production of alloys. Gallium arsenide (GaAs) and indium arsenide (InAs) are used in the fabrication of certain semiconductor devices, such as field-effect transistors and microwave integrated circuits, and in optoelectronics. Arsanilic acid and its derivatives 4-aminophenylarsonic and 3-nitro-4-hydroxyphenylarsonic acids are, in some countries, added to cattle and poultry feed at a concentration of 25–45 mg Kg^{-1} for use as growth-stimulating agents [37].

As a consequence of the many different uses of arsenic and arsenicals, there is a wide spectrum of situations in which humans can be exposed to this element.

2.3.3 Sources for humans

The sources of exposure to inorganic arsenic are both natural and anthropogenic. The latter include soils which can contain residues from arsenic purification/transformation. As examples, the soil can contain As-pesticide residues or the air surrounding non-ferrous smelters can contain As-compounds [30]. Natural sources include water, food, soil and air [30]. The release of arsenic from natural processes can be caused by the reduction of iron hydroxides and the oxidation of pyrite minerals including orpiment (As_2S_3) and realgar (As_2S_2). The possible mobilization of As in soils, and subsequent leaching into ground or surface water and subsequent entry into the human food chain, should always be considered as a serious hazard. In the case of arsenic ingestion, the main exposure sources are drinking water and diet [38]. Naturally occurring arsenic in drinking water supplies may affect more than 100 million people worldwide, including countries such as Bangladesh, India, China, Chile, Argentina, Mexico, Hungry, Taiwan, Vietnam, Japan, New Zealand, Germany and the United States. At present, twelve countries in Asia have reported high As levels in part of their groundwater resources. Bangladesh has the highest percentage of contaminated shallow tube wells (STWs) and an estimated 30 million people are dependant of those wells for domestic purposes [39-43].

Exposure to arsenic in drinking water occurs for the most part through the oral route, although dermal exposure may occur from bathing in arsenic-contaminated water. Since arsenic can be concentrated in liver, kidney, lung and skin tissues by its ingestion in drinking water, chronic exposure to arsenic in drinking water is a concern for regulatory agencies and public health organizations worldwide. This concern is based on the known epidemiological association between the exposure to arsenic-contaminated drinking water and the development of cancer in skin and internal organs. As a result of this association, in 1993 the WHO recommended a provisional guideline value of 10 μg As L^{-1}, and a regulatory decision was made in 2001 by the USEPA to lower the As drinking water standard (maximum contaminant level, MCL) from 50 to 10 μg As L^{-1} [30, 39]. This administrative guideline became enforceable in 2006 and ought to be re-examined every 6 years [38].

Considering that there are many contaminated drinking-water STW sources, a high percentage of contaminated irrigation STWs can also be anticipated. In accordance with FAO investigations, it has been estimated that water extraction from the shallow aquifer for irrigation adds 1 million Kg of As per year to the arable soil in Bangladesh, mainly in the paddy fields [39]. A number of studies from Bangladesh and West Bengal (India) have reported increased concentrations in soils and crops because of irrigation with As-contaminated groundwater. In these areas rice consumption is quite high (approximately 80 kg/year per capita) therefore the arsenic in rice can contribute considerably to arsenic ingestion in affected areas. Similar situations can be anticipated elsewhere in the region where As-contaminated irrigation water is used.

As the exposure to inorganic arsenicals in drinking water is decreased (the result of regulatory actions), dietary arsenic will become a greater component of the overall arsenic exposure.

Agricultural activities in soils contaminated with arsenic has led to crops with elevated levels of arsenic. Well-known is the Bangladesh situation and surrounding areas where irrigation of paddy rice fields with arsenic-contaminated groundwater has a demonstrated impact over the increased levels of As in rice grain. In 2005, Williams et al., reported high levels of As in rice cultivated in the United States due to the usage of arsenic herbicides in traditional cotton growing areas which have subsequently switched to rice production [44]. In 2006 at the heart of Montreal, Canada; certain community gardens (e.g. Baldwin, Laurier) were closed due to high levels of As found in vegetables cultivated in these soils. Technical reports indicate that both gardens were situated on former industrial sites [45, 46].

Estimated daily intakes of inorganic arsenic from environmental media by various age groups (from 0 to 70 years) in the Canadian population indicates that ingestion in food represents the principal route of inorganic arsenic intake for all age groups, followed by dirt and soil in infants and children, and water and air for all age groups. It was suggested that an average total daily intake ranging from < 0.1 to 2.4 μg Kg^{-1} -bw day^{-1} is ingested [29]. Intake of inorganic arsenic may be higher, however, in communities near point sources such as smelters, tailing areas, geological sources and areas with a history or arsenical pesticide application. The total daily intake of inorganic arsenic from these areas has been estimated to ranges from < 0.1 to 35 μg Kg^{-1}-bw day^{-1} [29].

2.3.4 Toxicological effects

Arsenic has been used in the treatment of several health disorders. Paradoxically, it is also carcinogenic. Arsenic is perhaps the only human carcinogen for which there is adequate evidence of carcinogenic risk by both inhalation and ingestion. Inorganic-arsenic compounds are known human carcinogens whereas the toxicities of arsenosugars and arsenobetaine are low or practically negligible to humans [47].

Arsenic is metabolized quite differently in the body depending on the chemical species administrated in foods and water, and also on the animal species even when the same chemical specie is administrated [47]. Natural organo-arsenic compounds, such as arsenobetaine, arsenocholine and arsenosugar, are taken up and absorbed effectively, and then excreted rapidly in their intact form into the urine without appreciable effects on the body, except arsenosugars. On the other hand, arsenite and arsenate are absorbed efficiently by animals. When administrated to animals, inorganic arsenic is metabolized by a series of consecutive reduction and methylation reactions, as presented in Figure 2.4. Arsenate and monomethylarsonic acid reductases in mammalian cells catalyze the reduction of arsenate to arsenite and of MMA(V) to MMA(III). The methylation of arsenite is catalyzed by arsenite methyltransferase with S-adenosylmethionine (SAM) as a methyl group donor. The first methylation step forms MMA(V), and then reduced to MMA(III) and further methylated to yield DMA(V) in the presence of MMA(III) methyltransferase. Similarly, reduction of DMA(V) to DMA(III) is a pathway for the third methylation step forming trimethylarsenic oxide (TMAO) [47-49].

Once absorbed, arsenic is transported by the blood to various organs in the body, mainly in the form of MMA and traces of AsB, DMA(V), ans iAsIII and is finally excreted into the urine mostly in the form of DMA, as can be seen in Figure 2.4.

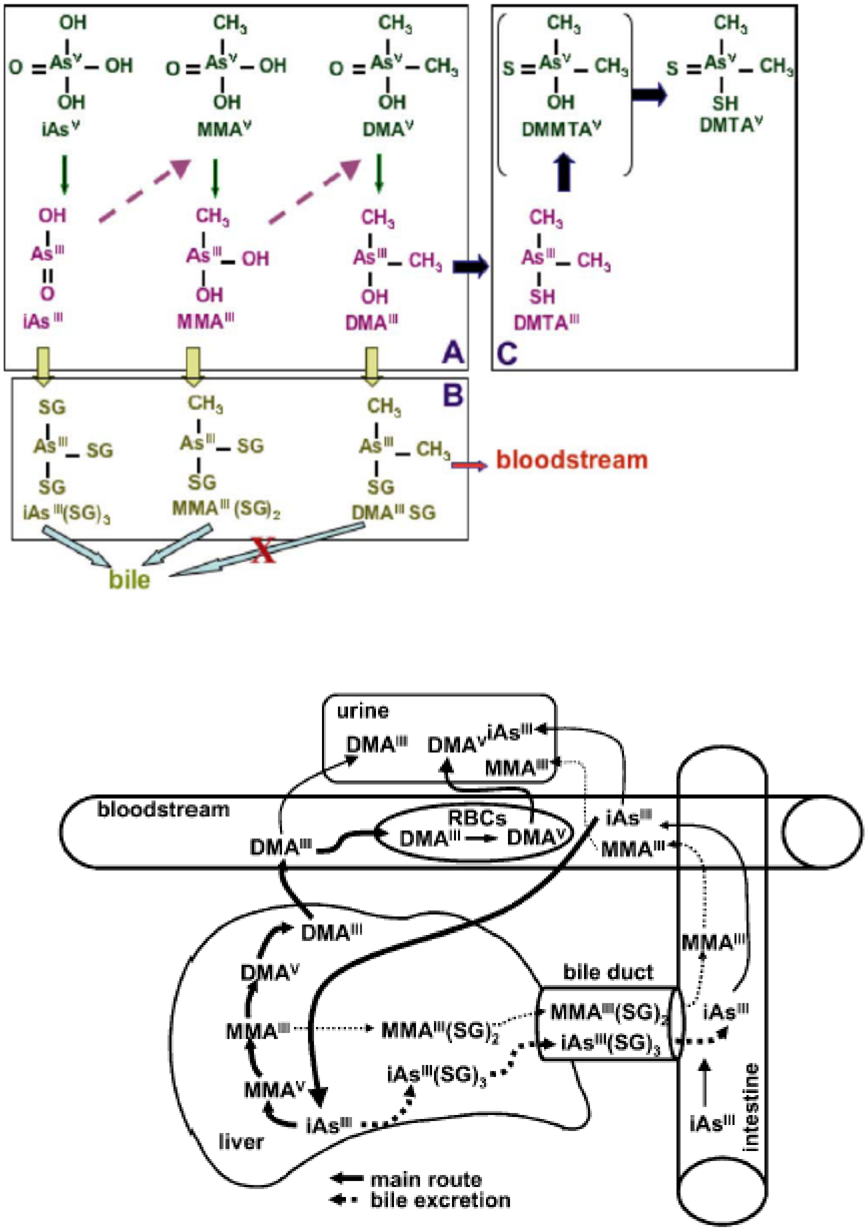

Figure 2.4 Proposed metabolic pathway for inorganic arsenic. Arsenate (iAsV); arsenite (iAsIII); dimethylarsinous acid (DMAIII); dimethylarsinic acid (DMAV); dimethylthioarsinous acid (DMTAIII); dimethylthioarsinic acid (DMTAV); monomethylarsonous acid (MMAIII); monomethylarsonic acid (MMAV); arsenotriglutathione {iAsIII(GS)$_3$}; monomethylarsenodiglutathione {MMAIII(GS)$_2$} and dimethylarsenodiglutathione {DMAIII(GS)}, adapted from [48, 49].

Arsenic exposure can result in carcinogenic and non-carcinogenic responses in humans. Arsenate and arsenite are known to be human carcinogens. The mechanism of reaction of arsenic compounds is quite complicated. It has been suggested that arsenite binds to sulfhydryl groups of dihydrolipoamide inhibiting pyruvate dehydrogenase. Consequently, conversion of pyruvate to acetyl coenzyme A (CoA) is decreased, citric acid cycle activity decreased, and production of cellular ATP is drastically diminished. The binding of arsenite to thiol groups inhibits cellular glucose uptake, gluconeogenesis, fatty acid oxidation, and further production of acetyl CoA, it also blocks the production of glutathione, which prevents cellular oxidative damage.

The effects of arsenate occur in part because of its transformation to arsenite, thus toxicity proceeds as outlined previously. More important is the structural resemblance between arsenate and inorganic phosphate. Arsenate can substitute for phosphate in glycolytic and cellular respiration pathways and as a result, the uncoupling of oxidative phosphorylation occurs. This suggests that in presence of arsenate, adenosine diphosphate (ADP) forms ADP-arsenate instead of forming ATP [29, 32, 37-43, 47-49].

The USEPA designation of arsenic compounds as carcinogens is based on increased lung cancer mortality in multiple human populations exposed primarily through inhalation, increased mortality from multiple internal organ cancers (liver, kidney, lung, and bladder), and increased incidence of human cancer in populations consuming drinking water high in inorganic arsenic to support their designation.

Ingestion of groundwater with elevated As concentrations and the associated human health effects are prevalent in several regions across the world. Arsenic toxicity and chronic arsenicosis is of an alarrming magnitude (particularly in South Asia) is a major environmental health disaster [43]. Carcinogenic effects can only be observed when toxic effects are also observed.

The carcinogenic effects of arsenic are well recognised and it is in this context that the Agency for Toxic Substances and Disease Registry (ATSDR) based in the United States has ranked arsenic as number one on the Comprehensive Environmental Response, Compensation, and Liability Act (CERCLA) Priority List of Hazardous Substances since 1997 [50].

2.4 Oxyanions of Selenium

2.4.1 Physical and Chemical Properties

Selenium is a metalloid that was identified serendipitously by the Swedish chemist Berzelius in 1818 [2]. It occurs naturally in the environment and is generally acknowledged as one of the widely distributed elements on earth, estimated to be the 69th most abundant element in the earth's crust. Most of it, occurs in association with sulphide minerals (such as galena, chalcopyrite, arsenopyrite, pyrite, sphalente, marcasite, and pyrrhotite) or as selenides of copper, silver, lead, mercury and other metals [51-54].

As summarised in Table 2.4, selenium exists naturally in both environmental and biological samples, in a number of oxidation states of both inorganic and organic species.

Table 2.4 Most important selenium species in environmental and biological systems, adapted from [55]

Inorganic species

Elemental Se (Se0), selenide –(Se-II), selenate and selenite

Simple organic species

Methylselenol (MeSeH), dimethylselenide (Me_2Se), dimethyldiselenide (Me_2Se_2), trimethylselenonium cation (Me_3Se^+), dimethylselenoxide (Me_2SeO), methylseleninic acid anion ($MeSe(O)O^-$), dimethylselenosulfide (MeSSeMe), selenocyanato ($SeCN^-$) and selenourea [$Se=C(NH_2)_2$]

Amino acids and low molecular mass species

Selenomethionine, selenocysteine, selenocytine, Se-methylselenocysteine, selenocysteic acid, Se-methylselenomethionine, S-(methylseleno)cysteine, selenomethionine selenoxide hydrate, selenohomocysteine, selenocholine, selenobetaine, selenoglutathione, γ-glutamyl-Se-methylselenocysteine, Se-adenosylselenohomocysteine

Other compounds

Selenopeptides, selenoproteins, selenoenzymes, selenosugars, Se-metal metallothionines

In the -2 oxidation state, selenium can be found as hydrogen selenide (H_2Se), sodium selenide (Na_2Se), di- and tri-methyl selenium, $[(CH_3)_2Se]$ and $[(CH_3)_3Se]$ respectively, and various selenoamino acids such as selenomethionine, selenocysteine, Se-methyl selenocysteine, selenocystatthionine and selenotaurine. Elemental selenium, Se(0), can be found in the dipeptide diglutathione. In the +4 oxidation state, selenium can exist as selenium dioxide (SeO_2), selenious acid (H_2SeO_3) or as sodium selenite (Na_2SeO_3). Finally in its most highly oxidized state (+6), selenium exists as selenic acid (H_2SeO_4) or as sodium selenate (Na_2SeO_4) [51-52].

The different chemical forms of Se can control its solubility, stability, and availability to organisms. Selenate, SeO_4^{2-}, is favoured under oxidizing conditions (pH > 14.5) and is highly soluble in water, and is generally considered to be the most toxic form [54]. Selenite, SeO_3^{2-}, occurs in oxic to suboxic environments (pH between 7.5 and 14.5) and is less available to organisms because of its affinity for sorption sites of sediment and soil [54]. In most agricultural soils, selenium is present as selenite and selenate compounds. Under anoxic conditions, elemental Se and selenide are the thermodynamically stable forms. Se(0) is relatively insoluble and selenide precipitates as metal selenides (such as FeSe) of very low solubility and hence are unavailable in agricultural soils for plant uptake. Organic selenide compounds (e.g., selenomethionine, selenocysteine) can accumulate in soil and sediments or be mineralize to inorganic selenium compounds, either as selenites or selenates. An Eh-pH diagram (Pourbaix-diagram) can be consulted in Figure 2.5. Therefore; selenites, selenates and organic selenides are the most important soluble forms of selenium in natural environments [54-57].

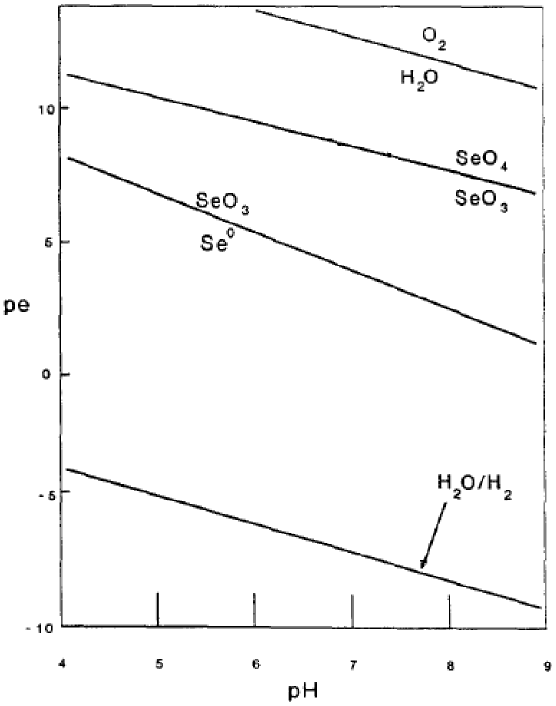

Figure 2.5 The Eh-pH diagram for Se at 25ºC and 1atm, adapted from [54].

2.4.2 Uses

The history of the use of selenium by humanity has been filled with contradictions and controversies. In its biological applications, these have taken the form of initial fears of its toxic qualities, later mitigated by classification of this element as an ultra-trace essential nutrient. The discovery in 1957 that selenium was an essential nutrient led to an entirely new era of research that continues to this day [58]. Instead of primary concerns with the toxicity of selenium, nutritionists have turned their attention to the metabolic functions of this element and the consequences of its deficiency. Selenium is an essential component of the enzyme glutathione peroxidase (GPX) that participates in the antioxidant protection of cells by reducing hydroperoxides. Selenium essentiality also appears to be the result of the formation of the active selenol group of selenoproteins, which contain Se in a highly specific form, selenocysteine. It has been also documented that Se and vitamin E (a lipid soluble radical-scavenging antioxidant) cooperate in the defense against oxidative stress in cells by detoxifying and inhibiting the formation of lipid hydroperoxides. Se compounds have also been found to inhibit tumorigenesis in a variety on animal models, and recent studies have indicated that supplemental Se in human diets may reduce cancer risks [55-61]. But, at the same time, it has been reported that selenium causes growth retardation, decreased fertility, embryotoxicity, fetotoxicity and teratogenic effects in animals. So its role in animal health is still not fully understood and remains controversial.

The principal selenium compounds of commercial importance are selenides (e.g., aluminium, arsenic, bismuth, cadmium, etc.); selenites (ammonium and sodium) and selenates (copper, potassium and sodium); selenium dioxide; selenium disulfide; selenium hexafluoride and selenium monosulfide. These compounds are used mainly in the manufacture of glass; in xerography; in conductors; rectifiers; electron emitters and insulators [51].

In agriculture, early uses of selenium compounds were for control of parasitic mites and insects; these compounds are no longer used for this purpose. Sodium selenite and selenate are presently used in agriculture as injectables and feed additives to control selenium-related deficiency disorders in livestock (e.g., liver degeneration in pigs, exudative diathesis and pancreatic degeneration in poultry) [62]. It is used as an active ingredient in remedies for eczemas and fungal infections in several pets [62].

Then, as all these applications increased, there has come apprehensions concerning the effects if any, of its continued, long-time application on the integrity of the environment [62,63].

2.4.3 Sources for humans

The occurrence of selenium in soils is of particular importance due to its recognised toxic effect on cattle foraging on plants which can accumulate the element from seleniferous soils. Selenium in soils is influenced by both the geochemical cycle of the element and the aqueous solution chemistry of the element. Hence, the accumulation of selenium in soil can arise from factors including: decomposition via the weathering of the host rock and subsequent transport of selenium by wind or surface waters; enrichment of the soil with selenium resulting from mining operations and the combustion of fossil fuels.

The selenium in the soil may occur in many forms (such as selenites, selenates, etc.). The accumulation of selenium by certain species of plants (*Astragalus*, *Haplopappus*, *Machaeranthera* and *Stanleya*) is well documented [52-54, 62-64]. Consumption of such plants by livestock is associated with the acute disease syndrome of blind staggers. Even before selenium had been discovered and named, there were reports of conditions in animals that, in retrospect, must have been caused by an excess of this element. Early reports of selenium poisoning by the consumption of these plants dates to Marco Polo’s travels to China in the 13th century [65]. In his travelogue he reported that ingestion of a toxic indigenous plant in today’s Gansu province of China killed cattle. Donkeys, oxen, and horses suffered hair loss and festers of theirs hooves and some of them even died [64].

Soluble oxyanions of selenium (selenite and/or selenate) are washed out from the soil and into waterways and consequently, selenium levels in ground and surface waters can range from 0.1 to about 400 µg L^{-1} [51, 52, 64]. However, depending on geological factors, groundwater can reach concentrations up to 6,000 µg L^{-1} [51]. Selenium is generally a minor constituent in potable water with concentrations ranging from 0.1 to 100 µg L^{-1} with a safe upper limit for selenium in drinking water considered to be 10 µg L^{-1} in accordance with EPA regulations [63]. In general, selenium in the drinking water does not add substantially to the selenium uptake, but its supposed implication in heart diseases makes its regulation mandatory. The selenium content in foods is highly dependant on the levels of selenium in soil and water. It is generally accepted that foods produced in some seleniferous farming areas contain high levels of selenium (e.g., milk, eggs, bread, bread and vegetables contained up to 1.2, 10,1.0, 8.0 and 17 mg Kg^{-1} respectively) [53].

Although atmospheric concentrations of selenium usually are of the order of a few nanograms per cubic meter, it should be well noted that point-source emission, primarily from the combustion of fossil fuels, can contribute to the local air pollution by selenium. SeO_2 is formed by the combustion of Se(0) present in fossil fuels with concomitant production of SO_2, which rapidly reduces SeO_2 to Se(0) , which is not available to plants or biosystems. Other possible sources of selenium in the atmosphere include the incineration of paper and rubber tires.

Because the difference between the essential (recommended daily allowance is 55 µg day^{-1}) and the toxic concentration level (more than 500 µg day^{-1}) of selenium is rather narrow, precise knowledge of the selenium content in the environment and food products is necessary.

2.4.4 Toxicological effects

There is an increasing recognition that selenium is an important trace element with industrial, environmental, biological, and toxicological significance. Its reported toxicology is often both conflicting and controversial. The toxicology of selenium is of considerable continuing interest for a variety of reasons including:

1. the long-establish selenium poisoning of domestic animals foraging on seleniferous plants;
2. health disorders in humans and animals resulting from selenium deficiencies;
3. its nutritional essentiality,
4. the protective effect of selenium against metal toxicity and the metabolic cooperation between selenium and vitamin E and other antioxidants;
5. the reported possibility of carcinogenicity of Se-compounds, and
6. the reported anticarcinogenicity, including a decrease in the incidence of hepatic, colon and mammary tumours. In addition, the enhancement of DNA repair processes and immunological mechanisms as well as the inverse relationships between the dietary intake of selenium and cancer mortality [51, 55, 58-65].

The many health benefits that have been attributed to selenium highlight the serrated road from a toxin to what may now be designated as a panacea. The International Agency for Research on Cancer (IARC) has determined that selenium and selenium compounds are not classifiable as to their carcinogenicity to humans [66]. The EPA has determined that only one specific form of selenium, selenium sulphide, is a likely human carcinogen but it is not present in foods [67]. The ATSDR ranked selenium number 140 on the CERCLA Priority List of Hazardous Substances since 1997 [50].

Chronic oral exposure to high concentrations of selenium compounds can produce a disease called selenosis. The major signs of selenosis are characteristic “garlic odor” of excess selenium in the breath and urine, hair and nail loss, thickened and brittle nails, lowered haemoglobin levels, skin lesions, mottled teeth, and neurological abnormalities (such as peripheral anesthesia, acroparesthesia and pain in the extremities) [68-70].

Humans absorb and retain the organic forms (SeMet, selenomethionine; SeCys, selenocysteine; SeMSC, Se-methylselenocysteine and Se-enriched yeast) of selenium more efficiently than the inorganic forms (Na_2SeO_3 and Na_2SeO_4); however, the metabolism of both organic and inorganic Se forms shows certain similarities, as can be observed in Figure 2.6 [68].

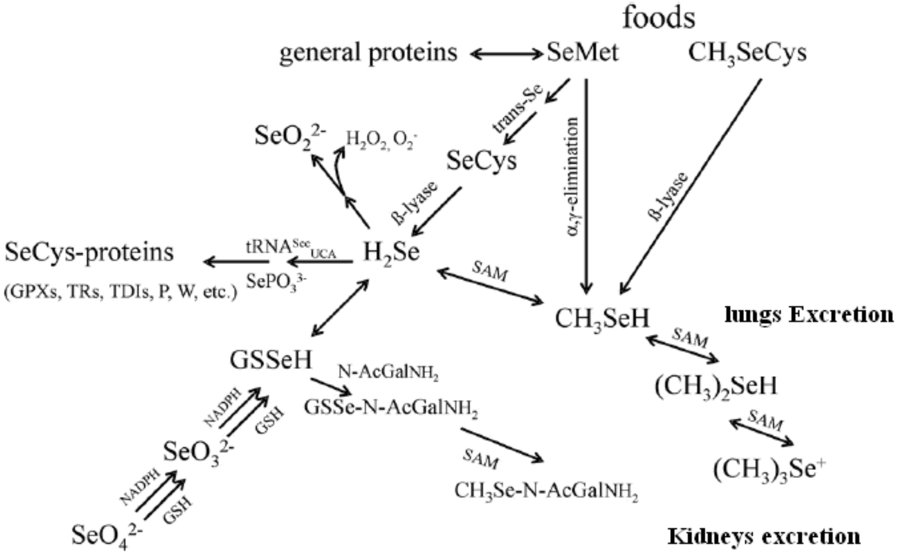

Figure 2.6 Proposed metabolic pathways for important seleno-compounds [59,68].

While the organic forms of Se are typically found in their reduced form (selenide), the inorganic salts need to be reduced from the oxidized forms to the selenide state. Upon absorption, selenite and selenate are reduced to the selenide state using GSH and NADPH (reduced forms of glutathione and nicotinamide adenine dinucleotide phosphate respectively) [59] . In contrast, the organic forms release selenide directly as a result of catabolism. Most of the Se in foods and dietary supplements is present as SeMet or SeCys. SeMet can either be metabolised to form SeCys or be incorporated non-specifically into proteins (without being distinguished from methionine) [69]. Intact SeCys in the diet is cleaved to H_2Se.

Selenide formation has a central role in Se metabolism being at the junction of two metabolic pathways. One pathway results in selenoprotein production, engaging the co-translocational synthesis of SeCys and its incorporation into specific selenoproteins. Because selenoprotein expression is tightly regulated, Se in excess of these needs enters an excretory pathway. The excretion occurs by the methylation or sugar derivatives of selenides, producing a series of metabolites: methylselenol (CH3SeH) and dimethylselenide ($[CH3]_2SeH$) which are excreted by the lungs, and trimethylselenonium ion $[(CH_3)_3Se^+]$ and 1-β-methylseleno-N-acetyl-D-galactosamine (CH_3Se-GalN) which are both excreted via the kidneys. Indirect evidence has suggested that CH_3SeH produced in the excretory pathway can play an important role as a key anticarcinogenic metabolite [61].

There is a very slender range of optimal activity between dietary levels of Se that result in deficiency and toxicity [67]. Therefore, the Se concentration is assumed to be well controlled in the body, being utilised either for the synthesis of selenoproteins or being disposed of after being methylated. The excessive intake of SeMet from certain varieties of plants has resulted in signs of toxicity in humans and livestock [62].

2.5 Remediation technologies for metal oxyanion-contaminated soils

Decontamination, commonly described as the inactivation, removal or destruction of toxic substances, is an important aspect of operations in a chemically or biologically contaminated environment.

The ultimate aim of researchers in the area of decontamination is to develop the perfect decontaminant – a substance that will degrade all contaminants but will leave surfaces and environments unharmed. To achieve this endeavour, there are certain criteria that must be kept in mind when applying remediation techniques. It is necessary for a decontaminant to accomplish complete destruction of the contaminant as rapidly as possible. Logistical considerations further emphasise the need for a highly reactive decontaminant. A conflicting requirement is for the decontaminant to be non-destructive to surfaces/ substrates. This presents a difficult situation. Ideally, the decontamination procedure is reactive with all contaminants but with no other components of the medium. It also should have no detrimental affect on sensitive equipment. An ease of application is also a desirable feature for logistic and training reasons.

Several techniques have been developed in order to remediate soils contaminated with inorganic or/and organic pollutants, a summary of the various remediation strategies is presented in Table 2.5.

Environmental remediation techniques currently used in the decontamination of toxic oxyanions are discussed in greater detail in the following sections.

Table 2.5 A summary of remediation technologies

Technology	Description	Applicability
Containment		
Physical	Prevent movement by preventing fluid flow	Landfill covers and slurry walls
Encapsulation	Creation of an inert waste	Injection of solidifying agents
Vitrification	Application of electrical energy to vitrify contaminant	Shallow metal-contaminated soil, low volatility metals
***Ex situ* treatment**		
Physical separation	Froth flotation, gravity separation, screening	For high metal concentrations
Soil washing	Addition of surfactants and other additives to mobilize contaminants	For water soluble contaminants
Pyrometallurgical	Elevated temperature, extraction, and processing for metal removal	Highly-contaminates soils
***In situ* treatment**		
Reactive barriers	Creation of permeable barrier	Sorption or degradation of contaminants in barrier
Soil flushing	Water flushing to leach contaminants	For soluble contaminants
Electrokinetics	Application of electrical current	Applicable for saturated soils with low groundwater flow
Phytoremediation	Use of plants for metal extraction	Shallow soils and water
Biochemical	Extraction of metals by microorganisms	Use in low-contaminated areas

2.5.1 Solidification/stabilisation technologies - Vitrification

Vitrification is a solidification/stabilization process requiring thermal energy. It involves insertion of electrodes into the soil capable of carrying a current. The resulting moulten slag solidifies, as it cools. The steps in the vitrification process are: 1) insertion of electrodes into the soil and the placement of graphite and glass frit starter path to initiate vitrification; 2) subsidence of the soil during vitrification and 3) placement of backfill over vitrified monolith. Mixed wastes can also be treated in this manner. High clay and moisture contents and debris can affect the efficiency of the process. These solidification/stabilization processes are suitable for contamination in shallow depths and of large volume. Leaching of the contaminants must, however, be carefully monitored. Full-scale applications were reported by Mulligan et al. [71] for AsO_4^{3-} , AsO_3^{3-} , Pb and CrO_4^{2-} contaminated soils.

Another means of thermal vitrification of pollutants is with microwave energy. Microwave and radio frequency heating techniques have proven to be suitable as energy source for thermal processing of contaminated soils. The first attempt to remediate soils contaminated with CrO_4^{2-} was reported in 1991 by Dauerman et al., [72] who subjected soils contaminated with Cr(VI) in a Pyrex container surrounded by sand, to microwave irradiation. The methodology employed for the vitrification of CrO_4^{2-} ions is very simple, microwave energy is absorbed by a graphite or an iron rod inserted in the contaminated site. The set-up is shown in Figure 2.7. The rod becomes extremely hot and conducts the energy to the surrounding soil.

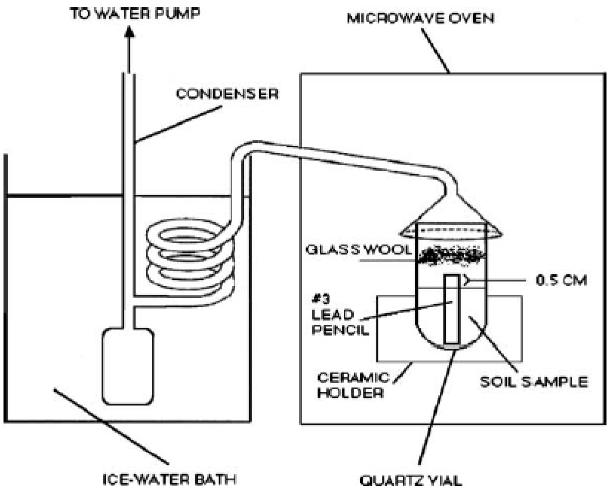

Figure 2.7 Microwave set-up for remediation purposes

When microwave energy is used, any water in the soil is volatilized rapidly. Such evaporation may well facilitate desorption of some undecomposed volatile organic materials (e.g., PCBs, PAHs), which would be trapped and collected via the built-in hood and vacuum system, and then remediated by known methods *ex situ*, making this technique useful for the remediation of soil contaminated with mixed pollutants (inorganic and organic) [73-74].

The advantages of the microwave method include: highly efficient *in situ* remediation, speed, and possible economies in the cost of energy. Further research studies remain to be performed in order to gain additional information about this vitrification strategy [73].

2.5.2 Pyrometallurgical separation

Pyrometallurgical processes use high temperature furnaces to volatilize metals from contaminated soil. Temperatures of 200-700 ºC are used to evaporate the contaminants. After volatilization, metals are then either recovered or immobilized. Although these methods are most applicable to mercury, gold or platinum, other inorganic species like AsO_4^{3-}, AsO_3^{3-}, cadmium, lead and CrO_4^{2-} are appropriate with certain other treatments. These later species may require pretreatment with reducing or fluxing agents to assist melting and provide a more uniform feed. This type of treatment is usually performed off site due to a lack of mobile units and is most applicable to highly contaminated soils (5-20%) where metal recovery is more profitable. The metal contaminants in soil then must be concentrated by physical or soil washing processes prior to pyrometallurgical procedures [71].

2.5.3 Chemical treatment

Chemical reactions can be designed to decrease the toxicity or mobility of metal contaminants. The three types of reactions that can be used for this purpose are oxidation, reduction and neutralization reactions. Changing the oxidation state of metals by redox reactions can detoxify, precipitate or solubilize metals. Chemical neutralization is used to adjust the pH balance of extremely acidic or basic soils and/or groundwater. This procedure can be used to precipitate insoluble metal salts from contaminated water, or in preparation for chemical oxidation or reduction.

Chemical treatment is often used as a pretreatment for solidification/stabilization (S/S) and other treatment technologies.

Reduction of CrO_4^{2-} to Cr(III) is the most common form of chemical treatment and is necessary for vitrified wastes containing CrO_4^{2-}. Trivalent chromium is readily precipitated by hydroxide over a wide range of pH values. Acidification can also be used to aid CrO_4^{2-} reduction. In groundwater, chromate reduction was enhanced in systems containing iron fillings in addition to the natural aquifer material, so that trenches (permeable walls) filled with zero-valent iron, Fe(0), have shown promise for those purposes.

Arsenic can be treated by chemical oxidation since AsO_4^{3-}, is less toxic, soluble and more mobile than AsO_3^{3-}. Research has indicated that arsenic stabilization can be achieved by precipitation or coprecipitation with ferric ion to form $FeAsO_4$ while low concentrations of AsO_4^{3-} can co-precipitate with $FeHO_2$ to form arsenic ferrihydride, a product that is resistant to acid or neutral leaching.

All of these chemical treatments can be performed either *ex situ* or *in situ*. However, *in situ* chemical agents must be carefully selected so that they do not further contaminate the treatment area. The primary problem associated with chemical treatment is the non-specific nature of the chemical regents. Oxidizing/reducing agents added to the matrix to treat a metal can also target other reactive metals and make them more toxic or mobile. Also, the long-term stability of reaction products is of concern since changes in soil and water chemistry might reverse the selected reactions.

2.5.4 Electrokinetics

Electrokinetics is an emerging technique for the remediation of contaminated land. It consists of applying a low level of direct electric current or a low voltage gradient across electrodes, which are inserted into the contaminated soil [71, 75-76]. As a result of this induced electric potential, electrolysis of water occurs at the electrodes producing hydrogen ions at the anode and hydroxyl ions at the cathode following the redox reaction shown in Figure 2.8.

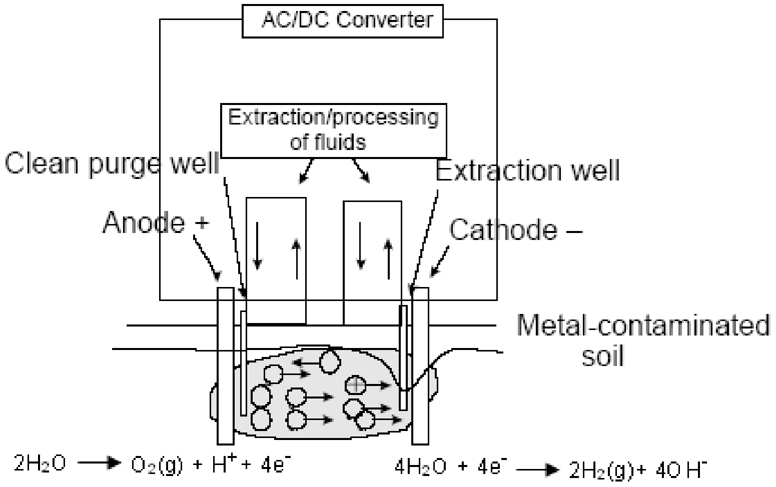

Figure 2.8 Electrokinetic process for soil remediation, adapted and modified from [71].

The generated O_2 gas and H_2 gas are permitted to escape out of the soil. The H^+ ions and OH^- migrate through the soil solution towards the cathode and anode respectively. The extent of their migration depends upon the buffering capacity of the soil. In soils with a low buffering capacity, a distinct pH gradient ranging from 2 near the anode and 12 near the cathode is generally developed. Under an induced electric potential, the soil contaminants will migrate towards either the cathode or the anode, depending on their net charge. For example, anionic species like; CrO_4^{2-}, AsO_4^{3-}, and AsO_3^{3-} migrate towards the anode whereas cationic Cr(III), Pb(II), Cd(II) species migrate towards the cathode. At the same time, electrokinetics also generates an electro-osmotic flow of water towards the cathode due to dipolar interactions of the water molecules with the surfaces of soil particles. This water flow is capable of transporting molecules, including uncharged organics {polycyclic aromatic hydrocarbons (PAHs), toluene, benzene, ethylbenzene and xylene (BTEX), etc.}, towards the cathode. The incorporation of water-soluble electrolytes, surfactants, complexing agents or acids at the anode can aid the removal of contaminants [71]. Previous research has demonstrated that the principal contaminant migration mechanisms that take place during the electrokinetic remediation process are: electroosmosis (movement of pore water under an electrical potential difference from the anode to the cathode); electromigration (movement of ions in the pore fluid of the soil under the influence of an electric current); diffusion and electrophoresis (transport of charged particles under the influence of an electric current) [75].

The feasibility and efficiency of electrokinetic remediation depends on the geologic, hydraulic, chemical, and electrical conditions of the contaminated site. One of the most important aspects of the electrokinetic process is its versatility. This process is able to remediate metal and organic co-contaminated soils as demonstrated by several research studies [71].

2.5.5 Biological treatment

Biological treatment technologies are available for remediation of metal-contaminated sites. These technologies are commonly used for the remediation of organic contaminants and are currently being applied for metal-oxyanion contaminated land. Biological treatment exploits natural biological processes that allow certain plants and microorganisms to aid in the remediation of pollutants. These processes occur through a variety of mechanisms, including adsorption, oxidation and reduction reactions, and methylation [26,71, 75-83].

2.5.5.1 Bioleaching

Bioleaching uses microorganisms to solubilize metal contaminants either by direct action of the bacteria, interactions with its metabolic products, or both. Mulligan et al. [71] have reported the use of *Thiobacillus sp*. Bacteria under aerobic and acidic conditions for the remediation of sites contaminated with uranium oxyanions. The potential exploitation of the fungus *Aspergillus niger* for the remediation of metal-contaminated soil has also been evaluated. It can produce citric and gluconic acids which can act as acids and chelating agents for the removal of metals such as copper from oxide mining residues.

2.5.5.2 Biochemical processes

Micro-organisms are capable of altering the redox state of toxic metals, organometalloids and radionuclide contaminants through direct and indirect biochemical processes [81]. A number of aerobic and anaerobic microorganisms are able to reduce CrO_4^{2-}. In the presence of oxygen, microbial reduction of Cr(VI) is commonly catalyzed [77] by soluble reductases in the cytosol of selected microorganisms (e.g., *Pseudomonas synxantha*, *Bacillus spp.*, *E. Coli* ATCC33456, *Shewanella alga* BrY-MT). By contrast, *Pseudomonas maltophilia* and *Bacillus megaterium* utilize membrane-associated reductases. Recently, two soluble Cr(VI) reductases have been isolated and purified from *Pseudomonas putida* MK1 and *E. Coli*. Under anaerobic conditions, both soluble and membrane-associated enzymes mediate the Cr(VI) reduction [77-79, 82, 83].

Natural metabolites of anerobic microorganisms, such as H_2S, produced by sulpahte-reducing bacteria (SRB), are effective chemical reductants of Cr(VI) under anoxic environments [77]. Some of the SRB for which detoxification of CrO_4^{2-} are well documented include *Pseudomonas fluorescens* and *Desulfovibrio desulfuricans*.

Precipitation of ^{99}Tc-oxides ($^{99}TcO_2$) was observed by the reduction of the highly soluble radionuclide ^{99}Tc(VII) mediated by *E. Coli*, *Desulfovibrio desulfuricans* or *Geobacter sulfurreducens* [78-80].

A number of bacteria that contain nitrate reductases are capable of reducing perchlorate (ClO_4^-). Pathogenic species *Staphylococcus epidermidis* and *Bacillus cereus* are capable of reducing ClO_4^- but their toxicity precludes further use in bioremediation [81]. However, some *Proteobacteria*, *Vibrio dechloraticans*, *Ideonella dechloratans*, *Wolinella succinogenes* have demonstrated outstanding reducing properties towards perchlorate.

Stolz et al., [83], have reported that several groups of bacteria can reduce arsenate and selenate. Among them are cited *Sulfurospirillum barnesii*, *Thaurea selenatis*, *Chrysiogenes arsenatis*. It has been proposed that oxyanions of arsenic and selenium can be used in microbial respiration as terminal electron acceptors with their subsequent transformation and mobilisation of arsenic and selenium [83].

The methylation of oxyanions by microorganisms is well documented but its potential uses are currently under development. It involves the attachment of methyl groups to form organometallic compounds, which are in some cases more toxic and mobile than other metal forms [82]. Recent attempts with *Candida humicola* have been made to accelerate the rate of Se biomethylation/volatilization and to assess its usefulness in a bioremediation program. This permanent removal of Se with the release of volatile Se species from Se-contaminated agricultural soils has shown some promise [82, 83].

2.5.6 Phytoremediation

Phytoremediation refers to the specific ability of plants to remove contaminants from soil and groundwater or to lower contaminant mobility [84-87]. Some plants have developed the ability to remove ions selectively from the soil to regulate the uptake and distribution of metals. Most metal uptake takes place in the root system, usually via absorption, where many mechanisms are available to prevent metal toxicity due to high concentrations of metals in the soil solution. The above ground shoots can be harvested to remove metals from the site and subsequently disposed as hazardous waste or treated for the recovery of metals [86].

Potentially useful phytoremediation techniques to remediate metal-contaminated sites include phytoextraction, phytostabilization (use of plants to limit the mobility and bioavailability of metals in soil) and rhizofilatration (this technique is use to treat contaminated water rather than soil) [84].

Phytoextraction is an innovative and cost-effective technology for non-destructive remediation of heavy metal-contaminated soils. It has become a promising remediation technique with the discovery of hyperaccumulators; plants that are able to accumulate large quantities of metals [85]. The capability to both tolerate elevated levels of heavy metals, and to accumulate them to unusually high concentrations has evolved both independently and together in a number of different plant species. Various strains of the *Brassica*, *Alyssum*, *Arabidopis*, and *Petrisis* species have been the most widely studied of the more of 400 hyperaccumulating vascular plants [85-87]. The effectiveness of hyperaccumulators has been demonstrated for Zn, Mn, Ni, Co, Cr, Cu, Pb, As and Cd, Se. Certain cultivars of *Brassica juncea* (Indian mustard) have shown the highest shoot Pb accumulation as well as an ability to accumulate and tolerate CrO_4^{2-} [84].

The effectiveness of phytoextraction for remediation of heavy metal-contaminated soils is highly dependent on the availability of metals for plant uptake. Metals in the soil environment exist as components of several different fractions: 1) free metal ions, soluble oxyanions and soluble metal complexes in the soil solution; 2) metal ions occupying ion exchangeable sites and the fraction that is specifically adsorbed on inorganic soil constituents; 3) organically bound metals; 4) precipitated or insoluble compounds, particularly of oxides, carbonates and hydroxides; and 5) metals in the structure of silicate minerals. Anthropogenic metal contamination of soils results in metals occurring in fractions 1 to 4 whereas the metal content in fraction 5 is indicative of background or indigenous soil concentrations. A major hurdle for phytoextraction is that only fraction 1, and, possibly components of fraction 2 are readily available to plants. Manipulation of the soil environment to enhance the availability of metals is critical for effective phytoremediation. Recent studies have focused on the feasibility of sunflowers (*Helianthus annuus*), barley (*Hordeum vulgare L.*) to hyperaccumulate multiple heavy metals with the aid of chelating agents added to the soil [85-87].

It has also been reported that plant assisted bioremediation techniques, in which plant roots in conjunctions with their rhizospheric microorganisms can be used to remediate soils contaminated with organics compounds (PAHs, PCBs, etc) [84].

2.5.7 Soil flushing/washing

Soil flushing involves the injection of water (with or without additives) into the contaminated soil *in situ* whereas soil washing requires the excavation of soil followed by extraction in the presence/absence of mobilization aids. These techniques are designed to recover the contaminants by increasing their solubility and mobility in the extracting phase. The efficiency of metal removal during soil washing/flushing depends not only on the degree and duration of contact between the extracting fluid and the contaminated soil but on the solubility of the metal pollutants in that extracting fluid and finally on the hydraulic conductivity of the soil (high permeability provides more efficient removal). Soil pH, type, cation exchange capacity (CEC), particle size, soil permeability, class of pollutants, and choice of extracting agents all affect the removal efficiency.

Since water solubility provides the controlling removal mechanism, additives are used to enhance efficiencies. In an analysis performed on a metal-contaminated site, it was determined that 400 years would be required to treat a site with water alone compared to 4 years of flushing in the presence of mobilization aids [71].

Soil washing is a treatment process used for remediating both organic and inorganic compounds from contaminated soils, sludges, and sediments [71,88-90]. This process involves high energy contact between the contaminated soils and an aqueous based washing solution. The steps involved in soil washing are: excavation of the contaminated soil; remedial treatment of the soil; solid/liquid separation of all contaminants; treatment or disposal of all residues and final soil deposition. There are numerous advantages to soil washing as a remediation technique [88]. First, the process takes place in a closed system which permits a better control of the conditions. Secondly, the application of this technique can result in a significant volume reduction of the contaminant mass. Thirdly, the cost of soil washing is relatively low compared to other multi contaminant technologies and significantly lower than the cost of landfilling. Lastly, the public's acceptance to the soil washing approach is high. But, soil washing has also disadvantages as a remediation technique. When the soil washing treatment is only a physical process, there is a little reduction in the toxicity of the contaminants and if chemical processes are involved, potentially hazardous chemicals that are used in the remediation process may then be difficult to remove from the treated soil and may remain on site [88-92]. This process has been primarily used to treat soils and sludges contaminated with only heavy metals or volatile organic compounds, however, it has not been extensively employed on soils that are contaminated with mixed pollutants (pesticides, heavy metals and volatile organic compounds) [88-90].

Chemically enhanced soil washing/flushing can be used to simultaneously removed mixed contaminants [91-93]. It includes the addition of organic and inorganic acids, NaOH (which can dissolve organic soil matter), small quantities of water soluble solvents such as methanol, chelating reagents {e.g. aminopolycarboxylic acids such as diethylenetriaminepentaacetic (DTPA) or ethylenediaminetetraacetic acid (EDTA), or nitrilotriacetic acid (NTA)} in combination with oxidizing/reducing agents, surfactants and/or cyclodextrines [91-100].

2.5.7.1 Use of surfactants preparations in soil remediation

There is an extensive body literature on the use of surfactants to enhance the removal of soil contaminants [92-95,100]. Surfactants are potential remediation agents as they promote the wetting, solubilization, and emulsification of pollutants (e.g. heavy metals, oxyanions and organic compounds) by altering the surface properties of liquids [91]. The fundamental properties of a surfactant are its amphiphilic structure made up of hydrophilic head and hydrophobic carbon tail, monolayer orientation at interfaces, and adsorption at interfaces. Being amphiphilic, the surfactant tends to migrate to interface where both moieties exists in preferred phase (e.g. oil-water, air-water, water and solid-liquid). This arrangement creates a third layer at the interface, decreasing interfacial tension between the two phases, hence reducing the surface tension of water which promotes the mobilization of contaminants from unsaturated soils [96]. A surfactant's ability to lower surface tension is an important factor determining the efficacy of the surfactant.

In addition, the amphiphilic structure causes the molecules to aggregate into micelles at a high concentration, which is a phenomenon unique to surfactants among amphiphilic molecules. Dynamic micelle aggregation permits the hydrophilic head to associate with water, while lipophilic tails to orient away from the bulk water phase. The micelle interior can be envisioned as pseudo-oil phase. Organic compounds preferentially partition into the interior of micelle, thereby increasing the solubility of organic compounds in a surface solution relative to its water solubility. The critical micelle concentration (CMC) is the minimum concentration of surfactant required for the formation of micelles. Beyond the CMC, the concentration monomer remains relatively constant. The micelle capacity to solubilize organic compounds makes these molecules suitable for soil remediation of hydrophobic contaminants [97,98].

The use of surfactants are attractive for the mobilization and mass transfer of mixed contaminants {such as oxyanions, heavy metals, and persistent organic pollutants (POPs)} from soil because not only are they often considered to be environmentally benign. Also once cleaned, they can be re-used for future mobilization/solubilization of pollutants from soil; they facilitate a rapid and permanent decontamination [100]. One of the constrains of the use of surfactant preparations as mobilization agents is the high price of commercially available surfactants, increasing costs for the overall soil remediation strategy.

Once the extractant fluid is pumped up to the soil surface for the flushing technique, or the washing solution is separated from the soil particulates fraction, the liquid needs to be treated to detoxify, transform, and or remove pollutants. Currently, some of the more widely used techniques for this treatment include the application ionization radiation, ultrafiltration or reduction with zero-valent metal.

2.5.7.2 Decomposition of pollutants using Ionizing radiation

Schmelling et al. [101] reported the treatment of industrial wastewater and extracting fluids (chelating agents or surfactants) from contaminated soils by ionizing radiation. This research has emphasized the role of the solvated electron in effecting the desired transformations of noxious species, primarily PCBs and heavy metals {Cr(VI), Hg, Pb, and Cd}. These transformations occur principally through the indirect effects of radiation in which interaction of gamma-ionizing radiation (^{60}Co γ-rays) with a solvent creates a suite of radical species that subsequently react with a contaminant solute. When an aqueous surfactant solutions containing metal ions is subjected to gamma radiation, reducing radicals are generated that react with the metal cations or oxyanions to reduce them to lower valence states where they precipitate and can be removed by filtration.

2.5.7.3 Removal of oxyanions using ultrafiltration

The application of surfactants {at concentrations above the critical micellar concentration (CMC)} to contaminated soils permits the entrapment of ionic solutes (like oxyanionic species) in solution. The increased hydrodynamic size of the solutes enables their rejection by polymeric ultrafiltration membranes and this process is known as micellar-enhanced ultrafiltration (MEUF).

Baek et al. [102] described the application of MEUF in order to remove CrO_4^{2-} and $Fe(CN)_6^{3-}$ from contaminated sites. Once a cationic surfactant was added, it forms micelles, surfactant aggregates that contain 50-100 surfactant molecules, above the CMC. Chromate and ferricyanide ions bind to the oppositely charged surface of the micelles. This solution is then passed through an ultrafiltration membrane with pore sizes small enough to block the passage of micelles. The rejection of micelles brings about the rejection of the CrO_4^{2-} and $Fe(CN)_6^{3-}$ adsorbed to the micelles. The unbounded ions and surfactant monomers pass through the ultrafiltration membrane and accumulate in the permeate.

To date, MEUF has been used to separate the organic pollutants, heavy metals, oxyanions, NO_3^-, SO_4^{2-} and sulfate using different surfactants. However, most of researchers on MEUF have focused on the single-pollutant system and few researchers reported mixed-pollutant system where competition due to difference in binding power of pollutants may inhibit the binding of those pollutants with weaker binding avidities. In 2004 Baek and Yang [103] demonstrated the feasibility of MEUF to treat sites contaminates with mixed contaminants (chlorinated aromatic hydrocarbons, NO_3^- and CrO_4^{2-}). They concluded that MEUF can be applied to treat sites contaminated with multi-pollutant systems.

2.5.7.4 Tansformation of pollutants using micro-Zero-Valent Metals

The use of zero-valent particles for the decontamination of common soil and water contaminants has been subject of numerous studies [104-120]. In the last decade, more than 200 hundreds peer-reviewed manuscripts have been published on this topic. Each metal possesses a characteristic standard reduction potential, which determines its thermodynamic ability to spontaneously react with several pollutants (either organic or inorganic substances).

Zero-valent iron (ZVI) has been the main focus of zero-valent metal particle studies [107-120]. Magnesium, silicon, tin and zinc have also been evaluated [104-106, 121-123]. Although many other metals (e.g., zinc, tin) reacts more rapidly with halogenated organic compounds than ZVI and can detoxify pollutants more rapidly than Fe(0), iron is still the most commonly used decontaminating reagent due to its low cost and non-toxicity [121].

The degradation of halocarbon compounds by ZVI has been sufficiently studied to permit certain conclusions: 1) hydrodechlorination occurs through a surface reaction with the metal as the ultimate electron donor; 2) the major determinants of degradation kinetics are mass transfer to, area of, and condition of metal surface; and 3) mediation by H_2 or metal impurities do not appear to be necessary for rapid degradation [104-107].

It has also been reported that the Fe(0)-mediated remediation of nitro aromatic compounds (NACs) such as trinitrotoluene (TNT), hexahydro-1,3,5-trinitro-1,3,5-triazine (RDX); of nitrosamine compounds (e.g., N-nitrosodimethylamine (NDMA) a potent carcinogen) and other compounds containing aldehyde, ketone, quinine, diamine, nitrile, oxime, imine, sulfoxide, and disulfoxide moieties occur rapidly [107].

So far, ZVI has been extensively used for the treatment of halogenated organic compounds by reductive dehalogenation and its use for other purposes continues to be investigated. It has already been demonstrated to be effective for the removal of several inorganic oxyanions including NO_3^-, NO_2^-, CrO_4^{2-}, AsO_4^{3-}, AsO_3^{3-}, SeO_4^{2-}, TcO_4^-, ReO_4^-, MoO_4^-, ClO_4^- and certain inorganic cations such as; UO_2^{2+}, Cu^{2+}, Cd^{2+}, Al^{3+}, Zn^{2+}, and Ni^{2+} [108-120]. The transformation rates of several oxyanions reduction vary appreciably depending on pH, zero valent iron (ZVI) concentration and source [120].

In contrast to organic compounds, the mechanism of detoxification of inorganic compounds is not yet fully elucidated nor have all the participating species been identified. It has been suggested that the mechanism of the oxyanion detoxification includes reductive precipitation, complex formation with iron oxides, or electrochemical reduction. The reactant specie depends on reaction conditions such as pH and amendments. To date, what has been proposed about this mechanism and the reactions involved in the decontamination sequence include the following. It seems that not only a direct electron transfer from the iron surface, but the formation of ferrous ion (Fe^{2+}) and further reaction with oxyanion to form its oxidized specie, ferric ion (Fe^{3+}). The iron surface can react with water to produce H_2, which seems to accelerate the reactions [107-120, 124-125]. The thermodynamic instability of ZVI in the presence of water and/or oxygen, mediate the oxidation of Fe^0/Fe^{+2} ion and the precipitation of iron species (α-FeOOH, α-Fe_3O_4, γ-FeOOH, $Fe(OH)_2$, $Fe(OH)_3$, and $FeCO_3$) on the ZVI surface [121]. As a consequence, the electron donor properties of the oxidised ZVI surface can be severely impeded, decreasing the transformation rate of Cr(VI) to Cr(III) reduction as an example. A schematic diagram proposing the mechanism of reduction of chromate by ZVI is presented in Figure 2.9.

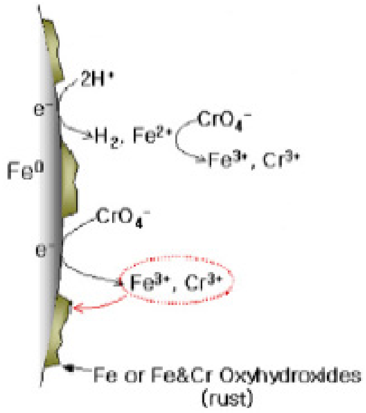

Figure 2.9 A schematic diagram of the main features of the Cr(VI) reduction by ZVI, adapted from [111].

Several attempts have been made to enhance the efficiency of this redox reaction and diminish the inactivating effects of the resulting passivation layer. On the one hand, adding with a second catalytic metal such as Pd, Pt, Ag, Cu, Zn or Ni to the iron particles have provided dramatic improvements in rates of detoxification for either organic or inorganic pollutants [125-127]. The addition of a second or third zero-valent metal on the iron surface serves not only as a catalyst but also as a protecting agent against surface corrosion [125]. For example, it has been suggested that the enhanced reactivity of palladised iron is likely due to the fact that Pd has the ability to intercalate hydrogen into its lattice and dissociate it into a powerful reductant [128-131].

Implementation of the zero-valent iron technology still faces several challenges:

1. decrease of metal reactivity over time, probably the result of the formation of surface passivation layers or the precipitation of various iron species {(α-FeOOH, α-Fe_3O_4, γ-FeOOH, $Fe(OH)_2$, $Fe(OH)_3$, and $FeCO_3$) on the surface of metal; and
2. engineering difficulties for constructing metal wall in deep aquifers (e.g. >30m) [120].

2.5.7.5 Tansformation of pollutants using nano-sized metallic particles

Oxyanion (e.g., arsenate, chromate, perchlorate or selenate) transformation mediated by metallic-based particles is a surface-mediated process; increasing the surface area of iron will increase the reduction rate [132-134]. By their nature, nanoparticles have an elevated surface/volume (*S/V*) ratio: approximately 35-40% of atoms are localized at the surface of a 10 nm nanoparticles compared with less than 20% for particles larger than 30 nm [133]. This high *S/V* ratio corresponds of specific surface area (SSA) that takes on very high values for nanoparticles might be associated with multiple intrinsic properties such as strong surface reactivity that are size dependent. There is appreciable evidence that nano-scale metal particles are more reactive than commercial micron-scale powders, most probably due to the high SSA and increased surface reactivity [132]. The increase in surface area and energy gained by using nanoscale particles has demonstrated a considerable increase in the decontamination potential of the particles [134-142].

The preparation of nanoparticles generally involves the reduction of metal ions in solution or in high temperature gaseous environments [135]. The high surface energy of these particles makes them extremely reactive, and most systems undergo aggregation without protection or passivation of their surfaces [143]. Agglomeration reduces the SSA and the interfacial free energy, thereby diminishing particle reactivity. A solid stabilizer can enhance dispersion (by decreasing agglomeration) of nanoparticles through (a) electrostatic repulsion and (b) steric hindrance. In addition to weakening the physical interactions, encapsulating with select stabilizers can also passivate the highly reactive surface. Although the surface passivating effect might also inhibit reaction with target contaminants, the net reactivity gain toward a target compound can be substantial because of the tremendous particle size reduction and the gain in SSA from the particle stabilization [143]. The selection of the solid support usually depends on the metallic nanoparticle that is intended to be stabilized, but the most extensively used supports to date are activated carbon, zeolite, silica, alumina, thiols, carboxylic acids, surfactants, and polymers [143-148].

Controversy remains about the novel size-dependent properties of nanoparticles (precisely the properties that make them desirable in technical and commercial uses). Concerns have been expressed in terms of the potential environmental or toxicological impacts of the release of this scale of particles [133, 149-151]. For instance, while it may be desirable from a standpoint of water or soil detoxification to have nanoparticles able to adsorb/transform a large quantity of ions or molecules in solution, this same trait may also have negative implications such as the adsorption of proteins and their denaturation [133]. A theoretical framework that relates properties of metallic nanoparticles to their biological effects is still needed in order to identify possible risks to human health and the environment.

Chapter

Three

Preface

In Chapter two, an overview of transition metal and non-metal oxyanions was presented in order to better understand toxicological effects and the nature of contamination in the environment and particularly in water, soil or sediment. In this chapter, ***s***everal remediation techniques that can be applied to heavy metal oxyanion contaminations were presented and a more detailed discussion was focused on the decontamination of sites using mobilizing agents (such as surfactants and chelating agents) and/or zero valent metals. The comprehensive literature review revealed the need for the development of efficient, fast, economical, and environmentally sustainable zero-valent metal technology for the mobilization of oxyanions from contaminated soils that can be coupled with the concurrent detoxification of the contaminants.

The first stage of this study involved the mobilization of chromate from soil using various surfactants preparations (Appendix 1). The selected preparation was reacted with various zero-valent metals under a selection of reaction conditions.

In the following chapter, the ability of several zero-valent metals to readily detoxify a surfactant preparation containing hexavalent chromium is evaluated. Finally, metallic nano-sized particles (Cu and Fe) are prepared in the presence/absence of a solid support (alumina and polymeric structures). Their reactivities towards the reduction of hexavalent chromium under slight and more acidic conditions are reported.

A portion of this chapter has been published in **J. Environ. Monit., 2009, 11, 1072 - 1079**. Authors: M. Rivero-Huguet, W.D. Marshall.

Chapter

Three

Reduction of hexavalent chromium mediated by micron- and nano-scale zero-valent metallic particles

3.1 Introduction

Chromium is a common pollutant found in brownfields, as well as surface and subterranean waters throughout the industrialized world. Whereas chromium(III) is an essential element for living organisms at ultra-trace levels, hexavalent chromium engenders environmental and health problems because of its acute toxicity, mutagenicity and carcinogenicity [24,25]. Over the last several years, a great deal of effort has been expended to identify and improve strategies to mitigate chromium(VI) contamination. In particular, several studies have demonstrated that zero-valent iron (ZVI) is an efficient and inexpensive reductant for Cr(VI) [109,111,152,153]. Under appropriate conditions, complete removal of Cr(VI) from solution has been reported in several laboratory studies and in both pilot and field-scale iron metal permeable reactive barriers. The rates of Cr(VI) reduction vary appreciably depending on pH, zero valent iron (ZVI) concentration and source. However, the thermodynamic instability of ZVI in the presence of water and/or oxygen, mediate the oxidation of Fe^0/Fe^{+2} ion and the precipitation of iron species (α-FeOOH, α-Fe_3O_4, γ-FeOOH, $Fe(OH)_2$, $Fe(OH)_3$, and $FeCO_3$) on the ZVI surface [124]. As a consequence, the electron donor properties of the oxidised ZVI surface can be severely impeded, decreasing the transformation rate of Cr(VI) to Cr(III). Several attempts have been made to enhance the efficiency of this redox reaction and diminish the inactivating effects of the resulting passivation layer. On the one hand, adding with a second catalytic metal such as Pd^0, Pt^0, Ag^0 or Ni^0 to the iron particles can accelerate the detoxification of Cr(VI) solutions. The second zero-valent metal on the iron surface serves not only as a catalyst but also as a protecting agent against surface corrosion. For example, it has been suggested that the enhanced reactivity of palladised iron is likely due to the fact that Pd has the ability to intercalate hydrogen into its lattice and dissociate it into a powerful reductant [106,128,130,131]. Hexavalent chromium reduction by Fe-based particles is a surface-mediated process; increasing the surface area of iron will increase the reduction rate. There is appreciable evidence that nano-scale metal particles are more reactive than commercial micron-scale powders, most probably due to the high specific surface area and increased surface reactivity [134].

The limitations for practical applications with ZVI technique have encouraged scientists to evaluate other zero-valent metals as electron donors. Several other metals, particularly those with very negative reduction potentials (e.g., Zn^0, Sn^0, Si^0, Al^0) can be substituted for iron as reductants. Zinc and Sn^0 have been demonstrated to dehalogenate organic compounds more rapidly than ZVI [106,121].

We report here the mobilisation and detoxification of Cr(VI) from a contaminated site. The Cr(VI)-contaminated soil sample was treated with a several surfactant formulations, as a mobilisation aid to dislodge the target ion from the particulate surfaces. The resulting solution was reacted with various zero-valent formulations (Al^0, Cu^0, Fe^0, Mg^0, Ni^0, Si^0 or Zn^0), with nanometer-sized Cu^0 and Fe^0 particles, and with nano-particles (NPs) stabilised with γ-Al_2O_3, carboxymethylcellulose (CMC) or soluble starch.

3.2 Experimental

3.2.1 Reagents and materials

Test surfactant (Tween® 20), $AgNO_3$ (99.8% purity), $CuSO_4{\cdot}5H_2O$ (≥98% purity), $ZnSO_4{\cdot}7H_2O$ (99% purity), $CoCl_2{\cdot}6H_2O$ (98% purity), $NiCl_2$ (98% purity), $MgCl_2{\cdot}6H_2O$ (≥99.0% purity), $Al_2(SO_4)_3{\cdot}18H_2O$ (≥98% purity), Na_2SiO_3 (SiO_2 44-47% purity), ethylenediaminetetraacetic acid copper(II) disodium salt (≥97.0% purity), 1,10 phenanthroline (≥99% purity), $NaBH_4$ (10-40 mesh, 98% purity), Al_2O_3 (150 mesh, 58Å, surface area 155 m^2 g^{-1}), soluble starch (ACS quality reagent), sodium carboxymethylcellulose (NaCMC, mean MW, 90,000) were used as received from Sigma-Aldrich, Oakville, ON, Canada.

Zero valent metals; iron metal (40 mesh, specific surface area 1.01 m^2 g^{-1}), copper powder (100 mesh, 99.5%, specific surface area 0.048 m^2 g^{-1}), zinc powder (100 mesh, 99.9%, specific surface area 0.059 m^2 g^{-1}), Magnesium granules (20 mesh, 98%, specific surface area 0.0786 m^2 g^{-1}), aluminium (200 mesh, 99% purity) and silicon powder (325 mesh, ≥99% purity), *S*-diphenylcarbazide, HCl (37% v/v), H_2SO_4 (95.0-98.0% purity) ACS reagent grade ethanol and acetone were obtained from Fisher Scientific, Napean, ON, Canada.

Potassium hexachloropalladate (K_2PdCl_6) and Ni^0 powder (99.7% purity, -50 +100 mesh) were purchased from Alfa-Aesar, Ward Hill, MA, USA.

Distilled de-ionised water (DDW) was obtained from a Millipore-Q purification system (Millipore Bedford MA, USA) with a resistivity of 18.0 MΩ·cm and was used for the preparation of all aqueous solutions.

Aqueous metal standard solution of Cr and Fe 1,000 mg L^{-1}, traceable to the National Institute of Standards and Technology (NIST) primary standard] and multi-element standard solution used for quality control (Cr 200.2 mg L^{-1} and Fe 1001 mg L^{-1}) were purchased from SCP Chemical Co., St-Laurent, Qc, Canada.

3.2.2 Acid pre-treatment of zero valent iron

Acid-washed iron was used in all the experiments. A known quantity of iron granules were washed copiously with 6M HCl and rinsed five times with distilled water, three times with ethanol and a further three times with acetone then dried in a N_2 stream for 2 h. To inhibit oxidation, the iron powder was stored under a nitrogen atmosphere prior to use.

3.2.3 Determination of hexavalent Chromium adapted to a microscale

The original phenylcarbazide method recommended by the APHA, was adapted to work on a microscale level [154]. Once filtered, the samples were immediately inserted into the Hach test tube with a freshly prepared phenylcarbazide solution in acetone (200 µL, 5 g L^{-1}) and H_2SO_4 (5 µL, 10% v/v). The reaction was permitted to continue for 5-10 min then diluted with 10 mL DDW.

3.2.4 Determination of Ferrous ion in the extract of surfactant solution

The standard Analysis Method 3500-Fe [B] based in the colorimetric reaction with 1,10-phenantroline was followed [154].

3.2.5 Metal determination by Atomic Spectroscopy

Total chromium, copper or iron determination was performed by flame atomic absorption spectroscopy (FAAS) at 357.9 nm, 324.8 nm or 248.3 nm respectively using a GBC 903 (GBC Scientific Equipment Pty Ltd., Australia) or by inductively coupled plasma optical emission spectrometry (ICP-OES) using a Varian Vista-MPX spectrometer (Varian Australia Pty Ltd., Australia) and multiple emission lines (267.72 nm; 283.56 nm; and 357.87 nm for Cr, 327.39 nm; and 324.75 nm for Cu, 238.20 nm; 259.94 nm; and 234.35 nm for Fe, 396.15 nm; 308.22 nm; and 309.27 for Al, 251.61 nm; 251.43; and 288.16 for Si, 213.85 nm; 202.55 nm; and 206.20 nm for Zn, 279.55 nm; 280.27 nm; 285.21 nm for Mg, 231.60; 230.30; and 221.65 nm for Ni) for each element were selected to assess the spectral interferences and a FACT (fast automated correction technique) model was used to correct the possible interferences.

3.2.6 Preparation of nanometer sized metal particles (Cu and Fe)

Zero-valent metal nano-particles (Cu^0 and Fe^0) were prepared by modifying a water-soluble approach while working in a H_2 atmosphere to improve the reducing conditions of the iron or copper salt [135,136,144,145].

Solutions were prepared in DDW that had been purged with purified N_2 for 2h to remove dissolved oxygen (DO). Prior to the reaction, an aliquot of the $FeCl_3$ or ethylenediaminetetraacetic acid copper(II) disodium salt stock solution was added to the support material (water-soluble starch, NaCMC or γ-Al_2O_3) to provide a solution/suspension with the desired metal (Cu, Fe) content and support concentration [~0.5% (w/w)]. Nano-sized metal particles were synthesized by adding 250 mM $NaBH_4$ aqueous solution dropwise in a H_2 atmosphere to a 45 mM Cu or Fe aqueous solution. The flask was vigorously shaken by hand (magnetic stirring was avoided to reduce magnetically induced aggregation of the resultant iron NPs) during the reaction.

When gas (hydrogen) evolution had ceased (after ~15 min), the nano-particles were separated from the solution and then rinsed with water three or four times. Dry nano-particles were obtained by successive washings with ethanol and acetone followed by drying at 110 ºC for 6 h.

For comparison, non-supported NPs were also prepared following similar procedures in the absence of stabilizing material. Non-stabilised copper NPs were prepared using $CuSO_4·5H_2O$ as starting material.

3.2.7 Estimation of Uncertainties associated with concentration

The measurement uncertainty associated with the determination of Cr and Fe concentrations in the extract samples by spectroscopic techniques has been calculated using a cause-and-effect approach as previously reported [155].

3.3 Results and Discussion

It was envisaged that Cr(VI) ions, once mobilized from soil into a surfactant emulsion, could be detoxified by conversion to Cr(III) during passage through a reactor column containing zero-valent metal (ZVM). It was also anticipated that the Cr(III) reduction product would be sorbed on to the ZVM surface and that the surfactant suspension could be recycled back to the soil to extract more toxicant. Previous washing trials had indicated the loss of some 11 percent of the surfactant to the soil after three washes with the same charge of a 2% (v/v) surfactant emulsion [100]. Thus, the surfactant content in the recycled aqueous suspension might have to be supplemented with fresh reagent. In addition to a capacity to mobilize both metals and non-polar organic contaminants, this approach was anticipated to decrease the quantity of surfactant consumed by processing and the quantity of ZVM needed for efficient reduction, as well as limiting the quantity of wash water requiring treatment post processing.

3.3.1 Reduction of Cr(VI) using zero-valent metals (Al^0, Cu^0, Fe^0, Mg^0, Ni^0, Si^0 or Zn^0)

A soil that had been heavily field contaminated with hexavalent chromium was treated with one of eleven different surfactant formulations (anionic, non-ionic or cationic) to evaluate the relative efficiencies of Cr(VI) mobilization. Once the pollutant had been mobilized from the soil, the solution that resulted was reacted with a zero-valent metal (ZVM). A one-way analyses of variance (ANOVA) indicated that at a 95% confidence level (P value 0.799), differences in the reaction kinetics of Cr(VI) reduction in the Tween® 20 suspension *vs.* in DDW were not statistically significant. In subsequent trials, the working solution consisted of chromate in Tween® 20 surfactant solution (2% w/v). Soluble chromate removal using zero-valent iron can be described by a generalised pseudo-first-order kinetic model, where the rate is proportional to the Cr(VI) concentration with an expression of the form

$$-\frac{\mathrm{d}C}{\mathrm{d}t} = k_{\mathrm{SA}} a_{\mathrm{s}}\, \rho_{\mathrm{m}}\, C = k_{\mathrm{obs}} C \qquad (1)$$

where C is Cr(VI) concentration (mg L^{-1}) at time t (min), k_{SA} is the surface area normalised reaction rate constant (mL min^{-1} m^{-2}), a_s is the specific surface area of the metallic particles (m^2 g^{-1}), ρ_m is the mass concentration of the ZVM (g mL^{-1}), and k_{obs} is the observed pseudo-first rate constant [134]. The rate constants (k_{SA} or k_{obs}) can then be estimated by fitting the pseudo-first rate expression from eq. 1 to the experimental data. In subsequent experiments, this model was used despite the fact that other more complicated mixed-order models have been proposed and used successfully [134,156,157].

As summarised in Table 3.1 and Fig. 3.1, the data from certain of the ZVMs provided an acceptable fit to a pseudo-first-order-rate of decrease in $HCrO_4^-$ from the surfactant suspension at pH 2.0 or lower values. For Fe^0, relatively rapid and complete reduction of hexavalent Cr was observed for initial pHs less than 3.0, providing a modest increase in the observed pseudo-first-order rate constant of 4.47 and 7.71 mL min^{-1} m^{-2} at pH 2.0 and pH 1.0 respectively. When the initial pH was increased above 3.0, the reduction process was better modeled as the sum of two pseudo-first order reactions. In Fig. 3.1B two linear rates can be delineated for ZVI (■); the initial decay from 0 to 30min, provided a goodness of fit (r^2) of 0.969, k_{SA} 0.070 mL min^{-1} m^{-2} mL^{-1} and the second decay that dominated from about 30 to 2000 min (r^2 0.979, k_{SA} 5.7×10^{-3} mL min^{-1} m^{-2}). Initially, the dominant reaction is considered to occur at exposed Fe^0 active sites but once the passivating oxide/hydroxide layer had formed, the reaction rate was decreased but not totally inhibited. At longer reaction times, the reduction of Cr(VI) continued albeit at a decreased rate. This might have resulted from the agitation that abraded the Fe surfaces exposing reactive sites but it also seem likely that electrons were able to traverse the oxide/hydroxide layer and reduce the adsorbed $HCrO_4^-$. For Fe^0, an increase of pH from 3.0 to 7.0 resulted in little further change in area normalized rate constants (Table 3.1).

Table 3.1 Predicted surface area-normalized rate constant (k_{SA}), correlation coefficient and intersection time for the time dependant disappearance of Cr(VI) from unbuffered solution at various initial pHs (pH_i) in the presence of various micron-size ZVMs.

ZVM	M :Cr (w/w)	pH_i [a]	pH_f [b]	k_{SA1} [c] (mL min^{-1} m^{-2})	r^2_{KSA1}	k_{SA2} [d] (mL min^{-1} m^{-2})	r^2_{KSA2}	*I*-time[e] (min)
Fe^0	310	1.09	1.15	7.71	0.9891	N/A [f]	N/A	N/A
	300	2.11	2.19	4.67	0.9919	N/A	N/A	N/A
	305	3.06	4.14	0.070	0.9688	5.7×10^{-3}	0.9789	24
	309	4.81	6.25	0.067	0.9872	5.3×10^{-3}	0.9897	30
	297	5.71	6.98	0.058	0.9911	5.1×10^{-3}	0.9675	13
	289	7.23	8.11	0.050	0.9764	4.7×10^{-3}	0.9723	10
Mg^0	517	1.85	4.22	7.481	0.9901	N/A	N/A	N/A
	364	5.62	9.16	no appreciable Cr(VI) reduction observed [f]				
Zn^0	340	2.12	2.61	37.52	0.9888	N/A	N/A	N/A
	628	8.08	7.32	substrate (92%) remained after 30h				
Cu^0	299	2.11	2.33	24.33	0.9839	N/A	N/A	N/A
	374	5.86	6.15	substrate (94%) remained after 30h				
	543	8.08	7.40	substrate (86%) remained after 30h				
Pd^0/γ-Al_2O_3	823	2.14	2.59	no appreciable Cr(VI) reduction observed				
	378	5.78	5.93	no appreciable Cr(VI) reduction observed				
$Pt^0/\ \gamma$-Al_2O_3	780	2.01	2.50	no appreciable Cr(VI) reduction observed				
	590	5.89	6.21	no appreciable Cr(VI) reduction observed				

[a] initial pH, [b] final pH, [c] surface area normalized rate constant for the initial decay, [d] surface area normalized rate constant for the second decay, [e] *I*. time refers to the intersection time between the two modeled decays, [f] less than 2% decrease in [Cr(VI)] after 30h.

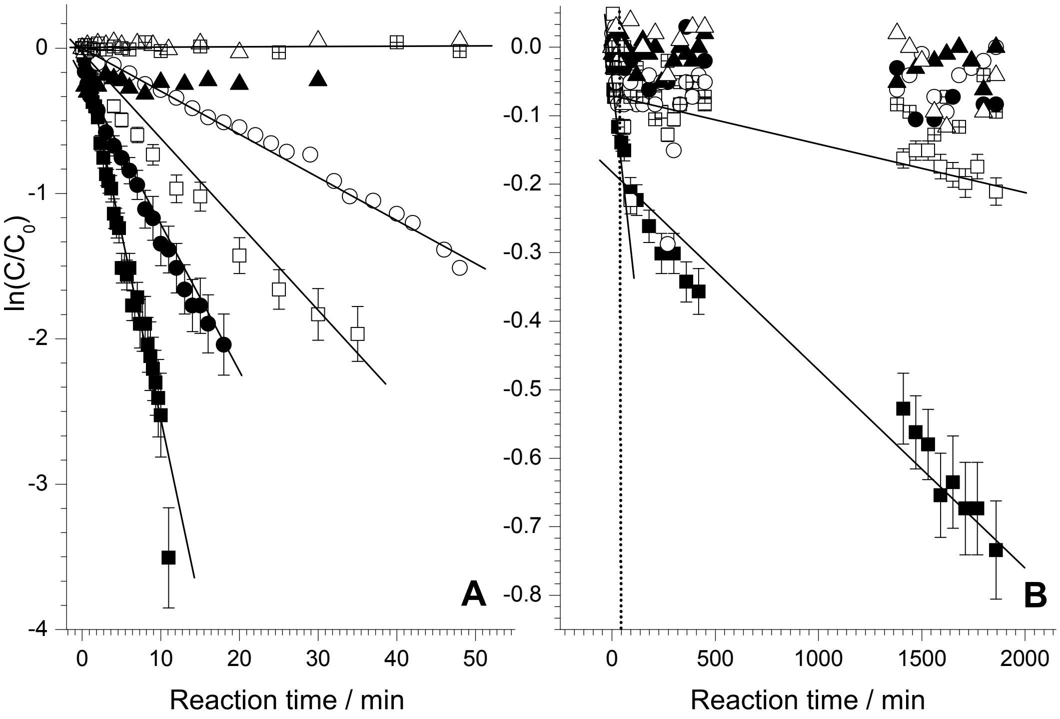

Figure 3.1. Plots of the variation with time of the ln of the mean Cr(VI) concentration (mg L^{-1}) when reacted at (A) pH 2.0± 0.1 or (B) 6.0± 0.1 with various micron-scale zero-valent metals. (■) Fe, (□) Cu, (●) Zn, (○) Mg, (▲) Ni, (Δ) Si and (⊞) Al. Uncertainty in the determination of selected Cr(VI) concentrations was omitted to facilitate the plot visualization. The vertical dotted line in pane B represents the *I*. time between the two exponential decay models.

The ability of several other zero-valent metals (Cu^0, Zn^0, Mg^0, Ni^0, Si^0 or Al^0) to mediate Cr(VI) reduction were also evaluated at various pHs. For certain metals (Ni^0, Si^0 and Al^0), no appreciable reduction of chromate was observed at any of the tested pHs, the ZVM to Cr ratio, or the amount of dissolved oxygen (DO) in the extract. A one-way analysis of variance was applied between the various Fe and Zn data sets (at pH 2.0 with a 99% level of confidence, p=0.01) to study the statistical significance of differences between kinetic models. The test indicated that at the 0.01 significance level the results are significantly different. It can be assumed that for the results for the other ZVMs which are slower are also significantly different from ZVI. The thermodynamic instability of these ZVMs in the presence of water favours the formation of oxides/hydroxides on the surface impeding (completely) the transfer of electrons from the metal surface to the adsorbed chromate. In the last decade, Si^0 has emerged as an efficient reductant of chlorinated hydrocarbons [105,158,159]. In the Si-H_2O system, the redox couple formed by Si and SiO_2 has a standard reduction potential (E_H^0) of -0.78 V (*vs.* SHE) making it a possible candidate as an electron donor following the reaction:

$$Si^0 + 3H_2O \rightarrow H_2SiO_3 + 4H^+ + 4e^- \qquad (2)$$

It has been demonstrated that silicon, when oxidized by oxygen and/or water, results in the formation of SiO_2, SiO groups and hydrogen-terminated silicon (≡Si-H) species on the metal surface that decreased reduction reactivity appreciably [159]. In our experiments, the reduction of chromate with commercial silicon was not observed for more alkaline pHs, increased mass concentration of Si^0 and/or de-oxygenating the chromate extract. As reported in Table 3.1 appreciable decreases of pH were observed (from 8.10 to 7.54 or from 10.04 to 8.15 (depending on the initial charge of Si^0 in the reaction mixture). This behaviour indicated the consumption of hydroxide ion (OH^-) possibly to form $HSiO_3^-$ ($SiO_2 + OH^- \rightarrow HSiO_3^-$) without further changes in the activation of the silicon surface and gaseous evolution was not observed. Studies have reported increased detoxification of certain pollutants at alkaline conditions when a combination of Si^0 and Fe^0 was used [105,159]. Experiments were performed at pH 10.0 using the Si-Fe system 60:40 (w/w). A decrease in pH from 10.0 to 9.12 was observed, and a chromate reduction rate (k_{SA1} of 7.3×10^{-3}; $r^2=0.9479$, k_{SA2} of 3.2×10^{-3} $mLmin^{-1}m^{-2}$; $r^2=0.9556$) comparable to the reduction rate using Fe^0 alone. On the other hand, the formation of soluble silicates (H_2SiO_3) is favoured only if the protective native oxide layer (SiO_2) is removed by HF [157]. For soil remediation, difficult manipulations with strong oxidant acids were to be avoided, since it is unlikely to be implemented in field-scale applications.

Reduction of chromate in the Tween® 20 formulation was observed with Cu^0, Zn^0 or Mg^0 in acidic media. In contrast to the iron particles, Cu^0, Zn^0 or Mg^0 metal particles were used as-received with no further pre-treatment to remove native oxides, yet virtually complete reduction of Cr(VI) was achieved. At more alkaline conditions these metals are thermodynamically unstable in water, so the formation of a protective layer of hydroxide and/or oxide was favoured, that impeded the transfer of electrons from the ZVM core to the adsorbed chromate. Although these zero-valent metals might be considered as possible substitutes, none of the tested metals proved to be as efficient as Fe^0 at mediating the reduction of Cr(VI) ions.

3.3.2 Reaction Probes

Figure 3.2 presents changes, with time, in the dissolved chromium and iron speciation for an initial pH of 2.0. It can be seen that the total chromium concentration remained relatively unchanged, indicating that the chromium hydroxide precipitation under these conditions was not appreciable or very slow, so that its adsorption to the iron surface was negligible. Alternately, it might be postulated that the $Cr(OH)_3$ might be retained within the interior of the surfactant micelle appreciable diminishing the precipitation onto the iron surface. Chromate was totally reduced to Cr(III) in less than 12 minutes. Total dissolved iron was gradually increased the result of ZVI dissolution, but only low concentrations of Fe^{2+} were observed if Cr(VI) remained in solution. In the presence of strong oxidizing agent (chromate), Fe^{3+} was dominant since it is more thermodynamically stable at such high oxidation-reduction potential. Appreciable quantities of Fe^{2+} were accumulated only after most of the $HCrO_4^-$ had been consumed. These observations corroborate the results from previous research [153,156,157,160].

The evolution of gas bubbles (likely H_2) from the Fe^0 surface were observed in the reactor. ZVI is considered to react In a series of redox reactions with adsorbed chromate, with water and/or with dissolved oxygen (DO) to generate Fe^{2+}, hydrogen gas and Cr(III). If excess chromate is present in solution, Fe^{2+} is further oxidized to Fe^{3+}. Since the total concentration of Cr was not altered, it can be assumed that the precipitation of $Cr(OH)_3$ or $Cr_xFe_{(1-x)}(OH)_3$ occur more slowly and/or at higher pH.

Further experiments (Table 3.2) were conducted in which the oxygen in solution was reduced to very low levels. Modest decrease in the pseudo first-order rate constant from 0.2313 to 0.1816 min^{-1} for pH 2 and comparable decreases in k_1 and k_2 for pH ~5 were observed together with a decrease of ferrous ion production indicating that dissolved oxygen is a facultative participant in Fe^0 oxidation.

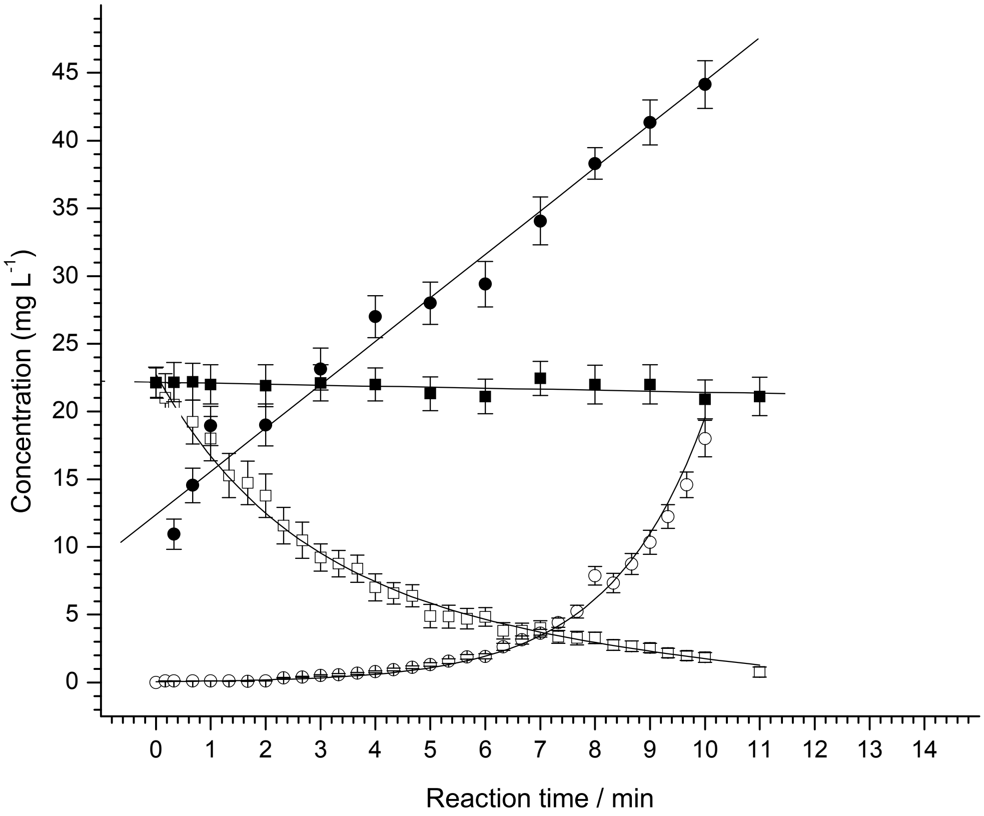

Figure 3.2. Variations, with time, in the soluble concentrations of total Cr, (■); Cr (VI), (□); total Fe, (●); or Fe^{+2}, (○).for reaction with initial conditions of pH 2.0±0.1 and [Cr(VI)] of 22.1 mg L^{-1} in the presence of Fe^0 granules (7.2 g L^{-1}).

Table 3.2 Variations in the observed pseudo-first order rate constant (*k*) following various pre-treatments of the micron sized Fe^0 surface prior to reactions at pH 2.0 or 5.0 for Cr(VI) and Fe concentration of 24.5 mg L^{-1} and 7.0 g L^{-1} respectively.

Treatment	**pH_i**	**k_1 [a] (min^{-1})**	**r^2_1**	**k_2 [a] (min^{-1})**	**r^2_2**	***I*.time [b] (min)**
Acid-washed ZVI	2.1	0.2313	0.9919	N/A [c]	N/A	N/A
	4.8	3.4×10^{-3}	0.9872	2.7×10^{-4}	0.990	30
Acid-washed ZVI then stored under H_2	2.2	0.4495	0.9911	N/A	N/A	N/A
	5.0	6.4×10^{-3}	0.9897	1.0×10^{-3}	0.9942	30
Acid-washed ZVI, equilibrated 24h under vacuum then stored in N_2	2.1	0.1582	0.9874	N/A	N/A	N/A
	4.9	2.1×10^{-3}	0.9896	2.3×10^{-4}	0.9921	30

[a] The sum of two exponential decays was used to model the observed kinetic results (k_1 and k_2), [b] *I*- time, intersection time between the two modeled decays, [c] N/A, not applicable.

Evidence to support the participation of hydrogen adsorbed on the iron particles was also sought. Zero-valent iron particles were stored either in a H_2 atmosphere for 60 min or in a vacuum for 24 h followed by storage under a N_2 atmosphere for 60 min. Table 3.2 summarizes the kinetic parameters obtained with storage pre-treatment for various ZVI pre-treatments. The greatest increase in the reaction rate was observed when working with ZVI that had been stored under a H_2 atmosphere. For reaction initiated at pH 5, a 3-fold increase of k_1 and a 4-fold increase of k_2 was observed. A fraction of the hydrogen adsorbed to Fe^0 might be in a dissociated form (hydrogen atoms) where it is a powerful reductant. Studies have suggested that iron can activate H_2 sorbed to noble metals such as palladium, where the hydrogen gas is dissociatively intercalated into the bulk of the metal to become a strong and efficient reductant [159,160].

3.3.3 Reduction of Cr(VI) using nano-sized metal particles

The synthesis of metal nano-partices reported by Zhang *et al*. (1998) produced metallic particles with a mean diameter of ~60 nm, and an average specific surface area of 33.5 m^2 g^{-1} [135,136,161]. It is presumed that the metal particles synthesized in the current studies were characterised by comparable dimensions. Analogous procedures were adapted for copper salts to synthesize nano-scale copper particles, with presumed dimensions between 5-30 nm and a specific surface area of 29.5 m^2 g^{-1} [162].

Rapid and extensive transformation of hexavalent chromium was achieved at most pHs using either nano-scale Fe^0 or nano-scale Cu^0 particles as summarized in Table 3.3 and Fig. 3.3. The salient observations included the enhanced reactivities of the nano-scale metal particles (relative to their micron-scale analogs) at both pHs. In contrast to mircon-scale Fe particles, with more circum neutral conditions, a single exponential decay model (r^2=0.984, k_{SA} 0.040 mL min^{-1} m^{-2}) provided an adequate fit to the observed data. Whereas for Cu^0 particles an increase from an almost negligible transformation of Cr(VI) to a 60% reduction in less than 10 min. (k_{SA} 24.3 mL min^{-1} m^{-2}). By this time, surface inactivation had become complete, as evidenced by a plateau in the disappearance curve of Fig. 3.3. This behaviour indicated that diffusion of chromate to the Fe^0 surface, adsorption and reduction of the toxicant were fast when compared with the rate of formation of a passivating layer of Cu (oxy)hydroxides.

Table 3.3 Pseudo-first order rate constant (*k*), surface-area normalized rate constant (k_{SA}), calculated half-life ($t_{1/2}$), surface area normalized half- life ($t_{SA\ 1/2}$), and correlation coefficient (r^2) for the pseudo-first order model of the time dependant disappearance of Cr(VI) from unbuffered solution at various initial pHs (pHi) in the presence of nano-size particles.

ZVM	**M:Cr (w/w)**	**pH_i**	**pH_f**	**r^2**	***k*** **(min^{-1})**	**k_{SA} ($mL\ min^{-1}\ m^{-2}$)**	**$t_{1/2}$ (min)**	**$t_{SA\ ½}$ ($min\ m^2\ mL^{-1}$)**
Fe	81	2.06	2.49	0.9794	0.919	0.549	0.75	1.3
	368	2.00	2.64	0.9835	4.62	2.76	0.15	0.25
	360	6.06	5.11	0.9837	0.067	0.040	10	17
Cu	193	2.03	2.50	0.9511	0.865	0.586	0.80	1.2
	398	5.31	7.45	0.9530	0.096	0.065	7.2	11
Supported nano-sized metal particles								
Fe^0/Al_2O_3	24	2.11	2.61	0.9862	5.58	2.23	0.12	0.31
	373	5.99	8.25	0.9853	0.219	0.089	3.2	7.8
Fe^0/CMC	40	2.01	2.55	0.9755	5.50	2.11	0.13	0.33
	381	5.99	6.15	0.9676	0.489	0.188	1.4	3.7
Fe^0/soluble starch	55	2.04	2.54	0.9862	2.00	2.00	0.13	0.31
	420	5.97	8.25	0.9853	0.223	0.223	1.4	8.6
Cu^0/Al_2O_3	103	2.00	4.02	0.9863	4.41	2.26	0.16	0.31
	340	5.07	7.30	0.9511	0.182	0.081	3.08	8.60
Cu^0/CMC	56	2.00	2.33	0.9801	8.35	4.07	0.083	0.17
	345	6.05	7.11	0.9633	0.408	0.199	1.7	3.5
Cu^0/soluble starch	266	2.04	4.02	0.9985	8.96	3.98	0.077	0.17
	206	6.30	7.30	0.9511	0.462	0.205	1.5	3.4

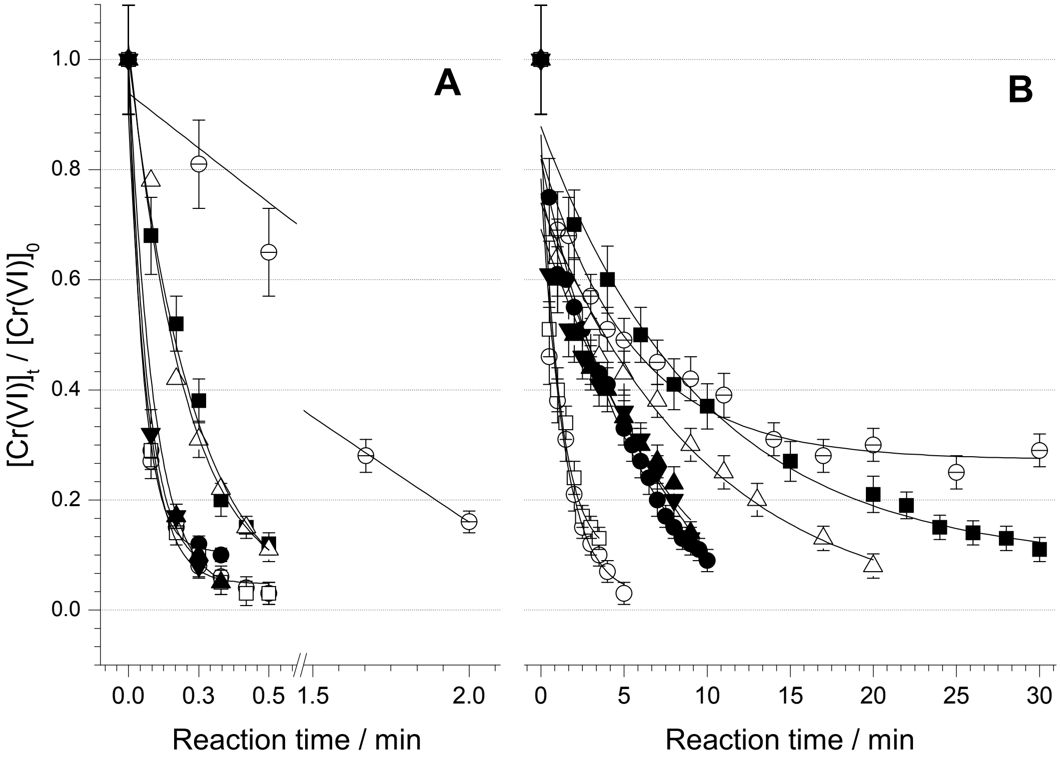

Figure 3.3. Plots of the variation with time of the mean Cr(VI) concentration (mg L^{-1}) when reacted at **(A)** pH 2.0± 0.1 or **(B)** 6.0± 0.1 with various nano-scale ZVM formulations. (■) Fe^0; (●) Fe^0/Al_2O_3; (o) Fe^0/soluble starch; (□) Fe^0/CMC; (⊖) Cu^0; (∆) Cu^0/Al_2O_3; (▲) Cu^0/soluble starch; (▼) Cu^0/CMC.

The enhancement of reactivity of these nano-scale particles were considered to be a consequence of their increased surface area and higher atom efficiency (fraction of metal atoms that can be used in the reaction). However, several attempts to prepare nano-scale particles of Zn^0 using similar methods were unsuccessful. The decomposition rates for nano-scale particles were adequately modeled by a single decay function at both pH 2 and at pH 6.

The inclusion of a stabilizing agent in the preparation of nano-particles seemed to prevent the agglomeration of the freshly prepared nano-scale metal particles which prolonged their increased reactivity [134,135,144,145,163,164]. Three different support materials {aluminum oxide, soluble starch and carboxymethylcellulose (CMC)} were evaluated for their influence on reactivity of the formulated nano-particles. At the more acidic pH, comparable initial rates were observed for nano-scale Cu^0 and Fe^0 particles supported on these materials. The one modest difference between the surface area normalized rate constants - the rate constant for the Al_2O_3 support was decreased by less than three-fold relative to the other two materials in the less acidic medium.

Chromate reduction was modestly enhanced for both Cu^0 and Fe^0 nano-scale particles when working with all three support materials. This phenomenon was caused by the ability of Fe and Cu ions to coordinate with hydroxyl/carboxylic groups on the surface of the starch or CMC polymer. UV-vis studies of the resulting solutions (coordinated Fe^{+3} and Cu^{+2} to their respective ZVMs) displayed monotonically increasing spectra of nearly exponential slope (characteristic of a bandlike electronic structure) toward shorter wavelengths, and complete disappearance of the prominent absorption peak) at 300 nm for starch- and CMC- complexed Fe^{+3} ions, or at 605 nm for corresponding Cu(II) compounds. These observations suggest that the reduced Fe and Cu particles do not exist as isolated atoms, but rather as clusters. The co-ordinating groups (hydroxyl, carboxylic) act as points of contact that anchor the cluster and impede the nano-particles from agglomerating. The observed reactivities are in agreement with previous reports for Cu^0 and Fe^0 nano-clusters [143,145,164].

For the Al_2O_3-supported nanometer scale metal particles, no changes were observed in the d-d transition band which suggested that the metal particles were retained on the Al_2O_3 surface by weaker forces (possibly Van der Waals forces). When compared to more-protected clustered nano-particles, stabilized Al_2O_3 particles present more exposed metal surface area in contact the aqueous media. The nano-particles remain susceptible to inactivation by passivation and/or agglomeration. The decreased formation of clusters by the Al_2O_3-supported nano-particles might explain the modest decrease for chromate reduction in alkaline media.

3.3.4 Comparisons of nano- *vs*. micron-scale ZV metals

A comparison of the surface area normalized rate constants (k_{SA}s) observed for Fe^0 and Cu^0 are summarized in Table 3.4. At pH 2, there were only modest differences among the k_{SA} values (3.00 ± 48%) for the Fe^0 micron-scale or nano-scale materials (bound or unbound). In contrast, differences in k_{SA}s for Cu^0 particles were appreciable (>28-fold). The k_{SA}s were decreased for both Fe^0 and Cu^0 at all conditions when the pH was increased from 2 to 6. For unbound nano-scale metal at pH 6, the rate constants were similar between the two metals (0.089 for Fe^0 vs. 0.064 for Cu^0) and this value approximated the k_{SA1} value (0.070) observed for micron-scale Fe^0 at the same pH. The one major difference was that this rate was maintained throughout the entire 30 min of monitoring. For Cu^0, the inhibitory effect of the oxyhydroxide layer was severe so that for micron-scale particles, some 86% of the Cr(VI) substrate remained after 2000 min of reaction at pH 8 and 94% of the substrate remained after this time at pH 6. Similarly, for nano-scale unbound Cu^0 despite an initially rapid rate, the reaction had essentially ceased after 15 min with ~26% of substrate remained (Figure 3.3). The binding of the nano-scale metal to a hydroxylic surface or to polyhydroxy compounds did not modify rates appreciably relative to unbound homolog. Other than a 4-fold increase in rate constant at pH 2 when Cu^0 was bound, other rate constants remained similar. None the less, for bound nano-scale Cu^0, the reaction was very extensive (>89%).

Even though nano-particles seems to overcome the drawbacks of inactivation and the consequent loss of reactivity, the potential health effects of their widespread use make their use of concern [165,166].

Table 3.4 A comparison of calculated specific area normalized rate constants observed for micron-scale *vs*. nano-scale (either bound or unbound) zero-valent metal (Fe^0 or Cu^0) at pH 2 or 6.

	Micron-scale			*Nanoscale*			
	Unbound			*unbound*		*Bound*	
pH	2.0 ± 0.1	6.0 ± 0.1		2.0 ± 0.1	6.0 ± 0.1	2.0 ± 0.1	6.0 ± 0.1
k_{SA}	k_{SA1}	k_{SA1}	k_{SA2}	k_{SA}	k_{SA}	k_{SA}	k_{SA}
Fe^0	4.67	0.070	0.005	2.76	0.089	2.11±12%	0.167±42%
Cu^0	24.33	NAR [a]		0.865	0.096	3.40±29%	0.162±43%

[a] NAR = no appreciable reaction {[Cr(VI)] decreased by 6% after 30h at pH 6 or by 14% after 30h at pH 8}.

3.4 Conclusions

The reductive remediation of chromate is strongly affected by the passivation of the metal surface and the consequent decrease in reactivity. The removal of (oxy)hydroxides from the metal surface by acid-washing substantially increased reactivity. Relative to conventional kinetic treatments, a model consisting of the sum of two exponential decays appreciably extended its applicability to higher pHs and to longer reaction times. The revised model can be used to compare efficiencies of various zero-valent metal / bimetallic formulations by comparing rates at exposed reactive sites (k_1) or through the oxyhydroxide layer (k_2). Additionally the intersection time (*I*-time) between the two models measures the protective effect(s) of metal pre-treatment and/or other additives in the reaction medium. Despite the increased reduction potentials of other metals (Al^0, Si^0, Cu^0 and Zn^0) relative to ZVI, their potential effectiveness in the field was restricted by the inactivating effects of rapid corrosion in aqueous media. The production of hydrogen gas and also ferrous iron ion should further encourage microbial growth that can also contribute to Cr(VI) reduction. Additionally it is anticipated that nano-scale iron particles can be used as efficient reducing reagents in regulating the standard reduction potential in the subsurface to mediate chemical and/or biological remediations. The enhancement of the rate of reduction of chromate was likely the result of an increased specific surface area to mass ratio, higher surface reactivity and the increased atom efficiency. Modestly increased rates of reduction were observed when freshly prepared nano-particles were anchored to carboxymethylcellulose or to soluble starch. Polymer activated rate increases supported the concept of the formation of intramolecular clusters of zero-valent metal. Further studies are needed to expand the applications for nano-sized metals and bimetallic mixtures to other toxicants. However, an important issue not addressed in these studies is the relative reactivities and atom efficiencies of nano-sized metal particles when measured over extended times that are relevant to the remediation of slow-moving plumes associated with permeable reactive barriers.

Chapter

Four

Preface

In Chapter three, the reactivity of various micron- and nano-sized zero-valent metal particles were evaluated for reactivity towards a surfactant preparation containing hexavalent chromium under selected reaction conditions. A rapid inactivation of the metallic surface due to the formation of (oxo)hydroxixde species caused a loss of reactivity, with the result that the reduction rate of hexavalent chromium was decreased dramatically.

When the hexavalent chromium reduction was performed (under similar reaction conditions) with nano-sized metallic particles, increased rates of reduction were observed. The enhanced rate of reduction of chromate was likely the result of an increased specific surface area to mass ratio, a higher surface reactivity and the increased atom efficiency.

In the current chapter, efforts are made to accelerate the rate of Cr(VI) reduction and to diminish and/or prevent the passivation of the metallic surface. A variety of mixed metallic particles are prepared and tested as accelerators for the detoxification of chromate. Observations relating to the reactivity and passivation of the micron-sized bi- and trimetallic mixtures relative to zero-valent iron, are presented and discussed. Selected nano-sized bimetallic analogs are also prepared, purified, and their reactivities towards the reductive remediation of a surfactant suspension containing chromate are reported under a selection of reaction conditions.

A portion of this chapter has been published in **J. Hazard. Mater., 169 (2009) 1081-1087**. Authors: M. Rivero-Huguet, W.D. Marshall.

Chapter

Four

Reduction of hexavalent chromium mediated by micro and nano-sized mixed metallic particles

4.1 Introduction

Chromium is a pollutant that is frequently found in brownfields, as well as in surface and subterranean waters throughout the industrialized world. Whereas chromium(III) is an essential element for living organisms at ultra-trace levels, hexavalent chromium engenders environmental and health problems because of its potent toxicity, mutagenicity and carcinogenicity [24,25]. Over the last several years, a great deal of effort has been expended to identify and improve strategies to mitigate chromium(VI) contamination. In particular, several studies have demonstrated that zero-valent iron (ZVI) is an efficient and inexpensive reductant for Cr(VI) [109,111,152,153]. Under appropriate conditions, complete removal of Cr(VI) from solution has been reported in several laboratory studies and in both pilot and field-scale iron metal permeable reactive barriers (PRBs). The rates of Cr(VI) reduction vary considerably depending on pH, zero valent iron concentration and type. However, the reactivity of ZVI in the presence of water and/or oxygen, mediates the oxidation of iron metal to ferrous ion and the precipitation of iron species (α-FeOOH, α-Fe_3O_4, γ-FeOOH, $Fe(OH)_2$ and $Fe(OH)_3$, $FeCO_3$) on the ZVI surface [124]. As a result, the rate of reduction of Cr(VI) to Cr(III) dramatically diminishes with time. Several attempts have been made to enhance the efficiency of this redox reaction by diminishing the inactivating effects of the resulting passivation layer [111,128,152]. On the one hand, adding a second catalytic metal such as Pd, Pt, Ag or Ni to the surface of the iron particles can accelerate the detoxification of Cr(VI) solutions. The second zero-valent metal on the iron surface serves not only as a catalyst but also as a protecting agent against surface corrosion. For example, it has been suggested that the enhanced reactivity of palladized iron is likely due to the fact that Pd has the ability to intercalate hydrogen into its lattice and dissociate it into a powerful reductant [128-131]. Hexavalent chromium reduction by Fe-based particles is a surface-mediated process; the increased surface area relative to the mass of iron increases the reduction rate. There is appreciable evidence that nano-sized metal particles are more reactive than commercial micron-scale powders, most probably the result of high specific surface area and increased surface reactivity [134]. However, the limitations for practical applications with ZVI techniques have encouraged scientists to evaluate other zero-oxidation-state metals as electron donors. Several other metals, particularly those with very negative reduction potentials (e.g., Zn, Sn, Si, Al) can be substituted for iron as reductants. Zero-valent Zn and Sn have been demonstrated to de-halogenate organic compounds more rapidly than Fe [106,121].

Here the mobilisation and detoxification of Cr(VI) from a contaminated site was evaluated. The Cr(VI)-contaminated soil sample was treated with one of several surfactant formulations, as a possible mobilisation aid to dislodge the target ion from the particulate surfaces. The resulting extract (Tween® 20) was reacted with various zero-valent formulation (Al, Cu, Fe, Mg, Ni, Si or Zn), bimetallic mixture (Ag/Fe, Al/Fe, Cu/Fe, Co/Fe, Mg/Fe, Ni/Fe, Pd/Fe, Pd/Cu, Pd/Zn, Si/Fe, Zn/Fe), trimetallic mixture (Cu/Zn/Fe, Pd/Cu/Fe or Pd/Zn/Fe) or nanometer-sized Cu and Fe particles, bimetallic ZVI nano-particles (Pd/Fe, Cu/Fe) as well as nano-particles that had been stabilized with γ-Al_2O_3, carboxymethylcellulose (CMC) or soluble starch. The detoxification of hexavalent chromium by reaction with micron- or nano-scale mono-metallic zero-valent formulation had been evaluated previously [167].

In the current report, an evaluation of the impact of a second metal (or a combination of two metals) doped onto the ZVM surface on the reduction of chromate at various pHs is described.

4.2 Experimental

4.2.1 Reagents and materials

Test surfactant (Tween® 20), $AgNO_3$ (99.8% purity), $CuSO_4 \cdot 5H_2O$ (≥98% purity), $ZnSO_4 \cdot 7H_2O$ (99% purity), $CoCl_2 \cdot 6H_2O$ (98% purity), $NiCl_2$ (98% purity), $MgCl_2 \cdot 6H_2O$ (≥99.0% purity), $Al_2(SO_4)_3 \cdot 18H_2O$ (≥98% purity), Na_2SiO_3 (SiO_2 44-47% purity), ethylenediaminetetraacetic acid copper(II) disodium salt (≥97.0% purity), 1,10 phenanthroline (≥99% purity), $NaBH_4$ (10-40 mesh, 98% purity), Al_2O_3 (150 mesh, 58Å, surface area 155 m^2 g^{-1}), soluble starch (ACS quality reagent), sodium carboxymethylcellulose (NaCMC, mean MW, 90,000) were used as received from Sigma-Aldrich, Oakville, ON, Canada.

Zero valent metals; iron metal (40 mesh, specific surface area 1.01 m^2 g^{-1}), copper powder (100 mesh, 99.5%, specific surface area 0.048 m^2 g^{-1}), zinc powder (100 mesh, 99.9%, specific surface area 0.059 m^2 g^{-1}), Magnesium granules (20 mesh, 98%, specific surface area 0.0786 m^2 g^{-1}), aluminium (200 mesh, 99% purity) and silicon powder (325 mesh, ≥99% purity), S-dephenyl carbazide, HCl (37% V/V), H_2SO_4 (95.0-98.0% purity) ACS reagent grade ethanol and acetone were obtained from Fisher Scientific, Napean, ON, Canada.

Potassium hexachloropalladate (K_2PdCl_6) and Ni powder (99.7% purity, -50 +100 mesh) were purchased from Alfa-Aesar, Ward Hill, MA, USA.

Distilled de-ionised water (DDW) was obtained from a Millipore-Q purification system (Millipore Bedford MA, USA) with a resistivity of 18.0 $M\Omega \cdot cm$ and was used for the preparation of all aqueous solutions.

Aqueous metal standard solution of Cr or Fe, 1,000 mg L^{-1}, traceable to the National Institute of Standards and Technology (NIST) primary standard and multi-element standard solution used for quality control (Cr 200.2 mg L^{-1} and Fe 1001 mg L^{-1}) were purchased from SCP Chemical Co., St-Laurent, Qc, Canada.

4.2.2 Acid pre-treatment of zero valent iron

Acid-washed iron was used in all the experiments. A known quantity of iron granules were washed copiously with 6 M HCl and rinsed five times with DDW, three times with ethanol and a further three times with acetone then dried in a N_2 stream for 2 h. To inhibit oxidation, the iron powder was stored under a nitrogen atmosphere prior to use.

4.2.3. Preparation of bi and trimetallic mixtures

The general preparations described by Zhang *et al*. were followed [136]. Pd/Fe, Ag/Fe, Cu/Fe, Zn/Fe, Co/Fe, Mg/Fe, Ni/Fe, Al/Fe, Si/Fe were prepared from pre-treated iron granules and Pd/Cu, Pd/Zn were obtained from the Cu or Zn zero-valent metal (ZVM), respectively, without previous pre-treatment. Sufficient K_2PdCl_6, $AgNO_3$, $CuSO_4$, $ZnCl_2$, $CoCl_2$, $MgSO_4$, $NiCl_2$, $Al_2(SO_4)$ or Na_2SiO_3 to result in the desired surface coverage on the iron (w/w) surface, was added to the aqueous metal suspension that was gently mixed on a rotary evaporator during 3h. A similar procedure was followed for the preparation of trimetallic mixture (Cu/Zn/Fe, Pd/Cu/Fe or Pd/Zn/Fe) in which the third metal was doped onto the bimetallic mixture (Zn/Fe or Cu/Fe) in a 2% (w/w) ratio.

4.2.4 Determination of hexavalent Chromium adapted to a microscale

The phenylcarbazide method recommended by the APHA, was adapted to work on a microscale level [154]. Once filtered, the samples were immediately inserted into the Hach test tube with a freshly prepared phenylcarbazide solution in acetone (200 µL, 5 g L^{-1}) and H_2SO_4 (5 µL, 10% v/v). The reaction was permitted to continue for 5-10 min then diluted with 10 mL DDW.

4.2.5 Determination of Ferrous ion in surfactant extract

The standard Analysis Method 3500-Fe B based in the colorimetric reaction with 1,10-phenantroline was followed [154].

4.2.6 Metal determination by Atomic Spectroscopy

Total chromium, copper or iron determination was performed by flame atomic absorption spectroscopy (FAAS) at 357.9 nm, 324.8 nm or 248.3 nm respectively using a GBC 903 (GBC Scientific Equipment Pty Ltd., Australia). Alternatively, determinations were performed by inductively coupled plasma optical emission spectrometry (ICP-OES) using a Varian Vista-MPX spectrometer (Varian Australia Pty Ltd., Australia) and multiple emission lines for Cr (267.71, 283.56, and 357.87 nm), for Cu (327.40, and 324.75 nm), for Fe (238.20, 259.94 and 234.35 nm), for Al

(396.15, 308.22 and 309.27), for Si (251.61, 251.43 and 288.16), for Zn (213.86, 202.55, and 206.20 nm), for Mg (279.55, 280.27, and 285.21) and for Ni (231.60, 230.30, and 221.65 nm) were selected to assess the spectral interferences and a FACT (fast automated correction technique) model was used to correct for potential interferences.

4.2.7 Preparation of nanometer sized bi-metallic particles (Cu and Fe)

Zero-valent metal nanoparticles (Cu or Fe) were prepared using a water-soluble approach while working in a H_2 atmosphere to improve the reducing conditions of the iron or copper salt [135,136,144,145].

Solutions were prepared in DDW that had been purged with purified N_2 for 2 h to remove dissolved oxygen (DO). Prior to the reaction, an aliquot of the stock solution of $FeCl_3$ or disodium ethylenediaminetetraacetate copper(II) complex was added to the support material (water-soluble starch, NaCMC or γ-Al_2O_3) to provide a solution/suspension with the desired metal (Cu, Fe) content and support concentration [~0.5% (w/w)]. Nano-sized metal particles were synthesized by adding 250 mM aqueous $NaBH_4$ dropwise in a H_2 atmosphere to 45 mM Cu or Fe aqueous solution. The flask was vigorously shaken by hand (magnetic stirring was avoided to reduce magnetically induced aggregation of the resultant iron nanoparticles) during the reaction.

When gas (hydrogen) evolution had ceased (after ~15 min), the nanoparticles were separated from the solution and then rinsed four times with water. Dry nanoparticles were obtained by successive washings with ethanol and acetone followed by drying at 110 °C for 6 h.

The Fe nanoparticles were used either directly as monometallic agent or loaded with a second metal (Cu or Pd) to yield bimetallic product. Loading of the second metal on the Fe nanoparticles was accomplished by adding known quantities of $CuSO_4$ or K_2PdCl_6 to the recently prepared Fe nanoparticles and permitting the reaction to proceed for 15 min under a H_2 atmosphere.

For comparison, non-supported nanoparticles were prepared following similar procedures in the absence of stabilizing material. Non-stabilised copper nanoparticles were prepared using $CuSO_4 \cdot 5H_2O$ as starting material.

4.2.8 Estimation of Uncertainties associated with concentration

Spectroscopic measurement uncertainties associated with the determination of Cr and Fe concentrations in the extract were calculated using a cause-and-effect approach as reported previously [155].

4.3 Results and discussion

4.3.1 Reduction of Cr(VI) using micron-scale metallic mixtures

A soil that had been heavily field-contaminated with hexavalent chromium was washed with various surfactant formulations (anionic, non-ionic or cationic) to evaluate the relative efficiency of Cr(VI) mobilization. Once the pollutant had been mobilized from the soil, the solution that resulted was reacted with various metallic mixtures. Previously, it had been observed that the presence of Tween® 20 in the extract of Cr(VI) had no perceptible effect on the reaction kinetics with ZVMs; they were adequately described by either a single or the sum of two pseudo-first-order kinetic models [167]. Table 4.1 summarizes the goodness of fit of a linear model to the experimental data (either a single exponential decay for pHs of ≤ 2.0 or the sum of two exponential decays for pHs ≥ 3.0) and the observed kinetic parameters {surface area normalized rate constant (k_{SA}) and surface area normalized half-life ($t_{SA\ 1/2}$)} for the tested metallic mixture. As reported previously for ZVI, if the initial pH was increased to 3.0 or above, a model consisting of the sum of two-pseudo first order reactions provided an appreciably better fit to the data than did the single exponential decay [167]. This was the case for all of the tested bimetallic mixtures. The first decay was considered to be dominated by reaction that occurred at exposed Fe active sites. Once the passivating (oxy)hydroxide layer had formed, a second decay function described the reaction rate that was decreased but not totally inhibited. The second decay function was considered to model reaction at the surface of the passivated layer. As summarised in Fig.4.1 and Table 4.1, relative to ZVI, only minor differences (less than two-fold) for Cr(VI) reduction rates were observed for certain of the bimetallic mixtures (Al/Fe, Si/Fe/ Pd/Cu or Mg/Fe) when working at the distinctly acidic condition. The other tested bimetallic mixtures (Pd/Cu, Pd/Zn, Pd/Fe, Ag/Fe, Ni/Fe, Zn/Fe and Cu/Fe) accelerated the reduction appreciably at pH~2. None of the bimetallic mixtures decreased the reduction rate appreciably.

It was observed that only palladized or argentized particles accelerated both k_{SA1} and k_{SA2} at pH 2.0 and at pH 6.0; the others bimetallic preparations displayed k_{SA2} rate constants that were almost unchanged relative to ZVI (less than 2-fold increase). However, the magnitude of the values of k_{SA2} were influenced only marginally by pH in the range between 3 and 10. As an example, for Pd/Fe at pHs between 3.1 and 9.3, k_{SA2} ranged between 0.71-0.60 x 10^{-3}.

Table 4.1 Predicted surface area-normalized rate constant (k_{SA}), and calculated surface-area normalized half-life ($t_{SA1/2}$) for the time dependant disappearance of Cr(VI) from unbuffered solution at various initial pHs (pH_i).

ZVM	Wt %	M:Cr (w/w)	pH_i [a]	k_{SA1} [b] (mL min^{-1} m^{-2})	r^2_{KSA1}	*I*.time[c] (min)	k_{SA2} [d] (mL min^{-1} m^{-2})	r^2_{KSA2}
Fe		300	2.11	4.67	0.992	N/A	N/A	N/A
		309	4.81	0.067	0.9872	30	5.3 x 10^{-3}	0.990
Pd/Fe	**0.02%**	337	2.04	4.32	0.978	N/A	N/A	N/A
		350	6.01	0.58	0.987	30	1.1x10^{-2}	0.992
	0.2%	340	1.03	10	0.993	N/A	N/A	N/A
		310	2.06	7.1	0.989	N/A	N/A	N/A
		300	3.01	0.63	0.994	31	3.6x10^{-2}	0.987
		318	9.10	0.53	0.983	32	6.0x10^{-3}	0.991
	1%	300	1.04	55	0.991	N/A	N/A	N/A
		305	2.13	26	0.984	N/A	N/A	N/A
		301	3.02	0.69	0.977	30	0.044	0.988
		310	5.01	0.65	0.991	31	0.015	0.989
		300	7.11	0.59	0.980	30	7.8x10^{-3}	0.978
		314	9.04	0.60	0.984	32	6.4x10^{-3}	0.990
	2%	301	1.02	86	0.994	N/A	N/A	N/A
		305	2.04	62	0.973	N/A	N/A	N/A
		312	3.11	0.71	0.987	29	0.051	0.991
		297	5.02	0.68	0.989	30	0.018	0.990
		305	8.50	0.61	0.983	31	8.9x10^{-3}	0.984
		300	9.32	0.60	0.986	32	7.5x10^{-3}	0.978
Ag/Fe	**2%**	350	1.42	31	0.990	N/A	N/A	N/A

		338	2.33	27	0.998	N/A	N/A	N/A
		312	3.12	0.33	0.989	41	0.019	0.988
		340	4.75	0.31	0.995	45	0.019	0.992
		406	9.70	0.30	0.991	40	$6.4\text{x}10^{-3}$	0.987
Cu/Fe	**2%**	287	2.07	8.6	0.961	N/A	N/A	N/A
		293	5.61	$3.9\text{x}10^{-2}$	0.965	120	$5.3\text{x}10^{-3}$	0.996
Zn/Fe	**2%**	328	2.01	16	0.984	N/A	N/A	N/A
		342	8.08	$2.0\text{x}10^{-2}$	0.967	180	$3.8\text{x}10^{-3}$	0.992
Co/Fe	**2%**	298	2.13	6.7	0.986	N/A	N/A	N/A
		302	6.11	$3.2\text{x}10^{-2}$	0.976	120	$4.9\text{x}10^{-3}$	0.989
Mg/Fe	**2%**	327	2.04	3.9	0.989	N/A	N/A	N/A
		315	6.98	$1.8\text{x}10^{-2}$	0.973	240	$4.9\text{x}10^{-3}$	0.981
Ni/Fe	**2%**	312	2.09	23	0.992	N/A	N/A	N/A
		306	6.23	$2.0\text{x}10^{-2}$	0.988	180	$4.6\text{x}10^{-3}$	0.992
Al/Fe	**5%**	301	2.24	2.2	0.988	N/A	N/A	N/A
		330	6.04	$3.0\text{x}10^{-2}$	0.976	120	$4.8\text{x}10^{-3}$	0.997
Si/Fe	**2%**	246	2.04	2.0	0.980	N/A	N/A	N/A
		310	6.57	$2.8\text{x}10^{-2}$	0.989	30	$3.4\text{x}10^{-3}$	0.978
Pd/Cu	**2%**	278	2.21	73	0.999	N/A	N/A	N/A
		256	8.10	0.67	0.987	150	0.283	0.996
Pd/Zn	**2%**	357	2.23	419	0.993	N/A	N/A	N/A
		259	8.10	1.2	0.988	150	0.244	0.995

[a] initial pH, [b] surface area normalized rate constant for the initial decay, [c] I. time refers to the intersection time between the two modeled decays, [d] surface area normalized surface area normalized rate constant for the second decay, [b,d] The sum of two exponential decays was used to model the observed kinetic results (k_{SA1} and k_{SA2}).

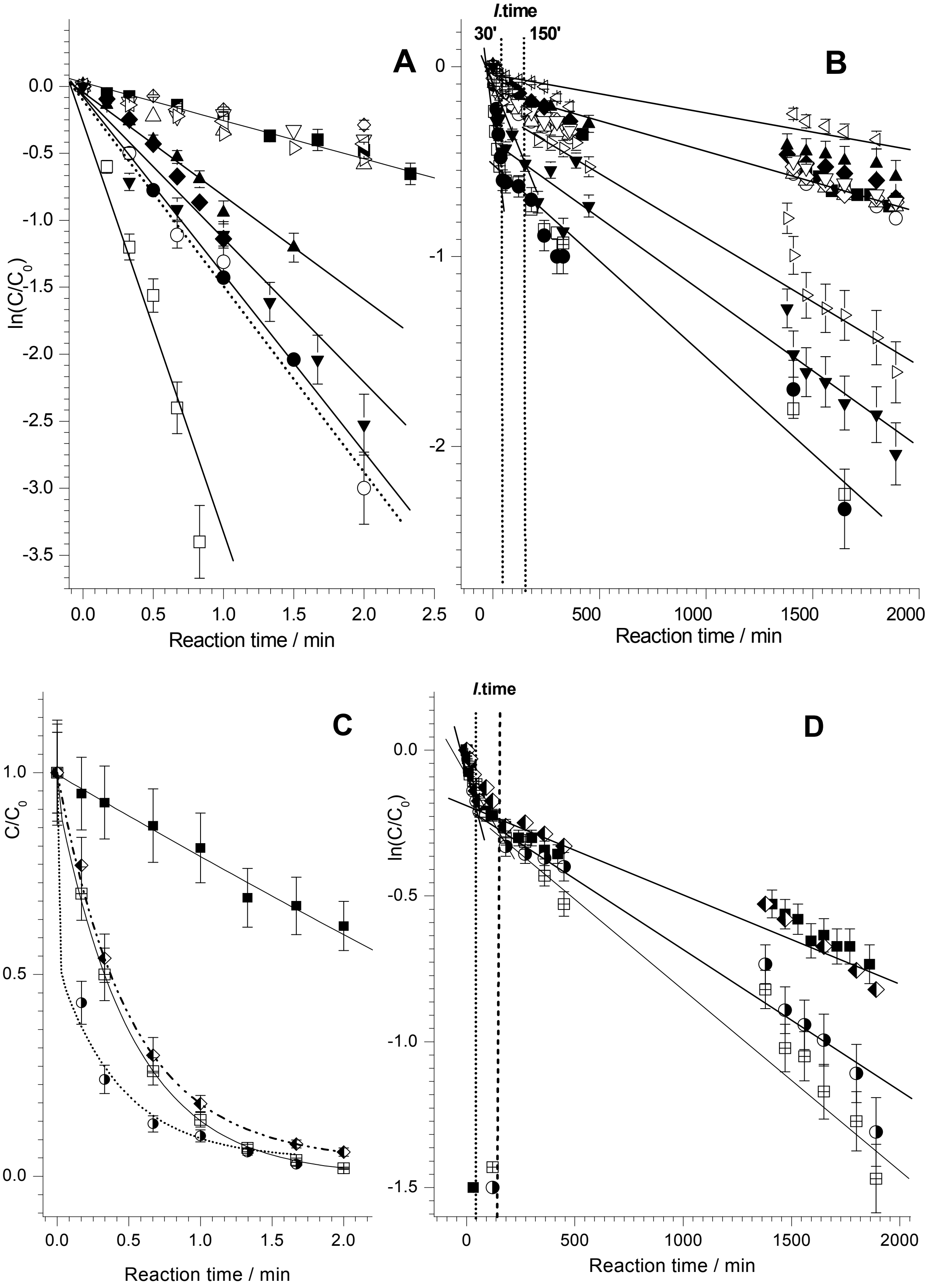

Figure 4.1 Plots of the variation, with time, of ln(C/C$_o$) or (C/C$_o$) where C is the concentration of Cr(VI) at time t and C$_o$ is the initial concentration (mg L^{-1}) when reacted (A) and (C) at pH 2.0± 0.1 or (B) and (D) at 6.0± 0.1 with various metallic

mixtures at a ZVM to Cr(VI) ratio (~300): Fe, (■); 2% Pd/Fe, (□); 2% Ag/Fe, (●); 2% Cu/Fe, (○);2% Zn/Fe, (▲);2% Co/Fe, (Δ);2% Mg/Fe, (◊);5% Al/Fe, (▽);2% Ni/Fe, (♦);2% Si/Fe, (◁); 2% Pd/Zn, (▼); Pd/Cu/Fe, (◑); Pd/Zn/Fe, (⊞); and Zn/Cu/Fe, (⬖). In 1D, the *I*.time, 30 min for Fe, or 120 min for Pd/Cu/Fe and Pd/Zn/Fe has been identified with a dotted line or with a dashed line respectively.

It was considered that k_{SA2} values in this range of pH, could be compared directly without introducing appreciable uncertainty. The approximately 100-fold decrease in rate between k_{SA1} and k_{SA2} was attributed to the rapid formation of a passivating oxyhydroxide layer at the metal surface that impeded the transfer of electrons to the adsorbed chromate.

For certain bimetallic mixtures, there was an appreciable increase in the intersection time between the two models (*I*.time, Table 4.1). This might have resulted from the fact that the cementation of a second metal tended to retard the rate of formation of the passivating oxide/hydroxide layer. The duration of the first step (dominated by the reduction at exposed active sites) was extended eight-fold in the case of Mg/Fe (240 min *vs.* 30 min for ZVI alone). Yet for other bimetals (Pd/Fe or Si/Fe), the duration of the initial stage remained unchanged relative to ZVI.

By contrast, other bimetallic mixtures appreciably increased the rate of reduction of chromate. Based on surface-area normalized pseudo first order rate model, the order of reactivity of the bimetallic mixtures was observed to be: Pd/Fe > Pd/Zn > Ag/Fe > Ni/Fe > Zn/Fe > Pd/Cu > Cu/Fe, suggesting that that one or more might be a suitable alternate material for a permeable reactive barrier (PRB). However, the release of metal ions other than iron, magnesium or possibly aluminium into the soil pore water can raise toxicological concerns.

Among the iron-based bimetallic mixtures, the palladized particles exhibited the highest reactivity. The rate of Cr(VI) disappearance increased with the Pd loading suggesting that the Pd particles are uniformly dispersed on the iron surface.

Fig. 4.2 summarizes the variations in observed rates for metal:Cr(VI) ratios (*w*/*w*) between 40 and 1200 in the presence/absence of palladium or silver metal. For bimetallic mixtures, the surface area normalized pseudo-first rate constant appeared to be linearly related to the Fe to Cr(VI) ratio. Moreover, at similar Fe:Cr(VI) ratios, the rate constants for bimetallic mixtures were increased ~10-fold relative to ZVI. For

Fe-based bimetallics, the increase in rate appeared to be linearly related to the Fe:Cr(VI) ratio. The magnitude of the slope for the various Pd/Fe mixtures (0.2, 1 or 2%) was approximately constant (~0.17) and similar to the slope observed with Ag/Fe. The minor variation in reactivity observed with the bimetallic preparations can be ascribed to differences in the catalytic properties of Pd vs. Ag and are likely due to differences in surface concentration, atomic structures, and/or their electronic properties.

By contrast, for ZVI, when a linear regression was forced through the first five data points (dashed line, Fig 4.2) the resulting slope was much less (0.010). The curvilinear response for ZVI suggested that for relatively low Fe/Cr(VI) ratios (< 200) small changes did not affect k_{SA} appreciably. Possibly, active sites became saturated with substrate, and kinetics were controlled by rates of reduction and/or release of the product from the active sites. At moderate Fe/Cr(VI) ratios (200-800), the increased number of sites relative to substrate lead to appreciable rate increases and at high Fe:Cr(VI) ratios (>800), a sufficient excess of sites caused the number of sites to have no influence of the reduction kinetics.

Noble metals are well known for being efficient catalysts. In the current application, they can function both as a catalyst and as a surface protectant. It can be inferred that they accelerate the corrosion reaction of the iron surface favouring the production of ferrous ion which readily reacts with Cr(VI) resulting in a net increase in the rate of Cr(VI) reduction. The remarkable capability of palladium to sorb H_2 dissociatively provides a source of strong reductant [161,163,168]. In addition, as transition metals, Pd, Ag, Ni, Cu, Zn have vacant *d* or/and *f* orbitals, which can form metal complexes with the non bonding electron pair or π bond of the oxygen atom in the chromate facilitating its adsorption onto the surface and decreasing the activation energy. It should be also noted, that no reaction was observed in the presence of Pd particles alone [167], probably because no electron donor was present. Pd possesses an elevated standard reduction potential (E_H^0, 0.987V *vs.* SHE) yet remains an inefficient electron donor for chromate reduction. Only when Pd was deposited on to the surface of Fe^0 to form an integrated bimetallic mixture, an enhancement of the reactivity achieved.

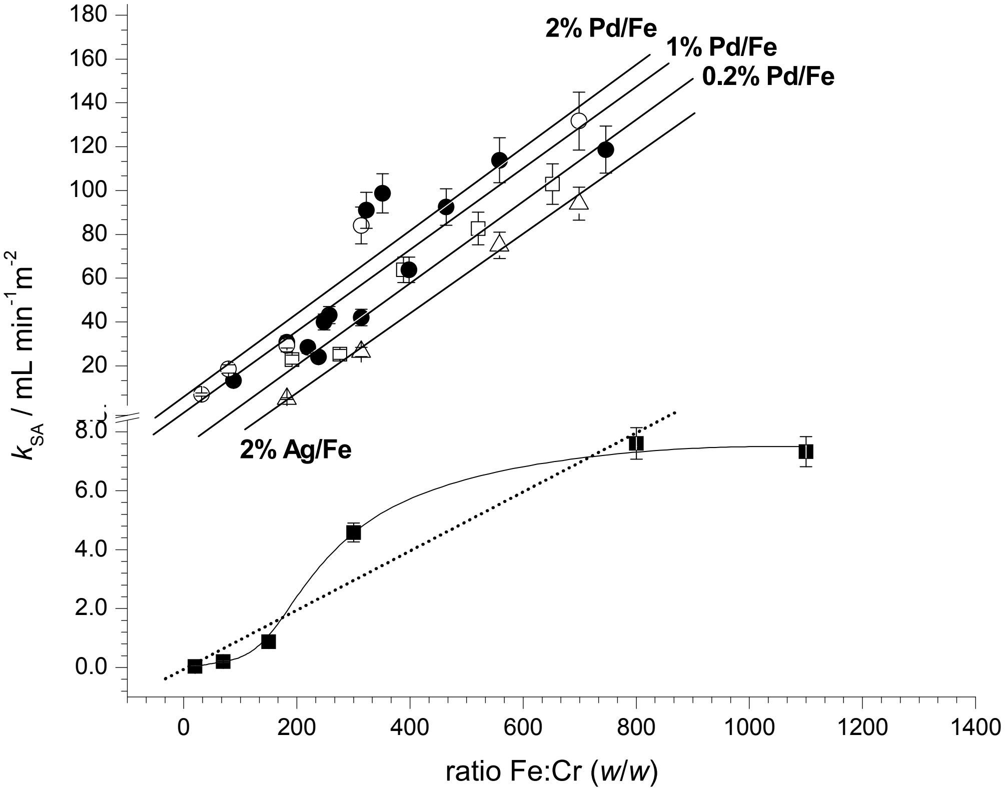

Figure 4.2 Variations, at pH 2.0± 0.1, in the mean surface area normalized pseudo-first order rate constant (k_{SA}, mL min^{-1} m^{-2}) for Fe^0 (■) or selected bimetallic mixtures, (□) 0.2% Pd/Fe, (●) 1% Pd/Fe, (○) 2% Pd/Fe and (Δ) 2% Ag/Fe as a function of the ratio of zero-valent iron to the concentration of Cr(VI).

In further experiments, a third zero-valent metal was cemented onto selected bimetallic preparation to yield: Pd/Cu/Fe (2:5:93 w/w), Pd/Zn/Fe (2:5:93 w/w) or Zn/Cu/Fe (5:5:90 w/w). Evaluations were conducted using the trimetallic formulations at pH 2 and 8; the results are summarized in Table 4.2. The palladized trimetallic mixtures were characterized by increased reactivity at both acidic and more circum-neutral conditions. For these preparations, an optimal kinetic model consisted of the sum of two pseudo-first order decays at both acidic (pH ~2, Fig 4.1C) and more circum neutral conditions (Fig 4.1D). The trimetallic mixtures were characterized by kinetic parameters that were very similar to each other (at pH ~2, k_{SA1} 38 whereas at pH 8, k_{SA1} 0.05, k_{SA2}, 0.008; *I*.time ~140 min). Thus, it seems possible to modify the composition of mixtures so as to extend the duration of initial decay while retaining much of the reducing activities of the mixture. Relative to ZVI, k_{SA1} was increased ten-fold at pH ~2 but was unchanged at pH 8, k_{SA2} was doubled and the intersect time was increased by four to six-fold. The trimetallic mixture Zn/Cu/Fe (5:5:90, w/w/w) represents a cost-effective alternative to the palladized bimetallic mixtures and provides comparable or improved kinetic parameters for the reduction of hexavalent chromium within a surfactant suspension.

4.3.2 Reduction of Cr(VI) using nano-sized bimetallic particles

A rapid and virtually complete reduction of hexavalent chromium was achieved at two pH conditions using either Fe or Cu nano-scale particles as summarised in Table 4.3 and Fig. 4.3. The salient observations for nano-scale zero-valent metal (NS-ZVM) included enhanced reactivity of the nano-scale metal particles under more circum-neutral conditions. Whereas the kinetics for micron-scale ZVI at circum-neutral pH was distinctly biphasic and micron scale Cu displayed virtually no activity, the kinetics of NS-ZV Fe or Cu was characterized by a single exponential decay with k_{SA} 4×10^{-2} at pH 6. This improvement reflects the increased surface area and higher atom efficiency of nano-scale particles. Experiments were also conducted with NS bimetallic particles (Pd/Fe, Cu/Fe or Pd/Cu). The formulation of catalyst into bimetallic mixtures further increased reactivity. The increase in k_{SA} (2- to 4-fold) was consistent yet modest at pH 2 and somewhat more appreciable at pH 5 (3- to 6-fold increase). Again, a cost saving can accrue if Cu/Fe is substituted for Pd/Fe or Pd/Cu. The proposed model for chromate reaction using bimetallic nano-particles might involve the oxidation of iron to galvanically protect the more noble catalyst metal (e.g., Pd, Cu).

Table 4.2 Predicted surface area-normalized rate constant (k_{SA}), and calculated surface-area normalized half-life ($t_{SA1/2}$) for the time dependant disappearance of Cr(VI) from unbuffered solution at various initial pHs (pH_i) for selected trimetallic mixtures.

Mixture	Ratio (w/w/w)	M:Cr (w/w)	pH_i[a]	k_{SA1} [b] (mL min^{-1} m^{-2})	r^2_{KSA1}	*I*.time[c] (min)	k_{SA2} [d] (mL min^{-1} m^{-2})	r^2_{KSA2}
Pd/Cu/Fe	**2:5:93**	720	2.03	4.3	0.998	>1	1.47	0.982
		468	8.08	$5.3x10^{-2}$	0.993	120	$8.5x10^{-3}$	0.985
Pd/Zn/Fe	**2:5:93**	340	2.04	2.0	0.999	>1	2.01	0.999
		610	8.10	$7.1x10^{-2}$	0.988	120	$1.1x10^{-2}$	0.990
Zn/Cu/Fe	**5:5:90**	440	2.03	2.0	0.999	>1	2.01	0.999
		360	8.04	$2.8x10^{-2}$	0.999	180	$6.7x10^{-3}$	0.993

[a] initial pH, [b] surface area normalized rate constant for the initial decay, [c] I. time refers to the intersection time between the two modeled decays, [d] surface area normalized surface area normalized rate constant for the second decay, [b,d] The sum of two exponential decays was used to model the observed kinetic results (k_{SA1} and k_{SA2}).

Table 4.3 Coefficient of correlation (r^2), pseudo-first order rate constant (k), surface area normalized rate constant (k_{SA}), half-life ($t_{1/2}$), surface area normalized half-life ($t_{1/2\ SA}$) and pH for Cr(VI) reduction with nano-size metallic particles in unbuffered solution.

Mixture	**M:Cr (w/w)**	**pH_i [a]**	**pH_f [b]**	**r^2**	**k [c] (min^{-1})**	**k_{SA} [d] ($mL\ min^{-1}\ m^{-2}$)**
Fe	368	2.00	2.64	0.984	4.6	2.8
	360	6.06	5.11	0.984	6.7×10^{-2}	4.0×10^{-2}
Pd/Fe	77	2.02	2.40	0.979	11	6.6
	310	5.99	5.18	0.985	0.24	0.15
Cu/Fe	122	2.03	2.40	0.960	10	5.9
	430	5.99	5.18	0.994	0.204	0.122
Cu	193	2.03	2.50	0.951	0.87	0.59
	198	6.12	7.05	0.942	6.1×10^{-2}	4.1×10^{-2}
Pd/Cu	150	2.01	2.35	0.961	5.3	3.61
	310	6.01	5.5	0.953	0.19	0.13

[a] initial pH, [b] final pH, [c] calculated pseudo-first order rate constant, [d] surface area normalized rate constant (specific surface areas: 33.5 $m^2\ g^{-1}$ and 29.5 $m^2\ g^{-1}$ for Fe and Cu nano-sized iron particles) [136,163,164].

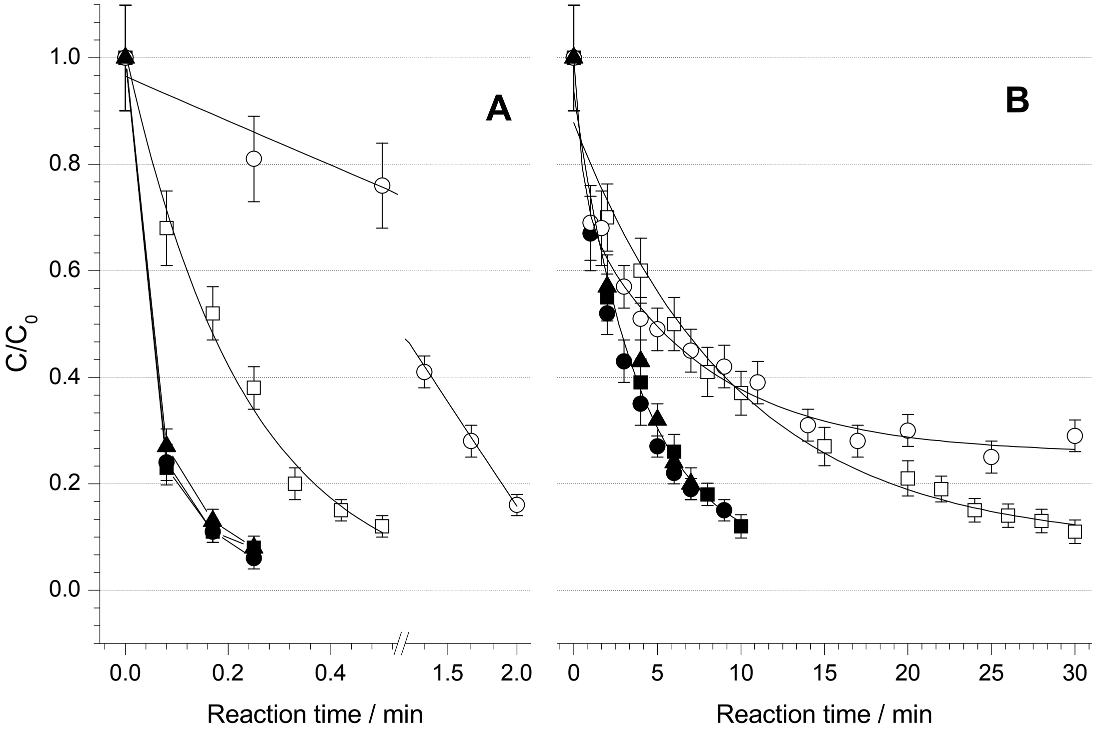

Figure 4.3 Plots of the variation with time of the mean Cr(VI) concentration (mg L^{-1}) when reacted at **(A)** pH 2.0± 0.1 or **(B)** 6.0± 0.1 with different nano-scale metallic formulations, (□) Fe; (●) Pd/Fe; (■) Cu/Fe; (○) Cu; (▲) Pd/Cu.

As iron corrodes, protons from water are reduced to adsorbed H atoms and to molecular hydrogen at the catalytic surface of the noble metal, while at the same time ferrous ions are produced. Chromate is adsorbed onto the surface of the bimetallic preparation where the transfer of electrons can take place from zero-valent metal (Fe or Cu).

In the last decade the use of nano-scale particles has emerged to apparently solve numerous problems in diverse disciplines such as electronics, contaminated site remediation and medicine. Despite a bright outlook for the future of nanotechnology, there is increased concern that human exposure to some engineered nanoparticles, can lead to adverse health effects particularly among susceptible individuals. Victims with a pre-existing or genetic disease, can be affected more severely [150,166]. Even though nanoparticles seems to overcome the drawbacks of inactivation issues and the consequent loss of reactivity, the potential health effects of their widespread use make their use of greater concern that must be taken into account when remediation techniques are intended for contaminated sites.

4.4 Conclusions

The reductive remediation of chromate in aqueous media is strongly affected by the passivation of the metal surface with the consequent loss of reactivity. The removal of (oxy)hydroxides from the metal surface by acid-washing can increase its reactivity substantially as demonstrated with the zero-valent iron. As soon as the metal surface is exposed to an aqueous solution, an oxide/hydroxide layer is formed in which the ratio to oxygen to metal varies as a function of depth from the surface.

The cementation of a second metal (Ag, Cu, Ni, Pd or Zn) on to the surface of the transition metal increased the reactivity of the preparation substantially. Catalytic metals, such as Pd or Ag, considerably increased the rate of disappearance of chromate either at acidic conditions or more alkaline pHs. The order of reactivity of the bimetallic mixtures based on surface-area normalized pseudo-first order rate constant was: Pd/Fe > Pd/Zn > Ag/Fe > Ni/Fe > Zn/Fe > Pd/Cu > Cu/Fe. Although the exact mechanism of the catalytic reduction of Cr(VI) has not been fully elucidated, it seems to be linked to: (1) their intrinsic catalytic properties which vary from metal to metal the result of differences in surface properties, atomic structures and electronic properties; (2) surface protectors that favour the release of ions (such as Fe^{+2}, or Cu^{+}, Cu^{+2}) from the metal surface which readily reacts with Cr(VI); (3) the ability of the formulation to sorb and activate H_2, and (4) the increase of adsorbed chromate onto the bimetallic surface. The Zn/Cu/Fe tri-metallic mixture represents a more cost-effective reductant relative to formulations based in noble metal catalysts.

The enhanced rate of reduction of chromate mediated by nano-sized particles is likely the result of increased specific surface area to mass ratio, higher surface reactivity and the increased atom efficiency.

An important issue to be investigated is the relative reactivity and atom efficiency of metal particles utilised in this study and particularly the nano-sized particles when measured over extended times that are relevant to remediation of slow-moving plumes in contact with a PRB.

Further studies are needed to delineate the underlying mechanistic steps of chromate reduction on metal surfaces and to expand the scope of synthetic method for nano-sized metal particles.

Chapter

Five

Preface

In Chapter three and four, the reactivity of various micro- and nano-sized zero-valent metal particles as well as metallic mixtures were evaluated towards the reductive transformation of hexavalent chromium under selected reaction conditions. Various zero-valent metal and bimetallic mixtures were characterised by a rapid inactivation and the loss of reactivity of the metallic surface caused by the formation of (oxo)hydroxides species. Consequently, the reduction rate of hexavalent chromium decreased dramatically.

Selected metallic mixtures accelerated the reduction rates of Cr(VI) at both acidic and circum neutral conditions. Nanoscale metallic particles improved the reductive remediation of Cr(VI) under selected reaction conditions.

In Chapter five, a variety of naturally-occurring molecules (containing α-hydroxyl carbonyl, α-hydroxyl carboxylate, α-carbonyl carboxylate, phenolate, carboxylates and/or thiol groups, siderophores, ascorbic acid); chelating agents (ethylenediaminetetraacetic acid derivates, acetyacetone) and others (acetylacetone, phenanthroline, urea) are examined their reducting activity towards a surfactant preparation (Tween® 20) containing Cr(VI) and Fe(0) under a variety of reaction conditions.

A portion of this chapter has been published in **Chemosphere, 76 (2009) 1240-1248.**
Authors: M. Rivero-Huguet, W.D. Marshall.

Chapter

Five

Influence of various organic molecules on the reduction of hexavalent chromium mediated by zero-valent iron

5.1 Introduction

Chromium is a pollutant that is frequently found in brownfields, as well as in surface and subterranean waters throughout the industrialized world. Chromium exists in several oxidation states but mainly as Cr(VI) or Cr(III) in the natural environment. These two oxidation states are fairly different in physical and chemical properties. Cr(VI) is highly soluble, mobile and toxic to humans, animals and plants. In contrast, Cr(III) is usually found in the form of $Cr(OH)_3$ which possesses low solubility and is readily absorbed to the surfaces of clay minerals [24,25]. Thus, one of the important approaches to control chromium contamination of soil, sediment or groundwater is to reduce Cr(VI) to Cr(III). The wide distribution of chromium contaminants in the environment is the result of the extensive exploitation of chromium to produce stainless steel, wood treatment products, tanning of leather or pigments [169]. Over the last several years, a great deal of effort has been expended to identify and improve strategies to mitigate Cr(VI) contamination. In particular, several studies have demonstrated that zero-valent iron (ZVI) is an efficient and inexpensive reductant for Cr(VI) [109,111,152,156,170]. Under appropriate conditions, complete removal of Cr(VI) from solution has been reported in several laboratory studies and in both pilot-plant and field-scale iron metal permeable reactive barriers (PRBs). The rates of Cr(VI) reduction vary considerably depending on pH, zero-valent iron (ZVI) concentration and type. However, the thermodynamic instability of ZVI in the presence of water and/or oxygen, mediates the oxidation of iron metal to ferrous ion and the precipitation of iron species (α-FeOOH, α-Fe_3O_4, γ-FeOOH, $Fe(OH)_2$ and $Fe(OH)_3$, $FeCO_3$) on the ZVI surface [124]. As a result, the rate of reduction of Cr(VI) to Cr(III) dramatically diminishes with time. Several attempts have been made to enhance the efficiency of this redox reaction by diminishing the inactivating effects of the resulting passivation layer. Doping a second catalytic metal such as Pd, Pt, Ag or Ni to the surface of the iron particles can accelerate the detoxification of Cr(VI) solutions. The second zero-valent metal on the iron surface serves not only as an accelerator but also as a protecting agent against surface corrosion [128-131]. During the last decades attention has been directed to evaluating the impact of naturally occurring organic molecules and/or co-ordinating reagents on the reduction rate of Cr(VI) mediated with ZVI [108,170-181].

Simple aliphatic organic acids with one to three carboxylic acid groups such as acetic, citric, formic, fumaric, lactic, oxalic, malonic, valeric, succinic, tartaric, and *p*-hydroxybenzoic acid occur frequently in soil and subsurface environments. These compounds are released by organisms or are produced during the decomposition of larger biopolymers. In anaerobic environments, a variety of thiols have been identified including glutathione, cysteine, methane thiol, and 3-mercaptopropionate [108,173,174]. These organic compounds can alter chemical processes in soils through complexation with metal ions in solution and ligand exchange reactions at soil surfaces. They can play a role in chromate reduction by ZVI via adsorption and complexation with the surface sites of Fe(0) and/or with the iron corrosion products.

It was anticipated that the reactivity of ZVI toward Cr(VI) would be accelerated by the presence of a limited set of additives that incorporate reducing and/or complexing activity resulting from the presence functional (carboxyl, carbonyl, alcohol, phenol and/or thiol) groups.

In the current report, the mobilisation and detoxification of Cr(VI) from a contaminated site was evaluated. The Cr(VI)-contaminated soil sample was treated with one of several surfactant formulations, as a possible mobilisation aid to dislodge the target ion from the particulate surfaces. The resulting extract (containing Tween® 20) was reacted with ZVI in the presence of naturally-occurring organic compounds that included a variety of polyols (glycerol, polygalacturonic acid, soluble starch), aliphatic organic acids (ascorbic acid, citraconic acid, citric acid, oxalic acid, acetic acid, formic acid, succinic acid, lactic acid, tartaric acid, glycolic acid, malonic acid, phytic acid, pyruvic acid, malic acid), and aromatic acids (p-hydroxybenzoic acid, phtalic acid, picolinic acid, 2,6-pyridine dicarboxylic acid, salicylic acid) or compounds bearing carboxylic and/or amino groups (humic acid, glutamic acid, L-histidine, cysteine, urea, thiourea, glutathione). Additionally, a variety of chelating reagents (that include cyclodextrin, deferoxamine {DFO}, ethylenediamine tetraacetic acid {EDTA}, diethylenetriamine pentaacetic acid {DTPA}, ethylenediamine tetrapropionic acid {EDTPA}, [*S*,*S*]-ethylenediamine disuccinic acid {EDDS}, ethylenebis(oxyethylenenitrilo) tetraacetic acid {EOTA}, methylglicine diacetic acid {MGDA}, 1,6-diaminohexane *N*,*N*,*N*',*N*'-tetraacetic acid {DHTA}, 1,3-diamino-2-hydroxypropane-*N*,*N*,*N*',*N*'-tetraacetic acid {DPTA}, 1,2-diaminopropane- *N*,*N*,*N*',*N*'-tetraacetic acid {MEDTA}, *N*-(2-Hydroxyethyl)ethylenediamine-*N*,*N*′,*N*′-triacetic acid (HEDTA), 1,10-phenanthroline {phen} or acetylacetone {acac}) were evaluated.

5.2 Materials and methods

All solutions and suspensions were prepared from distilled deionized water (DDW) with resistivity of 18.0 MΩ·cm, (Millipore Corp., Milford, MA, USA). Stock dichromate and other inorganic salt solutions were prepared from analytical-grade reagents (Fisher Scientific, Napean, ON, Canada) and filtered through a 0.2-*μ*m membrane filter (Fisher Scientific) prior to use. Organic reagents were obtained from Fisher Scientific (L-ascorbic acid, citric acid, *s*-diphenyl carbazide diethyenetriaminepentaacetic acid, L-glutathione, glycerol, L-histidine, oxalic acid, picolinic acid, 2,6-pyridine-dicarboxylic acid, soluble starch, thiourea, urea), Sigma-Aldrich {Tween® 20, acetic acid, acetylacetone, citraconic acid, β-cylcodextrin, L-cysteine, 1,6-diaminohexane *N*,*N*,*N*',*N*'-tetraacetic acid, deferoxamine mesylate salt, 1,6-diaminohexane *N*,*N*,*N*',*N*'-tetraacetic acid, ethylenediaminetetraacetic acid, formic acid, ethylenediaminetetrapropionic acid, ethylenebis(oxyethylenenitrilo) tetraacetic acid, 1,2-diaminopropane- *N*,*N*,*N*',*N*'-tetraacetic acid, heptakis(2,6-di-o-methyl)- β-cylcodextrin, humic acids, *N*-(2-Hydroxyethyl)ethylenediamine-*N*,*N*′,*N*′-triacetic acid, lactic acid, malic acid, malonic acid, 4-hydroxybenzoic acid, 1,10 phenanthroline, phtalic acid, phytic acid, polygalacturonic acid, pyruvic acid, salicylic acid, succinic acid, L-tartaric acid}, were purchased in the highest purity available and were used as received. [*S*,*S*]-ethylenediamine disuccinic acid (30% EDDS) was obtained as Octaquest E30 from Innospec Limited (Cheshire, UK) and the trisodium salt of methylglycinediacetic acid (86% MGDA) was purchased as Trilon® M from BASF (Ludwigshafen, Germany).

Iron metal (40 mesh, specific surface area 1.01 m^2 g^{-1}) was purchased from Fisher Scientific, (Napean, ON). Acid-washed Fe(0) was used in all the experiments. A known quantity of iron granules were washed copiously with 6M HCl and rinsed five times with DDW, three times with ethanol and a further three times with acetone then dried in a N_2 stream for 2 h. To inhibit oxidation, the iron powder was stored under N_2 prior to use.

The diphenylcarbazide (DPC) colorimetric method for the determination of Cr(VI) recommended by the APHA, was adapted to work on a microscale level [154]. Once filtered, the samples were immediately inserted into the Hach test tube with a freshly prepared phenylcarbazide solution in acetone (200 µL, 20 mM) and H_2SO_4 (5 µL, 10% v/v). The reaction was permitted to continue for 5-10 min then diluted with 10 mL DDW. Post reaction, the presence of test reagent did not have any perceptible influence on the Cr(VI)-DPC colour development.

The determination of Fe(II) in the surfactant extract was analyzed by the colorimetric reaction with 1,10-phenantroline following the standard Analysis Method 3500-Fe B [154].

Spectroscopic measurement uncertainties associated with the determination of Cr(VI) and Fe(II) concentrations in the extract were calculated using a cause-and-effect approach as reported previously [155].

The kinetics experiments were performed in strongly (pH 2.0) or weakly acidic solutions (pH 4.0-6.0). All reactions were carried out using a Tween® 20 extract suspension containing an initial concentration 390 µM Cr(VI) and a concentration of 7g L^{-1} Fe(0). In addition, 500 µmoles of the organic test reagent was added to result in a 500 µM reaction suspension. The reaction of Cr(VI) and the organic reagent was also studied in the absence of Fe(0). The suspension was mixed and shaken continuously. At convenient intervals, 0.5-1 mL aliquots were withdrawn, filtered through 0.45 µm membrane filter and added to a clean and dry Hach test tube.

Attenuated Total Reflectance (ATR)/FTIR spectra were collected by using Excalibur Series BIO-RAD spectrometer operating in the mid-infrared region (650-4000 cm^{-1}). The spectrometer was continuously purged with dry air from Balston dryer (Balston, MA, USA). The ATR device was placed in the nitrogen purged sample chamber and included the transfer optics through which IR radiation was directed to a detachable ZnSe crystal (45º and 11 internal reflections). A total of 256 scans were co-added at 4 cm^{-1} resolution and spectra were acquired in triplicate. FT-Raman spectra were obtained using a Varian 3100 FT-IR Spectrometer equipped with a FT-Raman accessory and Nd:YAG excitating laser operating at 1064 nm with a maximum power of 2 W. The system was equipped with a cryogenically cooled germanium (Ge) detector, near-IR beam splitter with a 180º reflective optics, and a fully motorized sample position adjustment feature. Data were collected at 8 cm^{-1} resolution with 256 scans summed. Spectra were used in the Raman shift range between 200 and 3600 cm^{-1}. The systems was operated using the Win-IR Pro Software and spectra were acquired in triplicate.

5.3 Results and discussion

A soil that had been heavily field-contaminated with hexavalent chromium was washed with various surfactant formulations (anionic, non-ionic or cationic) to evaluate the relative efficiency as mobilization aids for Cr(VI). Once the pollutant had been mobilized, the solution that resulted was reacted with various metallic mixtures. Previously, it had been observed that the presence of Tween® 20 in the extract of Cr(VI) had no perceptible effect on the reaction kinetics with zero-valent metals (ZVMs) and were adequately described by either a single or the sum of two pseudo-first-order kinetic models [167].

5.3.1 Reduction of Cr(VI) in the presence of organic acids (with one to three carboxylic groups)

Table 5.1 summarizes the goodness of fit of a linear model to the experimental data (either a single exponential decay for pHs of ≤ 2.0 or the sum of two exponential decays for pHs ≥ 3.0) and the observed kinetic parameters {surface area normalized rate constant (k_{SA})} for the various organic reagents tested in the presence of ZVI. As reported previously for ZVI, if the initial pH was increased to 3.0 or above, a model consisting of the sum of two-pseudo first order reactions provided an appreciably better fit to the data than did the single exponential decay [167]. This was the case for all of the organic reagents tested in this project.

Table 5.1 Predicted surface area-normalized rate constant(s) (k_{SA}) in the presence of Fe(0) and test reagent for the time dependant disappearance of Cr(VI) from unbuffered solution at various initial pHs (pH_i). Only data of organic acids (up to three carboxylic acids groups) that increased the reduction rate of Cr(VI) more than 2-fold are included.

	pH_i [a]	k_{SA1} [b] (ml min^{-1} m^{-2})	r^2_{KSA1}	*I*.time[c] (min)	k_{SA2} [d] (ml min^{-1} m^{-2})	r^2_{KSA2}
Fe(0)	2.1	4.67	0.992	N/A	N/A	N/A
	5.8	0.067	0.987	30	$5.3x10^{-3}$	0.990
Citric acid	2.3	37	0.989	N/A	N/A	N/A
	5.6	0.061	0.987	75	$6.5x10^{-3}$	0.980
L-Cysteine	2.0	26	0.990	N/A	N/A	N/A
	5.8	0.679	0.992	6	$1.2x10^{-2}$	0.962
Glycolic acid	2.0	11	0.987	N/A	N/A	N/A
	6.0	0.065	0.979	60	$7.1x10^{-3}$	0.981
Lactic acid	2.1	27	0.991	N/A	N/A	N/A
	5.9	0.059	0.990	60	$6.7x10^{-3}$	0.986
Malic acid	2.1	35	0.987	N/A	N/A	N/A
	5.7	0.045	0.982	120	$8.9x10^{-3}$	0.993
Picolinic acid	2.0	12	0.991	N/A	N/A	N/A
	5.9	0.089	0.983	60	$1.6x10^{-2}$	0.979
Pyruvic acid	2.1	25	0.996	N/A	N/A	N/A
	6.2	0.045	0.986	60	$7.5x10^{-3}$	0.982
Tartaric acid	2.0	37	0.995	N/A	N/A	N/A
	5.9	0.057	0.982	75	$6.3x10^{-3}$	0.986

[a] initial pH, [b] surface area normalized rate constant for the initial decay, [c] *I*. time refers to the intersection time between the two modeled decays, [d] surface area normalized rate constant for the second decay.

[b,d] The sum of two exponential decays was used to model the observed kinetic results (k_{SA1} and k_{SA2}).

The first decay was considered to be dominated by reaction that occurred at exposed Fe active sites. Once the passivating (oxy)hydroxide layer had formed, a second decay function described the reaction rate that was decreased but not totally inhibited. The second decay function was considered to model reaction at the surface of the passivated layer. Of twenty two organic compounds containing up to three carboxylic acid groups that were examined, only those reported in Table 5.1 appreciably increased Cr(VI) reduction relative to ZVI. None of the 22-carboxyl containing organic compounds decreased the reduction rate appreciably. As summarised in Fig. 5.1 and Table 5.1, relative to ZVI, appreciable increases for Cr(VI) reduction rates were observed in the presence of certain of the reagents (α-hydroxyl and α-carbonyl carboxylic acids, citric acid, malonic acid, cysteine) when working at pH~2, but only minor differences (less than two-fold) were detected at more circum neutral (pH ~6) conditions. In contrast, cysteine and picolinic acid accelerated the Cr(VI reduction rate (k_{SA2}) appreciable (2-fold and 3-fold respectively). This behaviour might be attributed to the reductant properties of these compounds.

As indicated in Fig. 5.2, a stoichiometry of the redox reaction with Cr(VI) is proposed, where α-hydroxyl acids readily react with Cr(VI) under acidic conditions to produce the corresponding α-keto acid. For these organic reductants, an initial, nearly instantaneous decrease in $[Cr(VI)]_{aq}$ (up to 70% decrease was observed in the first 10 s of reaction) can be clearly distinguished from a subsequent, more gradual decrease in $[Cr(VI)]_{aq}$, caused by a rapid Cr(VI) adsorption onto the ZVI surface followed by reduction of the adsorbed Cr(VI). Thus the adsorbed Cr(VI) reacts not only with the organic reductant but also with the iron surface. As the initial concentration of the pollutant was decreased, the remaining Cr(VI) had access to more Fe(0) active sites that are readily accessible for reaction. The effect of the α-hydroxyl carboxylic acids on the Cr(VI) reduction follows the order: tartaric acid > malic acid > lactic acid > glycolic acid. This is not surprising, since tartaric acid has two separate α-hydroxyl carboxylic acid functional groups, whereas lactic, malic and glycolic acids have only one. For compounds possessing a single α-hydroxy carboxylic acid functional group, changing the R substituent had an appreciable effect on the Cr(VI) reduction rate. Malic acid (R = $HOC(O)CH_2$-), was 1.3 times as reactive as lactic acid (R = H_3C-) and 3.18 times as reactive as glycolic acid (R = H-). The reactivities of these α-hydroxyl carboxylic compounds is considered to be caused by the inclusion of a second carboxylate group suitably positioned for chelating either Fe ions or Cr(III) formed in the reaction.

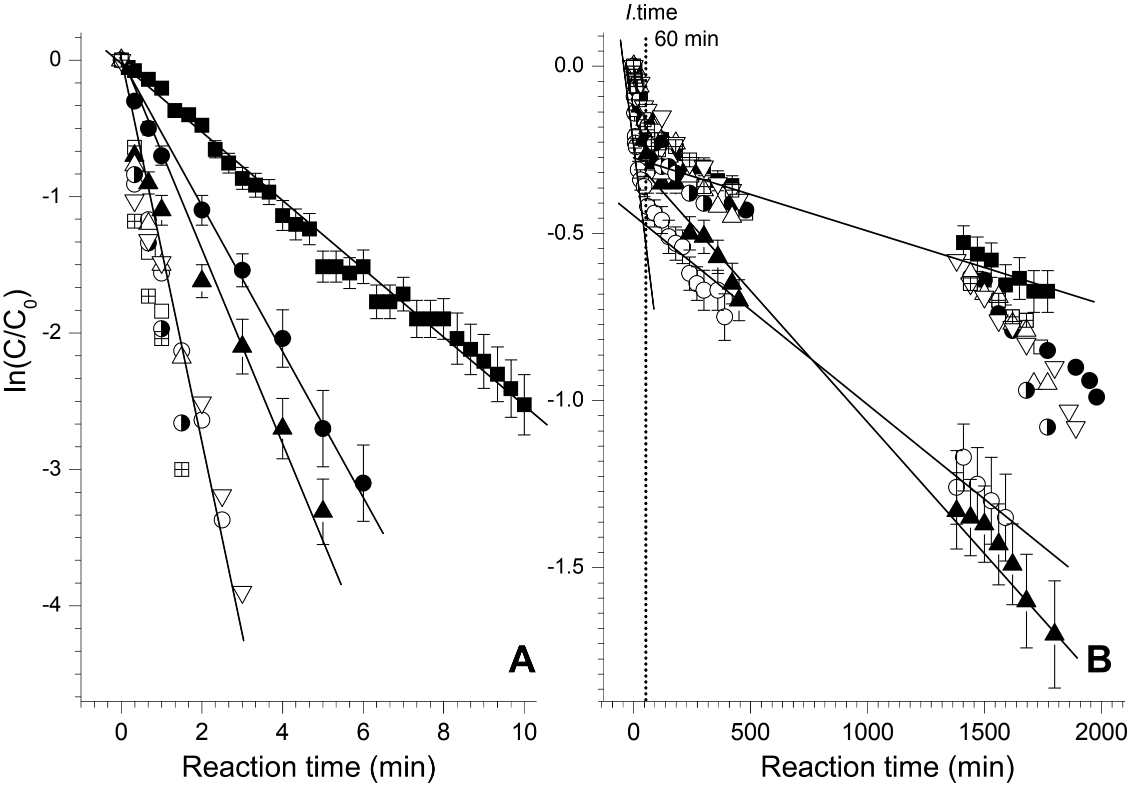

Figure 5.1 Selected plots of the variation with time of the ln of the ratio of the mean Cr(VI) concentration at time t to the initial concentration (μM) when reacted (A) at pH 2.0± 0.1 or (B) at 6.0± 0.2 with ZVI at a Fe(0) to Cr(VI) ratio (~300): Fe, (■); citric acid, (□); glycolic acid, (●); L-cysteine, (○); picolinic acid, (▲); lactic acid, (Δ); malic acid, (◑); pyruvic acid, (▽); and tartaric acid, (⊞), *l*.time (60 min) for glycolic, lactic, picolinic and pyruvic acids (dotted line). Uncertainties in the determinations of certain Cr(VI) concentrations were omitted to facilitate the plot visualization.

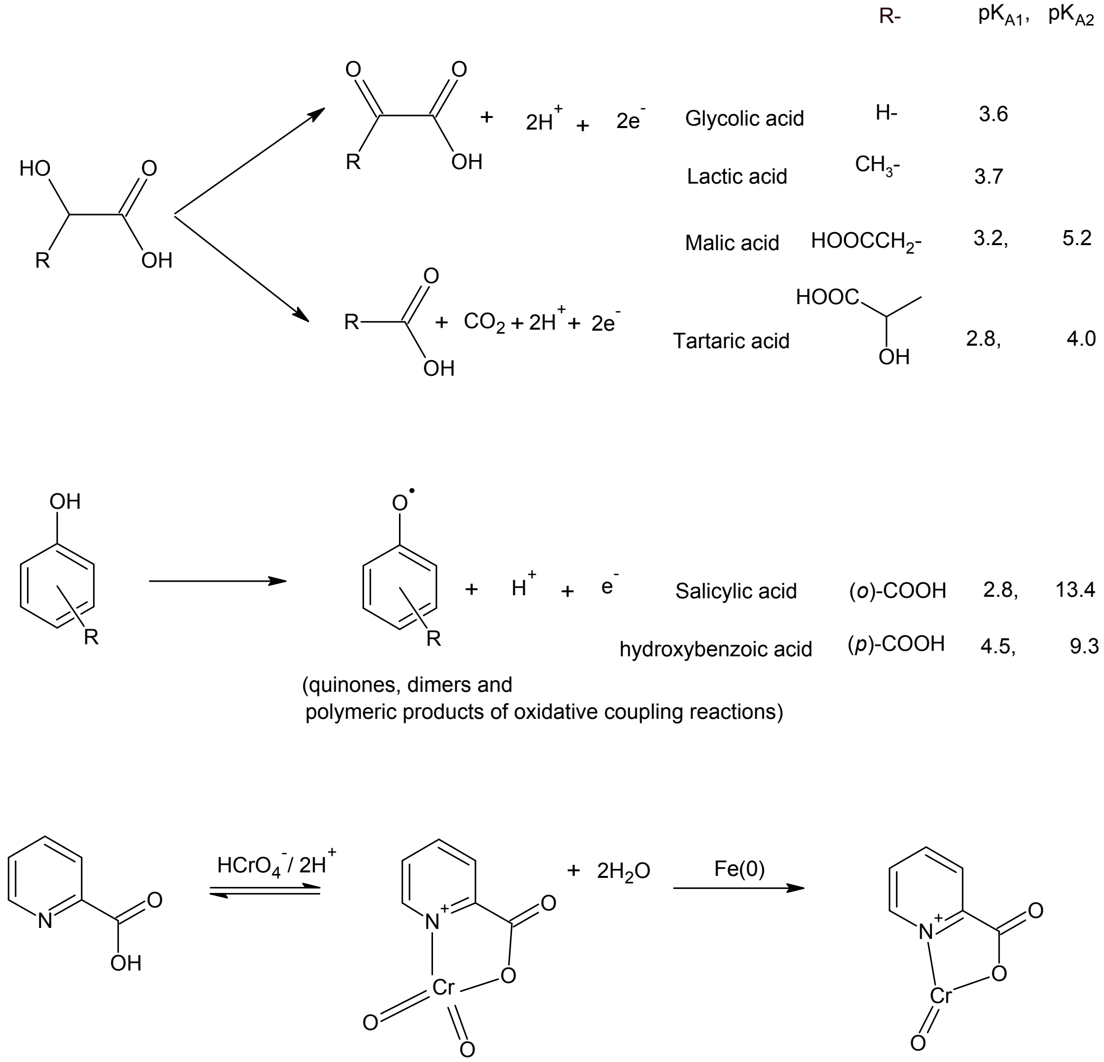

Figure 5.2 Possible oxidation products for selected organic compounds. p*K*$_a$ values are derived from Smith et al. [182].

An interesting effect was detected while studying the reduction of Cr(VI) by ZVI in the presence of picolinic acid (PA). It is well know that PA can act as an accelerator, although not as a true catalyst [183-186]. The inclusion of PA in the reaction system accelerated the reaction 3-fold under acidic conditions and up to 2-fold at more neutral pH. Islam et al. have demonstrated that PA does not get co-oxidised but is gradually lost during the reaction via the formation of inert Cr(III)-PA complex [186]. The enhanced reaction with hexavalent chromium is presumably the result of Cr(VI)-PA adduct formation which remains an active oxidant. Evidence of the formation of chromium picolinate was obtained from ATR/FTIR spectra of the reaction system. A shift of the symmetric and asymmetric stretches [$\Delta\nu$ = Δ(asym) – Δ(sym)] of the carboxylate group was observed when compared to that of the a surfactant solution of PA. $\Delta\nu$, was determined to be 271 cm^{-1} (1610 - 1339 cm^{-1}) suggesting that formation of only a monodentate interaction is the primary mechanism for binding PA to chromate extract [187]. The production of Cr(III)-PA complex was supported by the blue shift observed in the absorption spectra for the peak due to the transition $^4A_{2g}(F) \rightarrow {}^4T_{2g}(F)$ compared to the final suspension without PA. The absorption spectrum of the reaction mixture in the absence of PA had two maxima, at 409 and 581 nm, corresponding to the transitions $^4A_{2g}(F) \rightarrow {}^4T_{1g}(F)$ and $^4A_{2g}(F) \rightarrow {}^4T_{2g}(F)$ respectively [10]. The absorption spectrum of the reaction mixture with PA had two peaks at 410 and 549 nm in which the latter had undergone a blue shift that was consistent with the presence of a strong field donor site (heteroaromatic *N*-donor moiety).

The reduction rate of Cr(VI) with ZVI in the presence of cysteine is mediated by the initial reaction between Cr(VI) and the thiol group. FT-Raman studies of the reaction suspension corroborated the hypothesis of cystine interaction; the peak at 2550 cm^{-1} (S-H stretching vibrations) disappeared and a sharp peak at 501cm^{-1} appeared over the course of the reaction, which was attributed to the stretching vibration of a disulfide (S-S) linkage.

For each of the other organic compounds examined in this section, there was an appreciable increase (2-4 fold) in the intersection time between the two models (*I*.time, Table 5.1). This might have resulted from an interaction of the organic compound with the iron surface that retarded the rate of formation of the passivating oxide/hydroxide layer. The duration of the first step (dominated by the reduction at exposed active sites) was extended and values ranged between 60 and 120 min.

5.3.2 Reduction of Cr(VI) in the presence of polyamine carboxylates

In the presence of various polyamine carboxylate derivatives, only minor differences (less than two-fold) for Cr(VI) reduction rate parameters (k_{SA1}), were observed for certain compounds (DAHTA, DTPA, EDTA, EGTA, EDTPA, MEDTA or MGDA) when working at pH ~ 2. Figure 5.3 and Table 5.2 summarize the kinetic parameters for selected ethylenediamine carboxylic acids. At acidic conditions (pH ~2.0) EDDS, HEDTA and particularly DPTA increase the rate of reduction of Cr(VI) to Cr(III).

The tendencies of polyamine carboxylate ions to form stables coordinate complexes with numerous metals are well known [10,188,189]. The differences in k_{SA1} at acidic conditions (pH ~2.0) might be attributed to the selectivity and kinetic differences towards the formation of Fe stable complexes. A two-fold increase in the intersection time (*I*.time) was observed (relative to ZVI alone) which suggested that an initial interaction between Fe(0) and EDDS occurred retarding the rate of formation of the passivating oxide/hydroxide layer (Table 5.2).

Zhou et al., reported a dramatic enhancement in the reduction kinetics of Cr(VI) in the presence of Fe(0) and EDTA at more alkaline conditions (pH=4.0, 5.0, and 6.0) and a zero-order kinetic model [181]. Such differences with our results and kinetic model might be assigned to different experimental working conditions (0.224 g L^{-1}Fe(0); 100 µM Cr(VI); and 4000 µM EDTA *vs*. 7 g L^{-1} Fe(0); 390 µM Cr(VI); and 500 µM EDTA in a Tween® 20 medium in the current study).

Appreciable increases in the Cr(VI) reduction rates were observed in the presence of DPTA. At pH 2.0 ± 0.1, the reaction rate was increased more than five-fold and at pH 6.0± 0.2, the initial reaction rate (k_{SA1}) was increased 2-fold, the intersection time between the two exponential decays was increased by 50% and the k_{SA2} reaction rate was increased three-fold. The presence of hydroxyl groups in the aliphatic chain of DPTA caused a virtually immediate reaction with Cr(VI) to form the corresponding keto compound.

Trials performed in absence of Fe(0) at pH 2.0 in a Tween® 20 suspension of Cr(VI) and DPTA displayed a dramatic decrease in the initial Cr(VI) concentration during the first 20 seconds of reaction (by up to 25%), followed by a more gradual decline in the Cr(VI) concentration (33% remained after 30 min.) and a concomitant decrease in the pH, from 2.0 to 1.7, due to the release of H^+ during the oxidation of the hydroxyl group.

Table 5.2 Predicted surface area-normalized rate constant (k_{SA}), and calculated surface-area normalized half-life ($t_{SA1/2}$) for the time dependant disappearance of Cr(VI) from unbuffered solution at various initial pHs (pH_i) when reacted in the presence of various ethlyendiamine tetracetic acid derivates.

	pH_i[a]	**k_{SA1}[b] (ml min^{-1} m^{-2})**	**r^2_{KSA1}**	***I*.time[c] (min)**	**k_{SA2}[d] (ml min^{-1} m^{-2})**	**r^2_{KSA2}**
Fe(0)	2.1	4.67	0.992	N/A	N/A	N/A
	5.8	0.067	0.987	30	$5.3x10^{-3}$	0.990
EDTA	2.1	5.7	0.987	N/A	N/A	N/A
	5.9	0.069	0.975	30	$6.1x10^{-3}$	0.995
EDDS	2.1	9.8	0.994	N/A	N/A	N/A
	5.9	0.61	0.981	60	$7.5x10^{-3}$	0.984
DPTA	2.0	26	0.991	N/A	N/A	N/A
	6.2	0.15	0.987	40	$1.7x10^{-2}$	0.986
HEDTA	2.0	7.8	0.998	N/A	N/A	N/A
	5.8	0.067	0.986	60	$6.7x10^{-3}$	0.988
DTPA	2.1	5.9	0.988	N/A	N/A	N/A
	6.2	0.065	0.990	30	$6.0x10^{-3}$	0.978
EOTA	2.0	5.0	0.989	N/A	N/A	N/A
	6.2	0.062	0.990	30	$5.8x10^{-3}$	0.988
MGDA	2.1	5.9	0.988	N/A	N/A	N/A
	6.0	0.048	0.974	30	$7.3x10^{-3}$	0.993
DHTA	2.0	4.8	0.986	N/A	N/A	N/A
	6.1	0.065	0.990	30	$6.0x10^{-3}$	0.989
EDTPA	2.1	5.7	0.991	N/A	N/A	N/A
	6.0	0.063	0.978	30	$6.4x10^{-3}$	0.988
MEDTA	2.0	5.0	0.984	N/A	N/A	N/A
	6.1	0.059	0.979	30	$6.2x10^{-3}$	0.984

[a] initial pH, [b] surface area normalized rate constant for the initial decay, [c] *I*. time refers to the intersection time between the two modeled decays, [d] surface area normalized rate constant for the second decay.[b,d] The sum of two exponential decays was used to model the observed kinetic results (k_{SA1} and k_{SA2}).

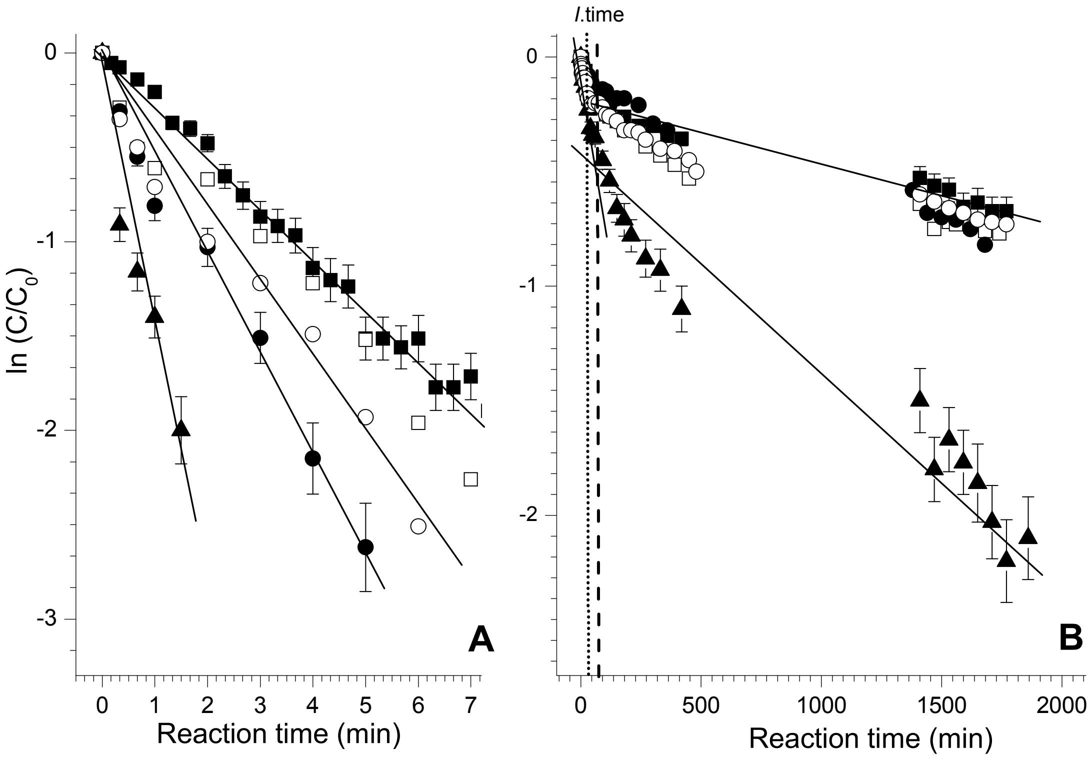

Figure 5.3 Selected plots of the variation, with time, of the ln of the ratio of the mean Cr(VI) concentration at time t to the initial concentration (μM) when reacted (A) at pH 2.0± 0.1 or (B) at 6.0± 0.2 with ZVI at a Fe(0) to Cr(VI) ratio (~300): Fe, (■); EDTA, (□); EDDS, (●); DPTA, (▲); and HEDTA , (○), *l*.time (30 min) for Fe(0) alone (dotted line), *l*.time (60 min) for EDDS and HEDTA reaction systems (dashed line). Uncertainties in the determination of certain Cr(VI) concentrations were omitted to facilitate plot visualization.

When ZVI was included in the reaction mixture, the decrease in the initial concentration of Cr(VI) caused the same number of active sites on the iron surface to be available to less Cr(VI) substrate resulting in an increased reduction rate of the Cr(VI) remaining (6-fold increase relative to ZVI alone). At more neutral pH (6.0 ±0.2), a 10% increase of initial Cr(VI) reduction rate was observed relative to ZVI alone during the first 30 min of reaction, likely the result of a slower oxidation of the hydroxyl group, with a gradual but continued increase of the Cr(VI) transformation that reached 92% after 31 h, compared to a 52% reduction with Fe(0) alone.

5.3.3 Reduction of Cr(VI) in the presence of diverse organic structures

Other molecular structures were also tested their ability to enhance Cr(VI) reduction during reaction with ZVI. The results were summarized in Table 5.3 and Fig. 5.4. None of the tested organic molecules (acetylacetone, ascorbic acid, cyclodextrin, deferoxamine, glycerol, humic acids, 1,10 phenathroline or phytic acid) decreased the Cr(VI) reduction rate. Only those compounds that either reacted with Cr(VI) (ascorbic acid or thiourea) or have strong affinity for Fe as chelating ligands (acetylacetone, deferoxamine, 1,10 phenanthroline) enhanced the Cr(VI) transformation.

At acidic conditions (pH~2.0) acetylacetone (acac) and phenathroline (phen) modestly increased the rate of Cr(VI) to Cr(III) transformation (less than two-fold relative to ZVI alone, Table 5.3). Under acidic conditions the formation of four-coordinate Cr(VI) intermediates [(phen)Cr(VI)O_2] has been proposed which may facilitate the Cr(VI) electron transfer reaction with a concomitant increase of the first-order kinetic rate constant [190]. Colour changes (from yellow to orange-red) during the course of the reaction suggested the production of Fe-acac and Fe-phen complexes. The absorption spectrum of the final reaction suspension corroborated the formation of Fe(III)-acac (absorption maximum at 480 nm) and Fe(II)-phen complexes (absorption maximum at 510 nm) [10].

At the more neutral pH, the presence of phen (o) did not have a major impact on the Cr(VI) reduction rate (Fig. 5.4B). As measured at 510 nm, a monotonic increase in the concentration of Fe(II) was observed in the presence of phen ($0.012x - 2.75$, $r^2=0.989$, SD= 3.23), however, in the absence of phen, virtually no Fe(II) was detected in solution.

Table 5.3 Predicted surface area-normalized rate constant (k_{SA}), and calculated surface-area normalized half-life ($t_{SA1/2}$) for the time dependant disappearance of Cr(VI) from unbuffered solution at various initial pHs (pH_i) for selected organic molecules.

	pH_i[a]	**k_{SA1}[b] (ml min^{-1} m^{-2})**	**R^2_{kSA1}**	***I*.time[c] (min)**	**k_{SA2}[d] (ml min^{-1} m^{-2})**	**r^2_{kSA2}**
Fe(0)	2.1	4.67	0.992	N/A	N/A	N/A
	5.8	0.067	0.987	30	$5.3x10^{-3}$	0.990
	9.0	0.026	0.976	25	$4.3x10^{-3}$	0.972
Acetylacetone	2.1	7.2	0.992	N/A	N/A	N/A
	5.8	0.085	0.994	50	$2.6x10^{-2}$	0.990
Ascorbic acid	2.0	32	0.986	N/A	N/A	N/A
	6.1	0.17	0.977	40	$1.4x10^{-2}$	0.980
Deferoxamine	2.1	12	0.987	N/A	N/A	N/A
	6.0	0.10	0.987	60	$1.7x10^{-2}$	0.982
	9.4	0.036	0.974	60	$5.3x10^{-3}$	0.986
1,10-phenanthroline	2.1	8.8	0.996	N/A	N/A	N/A
	5.9	0.050	0.997	60	$6.7x10^{-3}$	0.993
Thiourea	2.1	8.9	0.998	N/A	N/A	N/A
	5.9	0.075	0.976	45	$6.0x10^{-3}$	0.990

[a] initial pH, [b] surface area normalized rate constant for the initial decay, [c] *I*. time refers to the intersection time between the two modeled decays, [d] surface area normalized rate constant for the second decay.

[b,d] The sum of two exponential decays was used to model the observed kinetic results (k_{SA1} and k_{SA2}).

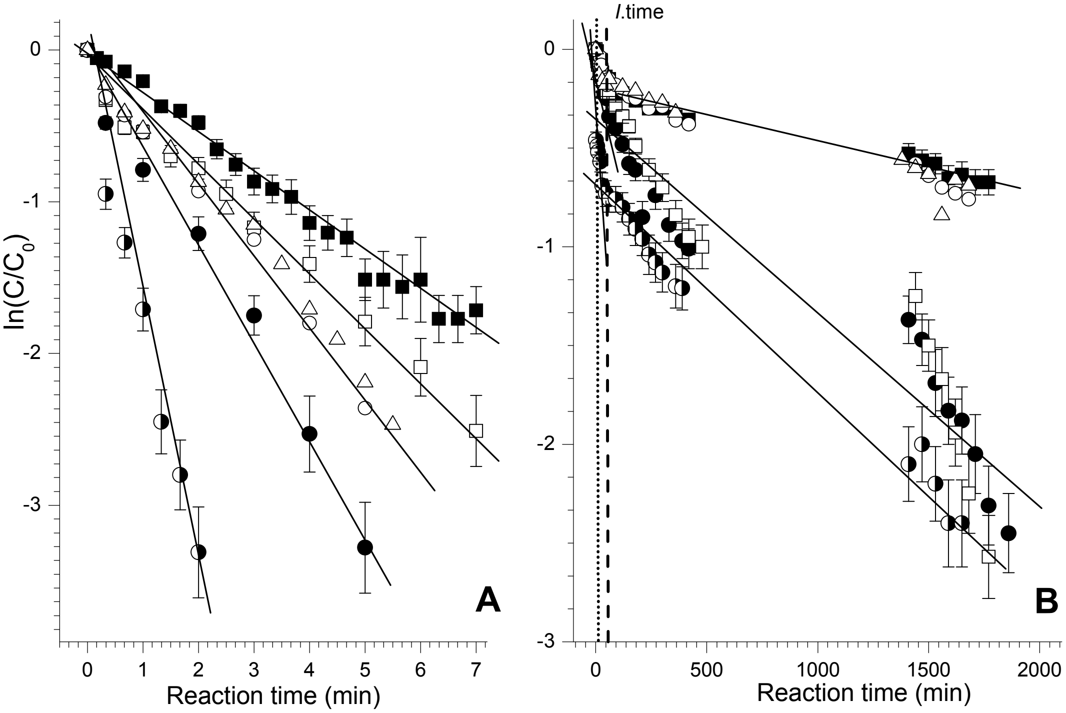

Figure 5.4 Selected plots of the variation with time of the ln of the ratio of the mean Cr(VI) concentration at time t to the initial concentration (μM) when reacted (A) at pH 2.0± 0.1 or (B) at 6.0± 0.2 with ZVI at a Fe(0) to Cr(VI) ratio (~300): Fe, (■); acac, (□); DFO, (●); tu, (Δ); ascorbic acid, (◑); and phen, (○),*l*.time (30 min) for Fe(0) alone (dotted line), *l*.time (60 min) for DFO and phen reaction systems (dashed line). Uncertainties in some the determinations of certain Cr(VI) concentrations were omitted to facilitate the plot visualization.

Zhou et al., reported a suppression of the zero-order-reaction between Fe(0) and Cr(VI) in the presence of phen at pH 4.0 (0.224 g L^{-1}Fe(0); 100 μM Cr(VI); and 1000 μM 1,10 phenanthroline) attributed to the formation of Fe(II) phen stable complexes [181]. For the current trials at pH 6.0±0.2, (7 g L^{-1} Fe(0); 390 μM Cr(VI) and 500 μM phen in a Tween® 20 media) the formation of Fe(II)-phen was observed (as discussed above), but no appreciable difference in the reduction rate relative to ZVI alone (k_{SA1} and k_{SA2}, Table 5.3) was recorded. The authors also reported a 45% reduction in the concentration of Cr(VI) during a period of more than 2000 min. After almost the same period of reaction, a 59% decrease in the initial Cr(VI) concentration (Fig. 5.4) was observed.

In the last decade, special consideration has been directed to siderophores of fungal or bacterial origin for their iron-chelating properties [191,192]. Deferoxamine (DFO) is a trihydroxamate siderophore with a terminal primary amino group, which generates thermodynamically stable high-spin Fe(III)-DFO complexes [192]. The inclusion of DFO in the Cr(VI)-ZVI reaction mixture resulted in a two-fold increase of the reduction rate at acidic conditions (Table 5.3, Fig. 5.4A). The formation of the hydroxamate-iron binding was revealed by the red shift in the UV-vis spectrum of the reaction suspension, (from 400 to 450nm corresponding to the hexaaquo Cr(III) and Fe(III)-DFO complex respectively) corroborating the formation of the hexacoordinate Fe(III)-DFO complex. A similar enhancement was also observed at the more circum neutral condition with an increase of two and three-fold in k_{SA1} and k_{SA2} relative to ZVI alone (Table 5.3). At more alkaline conditions (pH~9.4) a considerable increase in Cr(VI) reduction rate was achieved relative to ZVI alone (five and eight-fold increase for k_{SA1} and k_{SA2} respectively). At this pH, more than half of the hydroxamate groups are no longer protonated which favours complex formation and retards the formation of the oxide/hydroxide passivating layer on the iron surface.

Thiol-containing compounds are widely recognized as suitable reducing agents [193]. The impact of thiourea (tu) was evaluated as an accelerator in the ZVI mediated reduction of Cr(VI) at various pHs. At pH 2.0, a two-fold increase of the rate constant was observed (Table 5.3, Fig. 5.4). It can be presumed that a rapid reduction of Cr(VI) was accompanied by the formation of a disulfide or $RSCrO_3^-$ intermediate that facilitated Cr(VI) reduction [190]. The Cr(VI) reduction in the presence of thiourea was monitored by absorbance measurements during the course of the reaction. There was no evidence of Cr(VI)/thiol complex formation as characterized by a red shift of the chromate absorbance with an increase in absorbance at 430-450 nm

[194]. Experiments, performed in the absence of ZVI, demonstrated that reduction of Cr(VI) by thiourea was virtually complete after approximately 30h. ATR/FTIR spectra of the resulting solution displayed a decreased absorbance at 741 cm^{-1} (characteristic of the C=S stretching mode) and the appearance of sharp peak maximum at 1730 cm^{-1} characteristic of a carbonyl (C=O) stretching mode, indicating that the two-step reduction reaction was complete after this time [195]. No appreciable difference in the reduction rate was observed at increased pH. When trials were performed in the absence of ZVI, only 10% of Cr(VI) was transformed to Cr(III) after 30 h of reaction at pH~6.0. The formation of high-spin Fe(II) complexes with thiourea has been reported previously, but no evidence of the formation of Fe-TU complexes was detected over the course of the reaction [196].

Ascorbic acid (vitamin C, AA), a non-toxic biological reducing agent, has been reported to reduce Cr(VI) over a wide range of pHs [179]. In the current study, experiments carried out in the absence of Fe(0) at pH 2.0 for reaction of 390 μM Cr(VI)-Tween® 20 suspension with 270 μM AA demonstrated that 80% Cr(VI) had been reduced after 24 h. A model consisting of the sum of two-pseudo first order reactions provided an appreciably better fit to the data than did the single exponential decay with an intersection time (*I*.time) of 2 min ($k_1 = 0.16$ min^{-1}; $r^2 = 0.976$ and $k_2 = 5.5 \times 10^{-4}$ min^{-1}; $r^2 = 0.984$).

Under acidic conditions, complete reduction of Cr(VI) to Cr(III) was achieved in less than 2 min when the reaction mixture of Tween® 20-Cr(VI) and iron suspension was reacted in presence of 270 μM of ascorbic acid ([Cr(VI)] = 400 μM; pH 2.0; [Fe] = 7.2 g L^{-1}, Table 5.1 and Fig. 5.4A). This dramatic increase in the rate of Cr(VI) reduction in the presence of Fe(0) and AA probably was caused by the catalytic effects of Fe(III) in the oxidation of AA. Most likely, this process involves oxidation of AA to dehydroascorbic acid (DHA), following by hydrolysis that leads to opening the lactone ring to produce 2,3-diketoglulonic acid. Cleavage and further oxidation produce oxalic acid and L-threonic acid with a concomitant net increase of the Cr(VI) transformation [179,197]. As indicated in Fig. 5.4B, increasing the pH to 6.0, decreased dramatically the Cr(VI) reduction rate compared to more acidic pH values, yet an appreciable increase (~5-fold, Table 3) in rate, relative to Fe(0), alone was achieved.

5.4 Conclusions

The reductive remediation of chromate by ZVI in aqueous media is strongly affected by the passivation of the metal surface with the consequent loss of reactivity. The enhancement of the pseudo-first order rate constant was observed at circum neutral conditions only for those molecules that either reduced Cr(VI) (ascorbic acid, thiourea, cysteine, glycolic, lactic, malic and tartaric acids, 1,3-diamino-2-hydroxypropane-*N*,*N*,*N*',*N*'-tetraacetic acid) or formed stable complexes (citric acid, deferoxamine, acac, EDDS) with the reaction products. The formation of Cr(III) and Fe(III) complexes anticipated to inhibit the formation of insoluble precipitates, thus decreasing passivation of the Fe(0) surface. The rates of reaction of Cr(VI) in the presence of each of the tested molecules, were increased dramatically in acidic conditions (up to 50-fold).

This study demonstrated that the inclusion of these benign naturally-occurring organic molecules in a Cr(VI)-Fe(0) remediation system accelerate the reaction rate and can provide a protective effect for surfaces of iron metal permeable reductive barriers.

Chapter

Six

Preface

In Chapter five, a variety of naturally-occurring molecules (containing α-hydroxyl carbonyl, α-hydroxyl carboxylate, α-carbonyl carboxylate, phenolate, carboxylates and/or thiol groups, siderophores, ascorbic acid); chelating agents (ethylenediaminetetraacetic acid derivates) and others organic compounds (acetylacetone, phenanthroline, urea) were evaluated for their ability to accelerate the reduction of a surfactant preparation (Tween® 20) containing Cr(VI) and Fe(0) under a variety of reaction conditions. An appreciable enhancement (up to 50-fold) of the pseudo-first order rate constant was achieved at acidic and circum neutral pH conditions for those compounds capable of reducing Cr(VI) (α-hydroxyl carboxylate, ascorbic acid, cysteine). Comparable enhancements were obtained for certain chelating reagents which is attributed to the formation of complexes with reaction products that impeded the precipitation of Cr(III) and Fe(III) hydroxides and thus decreased passivation of the Fe(0) surface. The results suggest that these molecules might be used in effective remediation mediated by Fe(0) of Cr(VI)-contaminated soils or groundwater in a wide range of pH. The use of these compounds might increase reaction rates and extend the duration of the useful long-term performance of permeable reductive barriers.

Chapter six reports the influence of various transition metal and non-metal oxyanions (borate, phosphate) on the zero-valent iron mediated reduction rate of a surfactant preparation containing Cr(VI) under selected reaction conditions. Synergetic interactions among selected oxyanions are explored that lead to an improvement of the overall kinetic parameters of Cr(VI) reduction mediated by zero-valent iron. Such synergetic behaviour can be advantageous for brownfields that are burdened with a multiplicity of diverse pollutants.

Chapter Six

Impact of various inorganic oxyanions on the removal rate of hexavalent chromium mediated by zero-valent iron

6.1 Introduction

Although chromium is a naturally occurring substance, the majority of chromium raising environmental concerns is from anthropogenic sources [198]. Two possible oxidation states for chromium, Cr(III) and Cr(VI), exist in the environment. Cr(VI) is highly mobile in aquifers since it does not sorb strongly onto most soils, while Cr(III) is less water-soluble [111,160,198]. Cr(VI) is a strong oxidant, toxic, and potential carcinogenic. Contrarily, Cr(III) is relatively non-toxic and an essential human nutrient. It does not readily migrate in groundwater since it usually precipitates as hydroxides, oxides, or oxyhydroxides [199]. In recent years, a great deal of research efforts has gone to find better strategies to treat chromium contamination in the environment. In particular, a number of studies have demonstrated that zero-valent iron ZVI is an effective reductant for Cr(VI) [111]. It has been reported that ZVI is capable of degrading many chlorinated hydrocarbon solvents efficiently via reductive hydrodehalogenation and can mobilize other redox sensitive inorganic contaminants (CrO_4^{2-}, NO_3^-, MoO_4^{2-}, UO_2^{2+}, AsO_4^{3-}, TcO_4^-) [106,107,116,118]. ZVI-based technologies exploit the marked contrast of the toxicity and mobility between Cr(VI) and Cr(III) to remediate Cr(VI)-contaminated sites.

Although ZVI has been proven to be an effective and inexpensive material for the reduction of Cr(VI), its Cr(VI) reduction kinetics rate are prone to be adversely affected by the initial Cr(VI) concentration, pH, background electrolyte concentration, iron surface area and type, and presence of other dissolved contaminants. The rate of reduction of Cr(VI) to Cr(III) dramatically diminishes with time as a result of the thermodynamic instability of ZVI. The presence of water and/or dissolved oxygen causes the precipitation of iron species (oxides, hydroxides, oxyhydroxides and carbonates), producing a passivating layer on the iron surface. The transfer the electrons from the iron surface to the adsorbed Cr(VI) is significantly impeded.

It has been reported (Chapter 5) that simple aliphatic organic acids such as formic, tartaric, and citric acids naturally occurring in soil and subsurface environments can influence reductive detoxification mediated by ZVI via adsorption and complexation with the active surface sites of Fe(0) and/or iron corrosion products. In addition, major oxyanions such as sulfate, phosphate, and borate also present in the environment have been shown to decrease the removal kinetics of both arsenate and arsenite by Peerless Fe(0) [108,116]. The interaction of phosphate with iron oxides is strong and well documented. Recent Fourier transform infrared (FTIR) spectroscopic evidence for sulfate adsorption reveals that one monodentate surface iron complex is dominant over a wide range of surface coverages and pH values in the case of adsorption on hematite (α-Fe_2O_3) and goethite (α-FeOH·OH) [108,200]. Another recent FTIR study demonstrated that sulfate forms both outer-sphere and inner-sphere surface complexes on α-FeOH·OH at $pH < 6$ whereas at $pH > 6$, sulfate adsorbs on goethite as an outer-sphere complex [201]. Borate is also known to form inner-sphere complexes with iron oxides [202]. It has been shown that zerovalent-iron readily reacts with various oxyanions such as arsenate, chromate, nitrate, selenate, perchlorate, pertechnate, etc. The presence of one or more of these oxyanions can interfere in the removal and/or kinetic rate of reduction of chromate by zero-valent iron. The influence of these inorganic anions on chromate reduction by Fe(0) has not been fully elucidated nor quantified.

In the current report, the mobilization and detoxification of Cr(VI) from a contaminated soil was evaluated. The Cr(VI)-contaminated soil sample was treated with one of several surfactant formulations, as a possible mobilization aid to dislodge the target ion from particulate surfaces. The resulting extract (containing Tween® 20) was reacted with ZVI in the presence of competing oxyanions such as borate, silicate, molybdate, nitrate, nitrite, selenate, selenite, arsenate, phosphate, sulfate, perchlorate, periodate, permanganate.

6.2 Materials and methods

All solutions and suspensions were prepared from distilled deionized water (DDW) with resistivity of 18.0 MΩ cm, (Millipore Corp., Milford, MA, USA). Stock dichromate and other inorganic salt solutions were prepared from analytical-grade reagents (Fisher Scientific, Napean, ON, Canada) and filtered through a 0.2-*μ*m membrane filter (Fisher Scientific) prior to use.

Test surfactant (Tween® 20), Na_2SiO_3 (SiO_2 44-47% purity), 1,10 phenanthroline (99+% purity), $AgNO_3$ (99.8% purity), Na_2MoO_4 (98+% purity), NaH_2PO_4 (98% purity), Na_2SO_4 (98+% purity), NH_4ClO_4 (99.8% purity), Na_2SeO_4 (99% purity), Na_2SeO_3 (99% purity), were used as received from Sigma-Aldrich, Oakville, ON, Canada. Iron metal (40 mesh, specific surface area 1.01 m^2 g^{-1}), *S*-diphenyl carbazide, HCl (37% V/V), HF (48% V/V)), H_2SO_4 (95.0-98.0% purity), KNO_3 (98% purity), KNO_2 (99% purity), $KMnO_4$ (98+% purity), NH_4Cl (99% purity), KIO_4 (98-102% purity) ACS reagent grade ethanol and acetone were obtained from Fisher Scientific, Napean, ON, Canada. $Na_2HAsO_4 \cdot 7H_2O$ (98+% purity) was purchased from Alfa-*A*esar, Ward Hill, MA, USA.

Aqueous metal standard solution of As, B, Cr, Mo, P, Se, and Si 1,000 mg L^{-1}, traceable to the National Institute of Standards and Technology (NIST) primary standard, and multi-element standard solution used for quality control were purchased from SCP Chemical Co., St-Laurent, Qc, Canada.

Total arsenic, boron, chromium, molybdenum, phosphorous, selenium, and silicon was determined by inductively coupled plasma optical emission spectrometry (ICP-OES) using a Varian Vista-MPX spectrometer (Varian Australia Pty Ltd., Australia) and multiple emission lines (188.980 nm and 193.696 nm for As; 249.772 nm and 249.678 for B; 28.563 nm and 357.87 nm for Cr; 202.032 nm and 379.825 nm for Mo; 213.618 nm and 214.914 nm for P; 196.026 nm and 203.985 nm for Se; and 251.611 and 288.158 for Si) were selected to assess the spectral interferences and a FACT (fast automated correction technique) model was used to correct the possible interferences.

Acid-washed iron was used in all the experiments. In initial studies, a known quantity of iron granules was washed copiously with 6M HCl and rinsed five times with distilled water, three times with ethanol and a further three times with acetone then dried in a N_2 stream for 2 h. This procedure might produce soluble chloride interfering with quantification of chloride potentially produced by perchlorate reduction. Hydrochloric acid was subsequently replaced by 1.0 N HF in the acid-washing procedure. To inhibit oxidation, the iron powder was stored under a nitrogen atmosphere prior to use.

The original diphenylcarbazide (DPC) method recommended by the APHA, was adapted to work on a microscale [154]. Once filtered, the samples were immediately inserted into the Hach test tube with a freshly prepared DPC solution in acetone (200 μL, 5 g L^{-1}) and H_2SO_4 (5 μL, 10% V/V). The reaction was permitted to continue for 5-10 min then diluted with 10 mL DDW.

Total soluble ferrous ion (Fe^{+2}) in the surfactant extract was analyzed in accordance with the standard Analysis Method 3500-Fe [B] based in the colorimetric reaction between with 1,10-phenanthroline [154]. Chloride determination was carried out following the recommendation of the standard Analysis Method 4500-Cl^- [B], based in the precipitation of silver chloride [154].

Determination of ammonia, and nitrate/nitrite were performed using an automated ion analyzer QuikChem® 8500 Series Flow Injection Analysis System equipped with heating unit (Lachat Instruments, Inc., Loveland Colorado, USA) following the methods QuikChem® Method 10-107-06-2-C and 10-107-04-1-A respectively recommended by LACHAT Instruments.

Spectroscopic measurement uncertainties associated with the determination of Cr(VI) and Fe(II) concentrations in the extract were calculated using a cause-and-effect approach as reported previously [155].

The kinetics experiments were performed in strongly (pH 2.0) or weakly acidic solutions (pH 4.0 - 6.0). All reactions were carried out using a Tween® 20 extract suspension containing an initial concentration of 390 μM Cr(VI) and a concentration of 7g L^{-1} Fe(0). In addition, 500 μmoles of the inorganic test reagent was added to result in a 500 μM reaction suspension. The reaction of Cr(VI) and the organic reagent was also studied in the absence of Fe(0). The suspension was mixed and shaken continuously. At convenient intervals, 0.5-1 mL aliquots were withdrawn, filtered through 0.45 μm membrane filter, and added to a clean and dry Hach test tube.

6.3 Results and discussion

A soil that had been heavily field-contaminated with hexavalent chromium was washed with various surfactant formulations (anionic, non-ionic or cationic) to evaluate the relative efficiency as mobilization aids for Cr(VI). Once the pollutant had been mobilized, the solution that resulted was reacted with various metallic mixtures.

Previously, it had been observed that the presence of Tween® 20 in the extract of Cr(VI) had no perceptible effect on the reaction kinetics with ZVI, and were adequately described by either a single or the sum of two pseudo-first-order kinetic models [167].

Table 6.1 summarizes the goodness of fit of a linear model to the experimental data (either a single exponential decay for pHs of ≤ 2.0 or the sum of two exponential decays for pHs ≥ 3.0) and the observed kinetic parameters {surface area normalized rate constant (k_{SA})} for the various inorganic oxyanions tested in the presence of ZVI.

As reported previously for ZVI, if the initial pH was increased to 3.0 or above, a model consisting of the sum of two-pseudo first order reactions provided an appreciably better fit to the data than did the single exponential decay [167].

The first decay was considered to be dominated by reaction that occurred at exposed Fe active sites. Once the passivating (oxy)hydroxide layer had formed, a second decay function described the reaction rate that was decreased but not totally inhibited. The second decay function was considered to model reaction at the surface of the passivated layer. As summarised in Fig. 6.1 and Table 6.1, relative to ZVI, appreciable increases for Cr(VI) reduction rates were observed in the presence of certain reagents when working at pH~2, but minor differences (less than 2-fold) were detected for more circum neutral pH conditions.

The reduction rate of Cr(VI) mediated by ZVI at pH 2.0, was not appreciably modified by the presence of borate, molybdate, phosphate, or silicate. At selected intervals during the course of the reaction, the concentrations of total boron, molybdenum, phosphorous, and silicon were determined by ICP-OES. No detectable decrease in B or Si concentration suggest that no competition for active Fe sites occurred either by the sorption on the iron surface or the formation of surface complexes [111,202]. On the other hand the concentration of Mo had diminished by 16% after 15 min of reaction, which can be attributed to the reduction by ZVI of MoO_4^{2-} to Mo^{3+} which was then precipitated as $Mo(OH)_3$ [116].

At a concentration approximately equivalent to the Cr(VI), phosphate caused a significant decrease in Cr(VI) removal kinetics by ZVI at the acidic condition. Contrarily to previous findings, the sum of two-pseudo first order models provided an appreciably better fit to the data that did a single pseudo-first order model (Fig. 6.1 A and B). The first decay (*I*.time 1 min) can be considered to be dominated by the rapid reaction with the exposed Fe active sites (k_{SA} = 4.7 mL min^{-1} m^{-2} and k_{SA1} = 4.8 mL

min^{-1} m^{-2} with or without phosphate respectively). The second model is governed by the precipitation of iron-phosphate species on the iron surface [116].

Table 6.1 Predicted surface area-normalized rate constant(s) (k_{SA}) in the presence of Fe(0) and test reagent for the time dependant disappearance of Cr(VI) from unbuffered solution at various initial pHs (pH_i).

	pH_i[a]	k_{SA1}[b] (ml min^{-1} m^{-2})	r^2_{KSA1}	*I.*time[c] (min)	k_{SA2}[d] (ml min^{-1} m^{-2})	r^2_{KSA2}
Fe(0)	2.1	4.7	0.992	N/A	N/A	N/A
	5.8	0.067	0.987	30	$5.3x10^{-3}$	0.990
Arsenate	2.2	5.1	0.987	N/A	N/A	N/A
	6.0	0.022	0.965	30	$1.2x10^{-3}$	0.953
Borate	2.1	3.5	0.983	N/A	N/A	N/A
	5.8	0.062	0.985			
Molybdate	1.9	3.5	0.996	N/A	N/A	N/A
	5.7	0.058	0.984	45	$9.9x10^{-3}$	0.985
Nitrate	2.1	7.2	0.994	N/A	N/A	N/A
	5.7	0.059	0.990	60	$5.7x10^{-3}$	0.989
Perchlorate	2.1	7.8	0.983	N/A	N/A	N/A
	5.8	0.045	0.982	120	$8.9x10^{-3}$	0.993
Permanganate	2.1	6.3	0.989	N/A	N/A	N/A
Phosphate	1.9	4.8	0.996	1.0	2.59	0.984
	5.8	0.011	0.979	30	$9.9x10^{-3}$	0.994
Selenate	2.1	14	0.997	N/A	N/A	N/A
	5.8	0.093	0.982	30	$5.9x10^{-3}$	0.988
Silicate	2.0	4.2	0.993	N/A	N/A	N/A
	9.0	0.016	0.991	30	$2.4x10^{-3}$	0.987
Sulfate	2.1	5.5	0.995	N/A	N/A	N/A
	5.8	0.11	0.979	30	$9.9x10^{-3}$	0.986

[a] initial pH, [b] surface area normalized rate constant for the initial decay, [c] *I.* time refers to the intersection time between the two modeled decays, [d] surface area normalized rate constant for the second decay. [b,d] The sum of two exponential decays was used to model the observed kinetic results (k_{SA1} and k_{SA2}).

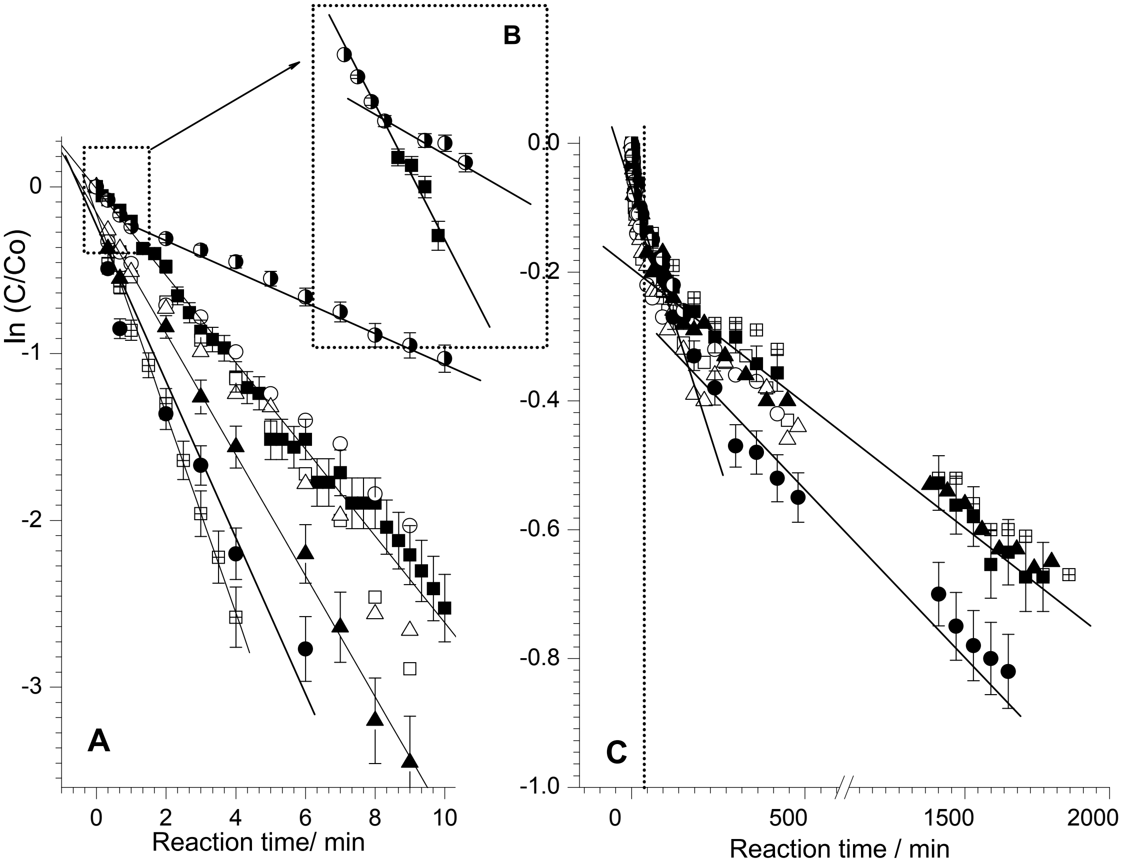

Figure 6.1 Selected plots of the variation with time of the ln of the ratio of the mean Cr(VI) concentration at time t to the initial concentration (*μ*M) when reacted (A) at pH 2.0 ± 0.2 or (C) at pH 6.0 ± 0.2 with ZVI at a Fe(0) to Cr(VI) ratio (~300): Fe, (■); arsenate, (□); perchlorate, (●); molybdate, (○); nitrate, (▲); sulfate, (Δ); phosphate, (◑); and selenate, (⊞), *l*.time (30 min) for ZVI (dotted line C). Plot (B) is an expansion of the intersection of the 2 models when reacting Cr(VI) in the presence of phosphate and ZVI (some points of the Fe plot were removed to improve visualization). Some uncertainties in the determinations of certain Cr(VI) concentrations were omitted to facilitate the plot visualization.

Such phenomenon was corroborated by a net decrease in the total P concentration in solution (75% decreased after 20 min reaction) and the appearance of whitish cloudiness in the reaction mixture after 1 min. Su and Puls (2001), reported a significant decrease in As(V) and As(III) kinetics mediated by Fe(0) in the presence of phosphate [116]. This was attributed to the formation of inner-sphere complexes with Fe with a consequent precipitation to form discrete solid phases on the iron surface.

This effect can be considered as advantageous, taking into account that ZVI technologies are capable of removing several inorganic oxyanions at the same (including, arsenate, arsenite, chromate, nitrate, perchlorate, etc.); however, excess of phosphate may reduce the effectiveness of the iron surface for certain of the contaminants (at least for As and Cr).

Under acidic conditions and arsenate concentration lower than 280 μM, arsenate seems to have little effect on Cr(VI) removal kinetics (data not shown), although As concentration slightly decreased after 10 min of reaction (3.7 %). If the initial arsenate concentration was greater than 500 μM a behaviour similar to that of phosphate occurred (Fig. 6.1 A and B). The sum of two first order models provide a better fit to the data (k_{SA1} = 7.5 mL min^{-1} m^{-2} and k_{SA2} = 2.3 mL min^{-1} m^{-2}, *l*.time 1 min). Over the course of the reaction, the concentration of total As diminished by 16 percent. At more circum neutral conditions (pH 6), this effect is more pronounced. The precipitation of Fe-arsenate species on the iron surface can impede the electron transfer from the iron surface to the adsorbed chromate [116]. It is likely that the As(V) competes with Cr(VI) for the active sites and the available electrons, causing a decrease in the rate of Cr(VI) reduction. Liu et al. 2009, reported similar results when reacting Cr(VI) with ZVI in presence of As(V) [203].

Fig. 6.2 summarises the effects of ZVI (■) mediated reduction of Cr(VI) in the presence of nitrate (●) and nitrite (□), together with the disappearance of inorganic nitrogen species (▲) and appearance of ammonia (○). In acidic conditions nitrate modestly accelerate the reduction of Cr(VI) (k_{SA} 7.2 mL min^{-1} m^{-2} relative to ZVI alone, k_{SA} 4.7 mL min^{-1} m^{-2}) while is being reduced at the same time by ZVI. This increment may be attributed to the iron corrosion caused by nitrate reduction:

$$NO_3^- + Fe^0 + 2H^+ \rightarrow NO_2^- + Fe^{2+} + H_2O \qquad (1)$$

$$NO_3^- + 4Fe^0 + 10H^+ \rightarrow NH_4^+ + 4Fe^{2+} + 3H_2O \qquad (2)$$

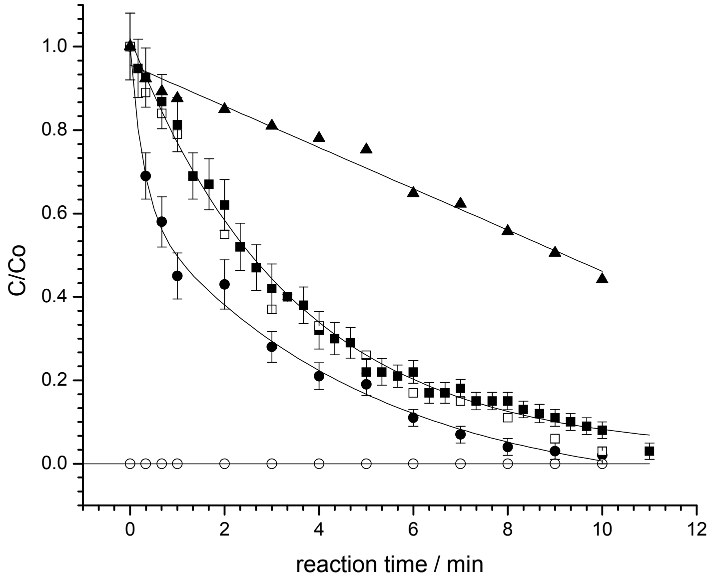

Figure 6.2 Variation with time of the C/Co the ratio of the mean Cr(VI), NO_3^-, and NH_4^+ concentration at time t to the initial concentration (*μ*M) when reacted at pH 2.0 ± 0.1 with ZVI at a Fe(0) to Cr(VI) ratio (~300): Fe, (■); chromate and nitrite, (□); chromate and nitrate, (●); concentration of NH_4^+, (○); disappearance of nitrate, (▲).

Negligible amount of ammonia was accumulated while nitrate (and chromate) was being reduced by Fe(0) (Fig. 6.2), thus it can be assumed that under the experimental conditions nitrate is first reduced to nitrite (pseudo-first order kinetic model k_{SA} 1.4 mL min^{-1} m^{-2}) following eq. (1).

The ZVI mediated reduction of Cr(VI) was not considerably affected by the presence of nitrite (k_{SA} 4.9 mL min^{-1} m^{-2} relative to ZVI, k_{SA} 4.7 mL min^{-1} m^{-2}).

At more alkaline conditions (pH ~ 6.0) Cr(VI) the rate of transformation was marginally affected by the presence of nitrate or nitrite (Table 6.1). Certain researchers have reported insignificant nitrate reduction at pH values greater than ~ 5, or in unbuffered deionized water [108, 109, 168].

A three-fold increase in the Cr(VI) kinetic rate constant at acidic conditions was observed in the presence of selenate (Fig. 6.1 A, Table 6.1). This enhancement in the rate of reduction might be attributed to the rapid reduction of Se(VI) to Se(IV) species mediated by ZVI, favouring the production of ferrous ion which readily reacts with chromate [117, 204]. Determination of total Se by ICP-OES, over the course of the reaction (less than 10 min), demonstrated that the concentration of soluble Se remained unchanged. It suggested that minimal adsorption of Se(VI) and/or Se(IV) species to the iron surface occurred under experimental conditions. In the absence of ZVI at pH~2, no interactions between selenate and chromate were observed.

The influence of selenite in the Cr(VI) transformation was also tested, with little variation to the constant rate (k_{SA} 5.1 mL min^{-1} m^{-2}). It has been considered that Se(IV) species reacts more slowly with Fe(0) than Se(VI) species and are more difficult to reduce {mainly to Se(0)} [117]. At more circum neutral pH value, selenate and selenite do not interfere with Cr(VI) reduction (Fig. 6.1, Table 6.1).

The presence of perchlorate in the reaction mixture modestly accelerated the Cr(VI) reduction rate at pH~2 but decreased the reduction rate ate pH~6 (Fig. 6.1, Table 6.1). From a thermodynamic standpoint, the perchlorate ion is anticipated to spontaneously degrade at ambient conditions through with the release of molecular oxygen {eqs. (3) – (5)} [81,205].

$$ClO_4^- + 8H^+ + 8e^- \leftrightarrow Cl^- + 4H_2O \qquad E^0 = 1.389\ V \qquad (3)$$

$$ClO_4^- + 2H^+ + 2e^- \leftrightarrow ClO_3^- + H_2O \qquad E^0 = 1.189\ V \qquad (4)$$

$$2H_2O \leftrightarrow 4H^+ + O_2 + 4e^- \qquad -E^0 = 1.229\ V \qquad (5)$$

However, perchlorate ion is relatively stable in solution. The low reactivity is caused by the slow kinetic liability rather than thermodynamic instability.

To follow the perchlorate reduction over the course of Cr(VI) reduction by ZVI, chloride evolution was monitored through the argentometric method [154]. The lack of cloudiness (silver chloride) led us to presume that perchlorate was partially reduced to chlorate ClO_3^- and/or chlorite (ClO_2^-) concomitantly with iron corrosion. The increase of ferrous ion may play an important role in the enhancement of chromate reduction. It should be pointed out that ZVI used in these experiments was washed with dilute HF solution to avoid the interference of soluble chloride trapped in the iron lattice. Perchlorate reduction in acidic media has been observed not only on zero-valent iron but also on aluminium, copper, and nickel [119,137].

For comparative purposes, periodate ion (IO_4^-) was added to the Cr(VI)-ZVI reaction mixture. In strongly acidic media, periodate moderate accelerate Cr(VI) reduction (k_{SA} 6.6 mL min^{-1} m^{-2}).

The presence of permanganate in the reaction mixture at pH ~ 2, slightly increased the transformation of Cr(VI) (Table 6.1, Fig. 6.3 (○)). The violet colour of the reaction suspension was rapidly discharged during the reaction, the appearance of a brownish precipitate (MnO_2) might involve a rapid reaction between Cr(VI) and Mn(VII) (favoured by the standard electrode potential) parallel to the reduction of MnO_4^- by Fe(0) [205].

$$MnO_4^- + 4H^+ + 3e^- \leftrightarrow MnO_2 + 2H_2O \qquad E^0 = 1.679\ V \qquad (6)$$

$$HCrO_4^- + 7H^+ + 3e^- \leftrightarrow Cr^{3+} + 4H_2O \qquad E^0 = 1.35\ V \qquad (7)$$

$$MnO_2 + 4H^+ + 2e^- \leftrightarrow Mn^{2+} + 2H_2O \qquad E^0 = 1.224\ V \qquad (8)$$

The brownish solid disappeared over the course of the reaction, likely caused by further reduction of MnO_2 to Mn^{2+} $\{[Mn(H_2O)_6]^{2+}\}$. Fig. 6.3 shows the alteration in total Mn concentration (●) when reacted with ZVI, where clearly can be seen that initially the Mn concentration diminished (precipitation of MnO_2) and after a while Mn concentration increased steadily (Mn^{2+}). Fig. 6.3 also shows the change in the UV-VIS spectra of MnO_4^- in reaction mixture. When permanganate reacted at pH 2.1with ZVI the sum of two pseudo-first order kinetic model better fit the data; k_{SA1} = 5.9 mL min^{-1} m^{-2}, r^2 = 0.995, *I*.time = 6 min, k_{SA2} = 8.3 mL min^{-1} m^{-2} , r^2 = 0.985 (Fig. 6.3, (□)).

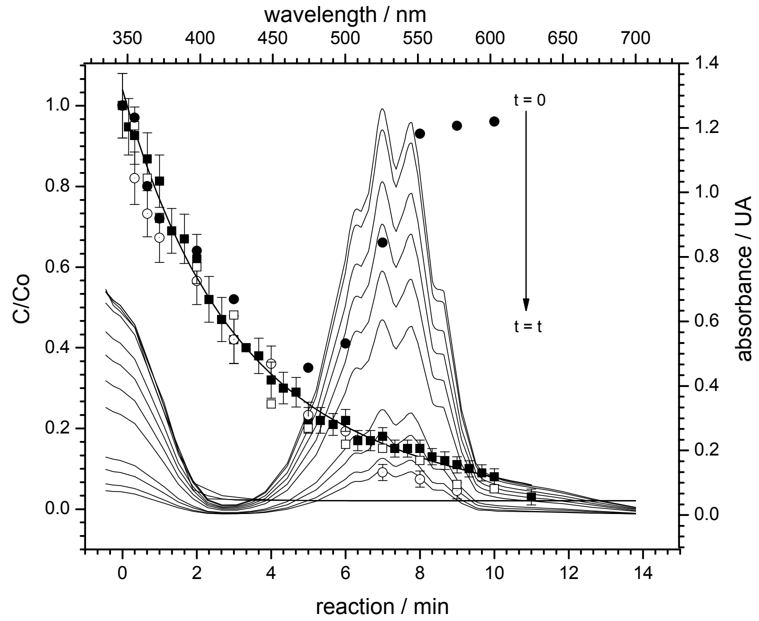

Figure 6.3 Variation with time of the C/Co the ratio of the mean Cr(VI), MnO_4^-, and total Mn at time t to the initial concentration (μM) when reacted at pH 2.0 ± 0.2 with ZVI at a Fe(0) to Cr(VI) ratio (~300): Fe, (■); chromate and permanganate, (○); total Mn, (●); disappearance of MnO_4^-, (□); background variation of UV-VIS spectra of MnO_4^- at time t.

6.4 Conclusions

The transformation of Cr(VI) mediated by zero-valent iron is highly dependent in iron corrosion reactions, with the consequent loss of reactivity caused by the passivation of the metal surface. Various oxyanions (nitrate, perchlorate, selenate), pollutants also found in contaminated sites, moderately accelerated the reduction of chromate by ZVI. It can be advantageous because brownfields usually are loaded with diverse pollutants. Zero-valent iron is capable of remove arsenate, arsenite, chromate, phosphate, perchlorate, etc., but only under certain conditions, simultaneous removal of oxyanions is achieved. The present study demonstrates that in a surfactant preparation (Tween® 20) containing chromate synergetic interactions occurred with various oxyanions (nitrate, perchlorate, selenate) at acidic pH values in the reaction with ZVI leading to an improvement of the overall kinetic model of Cr(VI) reduction and only moderate enhancement at circum neutral conditions. Neither improvement nor retardation of the Cr(VI) reduction kinetic parameters were observed in the presence of borate, molybdate, arsenate, silicate, and sulfate.

Chapter

Seven

Preface

In Chapters three to six, the disappearance of hexavalent chromium over the course of the reaction with metallic mixtures was monitored with the 1,5-diphenycarbazide colorimetric method. Toxic pollutants in the environment, such as hexavalent chromium, are strictly regulated by national and international legislation. Therefore, the analytical determination of such contaminants must be as precise and as accurate as possible. Moreover, an evaluation of the uncertainty associated with the result is essential. The report of an analytical result is, therefore, not considered complete without a formal statement of the uncertainty associated with it.

With increasing accreditation and qualtiy control (QC) procedures that are being implemented for all facets of analytical chemistry, measurement uncertainty is beginning to take on a higher profile. Indeed, analytical methods accredited in accordance with ISO Guide 17025 require an estimate of the associated measurement uncertainty. This wider use of properly calculated uncertainty estimates will ultimately permit improved intercomparability of anayltical results.

In this chapter, the evaluation of the uncertainty associated with the mass concentration of Cr(VI) is performed in accordance with the EURACHEM/CITAC Guide. The evaluation is approached in three stages: (1) a description of the measurement procedure and its model equation; (2) an identification of the main uncertainty sources and their quantification; and (3) the estimation of the combined and expanded uncertainties. Evaluation of the calculated uncertainty using dual or single wavelength spectrophotmetry for the determination of Cr(VI) is also investigated.

A portion of this chapter has been published in **Accred. Qual. Assur. 13 (2008) 711-716**. Authors: M. Rivero-Huguet, W.D. Marshall.

Chapter

Seven

Uncertainties when using dual-wavelength or single-wavelength spectrophotometry to monitor the course of hexavalent chromium reduction by zero-valent iron

7.1 Introduction

International trade, environmental protection, and science require increasingly reliable measurements. Nowadays, analytical laboratories producing any sort of measurement result (physical or chemical) are mandated by a formal (frequently legislative) requirement to provide results accompanied by a quantitative indication of the quality of the data. A parameter associated with the result of a measurement, that characterises the dispersion and quality of the value that can reasonably be attributed to the measurand is known as uncertainty. Its knowledge implies increased confidence in the validity of the measurement.

It is convenient to adopt a standard procedure to estimate the measurement uncertainty. The ISO guide to the expression of uncertainty in measurement (GUM) published by the International Standards Organization (ISO) is recommended by the Bureau International des Poids et Mesures (BIPM) and is followed by numerous outstanding analytical laboratories including the National Institute of Standards and Technology (NIST) and the Laboratory of Government Chemists (LGC) from the United States and the United Kingdom respectively. The EURACHEM/CITAC has also produced a guide that applies the GUM principles to analytical measurements [206,207,208].

Chromium is one of the common pollutants found in brownfields, as well as surface and subterranean waters throughout the industrialized world. Whereas chromium(III) is an essential nutrient in the diet of humans and animals in very small amounts, hexavalent chromium is potently toxic [24,25]. In recent years, a great deal of effort has been expended to identify and improve strategies to mitigate chromium(VI) contamination. In particular, several studies have demonstrated that zero-valent iron (Fe^0) is an efficient reductant for Cr(VI) [109,111,152,153]. The Cr(VI)-contaminated soil sample was treated with a surfactant solution (Tween® 20), as a mobilisation aid to dislodge the target ion from the particulate surfaces. The resulting solution was reacted with Fe^0 in acidic medium at ambient conditions. Sampling was performed after each 10 seconds of reaction and the Cr(VI) was analysed by the 1,5-diphenycarbazide colorimetric method [154].

Estimating the uncertainty in molecular spectroscopy is not an easy task. In practice, the combined uncertainty associated with the result can arise from several possible sources (that can include sampling, matrix effects and/or interferences, environmental conditions, uncertainties of masses and volumetric equipment and random variations) [209]. When estimating the combined uncertainty, it is frequently advantageous to treat each source of uncertainty separately to obtain the contribution from that source. Each of the separate contributions to uncertainty is referred to as an uncertainty component. When expressed as a standard deviation, an uncertainty component is known as standard uncertainty. However, for most purposes in analytical chemistry an expanded uncertainty (*U*) is used. The expanded uncertainty is obtained by multiplying the combined standard uncertainty $\{u_c(y)\}$, by a coverage factor *k*. In general, the value of the coverage factor *k* is chosen on the basis of the desired level of confidence to be associated with the interval defined by $U = k \cdot u_c(y)$. When the normal distribution applies and u_c is a reliable estimate of the standard deviation of y, $U = 2 \cdot u_c$ (i.e., $k = 2$) defines an interval having an associated level of confidence of approximately 95 %.

The general expression between the combined standard uncertainty $u_c(y)$ of a value *y* and the uncertainty of the parameters $x_1, x_2, \ldots\ldots\ldots x_n$ on which it depends is:

$$u_c(y(x_1, x_2, \ldots\ldots\ldots x_n)) = \sqrt{\sum_{i=1}^{n}\left[\frac{\partial y}{\partial x_i}u(x_i)\right]^2 + \sum_{i=1}^{n}\sum_{j=1}^{n}\frac{\partial y}{\partial x_i}\frac{\partial y}{\partial x_j}u(x_i, x_j)} \qquad (1)$$

where: $y(x_1, x_2, \ldots\ldots\ldots x_n)$ is a function of *n* parameters $x_1, x_2, \ldots\ldots\ldots x_n$,

$u_c(y(x_1, x_2, \ldots\ldots\ldots x_n))$ the combined standard uncertainty

$u(x_i)$ the standard uncertainty associated with x_i

$\frac{\partial y}{\partial x_i}$ the partial differential of y with respect to x_i, is a sensitivity coefficient

$u(x_i,x_j)$ is the covariance between x_i and x_j.

if $u(x_i,x_j) \neq 0$, variables are not independent but if $u(x_i,x_j) = 0$ variables are independent, and

$$u_c(y(x_1, x_2, \ldots\ldots\ldots x_n)) = \sqrt{\sum_{i=1}^{n}\left[\frac{\partial y}{\partial x_i}u(x_i)\right]^2} \qquad (2)$$

Therefore, the expanded uncertainty U is obtained by multiplying the $u_c(y)$ by the coverage factor *k.*

$$U = ku_c(y) \qquad (3)$$

It has been suggested that the use of dual-wavelength spectrophotometry (DWS) (or similar technique that makes use of the ratio of the absorbance at two selected wavelengths) can increase precision relative to the conventional method (single-wavelength spectrophotometry, SWS) that makes use of a single wavelength for the determination of trace amounts of a metal ion [210,211]. The modified approach can reduce the effect of spectral background due to impurities, solvent or radiation scattering. In this technique, the ratio of the absorbances at two wavelengths is plotted *vs.* the mass concentration of analyte to establish a calibration plot. Similar approaches have included the use of an isosbestic point as one of the wavelengths to compensate for variations in the quantity of colour-forming reagent, the β-correction technique to deduce the stoichiometric ratio of the product complex as well as it's molar absorptivity and stability constant and dual wavelength measurements to compensate for variations in mobile phase flow rate in a flowing system [212-216].

The objectives of the study were to evaluate the uncertainties associated with the spectrophotometric determination of hexavalent chromium mass concentration, γ(Cr), in the course of its reduction by zero valent iron. The evaluation was approached in three stages: (1) description of the measurement procedure and its model equation; (2) identification of the uncertainty sources and their quantification; and (3) estimation of the combined and expanded uncertainties. A further goal of this project was to compare the calculated uncertainty using the dual-wavelength and single-wavelength spectrophotometry for the determination of hexavalent chromium.

7.2 The standard procedure

The concentration of hexavalent chromium were determined colorimetrically by reaction with 1,5-diphenylcarbazide as described in the American Public Health Association (APHA) [154]. Procedures that were followed in this study are summarized in Figure 7.1. For the DWS method, the peak and valley absorption of the solution were determined at 540 and 630 nm respectively.

The mass concentration of Cr(VI), in mg L^{-1}, was calculated as:

$$\gamma(\mathrm{Cr}) = \frac{\gamma_\mathrm{o} M_\mathrm{f} d_\mathrm{o}}{M_\mathrm{o} d_\mathrm{f}} D \qquad (4)$$

Where γ_o is the Cr(VI) mass concentration obtained from the calibration curve (mg L^{-1}), M_f is the final mass of the solution (g), M_o is the sample mass (g), d_o and d_f are the densities (g mL^{-1}) of the initial and final solutions, and D is the dilution factor (when applicable).

The relative standard uncertainty associated with the mass concentration of Cr(VI) is:

$$\frac{u_\mathrm{c}(\gamma(\mathrm{Cr}))}{\gamma(\mathrm{Cr})} = \sqrt{\left(\frac{u\,(\gamma_\mathrm{o})}{\gamma_\mathrm{o}}\right)^2 + \left(\frac{u\,(M_\mathrm{f})}{M_\mathrm{f}}\right)^2 + \left(\frac{u\,(M_\mathrm{o})}{M_\mathrm{o}}\right)^2 + \left(\frac{u\,(d_\mathrm{o})}{d_\mathrm{o}}\right)^2 + \left(\frac{u\,(d_\mathrm{f})}{d_\mathrm{f}}\right)^2} \qquad (5)$$

7.3 Identification of the uncertainties sources and their quantification

In order to estimate the measurement uncertainty based on the EURACHEM/CITAC guide, the relevant sources of uncertainty that contributed in the determination of γ(Cr) were identified and quantified [208]. They are represented schematically in an Ishikawa diagram of Figure 7.2 [217].

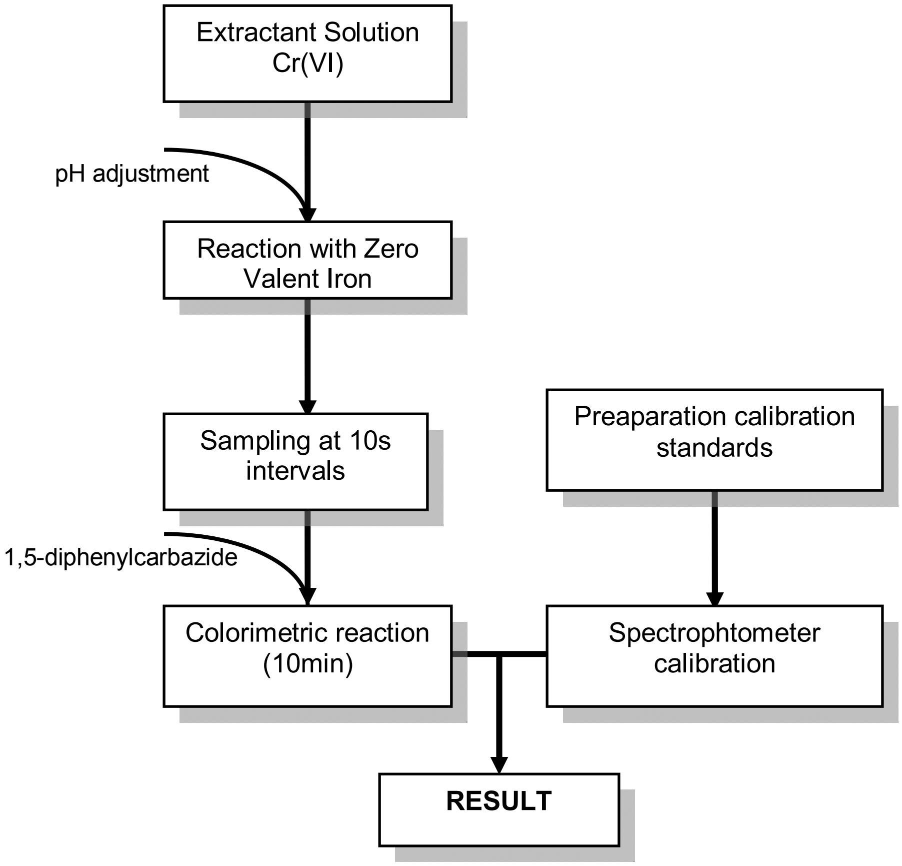

Figure 7.1 A summary of events to monitor the time dependant decline of γ(Cr) mediated by zero-valent iron.

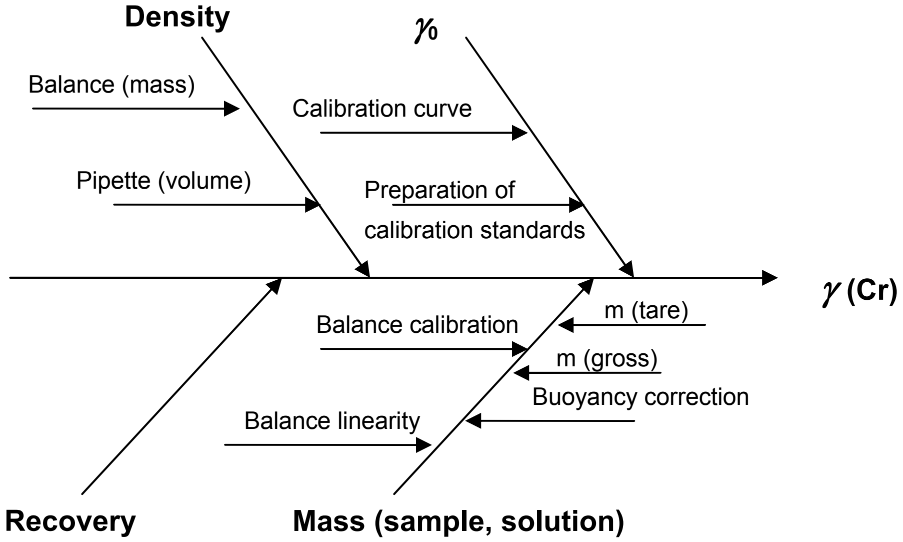

Figure 7.2 An Ishikawa diagram (cause-and-effect) for the spectrophotometric determination of the mass concentration of hexavalent chromium, γ(Cr).

7.3.1 Uncertainty related to mass concentration, $u(\gamma_o)$

When a solution of hexavalent Cr was mixed with zero-valent iron in a ratio 1:300 (*m*/*m*) and the pH was adjusted to (2.0 ± 0.1), the disappearance of Cr(VI) was virtually complete in less than 15 minutes. The mass concentration of hexavalent Cr was calculated using a manually prepared calibration curve. For this purpose six calibration standards were prepared, on a mass-by-mass basis, from (1001.0 ± 1.2) mg L^{-1} hexavalent chromium standard solution (Sigma-Aldrich, Oakville, ON) and reacted with 1,5-diphenylcarbazide. The absorbance (AU) was measured three times then the data were fitted to a linear least squares model. The linear least squares fitting procedure assumed that the uncertainties associated with the values of the abscissa were considerably smaller than the uncertainties associated with the values of the ordinate. Therefore, the usual uncertainty calculation procedures for γ_o reflect only the uncertainty in the absorbance and neither the uncertainty of the calibration standards, nor the inevitable correlations induced by successive dilution from the stock standard solution. The linear equation $A_j = b_1C_i + b_0$ represents the analytical curve, where A_j is the j^{th} measurement of the absorbance for the j^{th} calibration standard, C_i is the molar concentration of the i^{th} calibration standard, b_1 is the molar extinction coefficient and b_0 is the y intercept. The calculated values are b_0 = 0.01055 and b_1 = 0.8129 with a product moment correlation coefficient (*r*) of 0.99957, a standard deviation (s) of 0.01823, n = 18, *P* <0.0001, where the *P*-value is the probability of obtaining a value of the test statistic at least as extreme as the one that was actually observed.

In the case of the DWS method, the calibration curve was generated by plotting the mass concentration *vs*. the ratio of the absorbance at a wavelength corresponding to a peak maximum (A_p) for the coloured complex and a second wavelength corresponding to a peak minimum (A_v) for the complex. DWS absorbance = $[(A_p+1))/(A_v+1)]$. For this trace analysis procedure, arbitrarily one unit of absorbance has been added to both values to make them of comparable magnitude to background measures of the solution/colloidal suspension [210,211]. The equation $B_j = b_3C_i + b_2$ represents the analytical curve and the calculated values are b_3 = 1.00201 and b_2 = 0.78117, *r* = 0.99978, s = 0.01335 and for *n* = 18, p<0.0001.

The standard residual deviation, (s_{rd}), of the analytical curve was determined as:

$$s_{\mathrm{rd}} = \sqrt{\frac{\sum_{j=1}^{n}\left[A_j - (B_0 + B_1 C_j)\right]^2}{n-2}} \qquad (6)$$

The disappearance of hexavalent chromium was monitored with time at intervals of 10 s. Each sample was measured once, except at *t* = 0 where three replicate samples were measured (*n* = 3), that resulted in a different mass concentration γ_0 for each time interval. The uncertainty for γ_0, $u(\gamma_0)$, associated with the linear least square fitting procedure was calculated using Eqs. 6 and 7:

$$u\,(\gamma_{\mathrm{o}}) = \frac{s_{\mathrm{rd}}}{B_1}\sqrt{\frac{1}{p'} + \frac{1}{N} + \frac{\left(\gamma_{\mathrm{o}} + \bar{\gamma}\right)^2}{\sum_{j=1}^{n}\left(\gamma_{\mathrm{o}} - \bar{\gamma}\right)^2}} \qquad (7)$$

Where *p′* is the number of measurements performed to determine γ_0 and *N* is the number of measurements carried out to construct the calibration curve, $\bar{\gamma}$ is the average value of the different calibration standards, *i* is the index for the number of calibration standards and *j* is the index for the number of measurements that were used to obtain the analytical curve [208].

7.3.2 Uncertainty related to mass, $u(M)$

A Mettler Toledo PB303-S electronic balance was used. The manufacturer's literature identified three uncertainty sources for the tared weighing: the repeatability; the readability (digital resolution) of the balance scale and the contribution due to the uncertainty in the calibration function of the scale. This calibration function has two possible uncertainty sources, identified as the sensitivity of the balance and its linearity. The linearity of the balance is specified by the manufacturer as a tolerance, which represents the maximum deviation of the balance indication from the value that would be obtained by linear interpolation between the adjusting points (zero and internal/external weight loading) [218]. The calibration certificate of the balance specified a maximum deviation of 0.001 g identified as a tolerance. Assuming a uniform rectangular distribution for linearity, its uncertainty contribution is 0.001 g/$\sqrt{3}$ = 0.000577 g [208].

In this case, the balance was zeroed with the empty container on the pan and the container was then filled and weighed; therefore sensitivity contributions were neglected and the linearity uncertainty component should be counted twice (once for the tare and once for the gross weight, because each is an independent observation and the linearity effects are not correlated). This gives a standard uncertainty for each mass determination of $u(M)=\sqrt{2(0.000577)^2}=0.00082$ g.

In the course of this experiment, a correction for the effect of air buoyancy was performed so that all weighing were determined on a mass basis for weighing in a vacuum as defined by the Organisation Internationale de Métrologie Légale (OIML) [219]. Applying a correction factor to compensate for the buoyancy effect resulted in an increase in the mass of approximately 0.1% however the corresponding increase in the combined uncertainty brought about by this correction proved to be negligibly small.

7.3.3 Uncertainty related to recovery, $u(R)$

The bias of the analytical procedure was investigated using spiked solutions. The procedure involved in this work was a kinetic study, for which each determination was unique (with the exception of the measurement at t = 0). The significance of the bias should be determined in order to make a correction for the recovery percentage in the case that it is important. It was necessary to perform recovery studies to check not only the standard calibration curve but the stability of each of the reactants (i.e. the 1,5-diphenylcarbazide is known to decompose over time).

Two different samples (n) were spiked, and a mean recovery $(\overline{R})$ of 103.24% and standard deviation, s = 0.013357 was obtained. As a result, the standard uncertainty was calculated as the standard deviation of the mean

$$u(\overline{R})=s/\sqrt{n}=0.013357/\sqrt{2}=0.009445$$

A significance test was used to determine whether the mean recovery was significantly different from 1.0. The Student's t-test was calculated using the following equation (9):

$$t=\frac{|1-\overline{R}|}{u(\overline{R})}=\frac{|1-1.0324|}{0.009445}=3.43 \qquad (9)$$

This value was compared with the 2-tailed critical value t_{crit}, for n-1 degrees of freedom at 95% confidence (where n is the number of results used to estimate $\overline{R}$). If

t is greater or equal than the critical value $t_{crit,\ n-1}$ then $\overline{R}$ is considered to be significantly different from 1.0 and correction factor should be applied. For $n = 2$, t_{crit} is 12.7 and the calculated t is 3.43 (then $t<t_{crit}$). Hence the recovery tests indicated that no significant bias was present; it was inferred that there was no appreciable impact of the recovery on the final hexavalent chromium mass concentration.

7.3.4 Uncertainty related to density, $u(d)$

In this project, each of the volumes was measured as mass to obtain the actual volume; density rectifications were applied to each mass. A solution's density (mass per unit of volume) can be determined by weighing a known volume of that particular solution (with a volumetric pipette).

Then the combined standard uncertainty for the density can be estimated by the following expression:

$$u_c(d) = d\sqrt{\left(\frac{u(M)}{M}\right)^2 + \left(\frac{u(V)}{V}\right)^2} \qquad (10)$$

The volume has three major influences; calibration, repeatability and temperature effects.

Calibration: Uncertainty was stated by the manufacturer for a 10 mL pipette as ±0.02 mL measured at 20 ºC. The value of the uncertainty was provided without a confidence level or distribution information and the available information concerning the volume is limited; for a rectangular distribution, the standard uncertainty was calculated assuming a triangular distribution: $0.02/\sqrt{6} = 0.008$ mL

Temperature: According to the manufacturer, the volumetric pipette was calibrated at a temperature of 20 ºC, whereas the laboratory temperature varied within a range of ±2 ºC. Hence the uncertainty can be estimated from the temperature range and the coefficient of the volume expansion. Taking into account that the volume expansion of the liquid is considerably larger than that of the flask, only the former was considered for the calculations. The coefficient of volume expansion for water is $2.1\text{x}10^{-4}\ ^{o}\text{C}^{-1}$. Using a rectangular temperature distribution gives a standard uncertainty of $10\left(2.1\times10^{-4}\right)\left(4/\sqrt{3}\right) = 0.005$ mL

Repeatability: The standard uncertainty due to variations in filling was estimated from the standard deviation of 10 successive fill and weigh experiments. It provided a standard uncertainty of 0.009 mL. The three contributions are combined to give the standard uncertainty $u(V)$ for the pipette volume.

$$u(V) = \sqrt{0.009^2 + 0.005^2 + 0.008^2} = 0.01 \text{ mL}$$

Therefore the combined standard uncertainty due to the density is:

$$u_c(d) = d\sqrt{\left(\frac{u(M)}{M}\right)^2 + \left(\frac{u(V)}{V}\right)^2} = 1.03\sqrt{\left(\frac{0.00082}{10.003}\right)^2 + \left(\frac{0.01}{10.00}\right)^2} = 0.001 \text{ g mL}^{-1}$$

7.4 Calculation of combined and expanded uncertainty

The uncertainty associated with the mass concentration of hexavalent chromium was determined by combining the standard uncertainties of (a) the mass concentration; $u(\gamma_o)$, extrapolated from the linear regression (b) density; $u(d)$, and (c) mass of solutions; $u(M_o)$ and $u(M_f)$. Uncertainties were combined by using the rule of the propagation of uncertainties, following Eq. 5. To calculate the expanded uncertainty $U(\gamma(\text{Cr}))$ and presuming that a normal distribution applies, a k-value of 2 defines an interval having a level of confidence of approximately 95 %.

A graphical representation of the disappearance with time of γCr(VI) with its expanded uncertainty is presented in Figure 7.3 for both methods (SWS and DWS). An appreciable decrease in the calculated uncertainty using the dual-wavelength procedure can be observed for γ(Cr). It can be attributed to the fact that calculations were made using a relationship between the maximum (A_p) and minimum (A_v) absorbance of the solution [$B=(A_p+1)/(A_v+1)$] increasing repeatability and therefore diminishing the magnitude of uncertainties. It had been suggested that variations are decreased because of the tendency of the dependant variables (A_p and A_v) to vary in concert with each other.

When estimating the uncertainty related to a measurand, it is important to determine which contributions have a dominating influence on the final uncertainty result. Then, expediential improvements can be carried out in the experimental procedures to further decrease the uncertainty related to the measurand. Whereas the differences in uncertainties related to mass concentration, $u(\gamma(\text{Cr}))$, were appreciable between the two spectrophotometric techniques, differences in uncertainties related to mass ($u(M_0)$ or $u(M_f)$ or to density ($u(d)$)) were very small. Thus, the magnitude of differences in combined uncertainties was dominated by the contribution from the mass concentration estimates.

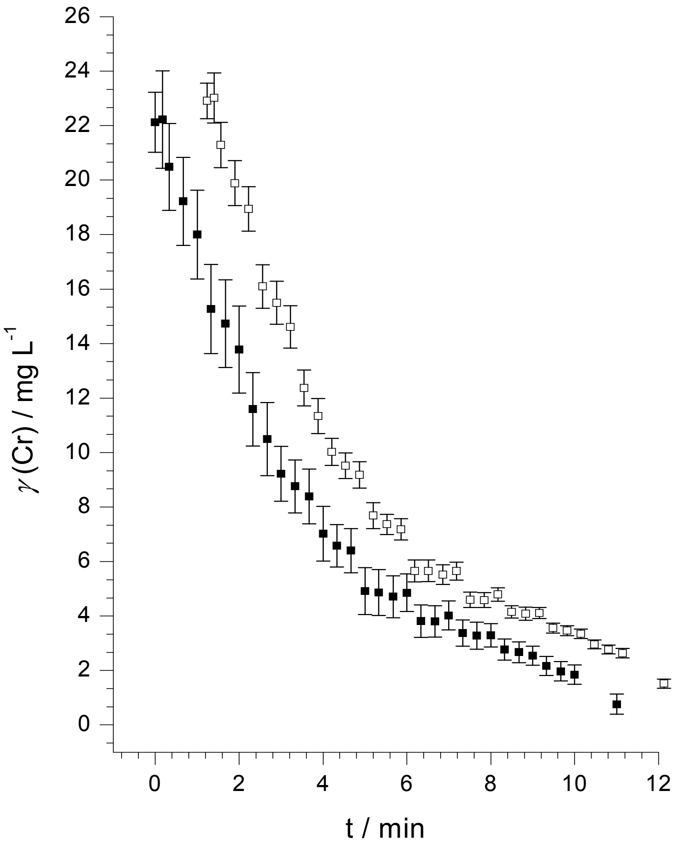

Figure 7.3 Plots of the variation with time of the mass concentration of hexavalent chromium, γ(Cr) in mg L^{-1}, together with their expanded uncertainty $U(\gamma(\text{Cr}))$, monitored by single-wavelength spectrophotometry (SWS) (■) or dual-wavelength spectrophotometry (DWS) (□). For clarity, the abscissa and ordinate for the (□) plot have been displaced by 2 min and 1 mg L^{-1} respectively.

A graphical representation of the $(\delta y / \delta x_i)u(x_i)$ is illustrated in Figure 7.4 which provides a comparison of the magnitude of each of the various contributions to the combined standard uncertainty $u_c(\gamma(\mathrm{Cr}))$. It can be seen that the standard uncertainty associated with the determination of $\gamma(\mathrm{Cr})$ and to a lesser extent the determination of volumes have dominating influences on the combined standard uncertainty.

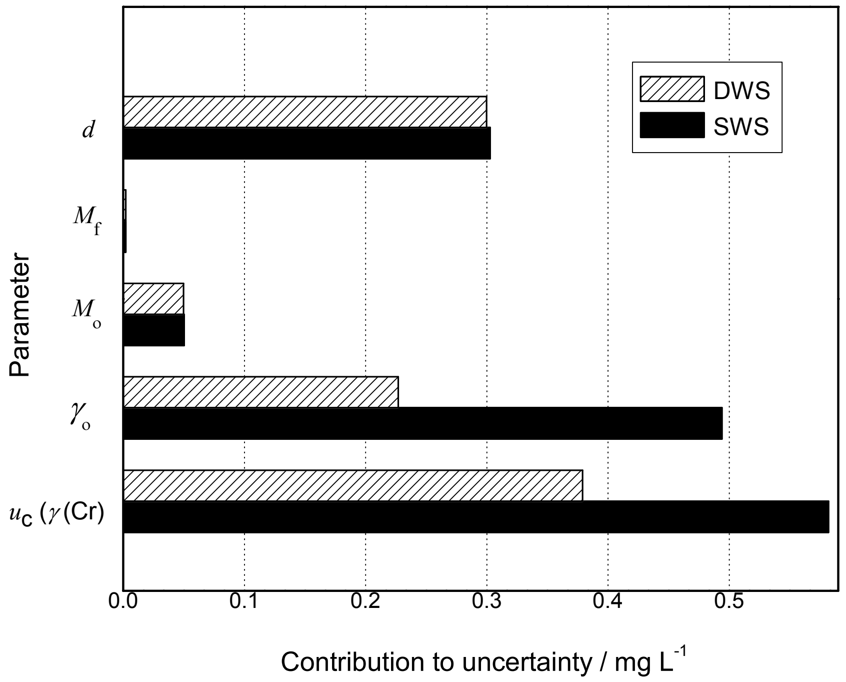

Figure 7.4 Representation of the uncertainty contributions to the combined standard uncertainty, $u_c(\gamma(\mathrm{Cr}))$, using single-wavelength (SWS) or dual-wavelength spectrophotometry (DWS) for the determination of Cr(VI) mass concentration (mg L^{-1}). γ_o; mass concentration extrapolated from the linear regression, d; density, M_o; sample mass and M_f is the final mass of the solution.

7.5 Conclusions

The estimation of measurement uncertainty is an important determinate for the reliability of measurement data and the process of estimation and interpretation should be easy to follow and practical. The use of the cause-effect diagram is an intuitive approach to identify the dominant contributions to the final uncertainty.

In the case of the kinetic study of the disappearance of hexavalent chromium in its reaction with zero valent iron, the major contribution to the uncertainty is the value derived from the calibration curve. One means of reducing the uncertainty resulting from the linear regression is working with dual-wavelength spectroscopy which also includes the measurement of absorbance at a second (valley) wavelength, increasing precision with little added effort. A lesser influence was detected for the process of determining volumes gravimetrically and correcting them by their densities; this approach permitted a saving of time and effort in the use of volumetric glassware and their calibration.

Chapter

Eight

Preface

These studies have investigated the mobilization of a carcinogenic oxyanion, chromate, using a surfactant preparation from a heavily contaminated soil and its reductive detoxification using micron- and nano-sized metallic particles. In parallel, the influence on the reductive rate of Cr(VI) of various organic compounds and inorganic ions commonly found in brownfields was also explored. These studies have demonstrated that the surfactant suspension mobilized appreciable quantities of hexavalent chromium from a soil. In addition, the conversion of the toxicant to an environmentally benign product using zero valent metallic particles was efficient. It was also demonstrated that certain mixed metallic preparations increased the reduction rate of Cr(VI) and nano-sized metallic particles drastically improved the reductive transformation of hexavelent chromium. Finally, the strategy of using naturally occurring organic and inorganic molecules to impede passivation of metallic and accelerate reduction rates was also investigated.

In the following chapter, a concise summary addresses the findings of this research in the chronological order. Secondly, a brief conclusion lists the contributions to knowledge and finally, some suggestions for further studies are presented.

-

Chapter

Eight

Summary, Conclusions, and Recommendations for Future Research

8.1 Summary

A general and historical background for the understanding of environmental pollution as well as major sources of inorganic toxicants which are present as anions (oxyanions) were provided in Chapter one. A brief introduction to the mobilization of oxyanions in the environment along with remediation technologies suitable for the detoxification of soil burdened with inorganic oxyanions were also included. This research was undertaken based upon the judgement that there remained a need for an efficient and cost-effective method that was capable of mobilizing mixed contaminants (organic, inorganic, and heavy) from soil. There remained a requirement for more a more efficient mobilization procedure for mixed contaminants. The techniques would be of wider interest if the mobilization procedure was (*i.*) capable of operating with recycled chemical reagents and (*ii.*) was coupled with a detoxification sequence that resulted in innocuous or less toxic products. A novel approach/technique of combining a surfactant preparation for the extraction of hexavalent chromium metal was proposed along with the reduction of Cr(VI) to Cr(III) mediated by micro and nano-sized metallic particles. Naturally-occurring organic and inorganic molecules, various chelating agents, and inorganic oxyanions commonly found in Brownfields were use to evaluate their influence on kinetic reduction parameters.

Chapter two, provided a brief overview of trace element oxyanions in order to better understand toxicological effects and the nature of contamination in water, soil, and sediment. Several remediation techniques directed to heavy metals and oxyanions were presented. A more detail discussion was focused on the decontamination of sites using mobilizing agents (including surfactants and chelating agents) and/or zero valent metals. The potential of nano-sized particles for the detoxification and removal of inorganic oxyanions from soils was examined in greater detail.

The reduction of hexavalent chromium in a surfactant preparation (Tween® 20) under a selection of reaction conditions was evaluated using a variety of zero-valent metals (Al, Cu, Fe, Mg, Ni, Si, and Zn) and various metallic nano-sized particles (Cu and Fe) was fully described in Chapter three. The results indicated that at circum neutral pHs, a rapid inactivation of the metallic surface was observed for almost all of the tested metals and complete reduction of Cr (VI) was achieved at acidic pH using only Cu, Fe, Mg or Zn.

A considerable increase in reactivity (up to 100-fold) was observed for reductive remediation mediated by nano-sized metallic particles. The use of a solid support as a dispersant and stabilizer circumvented the tendency of freshly prepared nano-particles to either react with surrounding media or agglomerate, resulting in the formation of much larger flocs and appreciable loss in reactivity. The formation of clusters by polymeric structures (water soluble starch, carboxymethylcellulose) provided an extra protection of the nano-particle surface with a striking improvement in their reactivity in particular at more alkaline conditions. Therefore, the incorporation of an innocuous stabilizer can substantially enhance the stability of metallic nano-particles for environmental transformations.

Chapter four discussed the preparation of various mixed metallic particles and their evaluation for reactivity towards Cr(VI) reduction in a Tween® 20 preparation. A variety of micron-scale bimetallic particles (Pd/Fe, Ag/Fe, Cu/Fe, Zn/Fe, Co/Fe, Mg/Fe, Ni/Fe, Al/Fe, Si/Fe, Pd/Cu, and Pd/Zn), micron-scale trimetallic particles (Pd/Cu/Fe, Pd/Zn/Fe, and Zn/Cu/Fe), and selected nano-sized bimetallic analogs (Pd/Fe, Cu/Fe, and Pd/Cu) were prepared and evaluated for reactivity. Relative to the reactivity of the zero-valent iron, the tested bimetallic mixtures (Pd/Fe > Pd/Zn > Ag/Fe > Ni/Fe > Zn/Fe > Pd/Cu > Cu/Fe) remarkably increased the pseudo-first order rate constant. The trimetallic preparation Zn/Cu/Fe, represented a cost-effective preparation providing comparable or improved kinetic parameters relative to the more expensive palladized bimetallic mixtures. The Pd/Fe, Cu/Fe and Pd/Cu nano-sized particles proved to be more reactive for the reductive detoxification of Cr(VI). The results were comparable when working with nano-sized Cu and Fe particles, suggesting that the cementation of a noble metal served not only as a reaction accelerator but also provided protection to the metallic surface, impeding its rapid inactivation.

A variety of natually-occurring organic molecules (containing α-hydroxyl carbonyl, α-hydroxyl carboxylate, phenolate, carboxylated and/or thiol groups, siderophore, ascorbic acid); chelating agents (ehtylenediaminetetraacetic acid derivates, acetylacetone) and others were examined their influence over the reduction of a surfactant preparation containing Cr(VI) mediated by zero-valent iron, was fully described in Chapter five. An appreciable enhancement (up to 50-fold) of the pseudo-first order kinetic rate constant was achieved at acidic and circum neutral pH values for those compounds capable of reducing Cr(VI) (α-hydroxyl carboxylate, ascorbic acid, cysteine). Comparable enhancements were obtained for certain chelating agents (ehtylenediaminetetraacetic acid derivates and siderophores) which was attributed to the formation of complexes with reaction products, such as Cr(III) and Fe(III), which were considered to impede the precipitation of Cr(III) and Fe(III) oxy/hydroxides and $Cr_xFe_{1-x}(OH)_3$. In consequence passivation of the iron surface was impeded. The results also suggested that these molecules might be useful in effective remediation of Cr(VI)-contaminated soils or groundwater in a wide range of pH values. Reaction rates are anticipated to be increased for both *ex-situ* applications and for the long-term performance of permeable reductive barriers.

Chapter six reported the influence of various transition metal and non-metal oxyanions on the reduction reaction of a surfactant preparation containing Cr(VI) mediated by zero-valent iron. Nitrate, perchlorate, and selenate (pollutants that are found frequeltly in brownfields) moderately accelerated (up to 4-fold) the reductive transformation of Cr(VI). Synergetic interactions occurred with various oxyanions at acidic pH values in the reaction with ZVI leading to an improvement of the overall kinetic parameters of Cr(VI) reduction but only moderate enhancement was observed at circum neutral conditions. Such synergetic behaviour can be advantageous for brownfields that are burdened with multiple diverse pollutants.

No changes in the rate of Cr(VI) reduction were observed in the presence of borate, molybdate, arsenate, silicate, and sulfate.

The evaluation of uncertainties associated with the spectrophotometric determination of hexavalent chromium in the course of its reduction by zero-valent iron was presented in Chapter seven. The recommendations provided by the EURACHEM/CITAC guide were followed to estimate the standard uncertainty in the determination of Cr(VI). The evaluation was approached in three stages: (1) description of the measurement procedure and its model equation; (2) identification of the uncertainty sources and their quantification; and (3) estimation of the combined and expanded uncertainties. A comparison of the calculated uncertainty using dual-wavelength (DWS) and single-wavelength spectrophotometry (SWS) for the determination of Cr(VI). The evaluation results suggested that the major contribution to the uncertainty was the estimate derived from the calibration curve. The use of the DWS, which involved the measurement of absorbance at a second wavelength, reduced the uncertainty resulting from the linear regression. Gravimetric determination of volumes (corrected by their densities) slightly influenced uncertainty related to Cr(VI) determination. It saved time and effort in glassware calibration.

8.2 Conclusions

These studies have identified novel approaches of using a surfactant preparation to mobilize chromate from contaminated soils and its detoxification mediated by micron- or nano-scale metallic particles. Combined procedures have been devised that make use of naturally occurring organic and inorganic molecules to impede passivation of metallic and accelerate reduction rates. This project is one of the few approaches that has involved an efficient mobilization of inorganic oxyanions from field contaminated soil followed by a chemical transformation to more innocuous and less mobile products. Based on the results from several experiments, this research dissertation has made the following major contributions to knowledge:

1. The use of a surfactant preparation as a mobilization aid for inorganic oxyanions (chromate, arsenate, etc.) permits the simultaneous removal of organic (including PCBs and PAH compounds) and inorganic pollutants (heavy metals).
2. Reductive chromate remediation is strongly affected by the passivation of the zero valent metal (ZVM) surface. Pretreatment by acid-washing of the ZVM surface dramatically increases metal surface reactivity.
3. The enhancement of the reduction rate of chromate, in a surfactant suspension, mediated by nanoscale metal particles is likely the result of an increased metal surface area to mass ratio, higher surface reactivity and the increased atom efficiency.
4. The cementation of a second or third metal (Ag, Cu, Ni, Pd, and/or Zn) onto the surface of the transition metal increased the reactivity of the preparation substantially. The Zn/Cu/Fe metallic preparation represents a more cost-effective reductant relative to formulations based in noble metal catalysts.
5. The accelerated reduction of Cr(VI) seems to be linked to: (1) the catalytic properties of the metal, surface properties, atomic structures and electronic

properties; (2) surface protectors that favour the release of ions from the metal surface (e.g. Fe^{+2}, Cu^{+}, Cu^{+2}) which readily reacts with Cr(VI); (3) the ability of the metallic preparation to sorb and activate H_2; and (4) the increased adsorption of chromate onto the bimetallic surface.

6. When compared to inorganic solid supports, increased rates of reduction are observed when freshly prepared metallic nanoparticles (NPs) are anchored to polymeric structures (such as soluble starch or to carboxymethylcellulose). These observations supports the concept of the formation of intramolecular clusters of zero-valent metal and polymeric structures as being responsible for for the positive impact on the reduction rates.
7. Bimetallic nano-sized particles accelerate Cr(VI) reduction rates appreciably. Kinetic parameters similar to those of NPs anchored on an inorganic support suggest that the second metal in the mixture serves not only as an accelerator for the reaction but also as a surface protector.
8. A reliable micro-scale adaptation for the determination of Cr(VI) (as recommended by the USEPA) was developed and validated for a surfactant preparation containing Cr(VI). A unique identification, evaluation, and estimation of uncertainties associated with the determination of Cr(VI) in the surfactant suspension was developed following ERACHEM/CITAC guide recommendations. The results indicated that the major contribution to the final standard uncertainty is the value derived from the calibration curve. One means of decreasing the magnitude of the contribution from this source is the use of a modified procedure involving dual-wavelength spectroscopy. The determination of volumes gravimetrically in this validated approach saved time and effort in the use of volumetric glassware and their calibration.

8.3 Recommendations for Future Research

Future studies that focus on the mobilization/detoxification of pollutants from contaminated sites (including soil, sediment or groundwater) mediated by zero-valent metals should include the following:

1. Further investigations are needed to explore and identify the fate of chromium species in the surfactant suspension during the reaction with zero-valent metals. Speciation studies of Cr compounds should be performed to understand precipitation rates that may cause the inactivation of the metal surface.

2. Further studies are needed to devise synthetic methods to delineate the underlying mechanistic steps of chromate reduction on metal surfaces.
3. The application of ultra-sonication as a means to decrease the rate of formation of (oxy)hydroxides on the iron surface so as to retain active surface sites exposed.
4. Environmentally benign reactants (such as biosurfactants and biodegradable reactants) should be evaluated for reactivity. Additionally, the capacity to recycle these surfactant preparations should be tested.
5. Current laboratory-based investigations should be extended to other field-contaminated soils (with different soil characteristics) and different types of contaminants admixed with inorganic oxyanions, heavy metals, and/or organic pollutants (PAHs, PCBs, BTEX compounds) is seen as a fruitful line of research.
6. Further investigations are need to devise new synthetic pathways to extend the scope of the synthesis methods for nano-sized metallic particles to metals other than iron and copper (e.g. zinc).
7. A further issue to be investigated is the relative reactivity and atom efficiency of nano-sized metal particles when measured over extended times that are relevant to remediation of slow-moving plumes with permeable reactive barriers (PRBs).
8. Despite the bright outlook for the future of nanotechnology, there is increasing concern that human exposure to some engineered nanoparticles, inadvertently or intentionally, might lead to adverse health effects. Even though nano-sized metallic particles seem to overcome the drawbacks of surface inactivation issues with the consequent loss of reactivity, the potential health effects of their widespread use must also be considered when remediation techniques are intended to be implemented at contaminated sites.

Appendix 1

Characterization of contaminated soil and detoxification of Cr(VI) using zero-valent iron in a surfactant solution

A.1 Soil Characterisation

Due to the anticipated high mobility of oxyanions and the low permeability of clay-type soils, a kaolin type soil was chosen for all experiments. Initial experiments characterised the soil with respect to particle size, pH, cation exchange capacity (CEC) was well as the original hexavalent chromium content of this soil**.** Relevant data are presented in Table A 1.1.

Table A1.1 Kaolin-type soil properties

	Gravel (%)	Sand (%)	Silt (%)	Clay (%)	Organic Content (%)	pH	Cr(VI) (mg Kg^{-1})	CEC (meq $100g^{-1}$)
Soil	0.0	4.0	18	78	< 1.0	4.9	< 5.0	1.0-1.6

A.2 Soil spiking procedure

The soil was soaked in a $K_2Cr_2O_7$ solution at a rate of 1 g of soil/10 mL of dichromate solution. The Cr(VI) solution provided a concentration that resulted in a final soil concentration of *ca*. 2400, 1200 or 700 mg Kg^{-1}. These concentrations were considered to be typical of hexavalent chromium concentrations that can be found in brownfields. The spiking procedure followed the procedure described by Shin and Barrington (2005), and consisted in shaking the soil in the dichromate solution at 150 rpm for 5 days on a water bath shaker, followed by removing the soil from the aqueous phase by centrifugation at 4000 rpm for 30 min [220]. The particulate fraction from the amended soil was air-dried and permitted to stand for 1 week in a forced air fume hood followed by analysis for hexavalent chromium content. The initial hexavalent chromium concentration in soil was determined using the extracting technique recommended by the USEPA alkaline digestion procedure, EPA 3060A, and Cr(VI) was quantified by the diphenycarbazide method in accordance with the American Public Health Association method [154,221].

A.3 Hexavalent chromium mobilization with surfactants

One of the biggest concerns of the remediation of oxyanions is their high mobility and low retention-adsorption at the disposal site. Although it has been reported that soil washing techniques for contaminated sites with high content of clay can be ineffective, the high solubility and mobility of inorganic oxyanions along with the low permeability of the kaolin type soil make conditions for soil washing less favourable [100].

Eleven surfactants that had been selected for this study included three anionic, six nonionic, and two cationic surfactants.

The surfactants selected included at least one from each of the four common groups of commercial surfactants: (i) ethoxylated alcohol (noninoic); (ii) ethoxylated alkylphenol (nonionic); (iii) sulphate (anionic); and (iv) sulfonate (anionic) functional groups. The choice of surfactant, on the basis of the percentage of chromate extracted and the concentration that remained in the contaminated soil is summarized in Table A 1.2. Even when three sequential washes were performed to remove chromate from the soil, only the first washing value was taken into consideration since the two subsequent washes were determined to have Cr(VI) that was near the limit of detection for the method (LOD = 5 mg Kg^{-1}). The efficiency of removal was virtually quantitative with a single extraction. Some of the surfactant molecules might have remained adsorbed to the clay mineral in the kaolin soil after separation from the supernatant fraction. The adsorption might have been driven by hydrogen bonding and/or van der Waals forces with the oxyethylene group. As well as providing sorption sites on the soil surface this might have decreased the amount of surfactant in suspension. A virtually complete recovery of chromate from this soil was demonstrated.

Table A1.2 Mean concentration (± 1SD[a]) of the initial hexavlent chromium burden, mean recovery percent by the extracting surfactant (± 1SD[a]) and mean concentration of the final hexavalent chromium burden (± 1SD[a]).

Extractant	Name	Cr(VI)[b] (mg Kg^{-1})	Recovery (%)	Cr(VI)[c] (mg Kg^{-1})
Water		2430 ± 187	99.5 ± 11.2	14.5 ± 4.2
SDS	sodium dodecyl sulfate	2430 ± 187	101.5 ± 3.8	23.9 ± 3.8
Triton XQS-20	Sodium octylphenoxyethyl phosphate ester	2430 ± 187	94.4 ± 3.8	37.8 ± 4.9
Triton X-301	Sodium octylphoxyethyl sulphate	2430 ± 187	103.0 ± 5.1	33.4 ± 3.9
Brij® 98	Polyoxyethylene (20) oleyl ether	2430 ± 187	103.5 ± 4.4	13.6 ± 3.0
Triton X-100	i-octylphenylethyleneoxide	2430 ± 187	101.5 ± 2.0	17.9 ± 3.9
Tween® 20	Polyoxyethylene (20) monolaurate	2430 ± 187	94.2 ± 4.2	18.2 ± 6.3
Tween® 40	Polyoxyethylene (20) monopalmitate	2430 ± 187	93.7 ± 5.8	25.6 ± 4.8
Tween® 80	Polyoxyethylene (20) monooleate	2430 ± 187	84.9 ± 7.4	18.6 ± 5.4
Tween® 85	Polyoxyethylene (20) trioleate	2430 ± 187	98.0 ± 4.9	13.6 ± 4.2
CPC	Cetylpyridinium chloride	2430 ± 187	80.7 ± 8.8	28.9 ± 8.8
Aliquat® 336	Tricaprylmethylammonium chloride	2430 ± 187	81.5 ± 9.9	31.6 ± 7.9

[a] SD = One standard deviation based on three replicates trials, [b] Cr(VI) initial concentration, [c] Cr(VI) final concentration in the soil.

A.4 Batch soil washing procedure

Batch experiments were performed by soaking three replicate 2.0 g samples of soil in 25 mL surfactant solution (2% v/v). The washing solution consisted of surfactant at a concentration well above (10-100 fold) its critical micellar concentration (CMC). The soil and surfactant solutions were equilibrated by shaking at 150 rpm in a water bath shaker for 24 h. The soil samples were removed from the soil by centrifugation at 4000 rpm for 30 min. A series of three successive batch washings was performed on soil samples by adding fresh solution of washing agent, shaking again for 24 h, and then removing the solution by centrifugation (4000 rpm, 30 min). For each wash, the supernatant was collected for hexavalent chromium analysis.

To determine the amount of hexavalent chromium desorbed from the samples, the surfactant fraction was analysed spectrophotometrically as suggested by the APHA [154]. Concurrently, hexavalent chromium analyses were also performed on the soil after the washing procedure in accordance with EPA 3060 so as to provide a mass balance for the analyte (Table A 1.2) [221].

A.5 Batch experiments with surfactants solutions and zero-valent iron

Detoxification reactions were performed in 50-mL vials containing 7 g L^{-1} Fe^0 (40 mesh, specific surface area 1.01 m^2 g^{-1}) and 20 mL of surfactant suspension containing Cr(VI), *ca*. 20 mg L^{-1}, in which the final pH had been adjusted to the desire value with a 1M H_2SO_4 or 1M NH_4OH. No attempt was made to control the pH over the course of the reduction. During the reaction, the vials were mixed on a rotating-table shaker at 180 rpm. Aliquots of the admixture (between 100 and 500 μL) were taken at 20 second intervals and filtered through 0.20 μm filters (Millipore). The filtered samples were directly inserted into Hach tubes {inner diameter 1.0 cm (O.D. 1.2 cm) x 10.0 cm} and Cr(VI) was determined by the 1,5-diphenylcarbazide method [154]. Minor modifications were made to the original spectrophotometric procedure in order to work at a micro-scale. The results are summarized in Table A 1.3 for acidic conditions. Each of the surfactant-mobilized chromate solutions followed a reduction pattern concordant with a pseudo-first order rate reaction and depending on the surfactant type slight to severe deviations from a reduction in a pure aqueous media were evident (one way ANOVA).

Even at low pH, the behaviour of the anionic surfactants tended to be similar which is consistent with adsorption of the surfactant on to the iron surface. In consequence, active sites on the surface of the Fe(0) were blocked and the reduction rate of hexavalent chromium was slowed (k_{SA} values Table A1.3).

The six non-ionic surfactants used belong to the group of polyethylene oxide (PEO) surfactants. The majority of these formulations have a total of 20 subunits of oxyethylene groups within their structure. Triton X-100 is the exception and possesses 9.5. The Tween® series of surfactants differ only in the fatty acid associated with the polyoxyethylene chain (monolaurate, monopalmitate, mooleate and trioleate). The identity of the fatty acid had an appreciable impact on the rate of reduction of hexavalent chromium with ZVI. Though they can also experience hydrogen bonding and van der Waals forces, it was observed that the major influence was the effect of steric crowding. The amount of fatty acids present in the structure and the size of the surfactant molecule seem to have an inverse relation with the reduction rate. The bigger the structure the bigger the micelle and therefore farther the chromate from the iron surface making harder their reaction. The Tween® 20 chromate solution shows the reductive behaviour (k_{SA}) more similar to that of an aqueous solution of chromate, which is in accord with the fact that it possess only a laurate substitution.

The cationic surfactants tested in this project had an prominent impact on the rate of Cr(VI) reduction mediated by ZVI, likely caused by a strong interaction between the chromate ion and the cationic molecule.

The working solution chosen for study was the chromate-Tween® 20 surfactant solution.

Table A1.3 Surface area normalized rate constant (k_{SA} ± 1SD[a]), coefficient of correlation (r^2) with the pseudo-first order model and parameters related to the one-way analysis of variance (ANOVA).

Extractant	k_{SA} ± 1SD ($mL\ min^{-1}\ m^{-2}$)	r^2	ANOVA Sum of squares	 Mean square	 F value	 P value
Water	5.3 ± 0.51	0.996				
Anionic						
SDS	3.9 ± 0.45	0.948	0.180	0.180	2.41	0.13[c]
Triton XQS-20	2.7 ± 0.32	0.966	0.059	0.059	0.654	0.42[c]
Triton X-301	3.9 ± 0.44	0.942	0.036	0.036	0.443	0.51[c]
Non-ionic						
Brij® 98	3.2 ± 0.40	0.900	0.014	0.014	0.171	0.68[c]
Triton X-100	3.1 ± 0.29	0.986	0.021	0.021	0.251	0.62[c]
Tween® 20	4.7 ± 0.50	0.992	0.0067	0.0067	0.066	0.80[c]
Tween® 40	2.1 ± 0.44	0.942	888	888	42	< 0.0001[b]
Tween® 80	1.5 ± 0.23	0.789	0.367	0.367	2.57	0.062[b]
Tween® 85	2.8 ± 0.33	0.979	0.399	0.399	3.59	0.056[b]
Cationic						
CPC	0.63 ± 0.76	0.979	0.428	0.428	4.83	0.037[b]
Aliquat® 336	0.54 ± 0.65	0.982	0.819	0.819	11.8	0.002[b]

[a] SD = One standard deviation based on three replicates trials, [b]At the 0.05 level (95% confidence level) the population means are significantly different, [c]At the 0.05 level (95% confidence level) the population means are not significantly different.

Appendix 2

An analysis of costs for soil washing with zero-valent iron treatment

Scientists are still searching to develop an efficient remediation process that is innocuous to biota, economical and capable of detoxifying soils that have been burdened with mixed contaminants (organic and inorganic pollutants).

The major obstacle in implementation of soil remediation techniques remains the high costs involved. Newer technologies have emphasized the detoxification of contaminants along with the recovery and reuse of reagents.

This short supplementary section attempts to estimate the cost of the chemical inputs requires to treat 1 Kg of soil contaminated with hexavalent chromium.

The main chemical reagents used to wash the soil and detoxify it, were surfactant and acid-washed iron. Hydrolysis of zero-valent magnesium was used to cause precipitation of $Cr(OH)_3$, so that recovery and reuse of the surfactant was possible.

Table A2.1 provides an estimate of the costs of chemicals (based on the Sigma-Aldrich 2008-2009 catalogue prices) consumed by a single soil wash, three approaches to detoxify Cr(VI) extract, and removal of Cr from the reaction mixture. This estimation of costs includes neither the cost associated with excavation, loading, transportation of soil samples, not the cost related with the safe disposal of the sludge waste stream.

Although not performed in this study, it is possible to recycle and reuse surfactant solution and ZVI (washing iron surface to reactive it and remove oxides) reducing direct and indirect costs (liquid waste disposal, transportation, loading).

Bimetallic mixture Pd/Fe dramatically accelerate Cr(VI) the rate of reduction under strongly or weakly acidic conditions but the elevated cost of Pd is anticipated to be the major limitation in using this approach. On the other hand, the presence of naturally occurring and environmentally benign organic molecules (such as citric acid) enhance the reduction rate of Cr(VI) with only an increment of 20% of the final cost.

Over all, it can be concluded that this technique is appealing because it serves not only to detoxify Cr(VI) but also various inorganic oxyanions (arsenate, nitrate, perchlorate, phosphate, selenate) and organic pollutants (such as PCBs).

The cost saving offered by recycling and reusing detoxification reagents can make it substantially relative to conventional remediation strategies, such as excavation and disposal and the added expense of recycling reagents is not appreciable.

Table A2.1 Cost comparison of soil washing with detoxification and precipitation using ZVI (Chapter Three), 2% Pd/Fe (Chapter Four), and ZVI with a500 μM citric acid solution (Chapter Five).

	Cost ($ g^{-1})	Reagent needed (g Kg^{-1} of soil)	ZVI ($ Kg^{-1})	2% Pd/Fe ($ Kg^{-1})	ZVI (500 μM citric acid) ($ Kg^{-1})
Iron granules	0.015	100	1.5	1.5	1.5
Acid washed iron	0.0016	100	0.2	0.2	0.2
pH adjustement	0.0054	31	0.2	0.2	0.2
Tween® 20	0.13	250	31.5	31.5	31.5
Mg granules	0.098	10	1.0	1.0	1.0
K_2PdCl_6	43	7.5	N/A	396	N/A
Citric acid	0.032	78	N/A	N/A	2.5
Surfactant recovery (~89%)			25.3	25.3	25.3
Total ($ Kg^{-1} of soil)			9.1	405.1	10.6

Appendix 3

Copyright release forms

Portions of this thesis are excerpts from previously published manuscripts; therefore copyright waivers from the various publishers have been included in this document. The manuscripts: “Reduction of hexavalent chromium mediated by micro- and nano-sized mixed metallic particles” and “Influence of various organic molecules on the reduction of hexavalent chromium mediated by zero-valent iron” that were published in the Journal of Hazardous Materials and Chemosphere respectively. The publisher for these journals is Elsevier and the author’s copyright permission states:

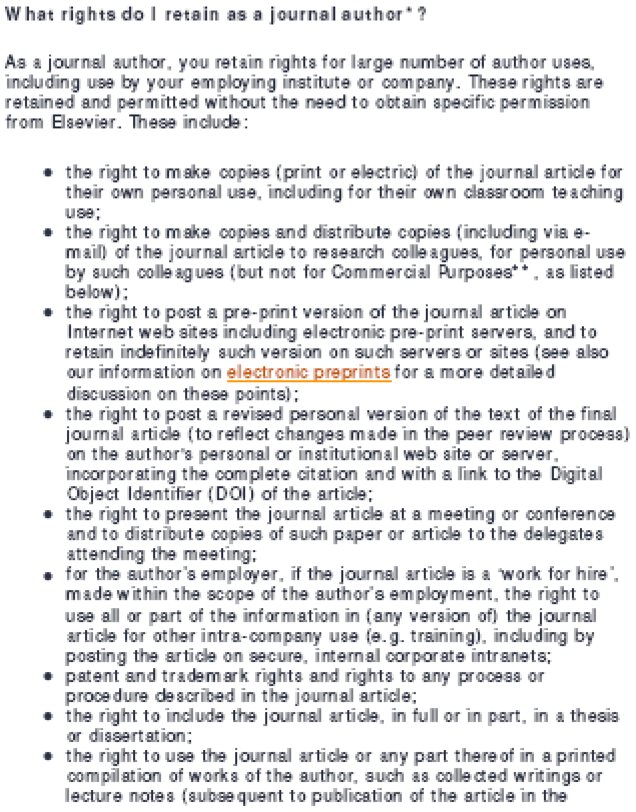

What rights do I retain as a journal author*?

As a journal author, you retain rights for large number of author uses, including use by your employing institute or company. These rights are retained and permitted without the need to obtain specific permission from Elsevier. These include:

- the right to make copies (print or electric) of the journal article for their own personal use, including for their own classroom teaching use;
- the right to make copies and distribute copies (including via e-mail) of the journal article to research colleagues, for personal use by such colleagues (but not for Commercial Purposes**, as listed below);
- the right to post a pre-print version of the journal article on Internet web sites including electronic pre-print servers, and to retain indefinitely such version on such servers or sites (see also our information on electronic preprints for a more detailed discussion on these points);
- the right to post a revised personal version of the text of the final journal article (to reflect changes made in the peer review process) on the author's personal or institutional web site or server, incorporating the complete citation and with a link to the Digital Object Identifier (DOI) of the article;
- the right to present the journal article at a meeting or conference and to distribute copies of such paper or article to the delegates attending the meeting;
- for the author's employer, if the journal article is a 'work for hire', made within the scope of the author's employment, the right to use all or part of the information in (any version of) the journal article for other intra-company use (e.g. training), including by posting the article on secure, internal corporate intranets;
- patent and trademark rights and rights to any process or procedure described in the journal article;
- the right to include the journal article, in full or in part, in a thesis or dissertation;
- the right to use the journal article or any part thereof in a printed compilation of works of the author, such as collected writings or lecture notes (subsequent to publication of the article in the

The manuscript: “Reduction of hexavalent chromium mediated by micro- and nano-scale zero valent metallic particles” published in the Journal of Environmental Monitoring which publisher is the Royal Society of Chemistry, the author’s copyright permission states:

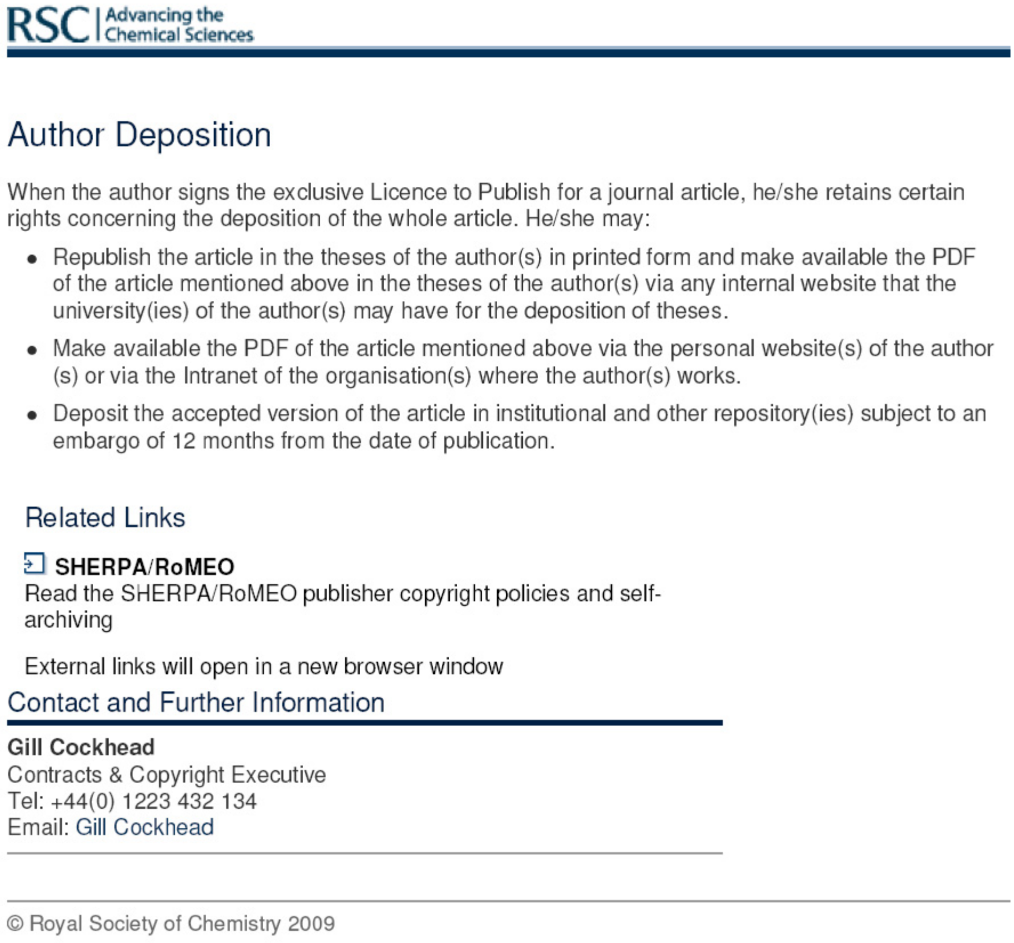

Author Deposition

When the author signs the exclusive Licence to Publish for a journal article, he/she retains certain rights concerning the deposition of the whole article. He/she may:

- Republish the article in the theses of the author(s) in printed form and make available the PDF of the article mentioned above in the theses of the author(s) via any internal website that the university(ies) of the author(s) may have for the deposition of theses.
- Make available the PDF of the article mentioned above via the personal website(s) of the author (s) or via the Intranet of the organisation(s) where the author(s) works.
- Deposit the accepted version of the article in institutional and other repository(ies) subject to an embargo of 12 months from the date of publication.

Related Links

SHERPA/RoMEO
Read the SHERPA/RoMEO publisher copyright policies and self-archiving

External links will open in a new browser window

Contact and Further Information

Gill Cockhead
Contracts & Copyright Executive
Tel: +44(0) 1223 432 134
Email: Gill Cockhead

The manuscript: "Uncertainties when using dual-wavelength or single-wavelength spectrophotometry to monitor the course of hexavalent chromium reduction mediated by zero-valent iron" published in the Journal of Accrediation and Quality Assurance (Journal for Quality, Comparability and Reliability in Chemical Measurement) whose publisher is Springer, the author's copyright permission states:

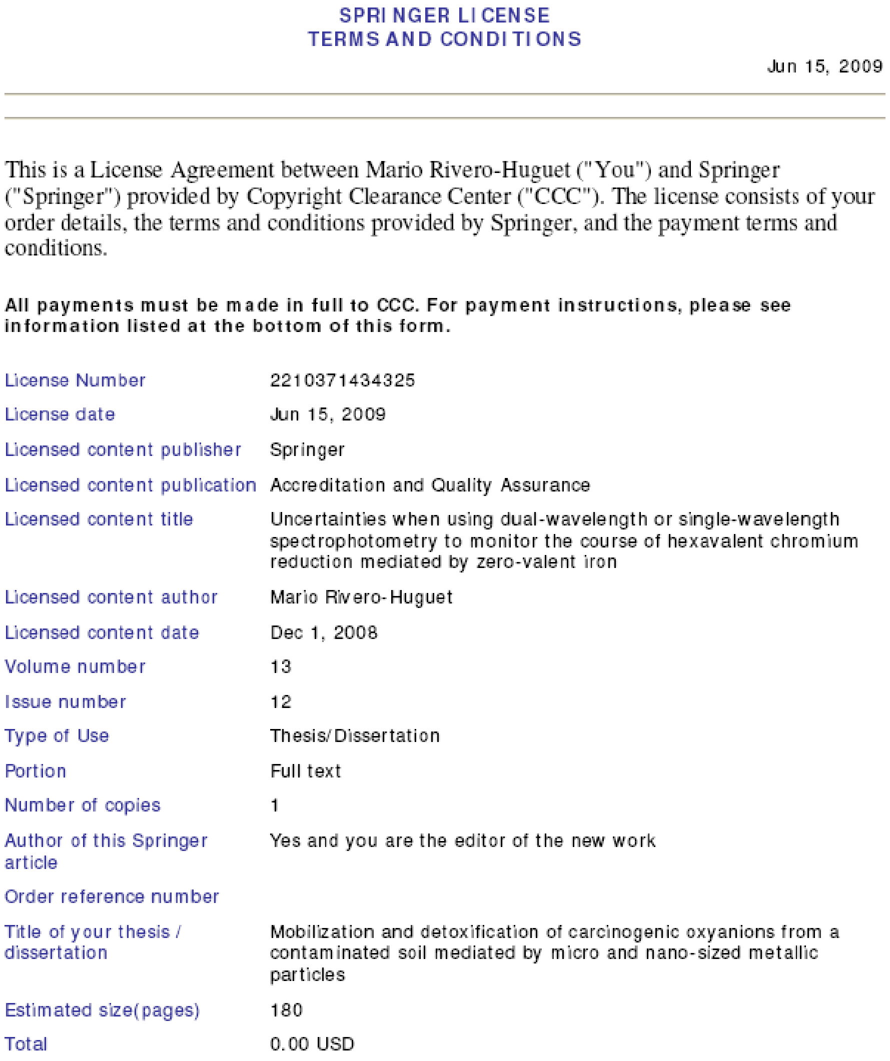

SPRINGER LICENSE
TERMS AND CONDITIONS

Jun 15, 2009

This is a License Agreement between Mario Rivero-Huguet ("You") and Springer ("Springer") provided by Copyright Clearance Center ("CCC"). The license consists of your order details, the terms and conditions provided by Springer, and the payment terms and conditions.

All payments must be made in full to CCC. For payment instructions, please see information listed at the bottom of this form.

License Number	2210371434325
License date	Jun 15, 2009
Licensed content publisher	Springer
Licensed content publication	Accreditation and Quality Assurance
Licensed content title	Uncertainties when using dual-wavelength or single-wavelength spectrophotometry to monitor the course of hexavalent chromium reduction mediated by zero-valent iron
Licensed content author	Mario Rivero-Huguet
Licensed content date	Dec 1, 2008
Volume number	13
Issue number	12
Type of Use	Thesis/Dissertation
Portion	Full text
Number of copies	1
Author of this Springer article	Yes and you are the editor of the new work
Order reference number	
Title of your thesis / dissertation	Mobilization and detoxification of carcinogenic oxyanions from a contaminated soil mediated by micro and nano-sized metallic particles
Estimated size(pages)	180
Total	0.00 USD

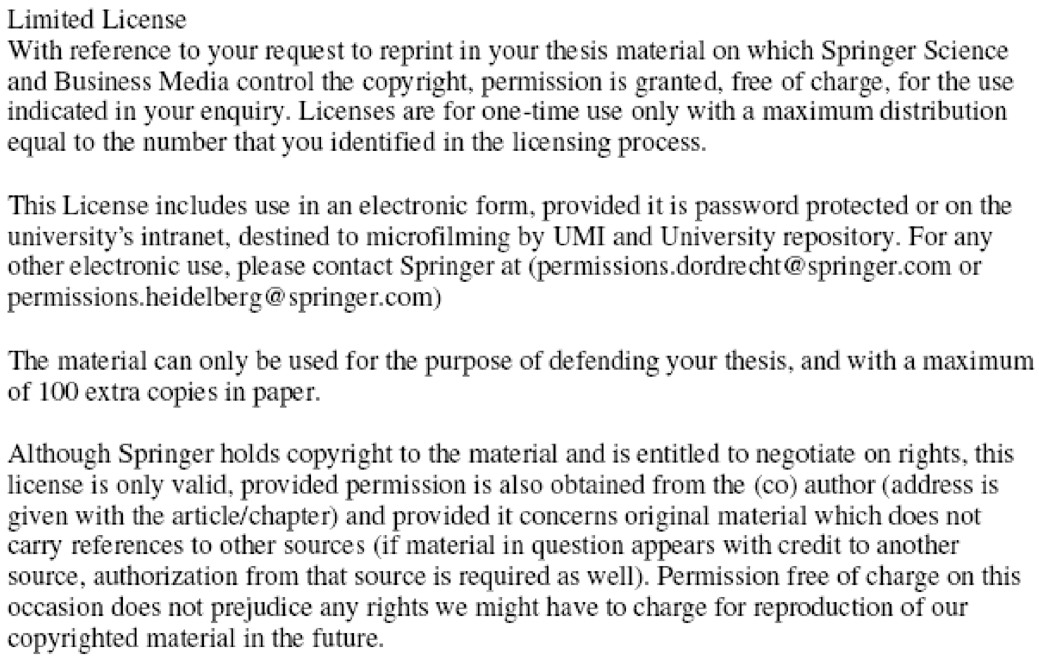

Limited License
With reference to your request to reprint in your thesis material on which Springer Science and Business Media control the copyright, permission is granted, free of charge, for the use indicated in your enquiry. Licenses are for one-time use only with a maximum distribution equal to the number that you identified in the licensing process.

This License includes use in an electronic form, provided it is password protected or on the university's intranet, destined to microfilming by UMI and University repository. For any other electronic use, please contact Springer at (permissions.dordrecht@springer.com or permissions.heidelberg@springer.com)

The material can only be used for the purpose of defending your thesis, and with a maximum of 100 extra copies in paper.

Although Springer holds copyright to the material and is entitled to negotiate on rights, this license is only valid, provided permission is also obtained from the (co) author (address is given with the article/chapter) and provided it concerns original material which does not carry references to other sources (if material in question appears with credit to another source, authorization from that source is required as well). Permission free of charge on this occasion does not prejudice any rights we might have to charge for reproduction of our copyrighted material in the future.

References

[1] A. Markham, A brief History of Pollution, Earthscan Publications Limited, UK, 1994.

[2] J. Nriagu, A History of Global Metal Pollution. Science 272 (1996) 223-224.

[3] C. De Sousa, Contaminated sites: The Canadian situation in an international context. J. Environ. Manage. 62 (2001) 131-154.

[4] A. Hursthouse, The relevance of speciation in the remediation of soils and sediments contaminated by metallic elements-an overview and examples from Central Scotland, UK. J. Environ. Monit. 3 (2001) 49-60.

[5] E. Van Hullebusch, P. Lens, H. Tabak, Developments in bioremediation of soils and sediments polluted with metals and radionuclides. 3. Influence of chemical speciation and bioavailability on contaminants immobilization/mobilization bio-process. Rev. Environ. Sci. BioTech. 4 (2005) 185-212.

[6] National Research Council. Biovailability of Contaminants in Soils and Sediments: Processes, Tools, and Applications. The National Academies Press, Washington, DC, 2003.

[7] J. Nriagu, The rise and fall of leaded gasoline. Sci. Total Environ. 92 (1990) 13-28.

[8] Canadian Council of Ministers of the Environment. Canadian Soil Quality Guidelines for the Protection of Environmental and Human Health: In: Canadian environmental quality guidelines, Canadian Council of Ministers of the Environment, CCME, Winnipeg, 2006.

[9] Ministère de l'Evironnement du Québec, Politique de protection des sols et de réhabilitation des terrains contaminés, Québec, 2006.

[10] F.A. Cotton, G. Wilkinson, Advanced Inorganic Chemistry; Wiley Interscience, NewYork, 6th ed, 1999.

[11] J.E. Huheey, Inorganic Chemistry; Principles of structure and reactivity; Harper Collins College Publishers, 4th ed, 1993.

[12] R. Colton, The Chemistry of Rhenium and Technetium, Interscience, London, 1965.

[13] K.V. Kotegov, O.N. Pavlov, V.P. Shvedov, Technetium. Advan. Inorg. Chem.

Radiochem. 11 (1968) 1-90.

[14] E.A. Katayev, Y.A. Ustynyuk, J.L. Sessler, Receptors for Tetrahedral Oxyanions. Coordin. Chem. Rev. 250 (2006) 3004-3037.

[15] Y. Marcus, H.D. Brook Jenkins, L. Glasser, Ion Volumes: a comparison. J. Chem. Soc. Dalton Trans. (2002) 3795-3798.

[16] D.G. Barceloux, Chromium. Clin. Toxicol. 2 (1999) 173-194.

[17] United States Environmental Protection Agency (USEPA), Toxicological review of hexavalent chromium (CAS No. 18540-29-9). USEPA, Washington, DC, 1998.

[18] D. Rai, L.E. Eary, J.M. Zachara, Environmental chemistry of chromium. Sci. Total Environ. 86 (1989) 15-23.

[19] Canadian Environmental Protection Act. Priority Substances List Assessment Report. Chromium and its Compounds. Government of Canada, 1994, revised 2006.

[20] J.V. Bhide, P.K. Dhakephalkar, K.M. Paknikar, Microbiological process for the removal of Cr(VI) from chromate-bearing cooling tower effluent. Biotechnol. Lett. 18 (1996) 667-672.

[21] J.O. Nriagu, In: Chromium in natural and human environment, Wiley New York, 1988.

[22] United States Environmental Protection Agency (USEPA), Supplemental guidance on interpretation of revised chromated copper arsenate (CCA) wood preservative labels, Washington, DC, 2002.

[23] United States Environmental Protection Agency (USEPA), Clean Water Act. USEPA, Washington, DC, 2002.

[24] M. Costa, Potential hazards of hexavalent chromate in our drinking water. Toxicol. Appl. Pharmacol. 188 (2003) 1-5.

[25] M.D. Cohen, B. Kargacin, C.B. Klein, M. Costa, Mechanisms of chromium carcinogenicity and toxicity. Crit. Rev Toxicol. 23 (1993) 255-281.

[26] K.H. Cheung, J.-D. Gu, Mechanism of hexavalent chromium detoxification by microorganisms and bioremediation application potential: A review. Int. Biodeter. Biodegr. 59 (2007) 8-15.

[27] International Agency for Research on Cancer (IARC). Monograph on Chromium, Nickel and Welding, Vol 49, Lyon, France, 1989.

[28] United States Department of Labor, Occupational Safety & Health Administration (OSHA), Toxic and Hazardous Substances, Chromium (VI)

Standard Number 1910.1026, 2006.

[29] Canadian Environmental Protection Act. Priority Substances List Assessment Report. Arsenic and its Compounds. Government of Canada, 1993, revised 2006.

[30] World Health Organization (WHO). Arsenic and Arsenic Compounds. Environmental Health Criteria Monograph 224, International Programme on Chemical Safety. 2nd edition, Geneva, 2001.

[31] Z. Gong, X. Lu, M. Ma, C. Watt, X.C. Le, Arsenic speciation analysis. Talanta 58 (2002) 77-96.

[32] D.A. Belluck, S.L. Benjamin, P. Baveye, J. Sampson, B. Johnson, Widespread Arsenic Contamination of Soils in Residential Areas and Public Spaces: An Emerging Regulatory or Medical Crisis?. Int. J. Toxicol. 22 (2003) 108-128.

[33] J. Gulens, D.R. Champ, R.E. Jackson, Influence of redox environments on the mobility of arsenic in ground water. In: E.A. Jenne (ed). Chemical modeling in aqueous systems, ACS Symposium Series 93. Washington, D.C, American Chemical Society, 1979, 81–95.

[34] S. Wolz, R.A. Fenske, N.J. Simcox, G. Palcisko, J.C. Kissel, Residential arsenic and lead levels in an agricultural community with a history of lead arsenate use. Environ. Res. 93 (2003) 293-300.

[35] C.F. Aten, J.B. Bourke, J.H. Martini, J.C. Walton, Arsenic and lead in an orchard environment. Bull. Environ. Contam. Toxicol. 24 (1980) 108-115.

[36] A.J. Bednar, J.R. Garbarino, J.F. Ranville, T.R. Wildeman, Presence of organoarsenicals used in cotton production in agricultural water and soil of the southern United States. J. Agric. Food Chem. 50 (2002) 7340-7344.

[37] World Health Organization (WHO). Chapter 6.1 Monograph on Arsenic. WHO Regional Office for Europe, Air Quality Guidelines 2nd edition, 2000.

[38] M.F. Hughes, E.M. Kenyon, K.T. Kitchin, Research approaches to address uncertainties in the risk assessment of arsenic in drinking water. Toxicol. Appl. Pharmacol. 222 (2007) 399-404.

[39] A. Heikens, Arsenic contamination of irrigation water soil and crops in Bangladesh: Risk implications for sustainable agriculture and food safety in Asia. Food and Agriculture Organization Regional Office for Asia and the Pacific, 2006.

[40] S. Bang, G.P. Korfiatis, X. Meng, Removal of arsenic from water by zero-

valent iron. J. Hazard. Mater. 121 (2005) 61-67.

[41] K. Ohno, T. Yanase, Y. Matsuo, T. Kimura, M.H. Rahman, Y. Magara, Y. Matsui, Arsenic intake via water and food by population living in an arsenic affected area of Bangladesh. Sci. Total Environ. 381 (2007) 68-76.

[42] K.G. Stollenwerk, G.N. Breit, A.H. Welch, J.C. Yount, J.W. Whitney, A.L. Foster, M. Nehal Uddin, R.K. Majumder, N. Ahmed, Arsenic attenuation by oxidized aquifer sediments in Bangladesh. Sci. Total Environ. 379 (2007) 133-150.

[43] P. Bhattacharya, A.H. Welch, K.G. Stollenwerk, M. McLaughlin, J. Bundscuh, G. Panaullah, Arsenic in the environment: Biology and Chemistry. Sci. Total Environ. 379 (2007) 2-3.

[44] P.N. Williams, A.H. Price, A. Raab, S.A. Hossain, J. Feldmann, A.A. Meharg, Variation in Arsenic Speciation and Concentration in Paddy Rice Related to Dietary Exposure. Environ. Sci. Technol. 39 (2005) 5531-5540.

[45] M. Beausoleil, N. Côté, Concentrations des métaux dans les légumes du jardin communautaire Baldwin. Evaluation des impacts à la santé. Agence de la Santé et des Services Sociaux de Montréal. Santé Publique de Montréal, 2006.

[46] M. Beausoleil, N. Côté, Evaluation de la contamination des sols du jardin communautaire Laurier, Arrondissement Rosemont/La Petite-Patrie. Agence de la Santé et des Services Sociaux de Montréal. Santé Publique de Montréal, 2006.

[47] J.G. Hering, Risk assessment for arsenic in drinking water: limits to achievable risk levels. J. Hazard. Mater. 45 (1996) 175-184.

[48] K.T. Suzuki, B.K. Mandal, Y. Ogra, Speciation of arsenic in body fluids. Talanta 58 (2002) 111-119.

[49] K.T. Suzuki, Metabolomics of arsenic based on speciation studies. Anal. Chim. Acta 540 (2005) 71-76.

[50] Agency for Toxic Substances and Disease Registry (ATSDR). Priority List of Hazardous Substances. Updated February 14, 2006, available at: http://www.atsdr.cdc.gov/cercla.

[51] L. Fishbein, Environmental Selenium and its Significance. Fund. Appl. Toxicol. 3 (1983) 411-419.

[52] H. Robberecht, R. Van Grieken, Selenium in environmental waters: determination, speciation, and concentration levels. Talanta 29 (1982) 823-

844.

[53] Y. Zhang, J.N. Moore, W.T. Frankenberger, Speciation of soluble selenium in agricultural drainage waters and aqueous soil-sediment extracts using hydride generation atomic absorption spectrometry. Environ. Sci. Technol. 33 (1999) 1652-1656.

[54] M.J. Blaylock, B.R. James, Redox transformations and plant uptake of selenium resulting from root-soil interactions. Plant Soil 158 (1994) 1-12.

[55] P.C. Uden, H. Totoe Boakye, C. Kahakachchi, J.F. Tyson, Selective detection and identification of Se containing compounds-review and recent developments. J. Chromatogr A. 1050 (2004) 85-93.

[56] K. Pyrzynska, Analysis of selenium species by capillary electrophoresis. Talanta 55 (2001) 657-667.

[57] R. Morales, J.F. López-Sánchez, R. Rubio, Selenium speciation by capillary electrophoresis. TrAC Trend Anal. Chem. 27 (2008) 183-189.

[58] National Academy Press. Selenium in Nutrition, revised edition. Subcommittee on Selenium. Committee on Animal Nutrition, Board on Agriculture and National Research Council, National Academy Press. Washington, DC, 1983.

[59] H. Zeng, G.F. Combs, Selenium as an anticancer nutrient: roles in cell proliferation and tumor cell evasion. J. Nutr. Biochem. 19 (2008) 1-7.

[60] G.F. Combs, W.P. Gray, Chemopreventive Agents: Selenium. Pharmacol. Ther. 79 (1998) 179-192.

[61] L. Schomburg, U. Schweizer, J. Kohrle, Selenium and selenoproteins in mammals: extraordinary, essential, enigmatic. Cell. Mol. Life Sci. 61 (2004) 1988-1995.

[62] J.E. Olfield, Risks and benefits in agricultural uses of selenium. Environ. Geochem. Health. 14 (1992) 81-86.

[63] H. Robberecht, R. Van Grieken, Selenium in environmental waters: determination, speciation and concentration levels. Talanta 29 (1982) 823-844.

[64] R.J. Shamberger, Selenium in the Environment. Sci. Total Environ. 17 (1981) 59-74.

[65] J.E. Oldfield, Selenium: A Historical Perspective in Selenium: Its Molecular Biology and Role in Human Health, Chap. 1, Washington, DC, 2nd ed., 2006.

[66] Internacional Agency for Research on Cancer (IARC). Some arizidines, N-, S-

, and O- Mustards and Selenium. IARC monographs on the evaluation of carcinogenic risk of chemicals to humans, vol.9., Lyon, France, 1975.

[67] United States Environmental Protection Agency (USEPA). Seleniun and its Compounds. National Primary Drinking Water Regulations. Washington, DC, 2007.

[68] K.T. Suzuki, K. Kurasaki, S. Ogawa, N. Suzuki, Metabolic transformation of methylseleninic acid through key selenium intermediate selenide. Toxicol. Appl. Pharm. 215 (2006) 189-197.

[69] Y. Shiobara, T. Yoshida, K.T. Suzuki, Effects of dietary selenium species on Se concentrations in hair, blood, and urine. Toxicol. Appl. Pharm. 152 (1998) 309-314.

[70] G. Yang, S. Wang, R. Zhou, S. Sun, Endemic selenium intoxication of humans in China, Am. J. Clinical Nutr. 37 (1983) 872-881.

[71] C.N. Mulligan, R.N. Yong, B.F. Gibbs, Remediation technologies for metal-contaminated soils and groundwater: an evaluation. Eng. Geol. 60 (2001) 193-207

[72] L. Dauerman, G. Windgasse, H.P. Gu, N. Ibrahim, E. Sedhom, Applications of microwave treatment of hazardous wastes: (a) non-volatile organics; (b) heavy metals. Mat. Res. Soc. Symp. Proc. 189 (1991) 61-66

[73] R.A. Abramovitch, L. Chang-Qing, E. Hicks, E. Sinard, In situ remediation of soils contaminated with toxic ions using microwave energy. Chemosphere 53 (2003) 1077-1085.

[74] R.A. Abramovitch, H. Bangzhou, D.A. Abramovitch, S. Jiangao, In situ decomposition of PCBs in soil using microwave energy. Chemosphere 38 (1999) 2227-2236.

[75] K.R. Reddy, U.S. Parupudi, S.N. Devulapalli, C.Y. Xu, Effects of soil composition on the removal of chromium by electrokinetics. J. Hazard. Mater. 55 (1997) 135-158.

[76] G. Maini, A.K. Sharman, C.J. Knowles, G. Sunderland, S.A. Jackman, Electrokinetic remediation of metals and organics from historically contaminated soil. J. Chem. Technol. Biot. 75 (2000) 657-664.

[77] W.L. Smith, G.M. Gadd, Reduction and precipitation of chromate by mixed culture sulphate- reducing bacterial biofilms. J. Appl. Microbiol. 88 (2000) 983-991.

[78] E.D. van Hullebusch, P.N.L. Lens, H.H. Tabak, Development in

bioremediation of soils and sediments polluted with metals and radionuclides. 3. Influence of chemical speciation and bioavailability on contaminants immobilization/mobilization bio- process. Rev. Environ. Sci. Biotechnol. 4 (2005) 185-212.

[79] N. Ishii, H. Koiso, H. Takeda, S. Uchida, Environmental conditions for the formation of insoluble Tc in water ponds located above paddy fields. J. Environ. Radioactiv. 99 (2008) 965-972.

[80] T. Barkay, J. Schaefer, Metal and radionuclide bioremediation: issues, considerations, and potentials. Curr. Opin. Microbiol. 4 (2001) 318-323.

[81] E.T. Urbansky, Perchlorate chemistry: Implications for analysis and remediation. Bioremediation J. 2 (1998) 81-95.

[82] E.T. Thompson-Eagle, W.T. Frankenberger, Protein-metiated selenium biomethylation in evaporation pond water. Environ. Toxicol. Chem. 9 (1990) 1453-1462.

[83] J.F. Stolz, R.S. Oremland, Bacterial respiration of arsenic and selenium. FEMS Microbiol. Rev. 23 (1999) 615-627.

[84] D.E. Salt, M. Blaylock, N.P.B.A. Kumar, V. Dushenkov, B.D. Ensley, I. Chet, I. Raskin, Phytoremediation: A novel strategy for the removal of toxic metals from the environment using plants. Bio/Technol. 13(1995) 468-474.

[85] N. Roosens, N. Verbruggen, P. Meerts, P. Ximénez-Embún, J.A. Smith, Natural variation in cadmium tolerance and its relationship to metal hyperaccumulation for seven populations of Thlaspi caerulescens from western Europe. Plant Cell Environ. 26 (2003) 1657-1672.

[86] F. Madrid, M.S. Liphadzi, M.B. Kirkham, Heavy metal displacement in chelate-irrigated soil during phytoremediation. J. Hydrol. 272 (2003) 107-119.

[87] M.C. January, T.J. Cutright, H. van Keulen, R. Wei, Hydroponic phytoremediation of Cd, Cr, Ni, As, and Fe: Can Helianthus annuus hyperaccumulate multiple heavy metals? Chemosphere 70 (2008) 531-537.

[88] R. Semer, K.R. Reddy, Evaluation of soil washing process to remove mixed contaminants from a sandy loam. J. Hazard. Mater. 45 (1996) 45-57.

[89] M. Jang, J.S. Hwang, S.I. Choi, J.K. Park, Remediation of arsenic-contaminated soils and washing effluents. Chemosphere 60 (2005) 344-354.

[90] R. Sheets, B.A. Bergquist, Laboratory treatability testing of soils contaminated with lead and PCBs using particle-size separation and soil washing. J. Hazard. Mater. 66 (1999) 137-150.

[91] W. Zhang, D.C.W. Tsang, I.M.C. Lo, Removal of Pb and MDF from contaminated soils by EDTA- and SDS-enhanced washing. Chemosphere 66 (2007) 2025-2034.

[92] W. Chu, K.H. Chan, The mechanism of the surfactant-aided soil washing system for hydrophobic and partial hydrophobic organics. Sci. Tot. Environ. 307 (2003) 83-92.

[93] C.N. Mulligan, R.N. Yong, B.F. Gibbs, Surfactant-enhanced remediation of contaminated soil: A review. Eng. Geol. 60 (2001) 371-380.

[94] C.N. Mulligan, R.N. Yong, B.F. Gibbs, S. James, H.P.J. Bennet, Metal removal from contaminated soil and sediments using biosurfactant surfactin. Environ. Sci. Technol. 33 (1999) 3812-3820.

[95] C.N. Mulligan, R.N. Yong, B.F. Gibbs, Removal of heavy metals from contaminated soil and sediments using biosurfactant surfactin. J.Soil Contam. 8 (1999) 231-254.

[96] D. Myers, Surfaces, interfaces, and colloids: principles and applications, 2002, 3rd ed. Wiley-VCH, New York.

[97] D.A. Sabatini, J.H. Harwell, R.C. Knox, Surfactant selection criteria for enhanced subsurface remediation. ACS Symposium Series (1999) 8-23.

[98] J.H. Harwell, D.A. Sabatini, R.C. Knox, Remediation of soils and aquifers with surfactants. Abstracts of Papers, 220th ACS National Meeting, (2000) 20-24.

[99] M.L. Brusseau, X. Wang,W. Wang, Simultaneous elution of heavy metals and organic compounds from soil by cyclodextrin. Environ. Sci. Technol. 31 (1997) 1087-1092.

[100] S. Ehsan, S.O. Prasher, W. Marshall, A washing procedure to mobilize mixed contaminants from soil: II. Heavy metals. J. Environ. Qual. 35 (2006) 2084-2091.

[101] D. Schmelling, D. Poster, M. Chaychian, W. Mclaughlin, J. Silverman, M. Al-Sheikhly, Applications of ionizing radiation to the remediation of materials contaminated with heavy metals and polychlorinated biphenyls. Radiat. Phys. Chem. 52 (1998) 371-377.

[102] K. Baek, B.K. Kim, H.-J. Cho, J.-W. Yang, Removal characteristics of anionic metals by micellar enhanced ultrafiltration. J. Hazard. Mater. B99 (2003) 303-311.

[103] K. Baek, J.-W. Yang, Simultaneous removal of chlorinated aromatic hydrocarbons, nitrate, and chromate using micellar-enhanced ultrafiltration.

Chemosphere 57 (2004) 1091-1097.

[104] P.G. Tratnyek, M.M. Scherer, T.L. Johnson, L.J. Matheson, Permeable reactive barriers of iron and other zero-valent metals. Chemical Degradation Methods for Wastes and Pollutants, 2003, Marcel Dekker Inc., New York.

[105] R.-A. Doong, K.-T. Chen, H.-C. Tsai, Reductive dechlorination of carbon tetrachloride and tetrachloroethylene by zerovalent silicon-iron reductants. Environ. Sci. Technol. 37 (2003) 2575-2581.

[106] Y.-H. Kim, E.R. Carraway, Dechlorination of chlorinated phenols by zero valent zinc. Environ. Technol. 24 (2003) 1455-1463.

[107] A. Agrawal, P.G. Tratnyek, Reduction of nitro aromatic compounds by zero valent iron metal. Environ Sci. Technol. 30 (1996) 153-160.

[108] C. Su, R.W. Puls, Nitrate reduction by zerovalent iron: effects of formate, oxalate, citrate, chloride, sulfate, borate, and phosphate. Environ. Sci. Technol. 38 (2004) 2715-2720.

[109] M.J. Alowitz, M.M. Scherer, Kinetics of nitrate, nitrite and Cr(VI) reduction by iron metal. Environ. Sci. Technol. 36 (2002) 299-306.

[110] J. Kumpiene, S. Ore, G. Renella, M. Mench, A. Lagerkvist, C. Maurice, Assessment of zerovalent iron for stabilization of chromium, copper, and arsenic in soil. Environ. Pollut. 2006; 144:62-69.

[111] Y.J. Oh, H. Song, W.S. Shin, S.J. Choi, Y.-H. Kim, Effect of amorphous silica and silica sand on removal of chromium(VI) by zero-valent iron. Chemosphere 66 (2007) 858-865.

[112] S. Bang, M.D. Johnson, G.P. Korfiatis, X. Meng, Chemical reactions between arsenic and zero-valent iron in water. Water Research 39 (2005) 763-770.

[113] S. Bang, G.P. Korfiatis, X. Meng, Removal of arsenic from water by zero-valent iron. J. Hazard. Mater. 121 (2005) 61-67.

[114] C. Su, R.W. Puls, Arsenate and Arsenite removal by zerovalent iron: kinetics, redox transformation, and implications for in situ groundwater remediation. Environ. Sci. Technol. 35 (2001) 1487-1492.

[115] N. Melitas, J. Wang, M. Conklin, P. O'Day, J. Farrell, Understanding soluble removal kinetics by zerovalent iron media. Environ. Sci. Technol. 36 (2002) 2074-2081.

[116] C. Su, R.W. Puls, Arsenate and Arsenite removal by zerovalent iron: effects of phosphate, silicate, carbonate, borate, sulfate, chromate, molybdate, and nitrate, relative to chloride. Environ. Sci. Technol. 35 (2001) 4562-4568.

[117] Y. Zhang, J. Wang, C. Amrhein, W.T. Frankenberger, Removal of selenate form water by zerovalent iron. J. Environ. Qual. 34 (2005) 487-495.

[118] K.J. Cantrell, D.I. Kaplan, T.W. Wietsma, Zero-valent iron for the in situ remediation of selected metals in groundwater. J. Hazard. Mater. 42 (1995) 201-212.

[119] A.M. Moore, C.H. De Leon, T.M. Young, Rate and Extent of aqueous perchlorate removal by iron surfaces. Environ. Sci. Technol. 37 (2003) 3189-3198.

[120] J. Liu, C. Wang, J. Shi, H. Liu, Y. Tong, Aqueous Cr(VI) reduction by electrodeposited zero-valent iron at neutral pH: Acceleration by organic matters. J. Hazard. Mater. 163 (2009) 370-375.

[121] R.-A. Doong, C.-C. Lee, K.-T. Chen, S.-F. Wu, Coupled reduction of chlorinated hydrocarbons and heavy metals by zero valent silicon. Water Sci. Technol. 50 (2004) 89-96.

[122] T. Boronina, K.J. Klabunde, Destruction of organohalides in water using metal particles: carbon tetrachloride/water reactions with magnesium, tin, and zinc. Environ. Sci. Technol. 29 (1995) 1511-1517.

[123] Z. Wang, W. Huang, D.E. Fennell, P. Peng, Kinetics of reductive dechlorination of 1,2,3,4-TCDD in the presence of zero-valent zinc. Chemosphere 71 (2008) 360-368.

[124] C.-C. Liu, D.-H. Tseng, C.-Y. Wang, Effects of ferrous ions on the reductive dechlorination of trichloroethylene by zero-valent iron. J. Hazard. Mater. B136 (2006) 706-713.

[125] S.J. Bransfield, D.M. Cwiertny, K. Livi, D.H. Fairbrother, Influence of transition metal additives and temperature on the rate of organohalide reduction by granular iron: implications for reaction mechanisms. Appl. Catal. B-Environ. 76 (2007) 348-356.

[126] D.M. Cwiertny, S.J. Bransfield, A.L. Roberts, Influence of the oxidizing species on the reactivity of iron-based bimetallic reductants. Environ. Sci. Technol. 41 (2007) 3734-3740.

[127] A. Ghauch, A. Tuqan, Catalytic degradation of chlorothalonil in water using bimetallic iron-based systems. Chemosphere 73 (2008) 751-759.

[128] T. Yuan, W.D. Marshall, Dechlorination of pentachlorophenol in supercritical carbon dioxide with zero-valent palladium magnesium bimetallic mixture. J. Environ. Monit. 4 (2002) 452-457

[129] Y.-H. Kim, E.R. Carraway, Dechlorination of pentachlorophenol by zerovalent iron and modified zero valent irons. Environ. Sci. Technol. 34 (2000) 2014-2017.

[130] C. Wan, Y.H. Chen, R. Wei, Dechlorination of chloromethanes on iron and palladium-iron bimetallic surface in aqueous systems. Environ. Toxicol. Chem. 18 (1999) 1091-1096.

[131] N. Korte, L. Liang, R. Muftikian, C. Grittini, Q. Fernando, The dechlorination of of hydrocarbons. Platinum Met. Rev. 41 (1997) 2-7.

[132] P. Varanasi, A. Fullana, S. Sidhu, Remediation of PCB contaminated soils using iron nano-particles. Chemosphere 66 (2007) 1031-1038.

[133] M. Auffan, J. Rose, M.R. Wiesner. J.-Y. Bottero, Chemical stability of metallic nanoparticles: A parameter controlling their potential cellular toxicity in vitro. Environ. Pollut. 157 (2009) 1127-1133.

[134] S.M. Ponder, J.G. Darab, T.E. Mallouk, Remediation of Cr(VI) and Pb(II) aqueous solutions using supported nanoscale zero-valent iron. Environ. Sci. Technol. 34 (2000) 2564-2569.

[135] C.-B. Wang, W.-X. Zhang, Synthesizing nanoscale iron particles for rapid and complete dechlorination of TCE and PCBs. Environ. Sci. Technol. 31 (1997) 2154-2156.

[136] W.-X. Zhang, C.-B. Wang, L.-H. Lien, Treatment of chlorinated organic contaminants with nanoscale bimetallic particles. Catal. Today 40 (1998) 387-395.

[137] Z. Xiong, D. Zhao, G. Pan, Rapid and complete destruction of perchlorate in water and ion-exchange brine using stabilized Zero-Valent Iron nanoparticles. Water Res. 41 (2007) 3498-3505.

[138] L.-H. Lien, Y.-S. Jhuo, L.-H. Chen, Effect of heavy metals on dechlorination of carbon tetrachloride by iron nanoparticles. Environ. Eng. Sci. 24 (2007) 21-30.

[139] B. Schrick, J. Blough, A. Jones, T. Mallouk, Hydrodechlorination of trichloethylene to hydrocarbons using bimetallic Nickel-Iron nanoparticles. Chem. Mater. 14 (2002) 5140-5147.

[140] S.M. Ponder, J.G. Darab, J. Bucher, D. Caulder, I. Craig, L. Davis, N. Edelstein, W. Lukens, H. Nitsche, L. Rao, D.K. Shuh, T.E. Mallouk, Surface and electrochemistry of supported zerovalent iron nanoparticles in the remediation of aqueous metal contaminants. Chem. Mater. 13 (2001) 479-

486.

[141] T.-T. Lim, B.-W. Zhu, Effects of anions on the kinetics and reactivity of nanoscale Pd/Fe in trichlorobenzene dechlorination. Chemosphere 73 (2008) 1471-1477.

[142] J. Cao, W.-X. Zhang, Stabilization of chromium ore processing residue (COPR) with nanoscale iron particles. J. Hazard. Mater. B132 (2006) 213-219.

[143] F. He, D. Zhao, J. Liu, C.B. Roberts, Stabilization of Fe-Pd nanoparticles with sodium carboxymethly cellulose for enhanced transport and dechlorination of trichloroethylene in soil and groundwater. Ind. Eng. Chem. Res. 46 (2007) 29-34.

[144] F. He, D. Zhao, Preparation and characterization of a new class of starch-stabilized bimetallic nanoparticles for degradation of chlorinated hydrocarbons in water. Environ. Sci. Technol. 39 (2005)3314-3320.

[145] P. Raveendran, J. Fu, S.L. Wallen, Completely “green” synthesis and stabilization of metal nanoparticles. J. Am. Chem. Soc. 125 (2003) 13940-13941.

[146] S.M. Ponder, J.G. Darab, T.E. Mallouk, Remediation of Cr(VI) and Pb(II) aqueous solutions using supported nanoscale zero-valent iron. Environ. Sci. Technol. 34 (2000) 2564-2569.

[147] H. Khalil, D. Mahajan, M. Rafailovich, M. Gelfer, K. Pandya, Synthesis of zerovalent nanophase metal particles stabilized with poly(ethylene glycol). Langmuir 20 (2004) 6896-6903.

[148] Q. Liu, Y. Bei, F. Zhou, Removal of lead(II) from aqueous solution with amino-funcionalized nanoscale zero-valent iron. Cent. Eur. J. Chem. 7 (2009) 79-82.

[149] E. Casals, S. Vázquez-Campos, N.G. Bastús, V. Puntes, Distribution and potential toxicity of engineered inorganic nanoparticles and carbon nanostructures in biological systems. TRAC-Trend. Anal. Chem. 27 (2008) 672-683.

[150] P.H.M. Hoet, I. Brüske-Hohlfeld, O.V. Salata, Nanoparticles – known and unknown health risks. J. Nanobiotchnol. 2 (2004) 1-15.

[151] R. Barrena, E. Casals, J. Colón, X. Font, A. Sánchez, V. Puntes, Evaluation of model nanoparticles eco-toxicity. Chemosphere 75 (2009) 850-857.

[152] R.M. Powell, R.W. Puls, S.K. Hightower, D.A. Sabatini, Coupled iron corrosion and chromate reduction: mechanisms for subsurface

remediation. Environ. Sci. Technol. 29 (1995) 1913-1922.

[153] S.E. Fendorf, G. Li, Kinetics of Chromate Reduction by Ferrous Iron. Environ. Sci. Technol. 30 (1996) 1614-1417.

[154] APHA, AWWA, WPCF. Standard Methods for the Examination of Water and Wastewater, 21st ed.; American Public Health Association: Washington, DC, 2005.

[155] M. Rivero-Huguet, W.D. Marshall, Uncertainties when using dual-wavelength or single-wavelength spectrophotometry to monitor the course of hexavalent chromium reduction mediated by zero-valent iron. Accred. Qual. Assur. 13 (2008) 711-716.

[156] N. Melitas, O. Chuffe-Moscoso, J. Farrell, Kinetics of soluble chromium removal from contaminated water by zerovalent iron media: corrosion inhibition and passive oxide effects. Environ. Sci. Technol. 35 (2001) 3948-3953.

[157] J.P. Gould J.P, The kinetics of hexavalent chromium reduction by metallic iron. Water Res. 16 (1982) 871-877.

[158] C.-C Lee, R.-A Doong, Dechlorination of tetrachloroethylene in aqueous solutions using metal-modified zero valent silicon. Environ. Sci. Technol. 42 (2008) 4752-4757.

[159] X. Zhou, M. Ishida, A. Imanishi, Y. Nakato, Roles of charge polarization and steric hindrance in determining the chemical reactivity of surface Si-H and Si-Si bonds and H-terminated Si(100) and –(111). J. Phys. Chem. B 105 (2001) 156-163.

[160] S.-S. Chen, C.-Y. Cheng, P.-H. Cahai, Y.-M. Chang, Reduction of chromate from electroplating wastewater from pH 1 to 2 using fluidized zero valent iron process. J. Hazard. Mater. 142 (2007) 362-367.

[161] E. J. Reardon, Anaerobic corrosion of granular iron: measurement and interpretation of hydrogen evolution rates. Environ. Sci. Technol. 29 (1995) 2936-2945.

[162] Z.-X. Zhang, Nanoscale iron particles for environmental remediation: An overview. J. Nanoparticle Res. 5 (2003) 323-332.

[163] Z. Chen, H. Meng, G. Xing, C. Chen, Y. Zhao, G. Jia, T. Wang, H. Yuan, C. Ye, F. Zhao, Z. Chai, C. Zhu, X. Fang, B. Ma, L. Wan, Acute toxicological effects of copper nanoparticles in vivo. Toxicol. Lett. 163 (2006) 109-120.

[164] C.-J. Lin, S.-L. Lo, Y.-H. Liou, Degradation of aqueous carbon tetrachloride by

nanoscale zerovalent copper on a cation resin. Chemosphere, 59 (2005) 1299-1307.

[165] M. Zhao, L. Sun, R.M. Crooks, Preparation of Cu nanoclusters within dendrimer templates. J. Am. Chem. Soc. 120 (1998) 4877-4878.

[166] G. Oberdörster, V. Stone, K. Donaldson, Toxicology of nanoparticles: A historical perspective. Nanotoxicol. 1 (2007) 2-25.

[167] M. Rivero-Huguet, W.D. Marshall, Reduction of hexavalent chromium mediated by micron- and nano-scale zero-valent metallic particles. J Environ. Monit. 11 (2009) 1072-1079.

[168] C. –P. Huang, H. – W. Wang, P. –C Chiu, Nitrate reduction by metallic iron. Wat. Res. 32 (1998) 2257-2264.

[169] X.R. Xu, H.B. Li, X.Y. Li, J.D. Gu, Reduction of hexavalent chromium by ascorbic acid in aqueous solutions. Chemosphere 57 (2004) 609-613.

[170] C. Li, Y. Lan, B. Deng, Catalysis of Mn^{2+} on the reduction of Cr^{6+} by citrate. Pedosphere 17 (2007) 318-323.

[171] P.R. Wittbrodt, C.D. Palmer, Reduction of Cr(VI) in the presence of excess soil fulvic acid. Environ. Sci. Technol. 29(1995) 255-263.

[172] P.R. Wittbrodt, C.D. Palmer, Effect of temperature, ionic strength, background electrolytes, and Fe(III) on the reduction of hexavalent chromium by soil humic substances. Environ. Sci. Technol. 30 (1996) 2470-2477.

[173] B. Deng, A.T. Stone, Surface-catalyzed chromium(VI) reduction: TiO_2-Cr(VI)-Mandelic acid system. Environ. Sci. Technol. 30 (1996) 463-472.

[174] B. Deng, A.T. Stone, Surface-catalyzed chromium(VI) reduction: reactivity comparison of different organic reductants and different oxide surfaces. Environ. Sci. Technol. 30 (1996) 2484-2494.

[175] S.J. Hug, H.U. Laubscher, Iron(III) catalyzed photochemical reduction of chromium(VI) by oxalate and citrate in aqueous solutions. Environ. Sci. Technol. 31 (1997) 160-170.

[176] Kabir-ud-Din, K. Hartani, Z. Khan, Unusual rate inhibition of manganese(II) assisted oxidation of citric acid by chromium(VI) in the presence of ionic micelles. Transit. Metal. Chem. 25 (2000) 478-484.

[177] Kabir-ud-Din, K. Hartani, Z. Khan,One-step three-electron oxidation of tartaric and glyoxylic acids by chromium(VI) in the absence and presence of manganese(II). Transit. Metal. Chem. 27 (2002) 617-624.

[178] S. Tandy, K. Bossart, R. Mueller, J. Ritschel, L. Hauser, R. Schulin, B.

Nowack, Extraction of heavy metals from soil using biodegradable chelating agents. Environ. Sci. Technol. 38 (2004) 937-944.

[179] X.R. Xu, H.B. Li, X.Y. Li, J.D. Gu, Reduction of hexavalent chromium by ascorbic acid in aqueous solutions. Chemosphere 57 (2004) 609-613.

[180] S. Çakir, E. Biçer, The interaction of cysteine with chromium(VI) ions under UV irradiation. Bioelectrochemistry 67 (2005) 75-80.

[181] H. Zhou, Y. He, Y. Lan, J. Mao, S. Chen, Influence of complex reagents on removal of chromium(VI) by zero-valent iron. Chemosphere 72 (2008) 870-874.

[182] R.M. Smith, A.E. Martell, R.J. Motekaitis, NIST Critical Stability Constants of Metal Complexes Database; NIST Standard Reference Database 46; U.S. Department of Commerce: Gaithersburg MD, 1993.

[183] J. Rocek, J.C. Drozd, Evidence for epoxides as intermediates in the chromic acid oxidation of olefins. J. Am. Chem. Soc. 92 (1970) 6668-6669.

[184] F. Freeman, K.W. Arledge, Chromyl chloride oxidations. VII. Kinetics and mechanism of the electrophilic addition to cycloalkenes. J.Org. Chem. 37 (1970) 2656-2662.

[185] A.K. Das, S.K. Mondal, D. Kar, M. Das, Micellar effect on the reaction of picolinic acid catalyzed chromium(VI) oxidation of mimethyl sulfoxide in aqueous acidic media: A kinetic study. Int. J. Chem. Kinet. 33 (2001) 173-181.

[186] M. Islam, B. Saha, A.K. Das, Kinetics and mechanism of picolinic acid promoted chromic acid oxidation of maleic acid in aqueous micellar media. J. Mol. Catal. A-Chem. 266 (2007) 21-30.

[187] G.B. Deacon, R.J. Phillips, Relationship between the carbon-oxygen stretching frequencies of carboxylate complexes and the type of carboxylate coordination. Coord. Chem. Rev. 33 (1980) 227-251.

[188] J. Byegård, G. Skarnemark, M. Skålberg, The stability of some metal EDTA, DTPA and DOTA complexes: Application as tracers in groundwater studies. J. Radioanal. Nucl. Ch. 241 (1999) 281-290.

[189] V. Nagaraju, T. Goje, A.M. Crouch, Determination of copper and iron using [*S,S'*]-ethylenediaminedisuccinic acid as chelating agent in wood pulp by capillary electrophoresis. Anal. Sci. 23 (2007) 493-496.

[190] M. Cieślak-Golonka, M. Daszkiewicz, Coordination geometry of Cr(VI) species: Structural and spectroscopic characteristics. Coordin. Chem. Rev.

249 (2005) 2391-2407.

[191] J.C. Renshaw, G.D. Robson, A.P.J. Trincini, M.G. Wiebe, F.R. Livens, D. Collison, R.J. Taylor,Fungal sideropohores: structures, functions and applications. Mycol. Res. 106 (2002) 1123-1142.

[192] A.V. Colnaghi Simionato, A.D. Cantú, E.Carrilho, Characterization of metal-deferoxamine complexes by continuous variation method: A new approach using capillary zone electrophoresis. Microchem. J. 82 (2006) 214-219.

[193] A. McAuley, M.A. Olatunji, Metal-ion oxidations in solution. Part XVIII. Characterization, rates, and mechanism of formation of the intermediates in the oxidation of thiols by chromium(VI). Can. J. Chem. 55 (1977) 3328-3334.

[194] P.H. Connett, K.E. Wetterhahn, In vitro reaction of the carcinogenic chromate with cellular thiols and carboxylic acids. J. Am. Chem. Soc. 107 (1985) 4282-4288.

[195] L. Bencivenni, S. Nunziante Cesaro, A. Pieretti, Matriz and ab initio infrared spectra of thiourea and thiourea-d4. Vib. Spectrosc. 18 (1998) 91-102.

[196] U. Russo, R. Graziani, S. Calogero, U. Casellato, Characterization of some high-spin iron(II) complexes with urea derivatives. The crystal structure of dichloreotetrakis(thiourea) iron(II). Transition Met. Chem. 4 (1979) 82-86.

[197] M.J. Arendse, G.K. Anderson, N.P. Rath, Oxidative degradation of the ascorbate anion in the presence of platinum and palladium. Formation and structures of platinum and palladium oxalates. Polyhedron 20 (2001) 2495-2503.

[198] T. Lee, H. Lim, Y. Lee, J.-W. Park, Use of waste iron metal for removal of Cr(VI) from water. Chemosphere 53 (2003) 479-485.

[199] K.C.K. Lai, I.M.C. Lo, Removal of chromium(VI) by acid-washed zero-valent iron under various groundwater geochemistry conditions. Environ. Sci. Technol. 42 (2008) 1238-1244.

[200] A.B. Cundy, L. Hopkinson, R.L.D. Whitby, Use of iron-based technologies in contaminated land and groundwater remediation: A review. Sci Total Environ. 400 (2008) 42-51.

[201] D. Peak, R.G. Ford, D.L. Sparks, An in-situ ATR-FTIR investigation of sulfate bonding mechanisms on goethite. J. Colloid Interface Sci. 218 (1999) 289-299.

[202] C. Su, D.L. Suarez, Coordination of adsorbed boron: A FTIR spectroscopic study. Environ. Sci. Technol. 29 (1995) 302-311.

[203] T. Liu, P. Rao, M.S.H., Mak, P. Wang, I.M.C. Lo, Removal of co-present chromate and arsenate by zero-valent iron in groundwater with humic acid and bicarbonate. Water Res. 43 (2009) 2540-2548.

[204] Y. Zhang, C. Amrhein, A. Chang, W.T. Frankenberger Jr, Effect of zero-valent iron and a redox mediator on removal of selenium in agricultural drainage water. Sci. Total Environ. 407 (2008) 89-96.

[205] Handbook of Chemistry and Physics David R. Lide Ed. CRC Press, 84th edition, 2003-2004.

[206] Guide to the expression of uncertainty in measurement (1993) BIPM/IEC ISO/IEC/IFCC/ISO/IUPAC/IUPAP/IOML International Organization for Standardization (ISO), Geneva, Switzerland (ISBN 92-67-10188-9).

[207] S.L.R. Ellison, V.J. Barwick, Using validation data for ISO measurement uncertainty estimation Part 1. Principles of an approach using cause and effect analysis. Analyst 123 (1998) 1387-1392.

[208] S.L.R. Ellison, M. Rösslein, A. Williams (Eds.), EURACHEM/CITAC Guide CG 4, Quantifying Uncertainty in Analytical Measurement, 2nd ed., EURACHEM, Berlin, 2000, Internet version: http://www.citac.cc/

[209] L. Sooväli, E.-I. Rõõm, A. Kütt, I. Kaljurand, I. Leito, Uncertainty sources in UV-vis spectrophotometric measurement. Accred. Qual. Assur. 11 (2006) 246-255.

[210] H.-W. Gao, L.-Q. Yu, Updated determination of trace amounts of zinc with dibromo- *O* – nitrophenylflurone by primary-secondary wavelength spectrophotometry. J. Anal. Chem. 55 (200) 870-873.

[211] H.-W. Gao, Y.C. Li, P.F. Zhang, M. Tao, L. Wang, Determination of trace amounts of cadmium with p-acetyl-benzenediazoaminoazobenzene by primary-secondary wavelength spectrophotometry. J. Anal. Chem. 56 (2001) 1007-1010.

[212] M. Thompson, D.J.W. Jones, Auto-standarisation in spectrophotometry. Analyst 101 (1976) 825-827.

[213] P. Jones, G. Nickless, Spectrophotometric determination of methylmercury in fish tissue with dithizone using a dual-wavelength procedure. Analyst 103 (1978) 1121-1126.

[214] H.-W. Gao, Dual-wavelength β-correction spectrophotometry for directly determining anionic detergents in environmental water. Anal. Proc. 32 (1995) 197-200.

[215] H.-W. Gao, β-correction spectrophotometry for composition determination of chelated copper(II) with its complexans. Anal. Proc. 32 (1995) 17-19.

[216] P. Jones, Major sensitivity improvements in ion chromatography determinations involving post-column spectrophotometric reaction detectors through elimination of pump noise using a dual wavelength monitoring procedure. Analyst 125 (2000) 803-806.

[217] ISO 9004-4:1993. Total Quality Management Part 2. Guidelines for Quality Improvement, International Standards Organization, Geneva, Switzerland.

[218] A.G. González, M.A. Herrador, The assessment of electronic balances for accuracy of mass measurements in the analytical laboratory. Accred. Qual. Assur. 12 (2007) 21-29.

[219] OIML IR No.33: Valeur conventionnelle du résultat des pesées dans l'air, 1979.

[220] M. Shin, S. Barrington, Effectiveness of the iodide ligand along with two surfactants on desorbing heavy metals from soils. Water Air Soil Poll. 161 (2005) 193-208.

[221] United States Environmental Protection Agency, Test Methods for evaluating soild waste, Method 3060A, Alkaline digestion for hexavalent chromium 1996.